FINAL REPORT

Decision-Scaling: A Decision Framework for DoD Climate Risk Assessment and Adaptation Planning

SERDP Project RC-2204

AUGUST 2016

Casey Brown
Scott Steinschneider
Sungwook Wi
University of Massachusetts

John Weatherly
Michael Case
Timothy Hayden
Anne Koster
US Army Corps of Engineers Engineering Research and Development Center

Linda Mearns
Melissa Bukovsky
Rachel McCrary
National Center for Atmospheric Research

SERDP
DOD ▪ EPA ▪ DOE

Page Intentionally Left Blank

Page Intentionally Left Blank

REPORT DOCUMENTATION PAGE

Form Approved
OMB No. 0704-0188

1. REPORT DATE *(DD-MM-YYYY)*	**2. REPORT TYPE**	**3. DATES COVERED** *(From - To)*
09-06-2016	Final Report	3/29/12-3/29/17

4. TITLE AND SUBTITLE
Decision-Scaling: A Decision Framework for DoD Climate Risk Assessment and Adaptation Planning

5a. CONTRACT NUMBER

5b. GRANT NUMBER

5c. PROGRAM ELEMENT NUMBER

6. AUTHOR(S)
Brown, Casey, Steinschneider, Scott, Wi, Sungwook, Weatherly, John, Case, Michael, Hayden, Timothy, Koster, Anne, Mearns, Linda, Bukovsky, Melissa, McCrary, Rachel

5d. PROJECT NUMBER
RC-2204

5e. TASK NUMBER

5f. WORK UNIT NUMBER

7. PERFORMING ORGANIZATION NAME(S) AND ADDRESS(ES) AND ADDRESS(ES)
University of Massachusetts
US Army Corps of Engineers Engineering Research and Development Center
National Center for Atmospheric Research

8. PERFORMING ORGANIZATION REPORT NUMBER

9. SPONSORING / MONITORING AGENCY NAME(S) AND ADDRESS(ES)
Strategic Environmental Research and Development Program
4800 Mark Center Drive, Suite 17D08
Alexandria, VA 22350

10. SPONSOR/MONITOR'S ACRONYM(S)
SERDP

11. SPONSOR/MONITOR'S REPORT NUMBER(S)
RC-2204

12. DISTRIBUTION / AVAILABILITY STATEMENT

Unlimited

13. SUPPLEMENTARY NOTES

14. ABSTRACT

This research presents and demonstrates a framework for assessing climate change risks to DoD installations and the built environment. The approach, which we call "decision-scaling," reveals the core sensitivity of DoD installations to climate change. It is designed to illuminate the sensitivity of installations and their supporting infrastructure systems, including water and energy, to climate changes and other uncertainties without dependence on climate change projections. In this way the analysis and results remain unclouded by the many choices and trade-offs required in the processing of projections from general circulation models (GCMs, also known as global climate models) and their associated uncertainties. The engine of analysis is the "climate stress test" which is an algorithm designed to stress the target system using systematic and exhaustive exploration of possible climate changes. Climate projections, including simulations from the NARCCAP are then used to inform the level of concern associated with each risk after the risks are identified via the climate stress test. The decision framework was applied to four sectors: water supply, energy costs, training and fire management and evaluated through piloting at four installations. The results show clear answers regarding the climate risks at each installation in each of these sectors, in terms that are quantifiably comparable across sectors. The expectation is the framework and assessment products are appropriate for application to all DoD installations and represent the very best approach for evaluating climate risks.

15. SUBJECT TERMS
Climate change, Risk Assessment, Decision Analysis, Adaptation, Water Supply, Fire Risk, Training, Energy Planning, Downscaling

16. SECURITY CLASSIFICATION OF:			**17. LIMITATION OF ABSTRACT**	**18. NUMBER OF PAGES**	**19a. NAME OF RESPONSIBLE PERSON**
a. REPORT	**b. ABSTRACT**	**c. THIS PAGE**		233	Casey Brown
					19b. TELEPHONE NUMBER *(include area code)*

Standard Form 298 (Rev. 8-98)
Prescribed by ANSI Std. Z39.18

Page Intentionally Left Blank

Abstract

This research presents and demonstrates a framework for assessing climate change risks to Department of Defense (DoD) installations and the built environment. The approach, which we call "decision-scaling," reveals the core sensitivity of DoD installations to climate change. It is designed to illuminate the sensitivity of installations and their supporting infrastructure systems, including water and energy, to climate changes and other uncertainties without dependence on climate change projections. In this way the analysis and results remain unclouded by the many choices and trade-offs required in the processing of projections from general circulation models (GCMs, also known as global climate models) and their associated uncertainties. The engine of analysis is the "climate stress test" which is an algorithm designed to stress the target system using systematic and exhaustive exploration of possible climate changes. Climate projections, including simulations from the North American Climate Change Assessment Program (NARCCAP) are then used to inform the level of concern associated with each risk after the risks are identified via the climate stress test. The decision framework was applied to four sectors: water supply, energy costs, training and fire management and evaluated through piloting at four installations. The results show clear answers regarding the climate risks at each installation in each of these sectors, in terms that are quantifiably comparable across sectors. The expectation is the framework and assessment products are appropriate for application to all DoD installations and represent the very best approach for evaluating climate risks.

Page Intentionally Left Blank

Contents

Tables

Figures

Acronyms

ACF	Apalachicola-Chattahoochee-Flint River Basin
A/E	Architecture/Engineering
AFB	Air Force Base
ARC	Atlanta Regional Commission
BCWCID	Bell County Water Improvement District
BRA	Brazos River Authority
BRAC	Base Realignment and Closure
CCAR	Climate Change Adaptation Roadmap
CMIP	Coupled Model Intercomparison Project
CWW	Columbus Water Works
DoD	Department of Defense
DOE	Department of Energy
DJF	December-January-February
EISA	Energy Independence and Security Act (EISA) of 2007
ENSO	El Nino-Southern Oscillation
EO	Executive Order
ERDC-CERL	Engineering Research and Development Center – Civil Engineering Research lab
ERDC-CRREL	Engineering Research and Development Center – Cold Regions Research and Engineering Lab
EUI	Energy Use Intensity
FEMP	Federal Energy Management Program
FY	Fiscal Year
GA	Genetic Algorithm
GCD	Gallons per capita
GCM	General Circulation Model
GSOD	Global Summary of the Day
HQ	Headquarters
HVAC	Heating, Ventilation and Air Conditioning
HYMOD	Hydrologic Model
KBDI	Keetch-Byram Drought Index
MGD	Million Gallons per Day
MGHPCC	Massachusetts Green High-Performance Computing Center
MNGWPD	Metropolitan North Georgia Water Planning District
NARCCAP	North American Regional Climate Change Assessment Program
NARR	North American Regional Reanalysis
NCAR	National Center for Atmospheric Research
NOAA	National Ocean and Atmospheric Agency
NSE	Nash-Sutcliffe Efficiency
NZP	Net Zero Planning
NZI	Net Zero Initiative

RCM	Regional Climate Model
RMSE	Root Mean Squared Error
SAC-SMA	Sacramento Soil Moisture Accounting
SCA	Snow Covered Area
SCE	Shuffled Complex Evolution
SERDP	Strategic Environmental Research and Development Program
SSTAs	Sea Surface temperature Anomalies
SWE	Snow Water Equivalent
TWDB	Texas Water Development Board
TMY	Typical Meteorological Year
USACE	United States Army Corps of Engineers
USAF	United States Air Force
USAFA	United States Air Force Academy
USGS	United States Geological Survey
VIC	Variable Infiltration Capacity
WARM	Wavelet Auto-Regressive Modeling
WBGT	Wet Bulb Globe Temperature

Objective

The Department of Defense (DoD) faces a wide array of real challenges and potential impacts of climate change. The DoD Climate Change Adaptation Roadmap (CCAR) described two broad areas of impacts: 1) effects on the operating environment, roles and missions and 2) effects on facilities, installations, training, testing, and other areas The effects may be moderated through successful adaptation planning or exacerbated by ill-formed plans. Thus there is an important and significant opportunity to inform DoD planning to increase the preparedness of the US military to climate change. The objective of this research effort was to develop a decision framework and methodology "fit to purpose" for doing so.

This report describes a decision framework and methodology specifically designed to guide decisions made under climate uncertainty, such as adaptation decisions. As described below, the framework also accommodates climate vulnerability and risk assessment as two special cases of decision making under climate uncertainty. The development of the decision framework and its illustration with a number of case studies was conducted for the Strategic Environmental Research and Development program (SERDP) project number RC-2204, "Decision-Scaling: A Decision Framework for DoD Climate Risk Assessment and Adaptation Planning." The specific objective for the research effort is to develop and apply the decision framework for the assessment of climate change risks to military installations. The methodology used, which is described fully in this document, is designed to illuminate the sensitivity of decisions to climate changes and other uncertainties without dependence on climate change projections. In this way the analysis and results remain unclouded by the many choices and trade-offs required in the processing of projections from general circulation models (GCMs, also known as global climate models) to make them useable in analysis at decision relevant spatial and temporal scales. Here, climate projections are used only in the final step of analysis to inform judgments corresponding to the "level of concern" that a decision maker might assign to a particular problematic climate change.

While the ultimate objective of this effort is the development and demonstration of a general decision framework for decision-making under climate uncertainty, there is immediate interest in understanding the vulnerabilities or risks that military installations face due to climate change. The framework presented here accommodates these kinds of assessments, and in fact, each of the case studies illustrates such assessments, rather than specific decisions per se. Here the term vulnerability is defined to mean a specific future condition (for example, a future climate change) that causes unacceptable performance for the system of interest, whether it be an infrastructure system (such as water supply) or activity (such as training). For example, a water supply can be said to be vulnerable to a reduction in mean precipitation of 10% or greater. Thus a vulnerability assessment attempts to identify the (climate) conditions that cause unacceptable performance. A climate risk assessment, in our usage, attempts to identify the climate risks of a system, where climate risks are based on assigning probabilities to the problematic climate conditions, or vulnerabilities, identified in the vulnerability assessment. The estimation of probabilities for specific climate changes is discussed further below. A vulnerability assessment can be considered a special case of the decision framework by using the vulnerability as a decision point: to take action (for the cases of unacceptable performance, meaning vulnerable) or to not take action (for the cases of acceptable performance, meaning not vulnerable).

The premise underlying the framework is that current decision frameworks for climate change decision-making are ill-suited for the nature of climate information currently produced. This is because existing decision frameworks depend on projections of future climate. Due to the immensity of choices related to the processing of climate projections (e.g., downscaling), the analyst engages in a quixotic search for the "best" processing approach, realizing the final results of the analysis will be largely dependent on the choices made at this initial stage. Yet the analyst has not have the context to know the implications and tradeoffs of different processing choices in terms of the climate factors that are most relevant, namely, those that cause vulnerabilities or that influence decisions.

The key innovation in the framework presented here is the removal from the analysis of the dependency on climate projections and other *a priori* climate change assumptions. Instead, the sensitivity of an infrastructure system or activity to climate changes is assessed directly, using systematic sampling of the response of the system to parametrically varied climate conditions. The sampling algorithm utilizes weather generation algorithms to insure spatial and temporal relationships are preserved, which insures the response is based on physically meaningful climate changes. The algorithmic approach allows sampling of a much greater range and variety of climate changes than a typical ensemble of climate change projections would offer.

The multidimensional sensitivity analysis, which we name the "climate stress test," reveals the climate conditions that are problematic and those that do not pose challenges. With this information climate information can be accessed to attempt to inform judgments as to the level of concern associated with the problematic conditions that were exposed. It should be noted, however, that while this framework presents a clear approach to marshaling information to make informed decisions under climate uncertainty, the selection of a best decision, given that information, is an underdeveloped topic and an area of strong research need.

The use of climate projections to estimate and assign probabilities to future climate changes remains an active area of research, to which contributions were made in this research effort. Nonetheless, the superposition of climate change projections on the vulnerabilities of infrastructure systems or activities reveals which projections and how many projections indicate problematic conditions would occur. This helps to frame the information provided by the projections. This information can also be used to inform the climate science investigation. For example, if only a single GCM or a small number indicated that the problematic conditions would occur, those models could be further investigated to discern whether they were credible in this location for the relevant climate processes. However, the methods for doing so remain to be developed.

The decision framework is designed to be generally applicable for the purposes of assessing climate risks and making adaptation decisions for the Department of Defense. Given the technical nature of the analysis, the framework is viewed as appropriate for sophisticated analysts residing within major command and headquarters units where strategic decisions and installation-level guidance is prepared. It also would be appropriate for implementation by consultants or contractors to investigate and assess climate risks at the installation and higher levels. At this point the use is better developed for vulnerability analysis and climate risk

assessment and for framing decisions. The process of developing an adaptation strategy requires further investigation although the framework is believed to be suitable for that.

While this report describes the general methodology and application to specific activities and infrastructure, the report does not describe the incorporation of these methods into a generally applicable framework for climate risk assessment of DoD installations. An accompanying Technical Guidance Manual does attempt to describe such a framework. This report is meant to demonstrate the utility of the general methodology and demonstrate that it can be applied effectively for relatively simply assessments as well as assessments that are very complex. The sector specific methods that we suggest for climate change analysis vary in their difficulty and complexity, from relatively simple to apply to many installations simultaneously (Fire Risk, Training), to those that are dependent on detailed understanding of the local infrastructure (Water Supply). It's worth noting that while screening level assessment of complex systems like water supply may be able to flag the need for further study, they cannot be effectively assessed using regional level analyses due to the large role of infrastructure and the importance of local context (infrastructure adequacy, water demand, etc.). To employ these methods appropriately as part of a comprehensive climate vulnerability assessment for DoD requires an overarching framework, the attributes of which we suggest here.

A comprehensive framework for vulnerability assessment of DoD installations that employs the Decision Scaling methodology would be based on a hierarchical approach, with screening analysis leading to the identification of installations and sectors that require further analysis. The more detailed and complex analysis would be employed only when deemed necessary according to the screening analysis. This framework is based on a similar concept we have developed for the World Bank (International Bank for Reconstruction and Development) and which they are currently employing to satisfy their new internal requirement. The results of such analysis would be useful for DoD planners to consider the level of investments that might be needed to adapt to climate change, the kind and location of such investments, and considerations regarding the long-term viability of installations.

This development of a screening process for use in the vulnerability assessment and development of the overall assessment framework were outside the scope of this study. In order to development a comprehensive vulnerability assessment framework, clarity is required on several issues, including: who would employ the framework, what specific decisions would the framework inform, and the ultimate objectives of the analysis. Based on our very positive experience with the World Bank and the successful uptake there, as well as the successful demonstration of methodology described here, we're confident that such an approach employing these methodologies could be an effective and successful climate vulnerability assessment framework for DoD.

Technical Approach

Overview of Methods

The methodology developed in this research effort is designed to address the challenge of developing a "fit to purpose" decision framework for the use of climate change information in the assessment of climate change risks to military installations. The general methodology is termed "Decision-Scaling" and is positioned as a method to use climate information to improve decisions made under climate uncertainty. The term derives from the concept of downscaling, a process for increasing the resolution of climate projections of GCMs, which is often the presumed first step in conducting climate impact assessments. However, given the numerous uncertainties and considerable computational effort required for downscaling GCM projections, and the often overwhelming number of choices these entail, it is not uncommon that efforts focusing on downscaling fail to produce insight for decision makers that is relevant to their decisions. As an alternative, Decision-Scaling inverts the usual order of analysis, focusing on understanding how decisions are sensitive to changing climate and using that insight to tailor the climate information provided by GCMs. The approach is based on an implicit acceptance of the inherent uncertainty of future climate and the futility of attempting to reduce that future uncertainty. Instead, the goal is to characterize the uncertainty in terms of its implications for decisions and identify the best decisions in view of uncertainty.

The general methodology consists of three steps: 1) Decision Framing; 2) Climate Stress Test; and 3) Estimating Climate Informed Risks. The decision framing step is used to identify the mission objectives, and metrics for quantifying them, the uncertain factors that affect the decision, such as future climate, the models or functional relationships needed to represent the system being investigated and if adaptations are being considered, any choices among adaptation alternatives. The climate stress test is a pragmatically designed multi-dimensional sensitivity analysis that reveals the fundamental sensitivity of the sector to climate changes, and/or, other uncertain factors. In doing so it exposes the climate conditions that are problematic for the sector. The final step is to prepare climate information, such as downscaled climate projections, to assess the level of concern that one might assign to the problematic conditions. This can be accomplished using both informal approaches and formal probabilistic methods, and both are illustrated in this report.

The climate risk screening analysis has been conducted in four illustrative sectors: water supply, fire risk, training, and energy planning. Each of these areas is assessed at four military installations, which were selected to represent separate regions expected to be at risk of climate change impacts and also to span a range of mission types. The installations are Ft. Benning (Southeast US, US Army), Ft. Hood (South central US, US Army), USAF Academy (Mountain West, US Air Force) and Edwards AFB (Southwest US, US Air Force).

The Decision-Scaling methodology is expected to yield benefits in at least three ways. First, the process will provide a clear delineation of the climate risks that are problematic for a particular sector, and the climate changes by which a sector is not threatened. These results are independent of climate projections, and thus are not subject to the various choices and uncertainties associated with processing steps such as downscaling. They also do not require

updating with every new generation of climate change projections. Second, the approach allows the characterization of climate change projections in terms relative to decisions and the revealed vulnerabilities. The effects of alternative methods for processing of climate change projections, including downscaling approaches (e.g., statistical vs. dynamical) and methods for estimating probability distributions of changes in climate variables can be presented in terms of their implications regarding the response of the system or sector to climate changes. The information provided by the projections can inform judgments made relative to the level of concern associated with any revealed problematic climate conditions or vulnerabilities of a particular sector. Similarly, the information can be used to inform judgments made relative to adaptation. In this way, the Decision-Scaling approach does not reject the use of climate change information or projections, but rather is designed to use them in the most decision-relevant and helpful way. Third, the approach is designed to facilitate robust decision making approaches, including quantification of the robustness of alternative decisions and clear indication of the expected risk reduction through alternative adaptations. This final benefit is not demonstrated explicitly here although the results should provide a conceptual understanding of how this would be possible.

Decision Framing

A premise of the Decision Scaling approach is that attributes of decisions have a significant and possibly critical effect on the utility of information produced to improve a given decision. In the context of climate change, this implies that the value of climate information and the best means of providing that information (in terms of both its attributes as well as the effort and expense to provide it) is best discovered by investigating vulnerabilities and decisions, rather than solely investigating the various ways of producing climate information. Therefore, the first step of the analysis is to frame decisions in terms of specific decision attributes and their context relative to climate change.

Following traditional approaches to decision analysis, a decision can be framed in terms of four categories:

- Choices (e.g., to adapt or not; to relocate a mission)
- Uncertainties (e.g., future climate; future population)
- Consequences (e.g., mission readiness; energy costs)
- Connections (e.g., work/rest tables; Energy Plus model)

The articulation of **choices** should include not only the specific options but also characteristics of the decisions, such as the decision hierarchy (what decision at what level) and the temporal nature of the decision (one shot, reversible, sequential, etc.). Uncertainties should include not only climate changes but also other relevant external factors, which will vary based on the specific decision. Consequences should be quantifiable metrics of performance that are meaningful to the decision maker. Ideally they would represent the measures currently used to assess the performance of a system or activity. Finally, connections are the way in which decisions yield consequences, and the way by which uncertainties affect them. The connections between climate and consequences often exist in functional relationships between weather or

climate and existing activities. For example, the IMPACT model estimates the allowable training activities of military personnel and equipment based on climate assumptions using average climate conditions at a location. The Energy Plus model uses a Typical Meteorological Year (TMY). Fire risk is estimated based on the relationship with the KBDI equation. In other cases, such as for water supply, new models or model combinations that relate climate to the reliability of water serving a particular installation may be required.

The framing serves to organize what can often seem a nebulous discussion of information and desires into categories that fit directly into the analysis framework. To whit, the decision maker faces choices that are to be evaluated in terms of their consequences that result from different realizations of the uncertainties. The consequences of choices are estimated based on our understanding of the connections between them, often represented by models or functions.

In this research project, analysis focused on assessment of current vulnerabilities and risk, and little attention was given to evaluating adaptation options, i.e., choices. This was a result of time and budget limitations rather than methodological difficulties or lack of interest. However, a review of representative decisions for the sectors analyzed was conducted. Specifically, the context for decisions related to climate change risks and adaptation was reviewed for each of the four focus areas: water supply, fire risk, training, and energy planning sectors. The specific facets of interest were 1) decision hierarchy (what decisions are made at what level), 2) characteristics of decisions (reversible, sequencing possible, etc.), 3) unique aspects of decisions within DoD, 4) current use of climate information, 5) nonclimate factors that are also relevant, and 6) framing regulations and directives.

The review of decisions within the four focus areas revealed broad commonalities and also some distinguishing features. It is worthwhile to report two overarching findings that affect all sectors. The first is that most decisions are strongly influenced by official guidance in the form of regulations and directives. The second finding is that there is no simple way to distinguish decision type by the level of the hierarchy at which the decision is made. In other words, decisions with long-term implications are made at the installation level as well as the command and headquarters levels. Likewise, decisions with operational implications occur at all levels.

Thus, planning for adaptation through influencing decisions is likely to require choices about where guidance can be best implemented. In the language of complexity science theory, points where influence is best exerted within complex systems are called “intervention points.” Given the scale of the challenge within DoD, the most effective intervention points for climate adaptation decision making are likely to be at the headquarters level, where tools can be provided and implemented quickly and where decisions have broad reach, and through directives that provide clear guidance for decision makers throughout the hierarchy. In particular, given the long term and uncertain nature of the climate information that can be provided, strategic planning decisions in terms of mission location and relocation, installation investment and future budget outlays may be the most beneficial decision applications for the tools developed in this research effort.

Our review of the current use of climate information in the representative focus areas has found the consistent use of historical information related to long term weather averages. These include

precipitation and temperature, as expected, as well as other variables such as relative humidity and wind. The values of these variables directly affect planning in the water sector and energy sector and also have implications for training, fire risk management and endangered species. In some cases, the updating of the historical dataset used may serve as a way to incorporate observed climate changes. For example, energy planning uses the "Typical Meteorological Year" (TMY) in the EnergyPlus tool. By using the most recent 30 years for the calculation of the TMY, the analysis will utilize the climate changes that have occurred during that period. However, since energy plan decisions often have long time horizons, the TMY might be quite different than that experienced in even the recent observed record.

In general, the analysis of decisions conducted in this study makes clear that there are entry points for climate information in many tools used to support planning decisions. These provide the opportunity to use the tools to conduct climate risk screening analyses. It is common for climate change analysis efforts to provide estimated mean projections of impacts based on GCM projections. In this analysis we instead adopt a risk-based approach, which provides valuable insights by allowing us to incorporate climate uncertainty into the context of impacts and decisions and to compare risks between sectors, missions and installations. The direct comparative analysis made possible by this approach will facilitate prioritization of adaptation activities and evaluation of risks to larger topics than a single impact sector, such as risks to entire installations or missions.

Climate Stress Test

The climate stress test is the term given to the multidimensional sensitivity analysis that is used to reveal the effects of possible climate changes, and other changes if desired, on the activity or system of interest. The general approach is to parametrically vary climate variables in a representation of the system or activity and infer from the results the response of the system to a wide range of climate changes. The representation of the system can range from simple empirical relationship to sophisticated models and sequences of models. The only requirement is that the representation includes some climate or weather inputs. For example, in this study the climate stress test approach was applied using a simple empirical representation of drought and fire risk based on KBDI, a sophisticated planning model, Energy Plus, and in the case of water resources assessment, a series of hydrologic models and water system models, some of which were created for the purposes of the study. The climate stress test approach is quite general. In principle, any model that could be used for assessing climate change impacts via climate projections can be used for a climate stress test, and likely more. And while the general approach can include non-climatic factors, for clarity this discussion focuses only on climate changes.

The climate stress test represents advancement over traditional sensitivity analysis. In the past single variable sensitivity analysis has been criticized because varying a single factor individually will fail to reveal sensitivities that are caused by the correlated behavior of multiple variables. For example, separately varying temperature and precipitation would not reveal problems that occur when both change together. However, varying multiple variables simultaneously requires preserving the physical relationships between these variables, if there are not independent, in order for the results to be physically meaningful. In the case of weather and climate variables, the particular challenge is maintaining spatial and temporal relationships in

fields like precipitation, temperature, wind, etc. However, the answer to this challenge resides in stochastic weather generators, which are statistical models that are designed to produce stochastically generated weather time series and have been used in the past in crop modeling and hydrologic modeling to create alternative historical time series, thus investigating the effects of possible alternative realizations of weather and climate variability. These models can serve as the basis of climate stress testing.

The attributes required for a multi-purpose climate stress testing algorithm include:

1) Physical fidelity – the algorithm must preserve known physical relationships between climate variables.
2) Spatial and temporal cogency – the algorithm must produce results that have a physically meaningful spatial and temporal scale (e.g., average annual temperature for a 30 year period over the spatial area of an installation). This allows the results to be linked to climate information, such as climate projections, which are always positioned in time and space.
3) Modifiable – the climate conditions must be able to be changed in a controlled and predictable way.
4) Representative variability – the representation of internal or "natural" variability, the unpredictable chaotic nature of weather time series, should be accurate to the degree possible. This is especially important because internal variability is typically dominant at the temporal and spatial scales of adaptation decision making and risk assessment. For example, at the spatial scale of a military installation and over a 30 year planning period, natural variability is likely to have a larger explanatory role in the conditions experienced than any trends in climate change.

For this study a climate stress testing algorithm was designed with these desired qualities. It is fully described in Steinschneider and Brown (2013). As illustrated in that paper, the climate stress testing algorithm can create a wider range of climate changes than that which could be derived from a typical downscaled, multi-model ensemble of projections. More important in some cases, the algorithm can more efficiently (in terms of the number of time series needed) sample a wide range of climate changes due to its systematic approach. This is important when the model or models used to represent a particular system is expensive in terms of computation time (e.g., the model representing the California water supply system). Not all applications require such a sophisticated approach. Water supply systems require careful simulation because they are expected to provide water at very high reliability and will only show sensitivity during critical periods, or rare events consisting of very dry conditions. In addition, they typically collect water from wide spatial areas, such as river basins, and the transport and storage of water defies simple linear representations. As a result, the detailed representation of temporal and spatial variability is required to accurately assess these systems. Other systems can be assessed using mean conditions at a point location and do not require the full features of a climate stress testing algorithm. Table 1 provides a summary of the stress testing approaches used in this study.

Table 1. Climate Stress Testing approach used in this analysis by sector.

Sector	Model	Climate Stress Test
Water Resources	Various – hydrology and water resources system models	Full climate stress tester (Steinschneider and Brown, 2013)
Energy Planning	Energy Plus	Simple alteration of Typical Meteorological Year (TMY)
Fire Risk	KBDI empirical relationship	Altered weather inputs in physically consistent way
Training	Work-Rest Tables	Altered weather inputs in physically consistent way

The stress test provides the analyst and decision-maker with a response function that relates a change in decision-relevant metrics measuring installation performance to changes in the climate and socioeconomic system, enabling the analyst to parse the space of future conditions into regions of 'acceptable' and 'unacceptable' performance. This functional relationship is extremely powerful in the decision-making process. For instance, it may indicate that the system is relatively insensitive to changes in climate or other stressors and further analysis is unnecessary. Alternatively, the stress test may reveal that the installation is extremely sensitive to even a modest change in one component of the climate system or small amounts of population growth, suggesting that proactive measures to improve the water supply system should be taken now.

Figure 1 shows an illustration of the results for a typical climate stress test. It shows a map of changes in climate (both precipitation and temperature) and the resulting impact. In this case, the area in red indicates that the impacts have exceeded an impact level (or a threshold) beyond which adaptation would be required. Thus, the climate changes represented by the red area indicate the climate changes that would cause adaptation to be necessary. The way of determining threshold levels is not necessarily dependent on any particular specified threshold; thresholds are completely malleable and can be specified by the individual analyst for the question of interest.

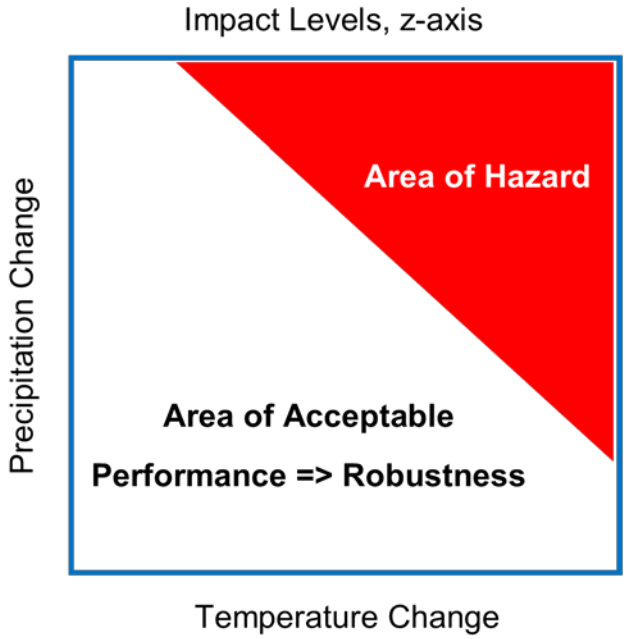

Figure 1 Illustration of Results for Climate Stress Test.

The climate stress test performed in this research provides an indication of the sensitivity of a sector or mission to climate change. A large red area indicates the system is very sensitive, whereas large areas of blue would indicate low sensitivity. Comparison of these areas can provide a first cut analysis of which activities, missions, etc. are more or less sensitive to climate change.

In the case of assessing vulnerabilities of a water system, a series of models is developed that can be used to identify the vulnerabilities of all components of the water resources system that serve the water demands of the installation. These models typically include the following three steps: 1) climate/weather generation, 2) hydrologic modeling, 3) water resources system modeling (Figure 2).

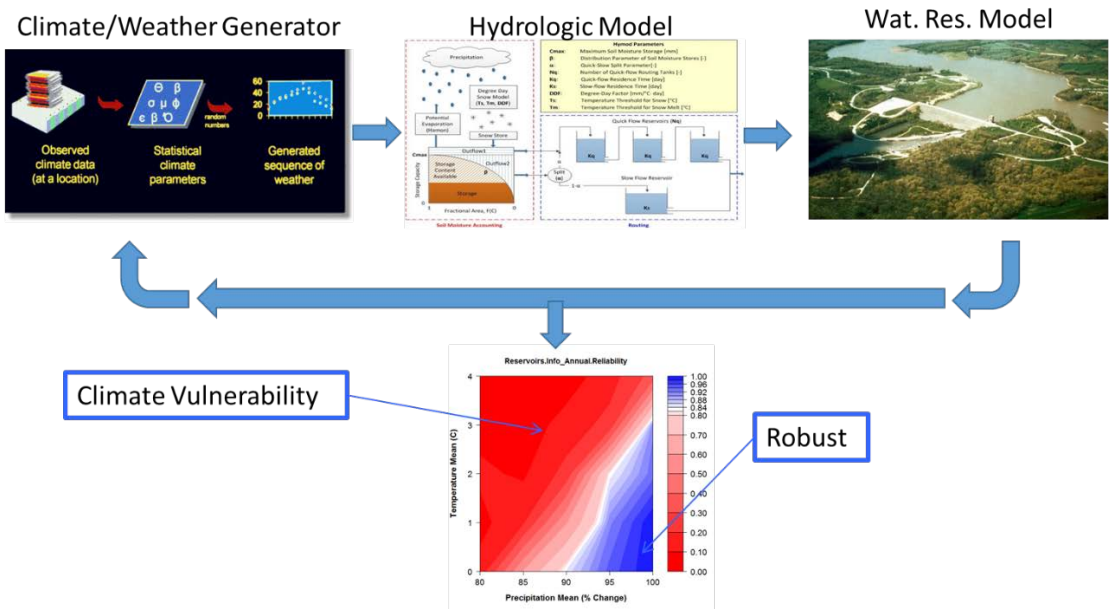

Figure 2 Three sequential elements of the vulnerability assessment modeling environment

Stochastic weather generators can create new sequences of climate that simultaneously exhibit different long-term mean conditions and alternative expressions of natural climate variability. A stochastic daily weather generator has been developed for this project to produce the climate time series over which to conduct the vulnerability analysis. The weather generator produces new sequences of weather variables that exhibit a wide range of characteristics, enabling detailed climate sensitivity analyses. The scenarios created by the weather generator are independent of any climate projections, allowing for a wide range of possible future climates to be generated. Furthermore, climate scenarios exhibiting the same mean climate changes can be stochastically generated many times to explore the effects of internal climate variability. Generated weather sequences are passed through a series of hydro-system models of the relevant river basins and infrastructure network to estimate how these changes in climate will translate into altered water availability for the customers and risks of flood and drought hazards etc.

The climate information from the weather generator is fed into a hydrologic model. A hydrologic model plays a role of translating changes in climate variables to hydrologic variables of interest (e.g., streamflow at inflow points to water infrastructure). The water resources model accepts hydrologic variables as inputs, as well as other driving variables (e.g., water demanded from domestic or agricultural users; environmental release requirements), simulates the infrastructure operation and conveyance plans that determine the flow of water through the engineered system and calculates the variables that are of interest for policy and management (e.g., reservoir storage, water delivered to users, water released to environment). Finally, the performance of proposed plans are evaluated for a range of climate conditions and the results are presented on a "climate response surface" that displays the climate changes that are problematic (Figure 2).

Estimation of Climate Informed Risks

The risk assessment framework based on the Decision-Scaling approach involves the estimation of likelihoods for the range of climate and socioeconomic changes explored in the stress test. To do that, evidence regarding possible future conditions can be considered, including projections from GCMs, information from historic observations, paleoclimate records, and population/water demand projections. Expert knowledge from climate scientists can be quite informative for the purpose of estimating the likelihood of changing climate and other conditions.

Figure 3 shows one example of how the climate risk screening resulting from the stress test could be used. In this figure, the result of the climate risk screening has been used to identify the number of climate projections indicating problematic/nonproblematic climate conditions. While these would not typically be interpreted as probabilities, they do provide an indication of risk. A reliable way to estimate probabilities given available climate projections would help the climate vulnerability screening analysis be more informative for decisions by allowing assessment on the probability of climate projections and consequent quantitative risk.

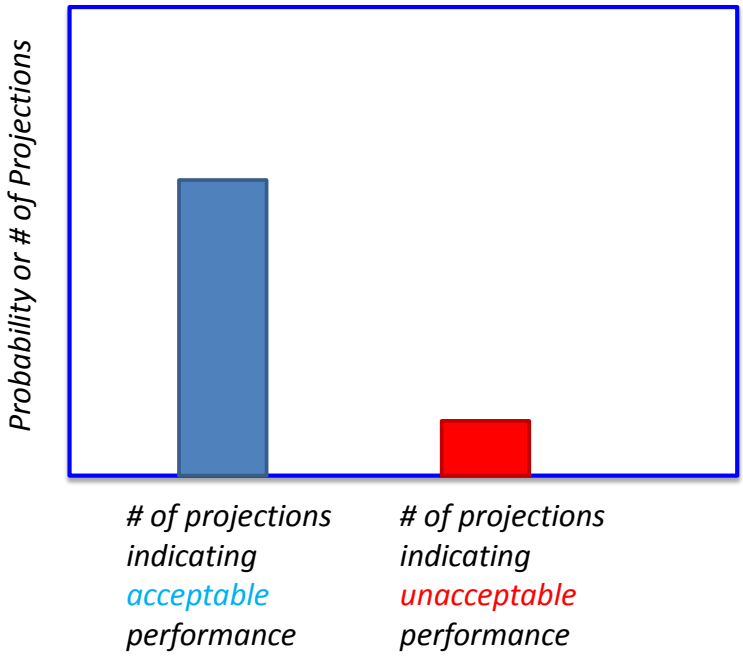

Figure 3 Climate projections in context based on climate risk screening analysis.

When the system is found to be sensitive to certain future scenarios, the stress test can be applied to all adaptation strategies as well. The results of this analysis reveal how well each adaptation strategy can preserve system performance over a wide range of futures. Specifically, this analysis determines which adaptations can preserve performance metrics above their thresholds across the range of future scenarios. The decision to accept a particular adaptation strategy then relies on an appraisal of the robustness of the various alternatives. For instance, the climate risk screening analysis can also be used to compare alternative plans or to evaluate the additional robustness

that a particular planned adaptation might provide. Figure 4 shows an illustration of how comparative analysis could be conducted using the results of the climate risk screening.

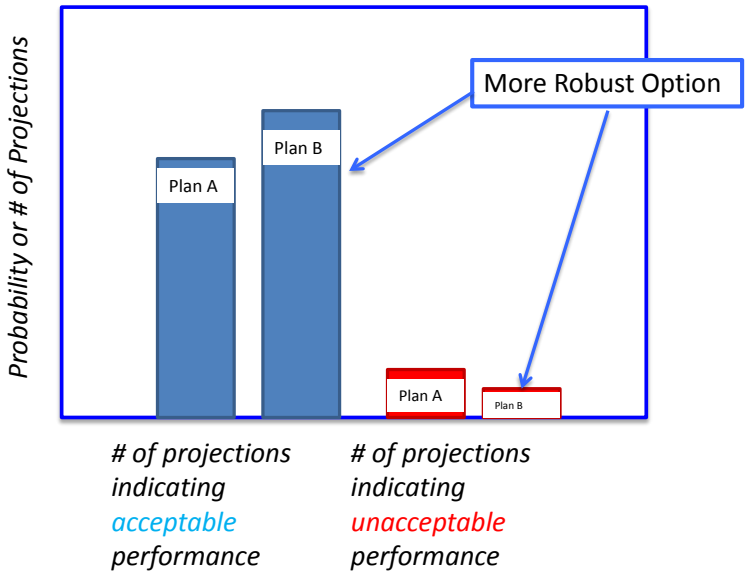

Figure 4 Comparing the robustness of alternative plans

The specific details of the process for each sector are described in the chapters that follow. Because the methodology differs for each of the focus areas, detailed analysis methods and results are described in the Results and Discussion section, which is organized by focus area. The results relate the decision framing for each sector and the climate risk assessment. Each climate risk assessment consists of a vulnerability assessment and assessment of future risks (based on climate change projections) and evaluation of system robustness.

Results and Discussion: Water Resources Installation-Level Assessment

Decision Framing

This section describes a decision framework for the Department of Defense (DoD) to use when responding to climate and other risks facing the water supply security of their training installations. A clean, reliable water supply is a mission critical resource for DoD installations. Even minor interruptions in the required quantity or quality of the water resources can disrupt the normal operations of an installation, and long-term or continuous disruptions in the water supply can threaten the viability of the installation for a particular mission.

Climate change poses a real threat to the water supply security of DoD installations. Regional changes to the climate regime across DoD locations can alter the expected water supply available to support installation operations by changing the historic conditions under which installations have been designed, managed, and stationed. Structured and effective decision processes for adapting installations to future water security challenges are critical for managing these risks and preventing them from interfering with necessary DoD operations.

The scale of analysis for water supply systems is defined by the system in question. For example, military installations located in Colorado Springs, CO, receive their water from Colorado Springs Utilities, which collects and treats water from sources that span much of the state. Much of their water is taken from the Colorado River Basin and is piped across the continental divide. As a result, a watershed level analysis such as Jenicek et al. (2011) that focused on the location of these military installations, which are all located in the Arkansas River Basin on the Atlantic side of the continental divide, would have almost no relevance to the water supply of these installations.

Expectations of climate changes are often summarized at region scales because this spatial scale is the scale at which climate projections have their greatest credibility. However, due to the modulating role of infrastructure, and the importance of other non-climate factors such as the water demand, a regional water supply analysis would have little meaning. However, a screening level analysis could be envisioned that accounted for local water supply and demand, combined with regional climate change estimations. Such an analysis would not yield conclusive results but would be useful for identifying specific locations that may be vulnerable and required further analysis. This study did not develop such a screening level analysis as the need for one did not surface until the study was already underway and the team was not funded to do so.

This section first discusses the decision processes and hierarchy for decision-making available to the DoD when adapting installations to water supply challenges due to climate change. The current and potential use of climate information is then discussed, followed by non-climate sources of information that could help inform the decision-making process. Finally, this section reviews the regulations and directives that frame DoD decisions for water supply adaptation.

DoD Decision Processes and Decision Hierarchy for Water Supply Adaptation

A three-tiered decision level hierarchy frames the decision processes available for installation-level adaptation to future water security challenges. The first tier of this hierarchy consists of decisions made and executed at the installations themselves. These include those actions that are

required to maintain the day-to-day operations of the installation. Examples of such actions include leak detection and repair for on-base infrastructure (e.g. water mains and pipes), the adoption of water reuse technologies, the instillation of water-efficient fixtures, and the imposition of conservation measures during drought conditions. Recommendations for these actions can be grouped into a set of best management practices (BMPs) and can be carried out by the civilian public works department or the commanding officers of the installation.

Beyond this simple set of actions, all other decisions for water resources adaptation will be made at higher levels in the decision hierarchy. The second tier of decisions in this hierarchy occurs at the command level. Command-level decisions regarding water supply will respond to medium-term (5-10 years) water issues that affect mission-oriented operations across multiple installations. A major type of decision made at this level of the hierarchy will include developing additional sources of water with infrastructure investments or the leasing/purchase of water from other entities (e.g. local utilities, other water rights holders) to meet growing installation water demands. Command-level decisions can also encompass directives requiring the adoption of certain water reuse or water efficient technologies across installations, rather than these technologies being adopted at the discretion of the commanders at the installation.

At the top of the hierarchy, adaptation decisions to water security issues are made at the headquarter (H.Q.) level. These highest-level decisions will consider water stress as it relates to operations across all DoD installations and their ability to meet broad mission goals. For instance, H.Q. will consider water stress as one important consideration among many when making decisions regarding Base Realignment and Closure (BRAC). If the water resources of a particular installation or set of installations becomes too stressed to support their current mission, H.Q. may decide to alter the mission of those installations, or in extreme circumstances, close them altogether.

Characteristics of DoD Decisions for Water Security Adaptation

The characteristics of the decisions made by the DoD for installation-level adaptation to water security risks vary greatly across the hierarchy described above. These characteristics include the frequency at which decisions are made, their reversibility, and whether actions can be phased in over time or must be carried through immediately. These characteristics are described below for each of the levels in the hierarchy.

Installation-level decision characteristics

Decisions made at the installation-level will occur with greater frequency in response to short-term water needs. For instance, water restrictions on the base may be imposed whenever there is a water shortage, which can occur and change over short (annual or monthly) timescales. The decisions to repair leaky infrastructure or adopt new water efficient technologies will not likely occur as frequently, but these actions may require annual or biannual decisions to be made by the public works department in the normal course of maintaining the water supply infrastructure of the installation.

Some installation-level decisions will be reversible. This is particularly true for operational decisions, such as the imposition of water use restrictions or other conservation measures in response to an immediate water shortage. However, not all decisions at the installation-level will

be easily reversed. Investments in on-base infrastructure or new water-efficient fixtures can only be reversed at a high cost to the installation.

Certain decisions made at the installation-level can also be phased in over time. For instance, a large repair effort to the infrastructure on an installation can be carried out in phases over time. The repair effort can be designed such that early phases of the repair can improve the water supply system without the additional improvements scheduled for the later phases of the job. This allows decision-makers to abandon those later stages of the effort if needed (due to a reduced budget, for instance) without having wasted the resources spent on the earlier phases of the repair. Other decisions made at the installation level will be carried through immediately. These decisions will likely be those that occur frequently and are highly reversible. An example of such an action would be the imposition of water use restrictions.

Command-level decision characteristics

Command-level decisions will tend to occur less frequently and in response to persistent water supply issues. If the operations at particular installations are continuously inhibited by water shortages and restrictions due to a limited supply, a command-level decision may be required to expand the supply of that installation through the development of new water resources. This can include investments in new infrastructure to acquire and treat raw water, but it can also include the purchase or lease of water from other entities. In either case, these decisions will likely occur at inter-annual timescales (5-10 years) in response to longer-term trends, such as population growth at an installation or diminished natural supplies due to the surrounding growth of civilian populations, climate variability, or climate change.

Many of the decisions made at the command level will be difficult to reverse. Any investments in hard infrastructure to develop new raw water resources cannot be reversed without partially or completely forgoing the capital used in the investment. Similarly, if command requires a set of installations to adopt new water reuse or efficient technologies, these investments cannot be reversed without capital loss. There are some command-level decisions that can be reversed, however. For instance, if water supplies at an installation are expanded through water leases or the outright purchase of water rights, these economic contracts can be terminated or sold if they are deemed unnecessary or undesirable in the future. The only capital that cannot be recovered will be that needed to connect the water infrastructure of the installation to the new water source.

While the long-term decisions made at the command level occur infrequently and are difficult to reverse, they can be phased in slowly over time. The expansion of a water supply can often involve the development or purchase of many different sources of new water resources (e.g. multiple raw water sources to develop, several water lease contracts with different entities, etc.). The decision to develop new water sources or enter into contracts with other water users can be implemented over multiple years, and during this time the number of water sources or contracts to develop can be adapted if water supply conditions change at the installation during this time.

H.Q.-level decision characteristics

Decisions made at the highest level of the hierarchy, the H.Q. level, will be the most infrequent. These high-level decisions will dictate the broad, long-term direction and mission of all DoD installations. The nature of these choices requires that they be infrequent; for an installation to perform effectively, its mission cannot be altered by H.Q. very often.

Because the decisions made at H.Q. occur very infrequently and dictate the broad direction of many DoD installations, they are very difficult to reverse. For instance, BRAC decisions in response to water stress would be extremely difficult to undo once they have been implemented. Due to the irreversibility of H.Q. decisions, they will respond only to the largest and most pressing water supply risks that seriously threaten the ability of installations to effectively operate for their respective missions.

The long-term, infrequent, and irreversible nature of H.Q. level decisions requires that they be phased in over time. BRAC-related decisions across a range of installations cannot be carried out quickly and simultaneously across all sites. Significant time is needed to redistribute troops, adjust the facilities at various sites to support mission realignment, and close installations that can no longer operate effectively. As such, these types of decisions must be phased in over time, allowing these decisions to be adjusted over the course of their implementation if water supply conditions change during the implementation of BRAC decisions.

Unique Aspects of DoD Water Supply Adaptation Decisions

Decisions regarding the water supply of DoD installations are distinct from other resource allocation and management decisions because they must account for the unique role of water as a public good that is shared amongst many users. DoD installations are often just one of many stakeholders within a local water supply district, and the installations themselves are commonly supplied by a local utility that serves the surrounding civilian community as well. Also, the water sources used to meet installation water demands often reside within a larger water resource system at the river basin scale, and sometimes operations at other facilities within that river basin can significantly impact the local availability of water for DoD installations or the utilities that serves them. Therefore, any thorough assessment of water supply risk at training installations used to inform decision-making must explore risks to all involved entities (e.g. the serving utility, stakeholder groups using the same water source, etc.) and across all appropriate spatial scales (i.e. the local watershed, larger river basin, full aquifer system). Also, the adaptation decisions themselves must account for the role of most training installations as customers to a serving water utility. This position may remove many supply-side adaptations available to the installation, as these decisions are made by the utility. Instead, adaptations available to the training installation could potentially be limited to demand management strategies.

The decision processes for water supply adaptation at DoD installations is complicated even further by the different water laws that vary locally across the United States and internationally. These laws govern how water is allocated between stakeholders, and depending on where DoD installations are located, the law can significantly affect the types of decisions available to DoD decision-makers. For instance, water law in the Western United States is governed by the Appropriation Doctrine, which states that the first person or persons to use a particular water source for a beneficial use has a right to continue that use, while subsequent users can use the remaining water available from that source provided they do not interfere with the rights of the previous users. Under this law, DoD installations may need to purchase or lease the water rights from priority holders if the installation requires additional water. In many parts of the Eastern United States, however, water use is governed by riparian water rights, which guarantee reasonable water allocations to those who own land adjacent to the water source. DoD

installations in these areas may need to engage large stakeholder groups of riparian water users to negotiate water allocations for the installation.

Current Use of Climate Information

There is an opportunity to inform the decision-processes described above with climate information available from various sources. State-of-the-art projections of future climate, as well as period-of-record observations, seasonal climate forecasts, and paleo-data records, can help inform water supply adaptation decisions. However, the utility of these data will differ across the decision hierarchy due to the nature of the decision-processes that occur at each level in the command chain.

At the installation-level, the utility of climate information will most likely be limited to historic observations of climate and streamflow data that can be used in engineering applications for the design or repair of on-base infrastructure. If expensive infrastructure is required to capture, store, and distribute water specifically for the installation, then there may be a use for projections of future climate or other more complex climate data sources in order to understand how that infrastructure may need to adapt to future conditions. Installation-level decisions could also potentially benefit from seasonal climate forecasts, which could provide some additional information on the likelihood of potential droughts. This could enable the installation to update its operations by making decisions to hedge against drought conditions when they are likely (e.g. postpone water intensive investments in the installation's grounds).

The potential utility of climate data becomes more varied when considering command-level decisions. These decisions, which concern the security of medium- and long-term water supply sources, can benefit from understanding how future climate conditions may affect the availability of supply for a particular region. Projections of future climate, such as those produced by state-of-the-art global circulation models (GCMs), provide plausible changes in regional precipitation and temperature that may occur under climate change. When used in conjunction with hydrologic models that relate climate conditions to river flows or groundwater levels, plausible changes can be extended to the supply of water available to DoD installations. Given the low to moderate skill of GCMs at reproducing historic climate conditions at regional scales, their output should not be considered as predictions of future conditions, but rather as plausible projections. However, these types of data can still be useful in discerning the likelihood of potential future changes, and these likelihoods can help inform decisions at the command-level. For instance, when deciding whether to manage water stress at an installation by expanding the installation's water supply with the purchase water rights or reducing the demands of the installation through investment in water reuse and water efficient technologies, it is important to understand the long-term threats that climate change poses to the supply-side option. If projections suggest that the water rights being considered are to a source that could likely dry up under increased temperatures, command may decide to avoid expanding the supply of the installation with that source and rather opt for a demand reduction strategy.

Climate information can also be useful for decisions made at the H.Q. level. Given their infrequent and irreversible nature, H.Q. decisions, like those concerning BRAC, could benefit greatly from climate information regarding the long-term water supply viability of different installation locations. GCMs can provide one source for this type of information, providing 50-100 year projections of future climate for regions across the country and the world. However,

other useful sources of information also exist. Where available, paleo-data, such as tree ring or sediment observations, can provide hundreds or thousands of years of climate data. These records can inform H.Q. about the potential threats of extreme droughts that have occurred in the distant past. Climate risks derived from the paleo-record would not drive H.Q. level decisions in isolation. However, these risks, when considered in conjunction with ominous GCM projections or recent declines in observed water supplies, could prove useful for H.Q. decisions like BRAC. By considering various sources of climate information, H.Q. can account for the likely water supply threats across all DoD sites when making broad decisions about the long-term direction and mission of DoD installations.

Non-Climate Factors

In the context of water security at DoD installations, climate variability and change govern the availability of water supply, but water demands are another critical issue that must be considered as well. These demands (and the ability to meet them) are dictated by a range of factors, including population growth, water-use efficiency, the construct of water rights surrounding water allocations, the relative price of water, and environmental requirements for ecosystem preservation. Increasing demands for water at DoD installations and the surrounding civilian populations, as well as new regulations at the state and federal level for environmental protection, will play a vital role in determining whether or not a given installation is at risk of losing its reliable supply of water.

Similar to projections of future climate, information is also available to describe the future population and water use of regions around the country. Population and water demand data are gathered regularly by various U.S. federal agencies at the state and county level. These data can inform DoD decision-makers about the recent changes in water use for the civilian communities surrounding DoD installations. Different metropolitan areas also provide long-term population and water demand projections that extend several decades into the future. Similar to the climate data, these historic data and future projections of water demands can inform longer-term DoD decisions about the threats of overuse posed to current water supplies, and may help indicate whether there is a need to expand current supply sources or hedge against future shortages by reducing on-base demand.

Framing Regulations or Directives

All decisions for installation adaptation to water resource security risks are framed by a series of recent laws and executive orders that describe federal and DoD policy related to installation water management. The Energy Independence and Security Act (EISA) of 2007 was the most recent law passed by Congress describing water efficiency requirements at DoD installations. Section 432 of this law requires that all Federal agencies must comply with an energy and water management benchmarking initiative. This initiative includes efforts to identify and evaluate the energy and water use of an agency's "covered facilities," as well as the implementation of certain energy and water efficiency measures. EISA 2007 was coupled with Executive Order (E.O.) 13423 – *Strengthening Federal Environmental, Energy, and Transportation Management*. Section 1c of this E.O. contains Federal targets for water use reductions and efficiency, including a goal to reduce water consumption by 2 percent annually through the end of fiscal year (FY) 2015 from baseline levels defined by water use in FY 2007. This equals a total reduction of 16% by the end of FY 2015. The Department of Energy (DOE) developed the Federal Energy Management Program (FEMP) to provide supplemental guidance to help Federal agencies

comply with E.O. 13423. This guidance, titled *Establishing Baseline and Meeting Water Conservation Goals of Executive Order 13423*, establishes and describes three key elements of compliance, including 1) water use intensity baseline development, 2) reduction of water use intensity, and 3) reporting procedures.

In response to the regulations and directives described above, the Army has set conservation goals for its installations to meet and exceed the requirements of Federal policy. The Army Net Zero Initiative (NZI) proposes a goal to manage installations on a net zero basis for energy, water, and waste. The Net Zero water initiative limits the consumption of freshwater resources by Army installations and promotes the return of those resources back to their original watershed to prevent surface water and groundwater depletion. The purpose of Net Zero Water Installations is to maintain the balance of water use and water availability to ensure a sustainable water supply into the future. These types of DoD initiatives, backed by aggressive Federal policy for water conservation, frame all additional measures taken to adapt DoD installations to water supply security risks due to climate change.

Analysis Methods

A multi-step methodology was used to identify the risks facing water supply security at DoD installations. The approach enables the identification and comparison of robust adaptation strategies for DoD installations to water supply risk in situations where future climate and socioeconomic conditions are highly uncertain. The results of the approach are designed to support the specific decision-processes available to the DoD and fit within its hierarchy of decision-making. These results are installation-specific and are therefore useful for informing adaptation decisions targeted for a particular location. However, the methodology is flexible enough to be applied in a wide array of contexts for installations across the country and those based internationally.

In simple terms, the framework can be described as first identifying which climate (or other) conditions lead to unacceptable water supply problems for DoD installations (i.e. a vulnerability assessment), and afterwards examining different sources of climate and other evidence (e.g. climate projections, the historic climate record, paleo-data, population projections, etc.) to determine whether those problematic futures are likely to occur. By separating the vulnerability assessment from the analysis of possible future conditions, the approach ensures that the water supply security of DoD installations is stressed over a sufficiently wide range of possible futures to identify important vulnerabilities. The framework is designed to identify the future conditions under which one water supply adaptation strategy would be preferred over others, illustrating the robustness of proposed alternatives. When coupled with information regarding the likelihood of different future conditions, this provides DoD decision-makers at various levels of the decision hierarchy with useful information regarding the robustness of adaptation strategies under different future states and how likely those different states are to occur. The framework presented here consists of four primary steps: 1) framing the problem, 2) conducting an installation-level vulnerability assessment to identify the future states that lead to unacceptable water supply challenges, 3) analyzing the likelihood of different types of problematic future conditions, and 4) appraising the robustness of alternatives to inform decision-making. These steps are described in more detail below.

Step 1.Framing the problem: Determine the appropriate context and scale of the analysis, identify key decision criteria and thresholds, and delimit adaptation options

A key principle of the proposed framework is tailoring the analysis to address the primary concerns of DoD decision-makers. In order to provide useful information to inform installation-level adaptations for water supply, it is critical to understand the water supply objectives of the installation, identify quantitative metrics that can measure those objectives, determine thresholds for those objectives that would indicate unacceptable water supply performance, determine the context and scale of an installation's water supply system, and identify the adaptation options available to the installation. All of these components are necessary to adequately frame the future water supply risks facing an installation and the possible actions that can be taken to manage those risks.

Communication with personnel on the installation is critical to help identify the water supply objectives that are important for operations. These personnel can also help to choose quantitative performance indicators or metrics that accurately characterize those objectives. It is important to identify these objectives early in the analysis to ensure that all additional work will be tailored to exploring the potential threats to these specific installation goals. While common objectives, such as water supply reliability, will always be included in the analysis, other objectives may become apparent through conversations with personnel at the installation that would otherwise have not been included in the results of the risk assessment.

Thresholds should also be set for all performance metrics in order to indicate unacceptable water supply performance. By taking the time to determine these thresholds, DoD decision-makers and analysts will better understand the level of water supply stress required to hinder the installation's normal operations and interfere with its mission. This information is important to distinguish between future water supply conditions that are inconvenient to an installation and those that truly threaten its operations. These thresholds will also be used in later parts of the analysis to determine the robustness of the current water supply system for the installation, as well as the robustness of different adaptation strategies under consideration. This component of the analysis can be quite difficult, as it requires analysts and decision-makers to communicate about the actual impacts of concern for the installation and the level of impact that actually interferes with the installation's mission. However, this step can also be extremely useful. The development of meaningful performance indicators and impact thresholds forces decision-makers to develop a strong understanding of the installation's water supply system and will help facilitate adaptation decision-making in the later stages of the process.

Early in the analysis it is also important to determine the appropriate context and scale for a risk assessment of the water supply system serving the installation. Here, basic information is gathered about the water supply system of the installation, such as the type of water source used (e.g. groundwater or surface water) and whether the installation is served by a utility. Information is also collected on external factors that can affect the water supply security of the installation. These include such factors as the source, amount, and growth of water demands of the surrounding civilian population, upstream water management strategies that can influence the local supply serving the installation, and federal and state environmental regulations that could limit the water available to meet demands. These type of data will determine the context of the water supply system and will dictate the tools that are needed to assess the risks facing the

system. This information will also indicate the appropriate scale for assessing all of the risks facing the installation's water supply. Execution of this step requires communication with DoD personnel about the installation's current water supply system design and operating policies, as well as any system weaknesses already identified from past experience. Decision-makers and analysts will need to use their judgment to determine which factors should be included in the analysis, but this process will help all parties better understand the range of factors that could influence the water supply security of the installation. This understanding will help in the preparation of adaptation measures that can address these potential threats.

After determining the water supply objectives of the installation and their associated quantitative metrics, thresholds used to determine when an objective is not met, and the appropriate context and scale of the water supply system, the analysts and decision-makers should compile an inventory of available adaptation options. This inventory should include all possible adaptation measures available to the installation for adapting its current water supply system to future threats. The merits of different measures will be determined later in the analysis to avoid any bias for one measure over another. By developing the adaptation option set early in the analysis, analysts can tailor their models of the water supply system to these available options in order to test their benefits and costs later in the analysis. This will ensure that the models created to inform the decision-making process are actually capable of doing so without substantial and expensive work required from the modeling team.

Step 2. Stress test: Identify installation vulnerabilities to climate and other relevant stressors

The next step in the process is to conduct a vulnerability assessment, or stress test, on the current system. The stress test is used to map changes in various climate conditions (e.g. precipitation and temperature) and other plausible stressors (e.g. increased water demand, more stringent environmental requirements, etc.) to the impacts on water security at installation sites. The stress test provides the analyst and decision-maker with a response function that relates a change in decision-relevant metrics measuring installation performance to different changes in the climate and socioeconomic system, enabling the analyst to parse the space of future conditions into regions of 'acceptable' and 'unacceptable' performance. This functional relationship is extremely powerful in the decision-making process. For instance, it may indicate that the system is relatively insensitive to changes in climate or other stressors and further analysis is unnecessary. Alternatively, the stress test may reveal that the installation is extremely sensitive to even a modest change in one component of the climate system or small amounts of population growth, suggesting that proactive measures to improve the water supply system should be taken now. If the results of the stress test indicate that the current system is sensitive to certain types of future conditions, then the stress test can be conducted for the installation updated with the various adaptation alternatives inventoried in step 1 in order to assess the improvements that each of the adaptations provides. That is, the stress test can also be used to identify the conditions under which one adaptation strategy would be preferred over others, illustrating the robustness of proposed alternatives.

In order to conduct the vulnerability assessment, a series of models is developed that can be used to identify the vulnerabilities of all components of the water resources system that serve the water demands of the installation. These models typically include the following three steps:

1. *A stochastic climate model that can generate alternative scenarios of climate variables.*

This model produces time series of precipitation, temperature, and other climate variables of interest that effect the water supply of the installation. The model can be used to impose transient changes in the statistics of these climate variables in order to develop a wide range of potential climate change scenarios that may occur in the future. The model can also be used to produce multiple climate time series that exhibit the same mean climate statistics, allowing the analyst to explore the effects of internal climate variability on installation water supply security. The stochastic climate model has three primary components, including 1) a wavelet decomposition coupled to an autoregressive model to simulate structured, low-frequency oscillations in large-scale climate drivers that drive local climate (El Nino – Southern Oscillation , sea surface temperature anomalies, seasonal wind anomalies, etc.), 2) a series of regressions that relate these large-scale climate drivers to seasonal/monthly climate variables over the watershed of interest, and 3) a quantile mapping procedure to enforce long-term distributional shifts in climate variables under climate change. These components allow the model to generate time series of climate variables that exhibit realistic characteristics at long-term (inter-annual) and mid-term (seasonal) timescales, and they also enable the creation of many climate change scenarios over which to stress the water supply system of an installation.

2. *Hydrologic models that can translate climate data into hydrologic data relevant to water supply systems*.
   The selection of an appropriate hydrologic model will depend on the particular water supply system serving the installation and the data available for model development. To develop and confirm the utility of the hydrologic models, each model is calibrated to a subset of historical data and then verified against another set of data that was not used during the calibration process. Inputs to these models often include time series of precipitation, temperature, and other climate variables (e.g., wind speed, relative humidity), all of which are provided by the stochastic climate model. The hydrologic models will output streamflow or groundwater levels at the location of interest selected for study.

3. *A water resources systems model that can simulate the operations of the water supply system.*
   This model simulates the operations of the water supply system serving the installation and tracks the ability of the system to meet water demands. This model is driven by the output of the hydrologic model, as well as time series of water demands for all users drawing from the water supply system. Other input data includes reservoir specs and operations (if applicable), environmental regulations, and other external factors influencing the system. Outputs generally are comprised of water deliveries to the installation and other water users, reservoir storages and releases, and streamflow at nodes throughout the model domain. The complexity of the systems model can vary significantly from a simple mass-balance model of a single reservoir to a basin-wide evaluation including multiple reservoirs, key water rights, and inter-basin transfers. Each model is calibrated to a historical data set that is often comprised of reservoir storages and releases, but may also include streamflow at gaged locations or groundwater levels. The model is verified against a time period in which the model was not calibrated to ensure its ability to accurately replicate system response. The output of the systems model will enable the quantification of key performance metrics that relate to the objectives of the installation, such as the reliability, vulnerability, and resilience of the installation's water supply. When coupled with the thresholds determined in step 1,

this output will enable the space of future conditions to be parsed into regions of acceptable and unacceptable performance.

Figure 5 provides an overview of how these models are used to conduct the vulnerability assessment. The stochastic climate model is used to generate a wide array of climate time series that drive the vulnerability assessment. The types of climate change explored can include transient changes in mean temperature, mean precipitation, precipitation variability, and serial correlation in annual precipitation, among others. In addition to these climate changes, changes in other stressors can also be defined, such as increased water demands and greater environmental water requirements. The series of models is run for every combination of these future climate and socioeconomic scenarios. Upon completion, an N-dimensional impact space (N being the number of stressors) is defined for each performance metric of interest. Given a performance threshold, both failing and acceptable conditions within each impact space can be established.

The range of future conditions under which to explore system performance is selected to ensure that they meet two conditions: 1) they extend beyond the range of projections provided by GCMs or water demand models, and 2) they extend far enough to cause the water supply system of the installation to fail. By requiring the stress test to encompass this wide range of future conditions, the analysis will better characterize the potential vulnerabilities of the system. This contrasts other methods that restrict the range of scenarios to those provided by climate or demand projections. These methods risk missing important vulnerabilities of the system if the projections are too narrow, and given the moderate to low skill of the models used to produce the projections, it is useful to identify vulnerabilities under "surprise" scenarios not encompassed by the projections. If those surprise scenarios are deemed implausible, they can be discounted later in the analysis to ensure that they do not unjustifiably influence the decision process. This is described in the next section.

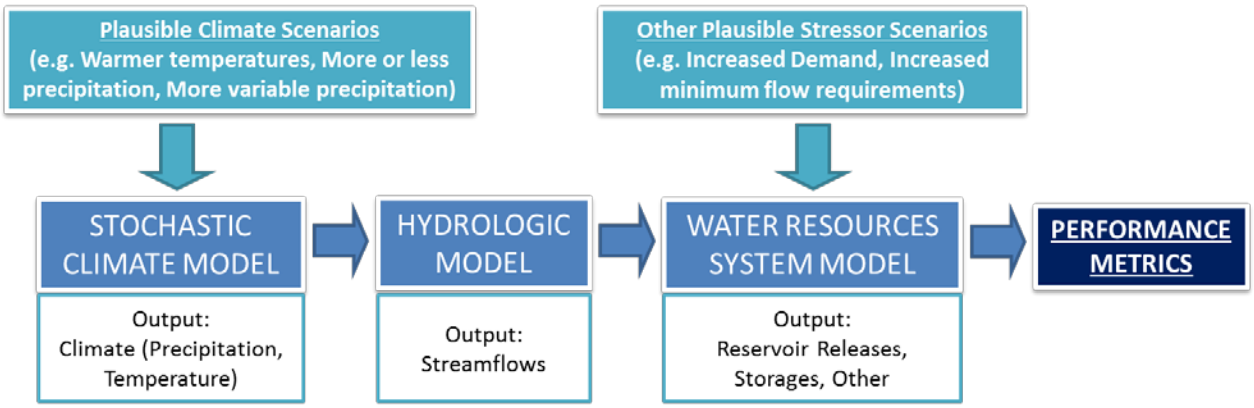

Figure 5 The Vulnerability Assessment Flow Chart.

Step 3. Estimate the likelihood of changing climate and other relevant stressors

The third step in the risk assessment framework involves the estimation of likelihoods for the range of climate and socioeconomic changes explored in the stress test. Here, all available evidence regarding possible future conditions is considered, including projections from GCMs,

information from historic observations, paleoclimate records, and population/water demand projections. Expert knowledge from climate scientists can be quite informative at this stage. All the evidence from each of these sources is synthesized to estimate the likelihood of possible future conditions.

The means by which available information is synthesized and presented in this part of the analysis should be tailored to improve the ability of decision-makers to interpret the data. This is particularly true for the climate information, as there is often a large amount of data available, whereas water demand projections are more rare and often do not include more than a single projection. For the climate data, certain decision-makers might prefer a formalized approach in which probabilities are developed from each climate information source (e.g. the historic record, GCM projections, paleodata) for the range of climate change space considered in the stress test. In this case, the analysis can draw on several methods available in the literature for developing probabilities of future climate states (Murphy et al. 2004, Stainforth et al. 2005, Tebaldi et al. 2005, Sexton et al. 2012). These probabilities will be subjective because there is no sample of future data against which they can be verified, but they do provide a formalized weighting of climate change space that can be used to inform the decision-making process. Alternatively, other decision-makers might not trust or completely understand formal probabilities of future climate, and therefore may prefer that climate information be presented more simply as ranges of possible change suggested by the different sources of climate information. For instance, the range of GCM projections may suggest a +/-20% change in mean precipitation by 2050, while the current trend in the historic record, if continued, might suggest that annual precipitation will fall 10% by that time. While not formalized into a statement of probabilities, this type of information still provides a means by which decision-makers can weigh the space of future climate. In either case, the likelihood information developed in this step can be used to help identify preferable decisions (discussed further in step 4).

As stated earlier, the likelihoods developed in this stage of the analysis can also reflect information embedded in the historic climate record (or paleo-record). As suggested by Stedinger and Griffis (2011), the uncertainty in the historic record remains the best starting place to understand how that risk might change in the future. In fact, for certain components of the climate system that have been argued to be beyond the scope of GCM projection information, the historic record may be the best available source of information from which to estimate the likelihood of potential changes.

One benefit of using climate and demand projections to estimate the likelihood of future change, rather than using them as a direct scenario generator, is that confidence in those data can be directly incorporated into the analysis. Knowledge about the particular strengths and weaknesses of the projections can be used to tailor the projections appropriately to maximize their credibility for the analysis. For instance, GCM projections of climate are known to exhibit greater skill at estimating changes in mean conditions over longer time scales (i.e. annual) and spatial scales. Also, there is greater confidence in their ability to estimate changes in temperature than in precipitation. The knowledge of these relative strengths and weaknesses can be highlighted when presenting the likelihood of possible changes suggested by the GCMs, making them more transparent to decision-makers. This contrasts the situation where GCM projections act as the

original source of climate scenarios and their weaknesses are embedded (i.e. hidden) in the climate sequences used to test the system.

Step 4. Appraise the robustness of the installation's water supply

In step 2 of the analysis (the stress test), the risk assessment framework identifies whether the current system is vulnerable to various types of future climate and socioeconomic conditions. If the status quo system is revealed to be insensitive to even the largest of changes tested, then no adaptation measures are necessary and the analysis is complete. A simple "wait-and-see" strategy can be employed where the system is monitored and the analysis revisited later if severe climate or water demand changes are observed. If, on the other hand, the system is sensitive to certain future scenarios, then the stress test is applied to all adaptation strategies as well. The results of this analysis reveal how well each adaptation strategy can preserve system performance over a wide range of futures. Specifically, this analysis determines which adaptations can preserve performance metrics above their thresholds (as defined in step 1) across the range of future scenarios.

The decision to accept a particular adaptation strategy then relies on an appraisal of the robustness of the various alternatives. The outcome of this process will depend on the level of confidence placed in the likelihood of future changes, as determined in step 3. To begin this approach, decision-makers can initially consider all possible future conditions tested in the stress test to be equally likely and plausible. Then, the adaptation measures can be ranked according the proportion of the space of future stressors over which they are able to maintain performance metrics above threshold levels. This proportion can be used to quantify the "unconditional robustness" of a particular adaptation approach. If a particular adaptation strategy is capable of maintaining performance metrics above threshold levels for a large range of future changes, then this adaptation can be considered robust. On the other hand, if a particular strategy only preserves performance metrics above threshold levels for a very limited proportion of the space of future scenarios, then this adaptation may be considered sensitive to climate change or water demand uncertainty. Potentially, one adaptation strategy will emerge that is much more robust across the entire space of changes compared to the other options. This information is very useful for decision-making, even before considering the likelihoods of future change.

Once the unconditional robustness of each adaptation measure is determined under the assumption of equal likelihoods, a data-informed judgment of robustness (i.e. "conditional robustness") can be developed using the likelihoods of change developed in step 3. Here, the likelihoods in step 3 are used to weight the space of future climate and socioeconomic conditions according to which changes are considered more likely. Decision-makers can explore which adaptation strategies are most robust under various assumptions about future change as suggested by the difference sources of climate evidence and population projections. Here, if one source of evidence is considered more credible than another, then decision-makers can choose to focus more on those adaptation policies that are robust under futures suggested by the more trusted information sources.

A major benefit of this approach is that decision-makers can immediately see whether different assumptions about future conditions influence their decision about a particular adaptation choice. It is possible that even after considering the likelihoods of future climate and water demands suggested by all difference sources of evidence, one or two adaptation policies emerge as the

most robust options available. Therefore, the choice of climate evidence or water demand projection is not particularly important and a decision can be made without extended debates regarding the value of one information source over another. On the other hand, the results may indicate that the robustness of one or another adaptation strategy significantly changes when different sources of evidence are used to develop the likelihoods of future change. This situation highlights how the approach makes transparent the effects of future change assumptions on the choice between adaptation policies. Here, decision-makers can consider which information source they trust more when considering which adaptation policy to choose. Also, the results under this situation reveal what types of information need to be refined and researched in order to help facilitate the choice between competing adaptation plans. In either case, the approach provides the means to facilitate the decision-making process when faced with an overwhelming and sometimes conflicting set of information sources.

Case Studies

The analysis methods described above were applied to four installation case studies: Fort Benning, GA, Fort Hood, TX, Colorado Springs, CO, and California Central Valley System, CA. In each case study, the entire methodology is presented: framing the water supply problem of each installation, conducting the stress test, and testing adaptation measures. Projections of future climate and water demands have also been gathered and used to develop estimates of conditional robustness for the status quo of each water supply system.

Case Study 1: Fort Benning, GA

Background and Problem Framing

For Benning is a major training installation located in central Georgia within the Apalachicola-Chattahoochee-Flint (ACF) River Basin (Figure 6). The waters of this river basin serve the needs of Georgia, Alabama, and Florida and are highly contested. Major conflicts exist between growing urban water needs in Georgia (Atlanta, Columbus), municipal water demands in eastern Alabama, and flows for fisheries and other environmental concerns in Florida. A decades-long, tri-state water conflict has resulted in numerous legal disputes, with a recent (June 2012) Supreme Court ruling allowing further allocations to the Atlanta metropolitan district.

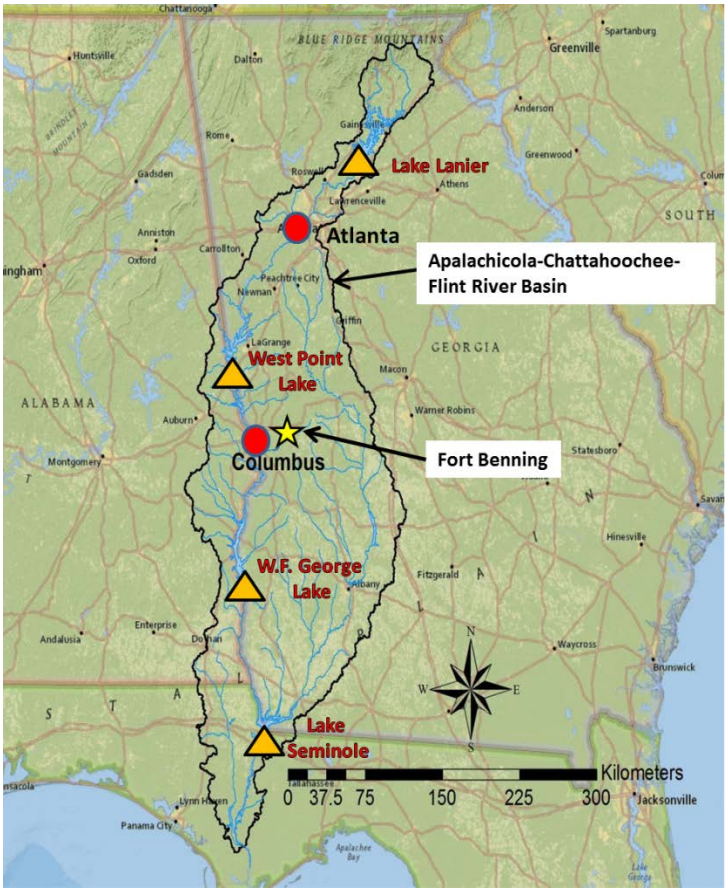

Figure 6 Map of Fort Benning (yellow star) located within the Apalachicola-Chattahoochee-Flint River Basin. Also shown are the major metropolitan regions of Atlanta and Columbus (red circles) and the major reservoirs operated by the U.S. Army Corps of Engineer (orange triangles).

Columbus Water Works (CWW) is the utility that serves Fort Benning. Fort Benning uses an average of around 5 million gallons per day (MGD) (between 2007 and 2009), but the total average demands for both Fort Hood and the surrounding counties served by CWW are much higher, around 33 MGD (Figure 7). This amount reflects a 50% increase over 1985 demands, although the demands have stabilized for these counties since 2000. To meet these water needs, CWW draws its water from Lake Oliver, a relatively small reservoir on the main stem of the Chattahoochee River. The Chattahoochee, along with the Flint and Apalachicola Rivers, are highly regulated by a series of 5 major dams operated by the United States Army Corps of Engineers (USACE), including Buford, West Point, Walter F. George, George W. Andrews, and Jim Woodruff. The first three dams have significant storage that forms large reservoirs (Lake Lanier, West Point Lake, and Walter F. George Lake). The operations of these reservoirs greatly impact the availability of water throughout the ACF system. Specifically, the releases made from West Point Lake dictate the amount of water available to CWW to meet the water demands of its customers, including Fort Benning. West Point releases are in turn dictated not only by the demands in the Columbus metropolitan area, but also by navigation and ecological flow targets far downstream. Therefore, a comprehensive water resources analysis is needed in order to adequately understand the sensitivity of Fort Benning's water supply to various climate and socioeconomic stressors.

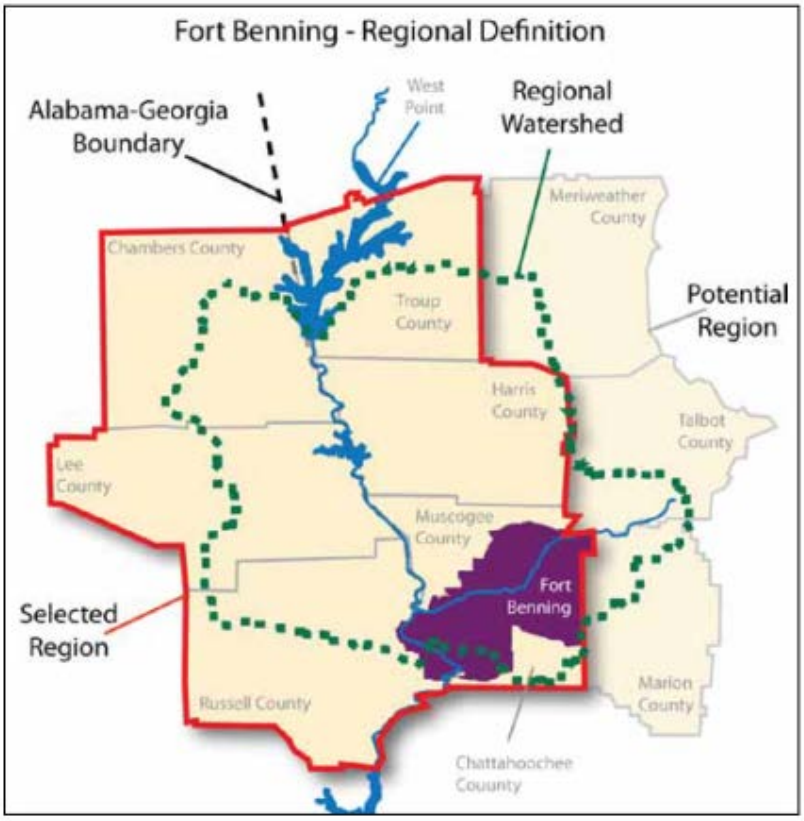

Figure 7 The local watershed for Fort Benning between the outlet of West Point Lake and the Chattahoochee River directly downstream of Lake Oliver. This figure is taken directly from Jenicek et al. (2011).

To measure the security and sustainability of the water supply of CWW and Fort Benning, three performance criteria are considered in this report. The first performance measure is the reliability of water supply at Columbus, which equals the proportion of time that water demands are fully met for the area. The second criterion is water supply vulnerability, which equals the average magnitude of shortfalls when full demand cannot be met at Columbus. Finally, the last performance measure considered is storage risk. This metric represents the minimum storage in the two upstream USACE impoundments (Lake Lanier and West Point Lake) during the simulation period. This criterion is important because there are times when water demands can be met but they require reservoir storage to be drawn down dramatically, a situation that reflects increased water supply risk for the system.

Thresholds are set for each of these criteria to delimit acceptable and failing future scenarios. For each metric, the threshold is set equal to the baseline value of the metric for the system under historic, observed climate and water demands. That is, this report assumes that the water supply for Fort Benning should be considered inadequate if a future scenario leads to any decrease in performance below that seen under the historic record. These thresholds are very conservative; in reality, some decline in water supply performance below historic levels would likely be acceptable. However, the threshold values chosen serve as a reasonable place to begin the

analysis, and they can be updated after further communication with personnel at Fort Benning and CWW.

Vulnerability Assessment

Both climate change and population growth can significantly stress the water resources of the ACF basin and thus could threaten the water supply security of Fort Benning. Because the water supply of CWW (and thus Fort Benning) is highly dependent on releases from West Point Lake, a vulnerability assessment must account for large-scale stressors of the system that influence major upstream impoundments. The water resources system in the ACF basin is highly integrated, with all major impoundments operated jointly to meet various water needs across all three states. Therefore, the vulnerability assessment conducted here evaluates the impact of population growth and climate change on the entire ACF system rather than just focusing on the operations of CWW. To evaluate each stressor's effect on the system, a stress test is performed on a 50-year planning period using monthly data to evaluate the system over a wide range of plausible futures. These represent changes in climate (precipitation and temperature) as well as water demand. Ensembles of stochastically generated precipitation and temperature data are used to drive calibrated hydrologic models for all inflow points throughout the system. Different demand scenarios across the region are also considered. The streamflow and demand data are used as the input to a system model of all reservoirs in the ACF. Details on each of these modeling components are presented below.

Stochastic Climate Generator

Historic daily climate data, including precipitation and maximum, minimum, and mean temperatures, were gathered for the ACF basin area over the period of January 1, 1949 to December 31, 2010 from the gridded observed meteorological dataset produced by Maurer et al. (2002). These data were aggregated to a monthly time step. The climate of the region exhibits a dual peak in precipitation, with one peak occurring in the summer between May and October and another occurring in the winter between the months of November and April. The stochastic climate generator simulates monthly climate variables from these two seasons separately and then combines them to form a continuous time series of climate data.

Precipitation and temperature during the winter (NDJFMA) season exhibit a moderate correlation with the wintertime (DJF) El Nino – Southern Oscillation (ENSO), while those same climate variables during the summer (MJJASO) season are correlated with summertime (JJA) sea surface temperature anomalies (SSTAs) in the North Atlantic Ocean. These large-scale climate drivers exhibit quasi-oscillatory low-frequency structure that propagates into the local climate of the ACF region. It is important that the stochastic climate generator be able to reproduce this structure when simulating monthly precipitation and temperature for the ACF.

To accomplish this, a wavelet auto-regressive modeling (WARM) approach is adopted (Kwon et al. 2007). The WARM approach extracts low frequency signals in the ENSO and SSTA data using wavelet decomposition and then stochastically simulates each signal using autoregressive time series models. By simulating each signal separately, the WARM model can better reproduce time series exhibiting a similar spectral signature to the observed data. A series of regressions between ENSO (North Atlantic SSTAs) and wintertime (summertime) average precipitation and temperature is used to translate the simulated large-scale climate drivers into seasonal climate across all locations in the ACF. Random samples from a multivariate-normal distribution fit to

the residuals of each regression for all sites are then added to the regression predictions. This approach propagates the appropriate amount of low-frequency structure into the simulated seasonal climate variables while maintaining a realistic level of statistical noise and between-site correlation. All seasonal climate variables are then disaggregated to a monthly time step using the method of fragments (Srikanthan and McMahon, 2001).

To impose various climate changes in the simulated time series, multiplicative factors are used to adjust the generated precipitation time series, while additive delta factors are used to adjust temperature values. All adjustments are transient. For example, if a 30% increase is desired for precipitation, then a time series of multiplicative factors is generated that begins with the value of 1 and ends with a value of 1.3, with a linear increase between the two values across the entire 50-year simulation period. This time series of multiplicative factors is then multiplied by the time series of generated monthly precipitation to create a climate-altered time series exhibiting the desired transient climate change. A similar approach is taken with the additive delta factors for monthly temperature.

Hydrologic Model

The *abcd* hydrologic model was selected to model monthly streamflow in the ACF system. This model structure was chosen because it has been recommended as an effective parsimonious model capable of efficiently reproducing monthly water balance dynamics (Alley, 1984; Vandewiele et al., 1992; Vogel and Sankarasubramanian, 2003). Martinez and Gupta (2010) examined the suitability of the *abcd* model structure for catchments throughout the United States, testing the model using several diagnostic statistics including Nash-Sutcliffe efficiency (NSE), bias, and variability error. That study found that the *abcd* model is a suitable structure for many catchments in and around the study region, showing good or acceptable performance over both calibration and evaluation time periods. These results support the model's use in this case study.

To calibrate the *abcd* model for the ACF system, unimpaired monthly streamflow data from 22 different inflow points were gathered over the period of January 1950 to December 1993 from a database developed as part of the Alabama-Coosa-Tallapoosa and Apalachicola-Chattahoochee-Flint River Basins Comprehensive Water Resources Study (USACE, 1997). Flows in that database were reconstructed in order to remove the effects of anthropogenic influences on the hydrologic data, such as municipal, industrial, and agricultural withdrawals and return flows, as well as evaporation, precipitation, and leakage associated with man-made reservoirs. These inflows serve as the input data into the water resources systems model of the ACF (described in the next section). The same historic climate data as described in the previous section were aggregated to each of these 22 different inflow points. In addition to precipitation, the *abcd* model requires potential evapotranspiration as an input. Monthly averages of maximum, minimum, and mean monthly temperatures were combined with estimates of monthly extraterrestrial solar radiation to produce a time series of potential evapotranspiration using the Hargreaves method (Hargreaves and Samani, 1982). Solar radiation was calculated using the method presented in Allen et al. (1998).

The *abcd* models were calibrated for each of the 22 different inflow points by minimizing the root mean squared error between simulated and reconstructed "observed" flows. The shuffled complex evolution (SCE) optimization algorithm presented in Duan et al. (1992) was utilized to conduct the calibration. At each site, the initial groundwater and soil moisture storage levels in

the model were also made available for calibration. This ensures that ill-specified initial conditions do not bias parameter estimates and removes the need to spin up each model before calibration. Model calibration was conducted over 30 years of data, leaving the remaining years for evaluation. For the evaluation period, the mean bias of the models equaled just +2.5%, but the largest and smallest biases ranged from +24% to -20%. However, besides those two outliers, the remaining 20 models had biases within +8.5% and -2% of the observed flows. Furthermore, 15 of the models had NSE values over 0.6 (a NSE of 1 indicates a perfect model, while a NSE of 0 indicates a model that predicts no better than the mean observed value). 7 models did have NSE values between 0.1 and 0.6, which suggests poor performance, but this can largely be attributed to errors in the reconstructed "observed" flows used for calibration, many of which had negative values throughout the record.

Water Resources Systems Model

This study utilizes a water resources systems model of the entire ACF system previous built to explore the effects of drought on the system and facilitate negotiations between stakeholders throughout the basin (Palmer et al. 1995). The systems model is constructed in the Stella software environment. Input data to the model include time series of monthly flows at 22 locations throughout the basin (now modeled by the *abcd* models), as well as net evaporation off of reservoir surfaces (now derived from the temperature and precipitation data simulated by the stochastic climate generator). The model also requires time series of water demands (and return flows) for municipal/industrial use, irrigation for agriculture, and thermoelectric cooling. The demands in the model have been updated to the data available for the year 2005 from county-level demand data provided by the United States Geological Survey (USGS) (Kenny, 2009). All performance criteria used to measure system performance (reliability, vulnerability, and storage risk) are available as output from the systems model.

Climate and Demand Alterations Considered

To conduct the vulnerability assessment, 50-year, monthly simulations of climate are run 25 separate times in the stochastic climate generator. Each of these simulations represents a different realization of internal climate variability for the region. For each of these 25 simulations, the precipitation and temperature time series are adjusted several times using multiplicative and additive factors (as described in the "Analysis Methods" section) to impose different climate changes. Two broad types of climate change are examined here, including alterations to the means of monthly precipitation and temperature. Changes to monthly precipitation means are ranged from ±40% of their historic values (i.e. 5 different changes: 60%, 80%, 100%, 120%, and 140%). Temperature delta shifts are ranged from 0 to 5 degrees Celsius at 1 degree increments (6 changes total). The ranges of these changes were chosen somewhat arbitrarily, except that they were designed to range beyond the changes suggested by GCM climate projections for this region. All changes are imposed by month. In total, 25×5×6=750 different climate simulations are considered. For each of these simulations, the climate data are used to force the *abcd* model and develop a time series of monthly streamflows, which are then run through the water resources systems model.

Demands are increased for all municipal and industrial (M&I) users throughout the system in order to evaluate the vulnerability of the water supply of Fort Benning to population growth across the region. Six different demand scenarios are considered, ranging from 100% to 300% of current demand levels (i.e. 100%, 140%, 180%, 220%, 260%, and 300%). All projections of

future demand are derived by projecting forward the county-level 2005 demands provided by the USGS. That is, six different time series of transient, multiplicative factors are applied to 2005 demand levels for all M&I users. Agricultural and thermoelectric demand changes are not considered in this study.

When the six demand scenarios are combined with the 750 climate simulations, a total of 750×6=4,500 scenarios of the ACF system are considered in this study. In order to avoid confusion, the ensemble of 4,500 runs will hereafter be referred to using the term "scenarios," while any information regarding the likelihood of future changes (discussed later) will be referred to using the term "projections". All of the future scenarios explored in this analysis are summarized in Table 2 below. The large number of generated climate and demand time series allows the system to be stressed over a wide range of plausible future conditions. This enables the identification of conditions that put the most pressure on the system and cause unacceptable levels of water supply risk for the Columbus area and Fort Benning.

Table 2 Climate and Demand Alterations Evaluated in the Vulnerability Assessment.

Stressor	**Range of Change (as a % of Historic Values)**	**Interval**	**Number of Changes**
Precipitation Mean	60% to 140%	20%	5
Temperature Mean	0 to 5 °C	1°C	6
Demand	100% to 300%	40%	6

Vulnerability Assessment Results

We first investigate how changes to various climate and socioeconomic stressors impact the water supply security at Columbus and Fort Benning. Figure 8 shows the results of the vulnerability assessment for water supply security at Fort Benning. Response surfaces for each of the three performance metrics (water supply reliability, vulnerability, and storage risk) are shown. Each response surface demonstrates how the performance metric changes in response to unit changes in two of the three stressors (i.e. precipitation and water demands, precipitation and temperature), with the third stressor held at its baseline level. These response surfaces show the performance metric averaged across all 25 realizations of stochastic climate variability. The dark solid line represents the performance metric under historic baseline conditions (i.e. the performance under the observed time series of climate and demands).

Figure 8(a) shows that water supply reliability responds strongest to changes in mean precipitation. Even slight decreases in precipitation over the region leads to rapid declines in water supply reliability at Columbus. This suggests that any precipitation decrease may lead to more frequent disruptions in the water supply to Fort Benning. Water supply reliability also decreases moderately as water demands around the region increase. The sensitivity of water supply reliability to both precipitation and water demand is demonstrated by the diagonal orientation of the response surface. This orientation can be interpreted as follows: when one stressor (e.g. precipitation) is altered, the same water supply reliability can only be maintained if the other stressor (e.g. water demand) is changed to offset the effect. In this case, if precipitation falls, reliability can only be maintained if water demands also decline. The angle of the diagonal orientation indicates which stressor has the stronger effect on reliability. In Figure 8(b), the near-vertical orientation of the response surface suggests that water supply reliability is only slightly

affected by increases in temperature. In fact, by comparing the angle of orientation between Figure 8 (a) and (b), it becomes clear that increasing water demands have a stronger influence on reliability than does increasing temperature.

The average water supply shortfall, or vulnerability, of the Fort Hood water supply system increases substantially when precipitation decreases from baseline levels (Figure 8(c)). However, this response fades when precipitation declines become more severe. This can be seen by the horizontal orientation of the response surface in Figure 8(c) when precipitation falls below 80%. The rise in vulnerability also appears to stop near this 80% precipitation threshold when comparing vulnerability under precipitation and temperature changes (Figure 8(d)). Vulnerability does not continue to rise as precipitation declines because the water supply system imposes a static reduction in water deliveries in response to drought. That is, when the water supply system becomes stressed, the system requires that all water users receive 10% less water than their full demand until the drought conditions have passed. The only way that shortfalls will rise above 10% of water demand is if the system enters a more critical drought condition, triggering a more stringent reduction in water deliveries. This system behavior also explains why the response surface in Figure 8(c) becomes horizontally oriented when precipitation declines below 80%. As demands increase, the actual volume of delivery shortfalls rises directly in proportion to the water demands, because shortfalls are by design set equal to 10% of demand. Finally, similar to reliability, water supply vulnerability is rather insensitive to increases in temperature, with only minor increases in the average shortfall volume as temperatures increase.

Water supply storage risk is highly responsive to declines in precipitation, with minimum storage ranging between 45% and 70% of capacity across all precipitation changes (Figure 8(e)). This range in storage risk is quite dramatic. Storage risk is also moderately responsive to water demands. The baseline storage risk (i.e. the thick, dark line) shows that demand effects across the range of water demand conditions (100% to 300% of baseline levels) equals the effects of precipitation change between -10% and +20% of the historic average. While precipitation clearly has the larger influence on storage risk, demands do exhibit some substantial influence. Temperature changes, on the other hand, impose a very small influence on storage risk, and cease to exhibit much impact at all when precipitation falls below 80% of historic levels (Figure 8(f)).

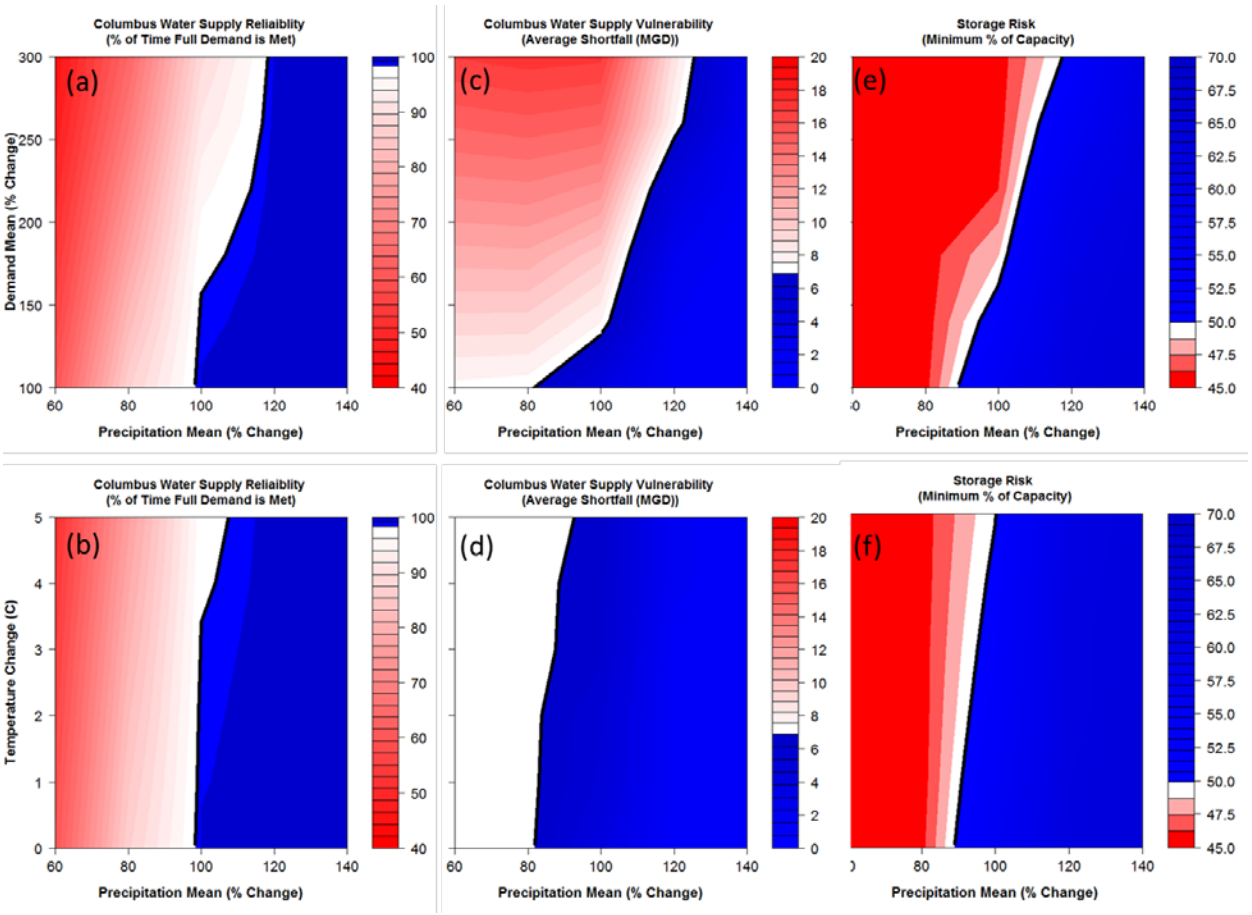

Figure 8 Response surfaces of each performance metric to changes in two stressors, with the third held constant at its baseline level. The performance metrics are contoured such that more favorable values are represented by blue while worse performance is represented by red. The thick, dark line represents the historic, baseline performance developed under the observed time series of climate and water demand.

After exploring the effects of climate change on the water supply security of Fort Benning, it is important to evaluate the effects of internal climate variability. Figure 9 shows the range of each performance metric under the 25 different runs of stochastic climate variability, but with no climate changes imposed or increases in water demand. These results show the range of each performance metric that can arise simply due to natural variations in regional climate. The results in Figure 9 suggest that variations in water security performance due to internal climate variability are not trivial. Water supply reliability values range from 100% down to almost 97%, which is significant given that water supply reliability is often considered inadequate if it falls into the low 90% range. Average water delivery shortfalls (i.e. vulnerability) range from 0 MGD to near 7 MGD, which is larger than the entire water demand of Fort Benning. The effects of climate variability can perhaps be seen best when examining storage risk. Across all 25 baseline climate simulations, the minimum storage in the two upstream impoundments (Lake Lanier and West Point Lake) ranges from 45% to 65% of capacity. This spread is very significant, and it suggests that the large amount of storage in those two reservoirs is crucial just to manage the natural, internal variability of the climate.

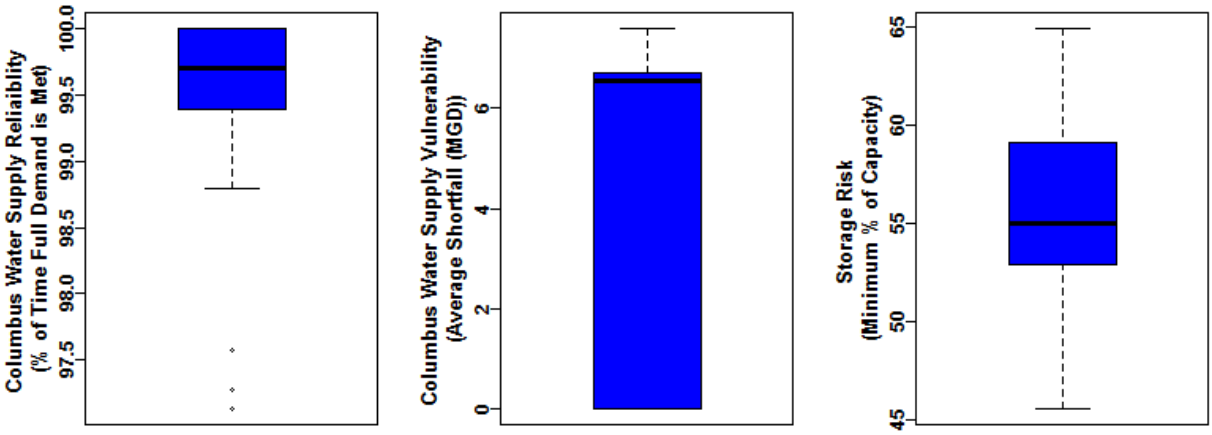

Figure 9 The range of each performance metric under all 25 different stochastic climate simulations.

The effects of internal variability can also interact with long-term climate and demand changes to compound the effects on water supply performance. Figure 10 shows the mean, minimum, and maximum value for each performance metric across the 25 climate simulations against one stressor variable (precipitation, temperature, or demand), with the other two stressors held constant at their baseline levels. This figure shows the relative impacts of climate variability on water supply performance and compares them to the effects of climate and socioeconomic long-term change. Several results emerge from Figure 10. First, it is clear that all performance metrics are substantially affected by climate variability, and for some, climate variability is as influential on performance as long-term change. For instance, in Figure 10(a), water supply reliability averaged across the 25 simulations is about 60% for a mean change in precipitation of 60%. However, reliability ranges between 50% and 70% across all 25 simulations for this mean precipitation change. This 20% uncertainty range is almost as large as the difference in mean reliability between a precipitation change of 60% and 80%. This result is similar for many of the metrics and stressors tested.

Another result that emerges from Figure 10 is that climate variability may have more or less impact on system performance depending on the long-term climate or socioeconomic change. In several instances (Figure 10 (a,b,d,g,h)), the range of performance across the 25 simulations narrows substantially if the long-term change of a stressor exceeds some threshold. For example, in Figure 10(a), the range of water supply reliability is minimal if the mean precipitation change is 100% of baseline or greater. It is only when precipitation declines to 80% or less that climate variability begins to show a substantial impact on performance. However, the opposite result is true for storage risk (Figure 10(g)). Here, the range of storage risk is very small when the average precipitation falls very low, but this range grows substantially when there is more precipitation on average. These results suggest that under wetter precipitation conditions, fluctuations in storage can manage drought conditions when they occur and prevent substantial water shortages. However, under persistently drier conditions, large reservoir storage is no longer capable of managing a particular series of dry months or years because every year is consistently too dry, so there is never any water available to refill storage after a drought has ended.

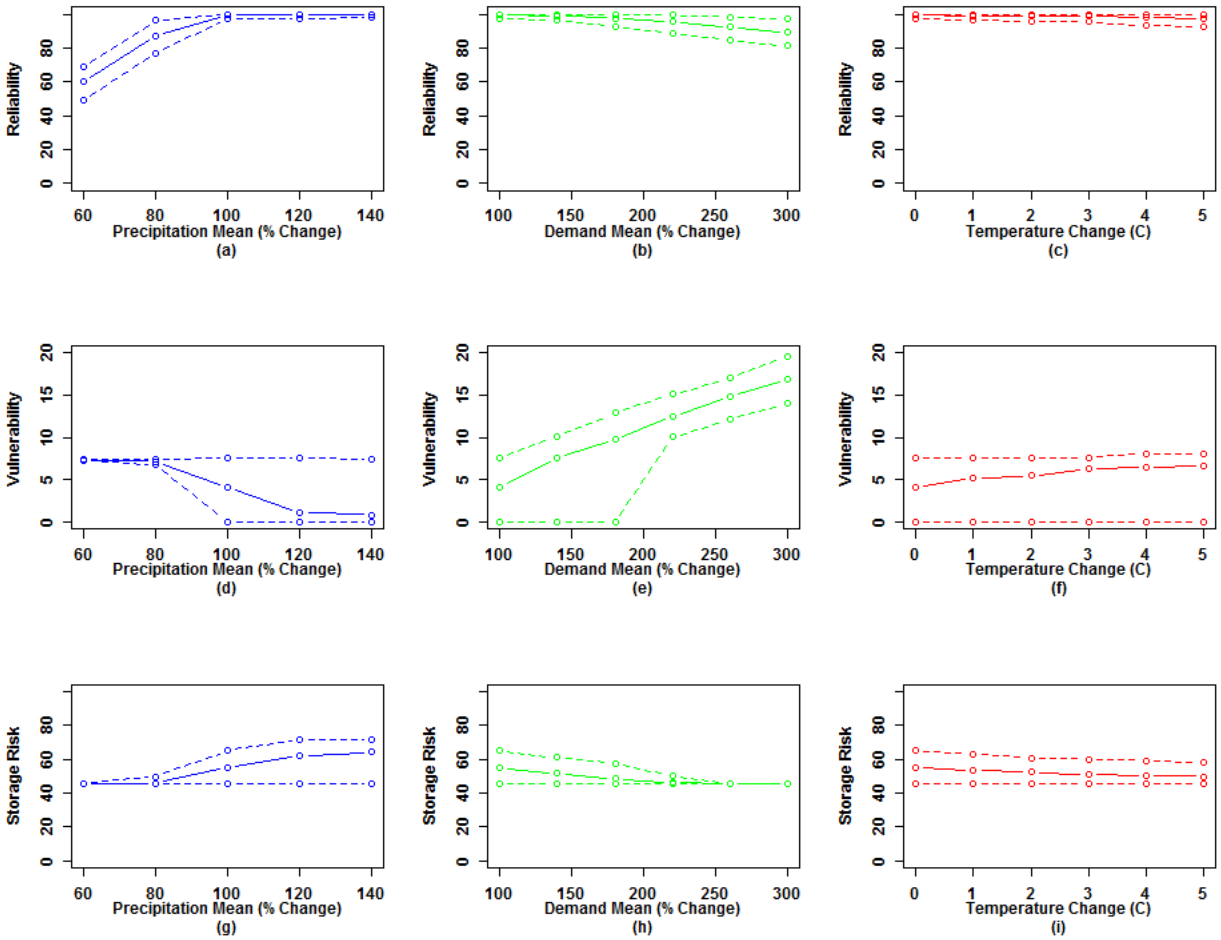

Figure 10 The response of each performance metric to a change in one stressor with the other two stresses held constant at their baseline levels. The solid line indicates the mean performance metric under all 25 stochastic simulations, while the dashed lines represent the minimum and maximum metric from the 25 simulations.

In summary, the results of the stress test revealed that the water security of Fort Benning appears most vulnerable to declines in precipitation over the ACF region. Increases in water demand also contribute moderately to the risk facing the water supply system, while the system appears only slightly sensitive to temperature increases. Internal climate variability also contributes significantly to the water supply risk of Fort Benning, particularly when long-term changes are unfavorable.

Likelihood of Future Changes

After assessing the vulnerabilities of Fort Benning's water supply system to a range of future conditions, projections of future climate and water demands are used to determine how likely those futures are. Again, all information regarding future likelihoods is referred to as a "projection", while the time series of future conditions used in the stress test are referred to as "scenarios". To estimate the likelihood of future climate changes, climate projections were gathered from the Coupled Model Intercomparison Project (CMIP). Two generations of climate

projections, CMIP3 and CMIP5, were gathered from this database (Reclamation, 2013). The CMIP database provides a large ensemble of future climate projections under a wide range of future carbon dioxide emissions scenarios and GCM structures. These data are available at very coarse resolutions, requiring that they be downscaled to the ACF region. While future research will explore the utility of different downscaling methods for DoD decision-making, this interim report only uses a single downscaling method for an initial assessment (the bias correction spatial disaggregation technique). Data from the downscaled climate projections were taken for a 30-year window around the year 2050 and compared against data for 1970-2000 to determine the projected change factors for both precipitation and temperature.

Figure 11 shows the range of changes projected for mean precipitation and mean temperature for the year 2050. Projections from both the CMIP3 and CMIP5 datasets are included. Both datasets project an increase in temperature somewhere between 0.5°C and 3.5°C, although the CMIP5 projections include a few warmer outliers than does the CMIP3 dataset. For precipitation, the two sets of projections show some interesting differences. The average across all CMIP3 projections suggests that mean precipitation will decline to 98% of baseline levels, but the projections range between 83% and 118% of the baseline. The CMIP5 projections have an average precipitation decline of 94% of baseline levels, but this dataset has far fewer outliers showing large precipitation increases. Furthermore, the CMIP5 dataset also contains a few projections suggesting steep declines in mean precipitation, as low as 77% of baseline levels. This precipitation decline would signify a dramatic change in the availability of water over the ACF region.

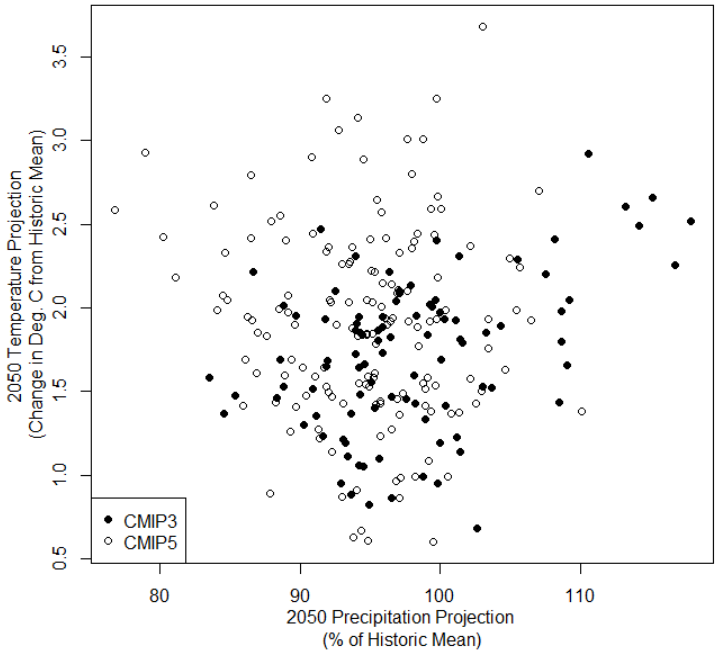

Figure 11 Distribution of mean precipitation and temperature projections for the year 2050 derived from the CMIP3 and CMIP 5 datasets.

Projections of future water demand were developed using projections of population and per capita water use for the metropolitan Atlanta region. These projections, which extend out to the year 2050, were compared against baseline water demand levels for this region (2006 water demands) to develop multiplicative change factors for municipal and industrial (M&I) water use in Atlanta. These change factors were then used as projections of the change in water demand expected for all M&I water use throughout the ACF system. In the stress test, water demands were changed by increasing M&I demands throughout the entire ACF system using change factors that ranged from 1 to 3 (i.e. 100% to 300% of historic demands). Thus, the projections of future water demand, in the form of change factors, can be directly compared to the changes made in the stress test. We recognize that other M&I water users in the ACF will not likely grow as fast as those of Atlanta over the next several decades, which will impose some error into the projections of water demand used in this study. However, there is limited data to project water demand for other metropolitan regions, and also, the M&I demands in Atlanta compose the vast majority of M&I demands throughout the ACF system. Therefore, the error in multiplicative demand projections for non-Atlanta regions will actually have little impact on the interpretability of the results.

Population projections were gathered from three different sources: the Metropolitan North Georgia Water Planning District (MNGWPD), Atlanta Regional Commission (ARC), and the state of Georgia (GA State). Two different projections were available from the ARC, leading to 4 population projections altogether (AECOM, 2009; ARC, 2009; State of Georgia, 2010; ARC, 2011). These projections are shown in Figure 12. Note that some projections were linearly interpolated out to 2050 because they ended in 2035. These projections suggest that population in the Atlanta region will increase from approximately 4.5 million in 2006 to between 8 and 10 million by 2050. The MNGWPD also provided three different projections of per capita water use. These projections included a baseline level of water use from 2006 (154.7 gallons per capita per day (gcd)), a status-quo projection for 2035 (146.7 gcd), and a 2035 projection under a proposed conservation plan (134.9 gcd). These 2035 per capita water use projections were used as 2050 projections. By multiplying the per capita water use projections by the population projections, 4×3=12 different water use projections were developed. These are shown in Figure 13. When compared to the 2006 baseline demand, these projections suggest 12 different multiplicative demand changes that range from 167% to 237% of baseline demand, with a mean change of 195%.

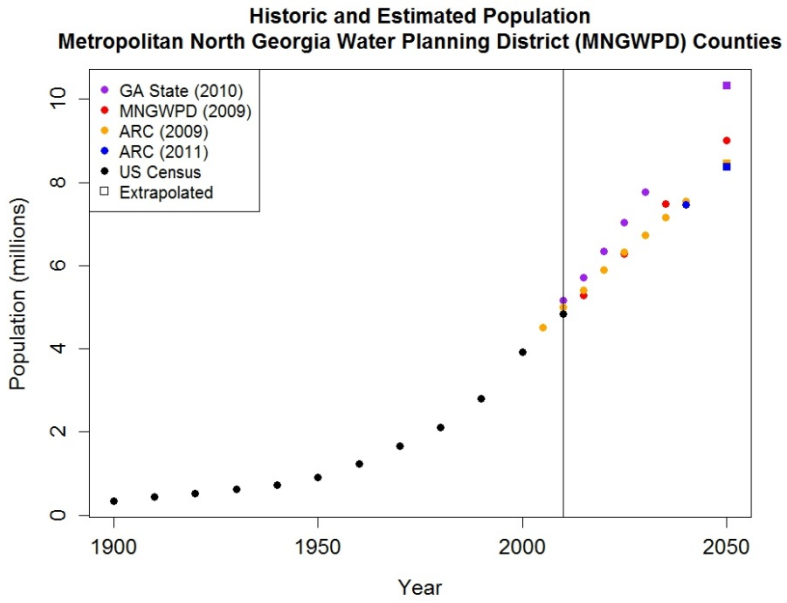

Figure 12 Historic population data and population projections for the Metropolitan North Georgia Water Planning District. Projections are included from three sources, including the MNGWPD, Atlanta Regional Commission (ARC), and GA State. Some projections only extended to 2035 and were linear extrapolated to the year 2050 (boxes). The vertical line separates historic data from the projections.

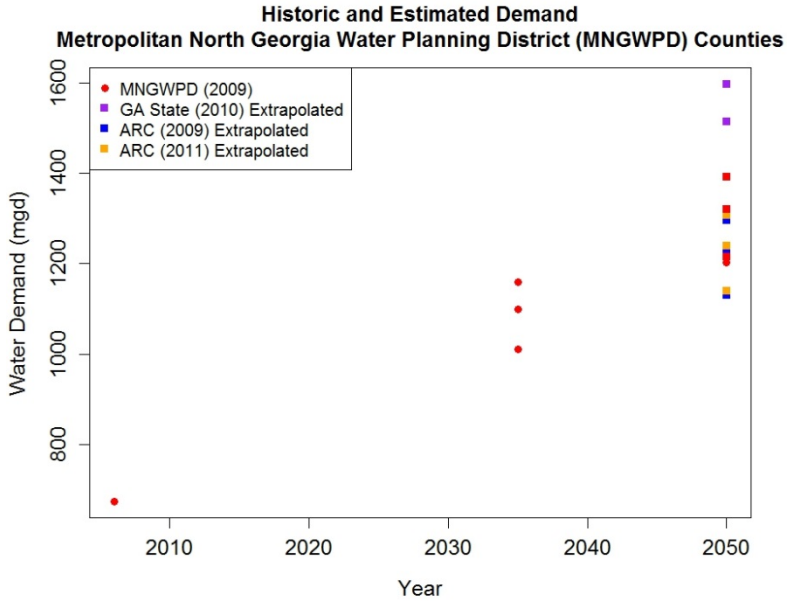

Figure 13 Water demand projections for the Metropolitan North Georgia Water Planning District. These projections are derived from the product of four population projections and three projections of per capita water use.

Assessment of Future Risks and System Robustness

The results of the vulnerability assessment can be coupled with the analysis of the likelihood of future change to determine how likely problematic futures are to occur and whether the water supply of Fort Benning is robust to these risks. Figure 14 shows the same vulnerability response surfaces as in Figure 8, but now the water demand and CMIP climate projections are superimposed on the surfaces to indicate which regions of the space are most likely to occur in the future. The CMIP3 and CMIP5 projections are distinguished using green and purple points, respectively. Because the climate and demand projections were developed independent of one another, each climate projection was coupled with every demand projection, leading to the horizontal orientation of the projections in Figure 14(a,c,e). Recall that the threshold of acceptable performance is set to the level of performance under historic, observed conditions (represented by the thick, dark line on each response surface). Any projection that falls to the left of this line (into the redder region) suggests that future performance will be unacceptable, while a projection that falls to the right of the threshold (into the bluer region) indicates acceptable future performance.

The results in Figure 14 suggest that there is a significant risk that future water supply performance for Fort Benning will be worse than it is presently and will fall below the threshold of acceptable performance. Future projections are particularly discouraging when considering changes in both precipitation and water demands (Figure 14(a,c,e)). Figure 14(a) shows a majority of projections in the unacceptable region of water supply reliability performance, with the CMIP5 projections (which are generally drier) having almost no projections in the acceptable region. This occurs because all demand projections show an increase in water demand of 150% of baseline levels or higher, and the region of unacceptable performance becomes substantially larger right at this level of 150% of baseline demand. These same results are seen for both water supply vulnerability and storage risk as well (Figure 14(c,e)).

When comparing projections of precipitation and temperature under baseline water demands, more than half of all projections suggest unacceptable future reliability performance (Figure 14(b)). Future projections are somewhat more promising for water supply vulnerability, with most projections falling to the right of the threshold line. Storage risk, however, also has a significant number of projections (~30%) falling into the unacceptable region of performance (Figure 14(f)).

The results from Figure 14 suggest that only a few projections of future conditions need to materialize in order to stress the water supply of Fort Benning beyond an acceptable level. On their own, modest increases in water demands or decreases in precipitation are enough to push the system into a stressful condition, and simultaneously these changes can cause severe problems for Fort Benning's water supply. Projections of future climate and water demand suggest that this simultaneous change is quite likely to occur, indicating that water supply at Fort Benning is at high risk of failure.

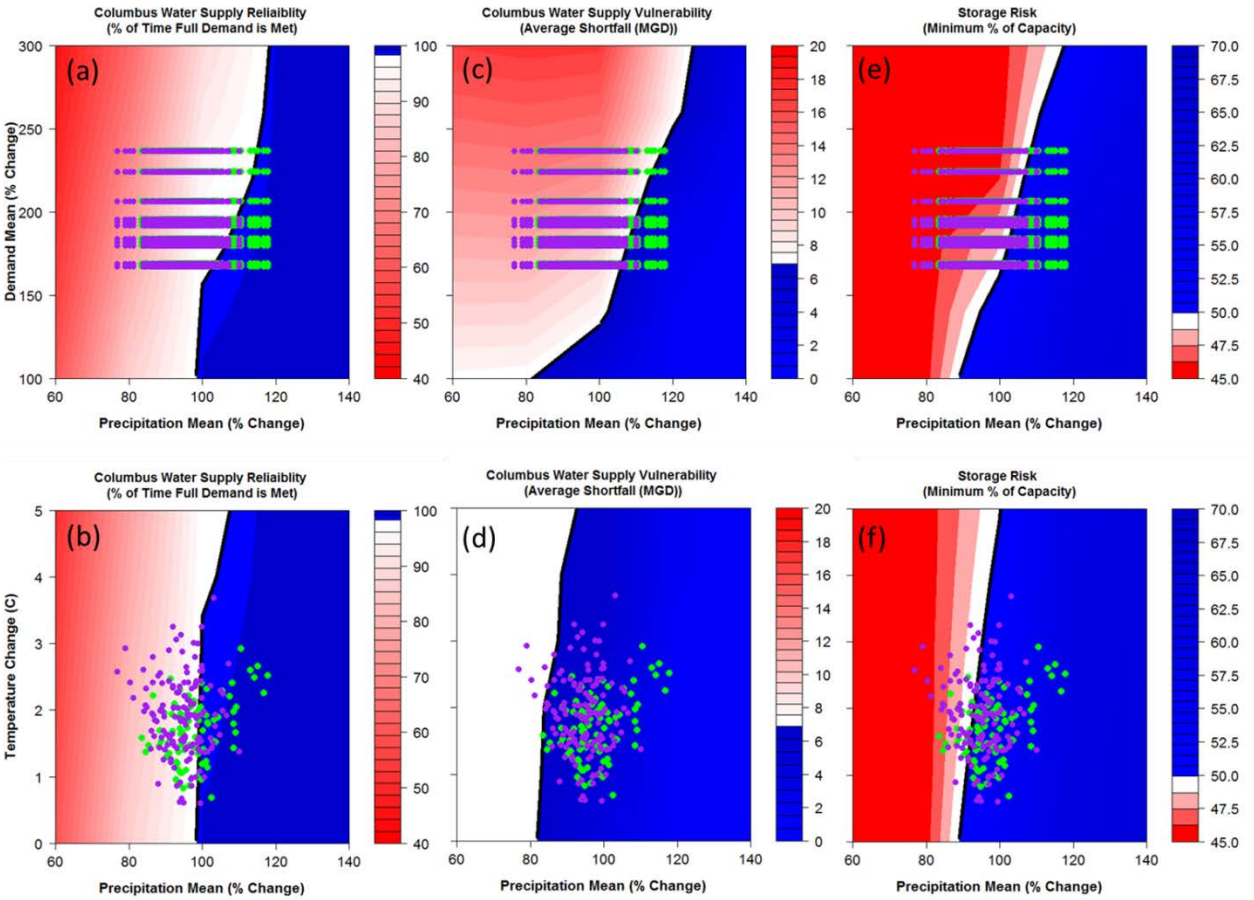

Figure 14 The same as Figure 8, except projections of future climate and water demands are superimposed. CMIP3 projections are denoted by green dots, while CMIP5 projections are colored purple. Because demand and climate projections were developed independently, all CMIP3 and CMIP5 precipitation projections were coupled with all demand projections in a,c, and e.

The information from the stress test and the assessment of future likelihoods can also be combined quantitatively to provide a metric of robustness that can help inform the decision process regarding Fort Benning water supply adaptation. This metric of robustness can also be independent of any projections of future change. In the latter case, the metric is termed unconditional robustness, and it simply equals the percentage of the future change space tested in the stress test that yields acceptable performance. That is, unconditional robustness equals the number of future scenarios that yield acceptable performance divided by the total number of scenarios tests (4,500 in total for this case study). This metric provides a snapshot of how well the current system performs over all the possible climate and socioeconomic changes that were considered. A different robustness metric can be developed for each performance measure. Note that this robustness metric is most useful when comparing multiple different adaptation measures, as it provides information on how much improvement a particular adaptation measure provides over the status quo system in terms the proportion of future conditions under which that adaptation can maintain acceptable performance.

Figure 15 shows the unconditional robustness calculated for each of the three performance metrics. These results suggest that water supply reliability is maintained above its threshold level across 40% of the entire space of future changes considered, while vulnerability and storage risk are acceptable across 28% and 35% of the space, respectively. These values indicate that water supply performance is very sensitive to many of the future scenarios that were tested. However, no information about future likelihoods is included in the unconditional robustness metric. This problem is resolved by using the conditional robustness metric. Conditional robustness is defined as the number of climate change and water demand projections that fall into an acceptable space of water supply performance divided by the total number of projections considered. Conditional robustness metrics for each performance measure are given in Figure 16. Two versions of conditional robustness are provided, one based on the water demand projections coupled with the CMIP3 climate projections (Figure 16(a)), and another based on demand projections coupled with CMIP5 (Figure 16(b)). For the CMIP3 projections, water supply reliability and vulnerability is acceptable for approximately 8% of all projections, while storage risk robustness is slightly above 19%. For the CMIP5 projections, reliability robustness is 3%, vulnerability robustness is slightly greater than 2%, and storage risk robustness is approximately 9%. The CMIP5 projections lead to worse robustness measures than those from CMIP3 because CMIP5 projections suggest somewhat drier conditions. However, both sets of projections lead to substantially worse robustness than that in the unconditional case, primarily because both projections include water demands that are greater than 150% of baseline levels. These increased water demands consistently degrade system performance below threshold levels unless climate projections indicate substantially wetter conditions, which the majority of climate projections do not predict.

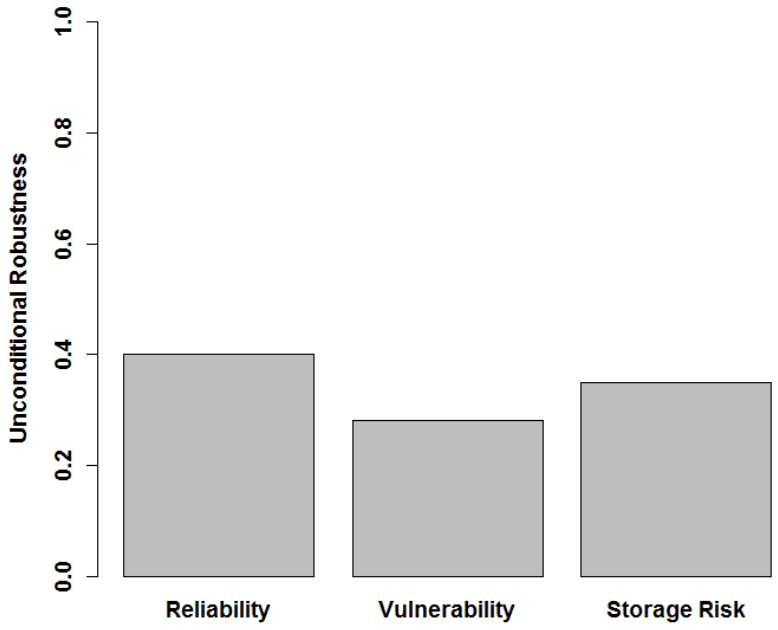

Figure 15 The unconditional robustness of each water supply performance metric, which equals the ratio of all acceptable climate and demand scenarios to the total number of scenarios tested.

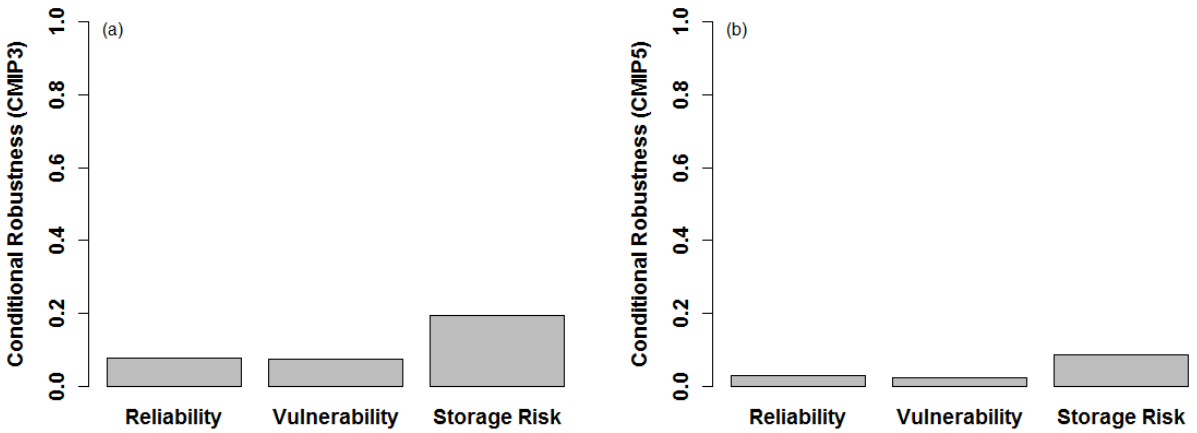

Figure 16 The conditional robustness of each water supply performance metric for the a) CMIP3 and b) CMIP5 projections. The conditional robustness equals the ratio of the number of climate and demand projections that are acceptable to the total number of projections examined.

Conclusions

This case study presented a risk assessment of the water supply system serving Fort Benning in Columbus, GA. An initial vulnerability assessment was used to determine the future conditions that led to unacceptable water supply performance for the installation. This analysis showed that Fort Benning's water supply is highly sensitive to small decreases in average precipitation over the region, moderately sensitive to increasing water demands, and relatively insensitive to increasing temperatures. Internal climate variability was also shown to strongly influence water supply performance, especially if underlying long-term trends were unfavorable for water supply security.

Climate and water demand information was then gathered to determine the likelihood of different future conditions. Climate projections showed a wide spread of possible outcomes, but many suggested that warmer and drier conditions were likely in the future. Demand projections all agreed that water demands would increase, but the magnitude of this increase ranged widely.

The results of the vulnerability assessment and the assessment of likelihoods of future change were combined to determine how robust Fort Benning's water supply system is to future change. Both unconditional and conditional robustness measures suggest that there is significant risk to the security of Fort Benning's water supply, although the conditional risks based on future climate and demand projections are extremely high. Overall, the results of the analysis suggest that adaptation measures should be considered to make the water supply of Fort Benning more robust to future climate and socioeconomic conditions.

Case Study 2: Fort Hood, TX

Background and Problem Framing

Fort Hood (Figure 17) is a major training installation located in the Brazos G Regional Water Planning Area, which consists of 37 counties, 30 major reservoirs, and covers 31,600 square miles. Region G is one of 16 regional water planning areas established by the Texas Water Development Board (TWDB) (BGRWPG, 2010). Region G is further separated into several sub regions and Fort Hood is located in the IH-35 Corridor sub region. The IH-35 Corridor consists of five counties and has been subject to rapid population growth, averaging 3.9 percent annually since 1970 (Jenicek at al., 2011).

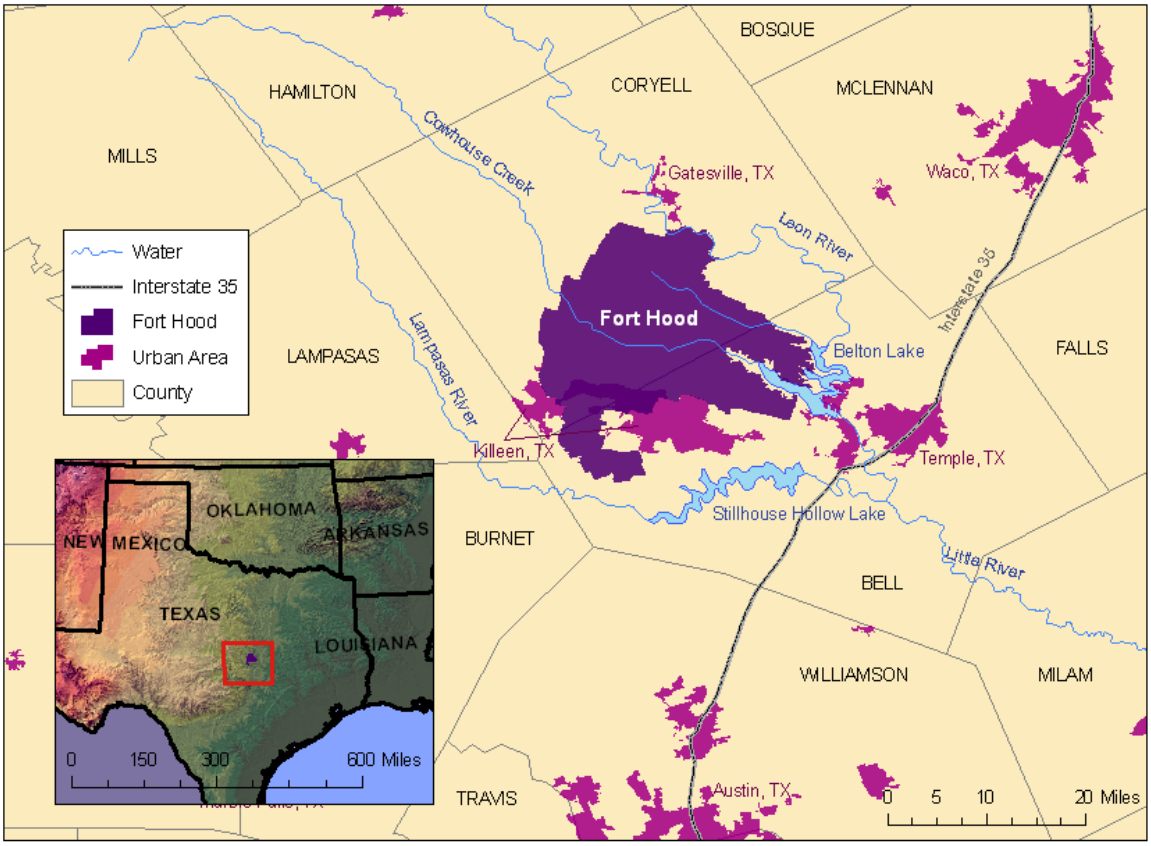

Figure 17 Map of Fort Hood, Texas as located near Belton Lake, the base's primary water supply. Also shown is Stillhouse Hollow Lake immediately south of Fort Hood, however, this lake does not contribute to the base's water supply. This figure is taken directly from Jenicek et al. (2011).

The primary water supply for the base is Belton Lake. This lake is located in Bell County, Texas within the Brazos River Basin and has a drainage area of approximately 3,740 square miles. The lake is owned by the U.S. Army Corps of Engineers (USACE) and serves two primary purposes; flood control and water supply. The capacity of the reservoir is approximately 1,100,000 acre-feet and the conservation pool is slightly greater than 435,000 acre-feet (nearly 40% of capacity). Flood control is managed exclusively by the USACE, while water supply is managed by several entities. The Brazos River Authority (BRA) and Fort Hood own the only water rights to Belton Lake, with the BRA owning the majority (100,257 acre-feet of the total authorized use per year

of 112,257). For other entities to use water from Belton Lake, each must obtain a contract with the BRA granting access/use. Major water providers with access to Belton Lake include the BRA, Bell County Water Improvement District (BCWCID No. 1), Bluebonnet Water Supply Corporation (BWSC), and the City of Temple. The largest water provider in Region G is the BRA which owns and operates 3 reservoirs and owns water rights to storage space within 8 reservoirs owned by the USACE within the region (Figure 18) (BGRWPG, 2010). While Belton Lake is used to serve Fort Hood and the immediately surrounding counties, it also is a source for many downstream water users. The BRA serves water users throughout the basin, and utilizes each of their reservoirs to meet the needs of the downstream users. From 1998 to 2011, Belton Lake was used by the BRA for downstream users in approximately 35% of those years. Fort Hood does not use groundwater despite its location above the Edwards-Trinity Aquifer and other smaller groundwater sources (Jenicek at al., 2011).

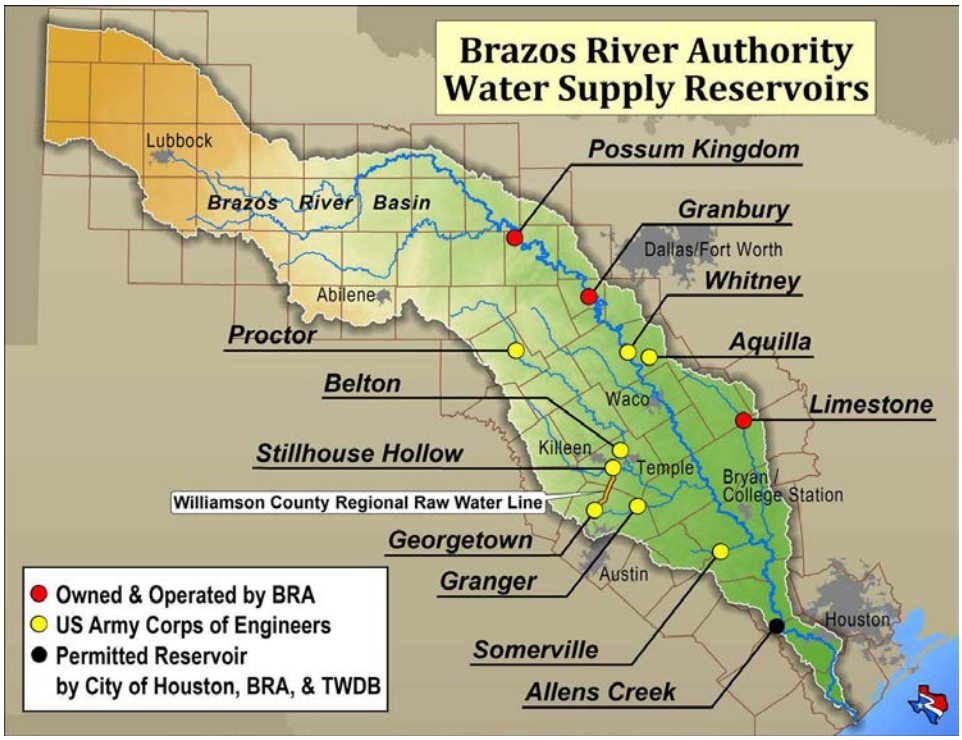

Figure 18 Map of the Brazos River Authority water supply reservoirs and the Texas portion of the Brazos River basin. This figure is taken directly from BGRWPG, 2011.

Two utilities serve Fort Hood; BCWCID No. 1 and Gatesville Regional Water Supply (GRWS). BCWCID No. 1 serves South and West Fort Hood, amongst other nearby cities. GRWS is a smaller water utility which serves only North Fort Hood. The water source for each of these utilities is Belton Lake. Fort Hood is authorized to use 12,000 ac-ft of water from Belton Lake each year (Jenicek at al., 2011), but currently use only around 8,600 ac-ft.

Vulnerability Assessment

According to the Brazos G Regional Water Plan of 2011, the anticipated two most impactful stressors on water supply are population growth (leading to increased demand) and droughts (leading to decreased runoff). To evaluate the Fort Hood water supply system over a wide range of plausible futures, a stress test is performed on a 50-year planning period using monthly data.

These represent changes in climate (precipitation mean and temperature mean) and demand (divided into local community users and downstream users). Ensembles of stochastically generated precipitation and temperature data is used to produces streamflows using the hydrologic model HYMOD. The streamflow data is used as the input to a system model built in R for Belton Lake. Multiple performance metrics (Minimum Elevation, Vulnerability, and Demand Reliability) are used to evaluate models' ability to reproduce system response.

Stochastic Climate Generator

Historic daily climate data, including precipitation and maximum, minimum, and mean temperatures, were gathered for the Belton Lake watershed over the period of January 1, 1949 to December 31, 2010 from the gridded observed meteorological dataset produced by Maurer et al. (2002). These data were aggregated to a monthly time step. The climate of the region exhibits a dual peak in precipitation, with one peak occurring in late spring between January and June and another occurring in the fall between July and December. The stochastic climate generator simulates monthly climate variables from these two seasons separately and then combines them to form a continuous time series of climate data.

Precipitation and temperature during the spring (JFMAMJ) season exhibit a moderate correlation with the wintertime (DJF) El Nino – Southern Oscillation 4 (ENSO4), while those same climate variables during the summer (JASOND) season are correlated with summertime (MJJ) sea surface temperature anomalies (SSTAs) in the North Atlantic Ocean. These large-scale climate drivers exhibit quasi-oscillatory low-frequency structure that propagates into the local climate of the Belton Lake region. It is important that the stochastic climate generator be able to reproduce this structure when simulating monthly precipitation and temperature for Belton Lake watershed. To accomplish this, the approach taken in the Fort Benning case study stochastic climate generator section is used.

To impose various climate changes in the simulated time series, multiplicative factors are used to adjust the generated precipitation time series, while additive delta factors are used to adjust temperature values. All adjustments are transient. For example, if a 30% increase is desired for precipitation, then a time series of multiplicative factors is generated that begins with the value of 1 and ends with a value of 1.3, with a linear increase between the two values across the entire 50-year simulation period. This time series of multiplicative factors is then multiplied by the time series of generated monthly precipitation to create a climate-altered time series exhibiting the desired transient climate change. A similar approach is taken with the additive delta factors for monthly temperature.

Hydrologic Model

The hydrologic model was built based on the HYMOD, a widely applied (Boyle et al., 2001; Moradkhani, 2005a, 2005b) five-parameter hydrologic model, for the combined inflow to Belton Lake. Two rivers flow into Belton Lake; the Leon River and Cowhouse Creek, each with respective drainage areas of 3012 and 728 square miles. Inputs to the model include monthly precipitation and potential evapotranspiration. The hydrologic model was calibrated against monthly USACE inflow measurement from 1985 to 1995 and validated over a four year period 1996 to 1999 (Figure 19). For the calibration procedure, historical monthly climate data over the entire Belton Lake Watershed was derived using $1/8^{th}$ degree gridded daily dataset (Maurer et al.,

2002) averaged over the basin. Historical potential evapotranspiration was calculated using the Hargreaves Method (1982). The calibration procedure was first performed automatically using the shuffled complex evolution algorithm followed by manual adjustments of the parameters which resulted in a Nash-Sutcliffe value of 0.62 and a small negative bias of 1.0. Several other hydrologic models were developed for the Belton Lake Watershed (ABCD, SAC-SMA, and VIC), but none performed as well as the HYMOD model.

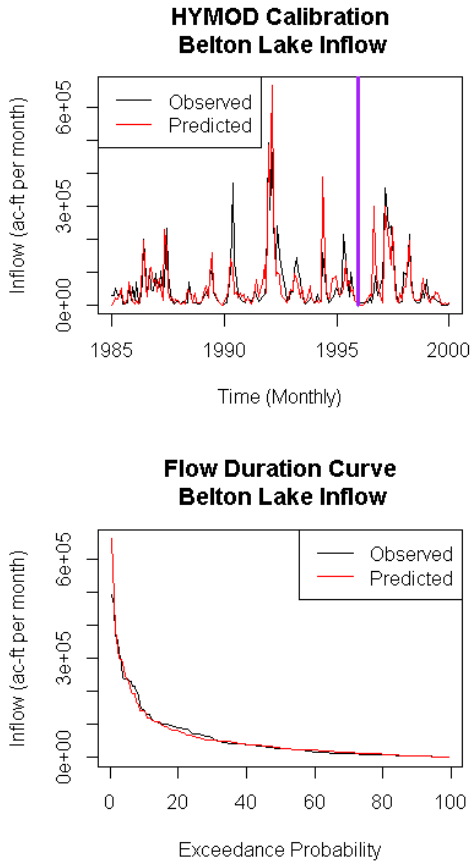

Figure 19 Hydrologic model calibration of the inflow to Belton Lake. The top figure shows the time series of predicted versus observed streamflows from 1985 to 2000. The purple vertical line indicates the separation between the calibration (to the left) and validation (to the right) periods. The bottom figure compares the predicted and observed flow duration curves.

Water Resources Systems Model

The system model is a simple mass-balance model of Belton Lake tracking inflows (river inflows, precipitation directly onto the lake) and outflows (controlled and uncontrolled releases downstream, demand, evaporation directly off of the lake). Parameters controlling reservoir releases from different storage zones designated by the USACE were adjusted to calibrate the model to historical release and storage data reported by the USACE from 1985 to 1995 and verified over a four year period 1996 - 1999 (Figure 20). Demands in the system model are automatically reduced during times of low storage according to the BRA 2012 Drought Management Plan. For the calibration, demands for users within local communities were estimated from USGS population data. No demand data was available for any Belton Lake

releases intended for downstream users in this time period. When the system model is run within the vulnerability assessment, demand projections for both users in nearby communities and downstream users are included. It is assumed that as demands increase, water rights will be renegotiated (as has been done historically) such that water rights will have no effect on the system model.

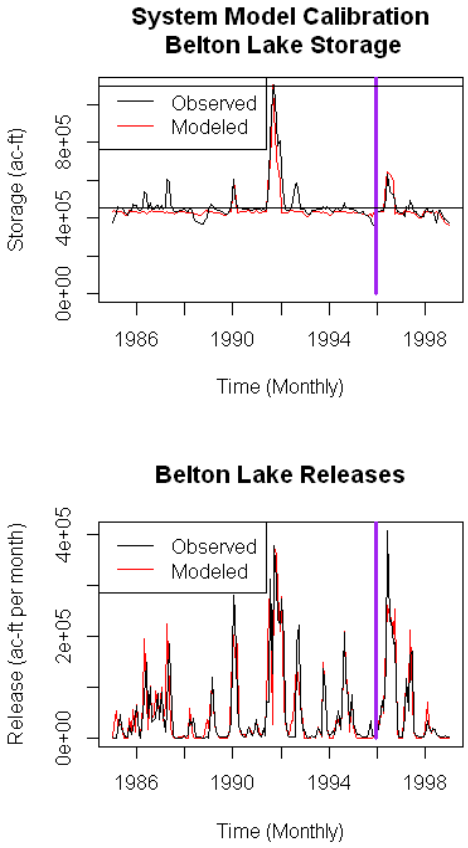

Figure 20 System model calibration for the Fort Hood water supply. The top and bottom figures show a time series of reservoir storage and releases for the predicted and observed from 1985 to 1999. The purple vertical line indicates the separation between the calibration (to the left) and verification (to the right) periods.

As part of the vulnerability assessment for the system model output, the following performance metrics are calculated:

- Water Supply Reliability:
  Defined as the percentage of monthly time steps in which full demands are met over the full simulation period
- Water Supply Vulnerability:
  Defined as the average demand shortfall over the full simulation period
- Storage Risk:
  Defined as the minimum storage of Belton Lake over the full simulation period

Climate and Demand Alterations Considered

To conduct the vulnerability assessment, 50-year, monthly simulations of climate are run 50 separate times in the stochastic climate generator, representing projections from 2010 to 2060. Each of these simulations represents a different realization of internal climate variability for the region. For each of these 50 simulations, the precipitation and temperature time series are adjusted several times using multiplicative and additive factors (as described in the "Analysis Methods" section) to impose different climate changes. Two broad types of climate change are examined here, including alterations to the means of monthly precipitation and temperature. Changes to monthly precipitation means are ranged from ±30% of their historic values (i.e. 7 different changes: 70%, 80%, 90%, 100%, 110%, 120%, and 130%). Temperature delta shifts are ranged from 0 to 5 degrees Celsius at 1 degree increments (6 changes total). The ranges of these changes were chosen somewhat arbitrarily, except that they were designed to range beyond the changes suggested by GCM climate projections for this region. All changes are imposed by month. In total, 50×7×6=2,100 different climate simulations are considered. For each of these simulations, the climate data are used to force the HYMOD model and develop a time series of monthly streamflows, which are then run through the water resources systems model.

Demands are increased for all municipal users throughout the system in order to evaluate the vulnerability of the water supply of Fort Hood to population growth across the region. Seven different demand scenarios are considered, ranging from 80% to 200% of current demand levels (i.e. 80%, 100%, 120%, 140%, 160%, 180%, and 200%). Demand changes are applied to the local community users only, i.e. the utilities/nearby cities with access to and authorized use of Belton Lake. 2010 demands are taken from county/utility annual demand estimates by the BRA (BGRWPG, 2011). No data was available for the Fort Hood region regarding monthly use, thus monthly demand data from a nearby watershed (Griffin and Chang, 1990) was used to parse annual demands into a monthly time series. All projections of future demand are derived by projecting forward the 2010 demands provided by the BRA. That is, seven different time series of transient, multiplicative factors are applied to 2010 demand levels for all nearby municipal users. Manufacturing, steam-electric, mining, irrigation, and livestock demand changes are minor in comparison and are not considered in this study. The downstream user demand is included in the analysis, but only applied at historical levels (each year Belton Lake has a 35% chance of being used, and the amount released from Belton Lake for the downstream users during the warm months (MJJASO) is randomly selected from a uniform distribution of yearly release data provided by the BRA from 2000 to 2010).

When the seven demand scenarios are combined with the 2,100 climate simulations, a total of 2,100×7=14,700 scenarios of the Belton Lake system are considered in this study. As done in the Fort Benning case study section, in order to avoid confusion, the ensemble of 12,600 runs will hereafter be referred to using the term "scenarios," while any information regarding the likelihood of future changes (discussed later) will be referred to using the term "projections". The large number of generated climate and demand time series allows the system to be stressed over a wide range of plausible future conditions. This enables the identification of conditions that put the most pressure on the system and cause unacceptable levels of water supply risk for Fort Hood.

All of the future scenarios explored in this analysis are summarized in Table 3 below.

Table 3 Climate and Demand Alterations Evaluated in the Vulnerability Assessment

Stressor	Range of Change	Interval	Number of Changes
Precipitation Mean	70% to 130%	10%	7
Temperature Mean	0 to 5 °C	1°C	6
Demand	80% to 200%	20%	7

Vulnerability Assessment Results

Figure 21 shows the impact of internal climate variability on several performance metrics of interest *under no change conditions*. Here, only the 50 different runs of stochastic climate variability for the combination of 100% precipitation mean, 100% demand, and 0 °C temperature change is shown. These results show the range of each performance metric that can arise simply due to natural variations in regional climate. The results in Figure 21 suggest that variations in water security performance due to internal climate variability are not trivial. Water supply reliability values range from 100% down to 98%, which is significant given that water supply reliability is often considered inadequate if it falls into the low 90% range. Average water delivery shortfalls (i.e. vulnerability) range from 0 acre-feet/month to near 700 acre-feet per month (7.5 MGD), which is roughly 70% the entire water demand of Fort Hood (10.7 MGD). The effects of climate variability can perhaps be seen best when examining storage risk. Across all 50 baseline climate simulations, the minimum storage ranges from 27% to 36% of capacity. Outliers tend to be the result of coinciding drought periods with releases from Belton Lake to meet downstream user demands. When this type of incident occurs, lake levels are subject to more severe drawdown and water use restrictions are put in place resulting in increased demand shortfalls.

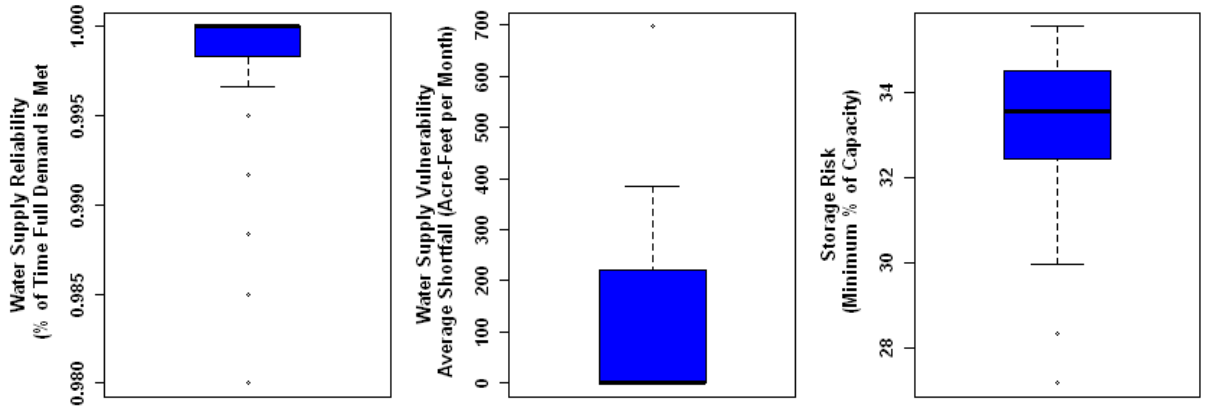

Figure 21 Boxplots of each performance metric representing no change to historical conditions over the 50 climate trials

Next, we investigate how the system responds to changes in both climate and demands. Figure 22 shows the results for water supply security at Fort Hood. Response surfaces for each of the three performance metrics (water supply reliability, vulnerability, and storage risk) are shown. Here, changes in precipitation mean are plotted against both changes in municipal demand and changes in temperature mean, with the third stressor held at its baseline level. The plots show how changes in these stressors influence the Water Supply Reliability, Water Supply Vulnerability, and Storage Risk of the Fort Hood water supply system. These response surfaces show the performance metric averaged across all 50 realizations of stochastic climate variability.

The dark solid line represents the performance metric under historic baseline conditions (i.e. the performance under the observed time series of climate and demands). The solid black line indicate the performance threshold, defined by running historical climate from 1950-2000 through the HYMOD model producing streamflows, then incorporating 2010 local community demands and 25 different time series of stochastically generated downstream user demands (calculated the same as described for the vulnerability assessment in the "Climate and Demand Alterations Considered" section for Fort Hood) through the water supply system model. The mean result from the 25 downstream demand trials is taken as the performance threshold for each metric.

The results show that precipitation mean changes have the largest impact on system performance, followed by demand and then, to a much lesser extent, temperature mean. All three metrics are highly responsive to changes in precipitation mean, as evidenced by the nearly vertical threshold line in Figure 22(b), (d), and (f). Alternatively, precipitation mean and demand changes are shown to strongly counteract each other in Figure 22(a), (c), and (e). The diagonal orientation of the threshold line indicates for an increase in precipitation, a decrease in demand must occur to attain the same metric value for any of the three metrics. In all scenarios, worst case conditions occur for an increase in demand of 200% and a precipitation mean change of 70% (top left corner of Figure 22(a), (c), and (e)). In this scenario, water supply reliability value falls to approximately 87%, water supply vulnerability increases to 700 acre-feet per month, and storage risk decreases to 20%. Conversely, best case scenarios occur when precipitation is increased to 130% and demand is lowered to 80%. In this scenario, water supply reliability value increases to nearly 100%, water supply vulnerability decreases to nearly 0 acre-feet per month, and storage risk increases to 33%.

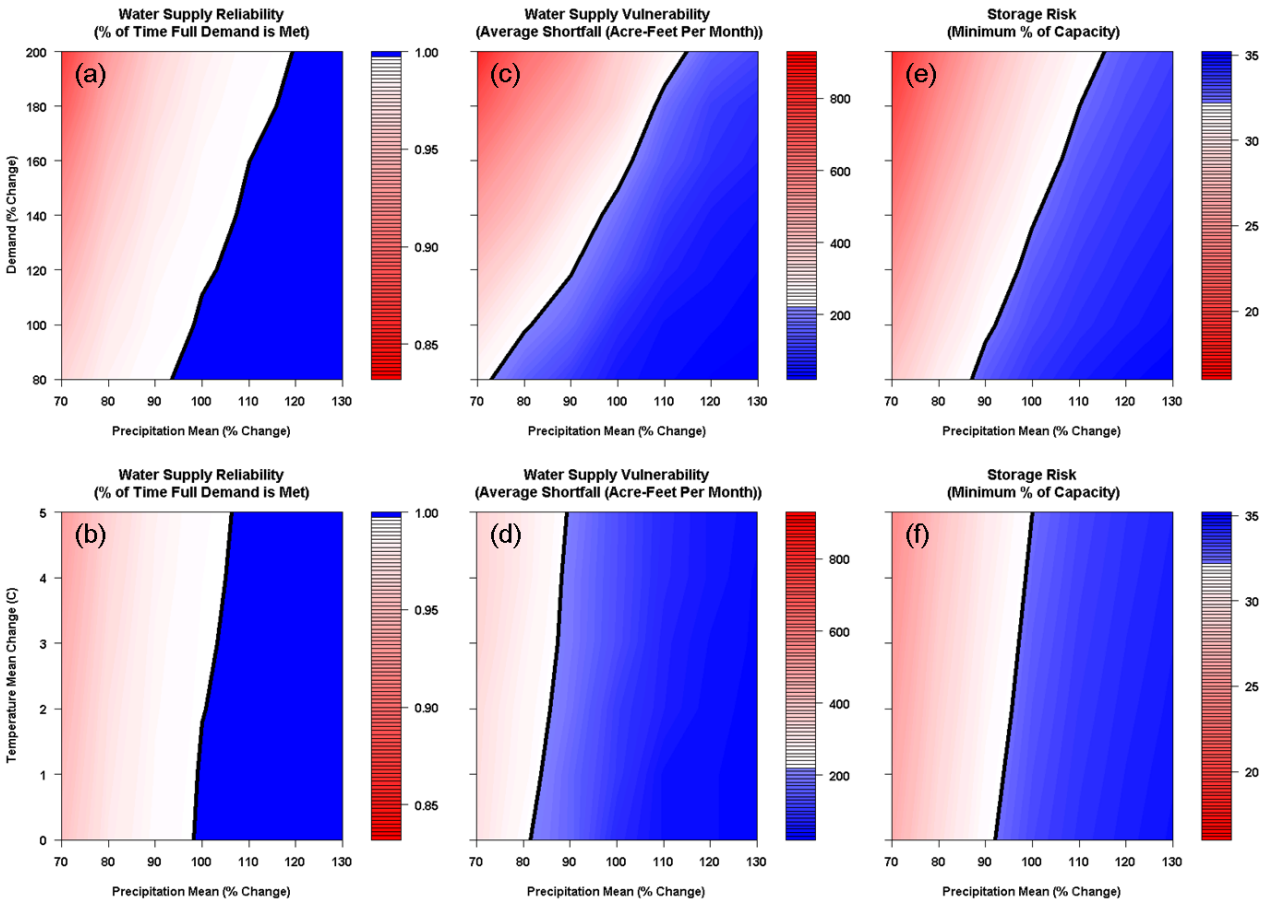

Figure 22 Response surfaces of each performance metric to changes in two stressors, with the third held constant at its baseline level. The performance metrics are contoured such that more favorable values are represented by blue while worse performance is represented by red. The thick, dark line represents the historic, baseline performance developed under the observed time series of climate and water demand.

The effects of internal variability can also interact with long-term climate and demand changes to compound the effects on water supply performance. Figure 23 shows the mean, minimum, and maximum value for each performance metric across the 50 climate simulations against one stressor variable (precipitation, temperature, or demand), with the other two stressors held constant at their baseline levels. This figure shows the relative impacts of climate variability on water supply performance and compares them to the effects of climate and socioeconomic long-term change. Several results emerge from Figure 23. First, it is clear that all performance metrics are substantially affected by climate variability, and for some, climate variability is as influential on performance as long-term change. For instance, in Figure 23(a), water supply reliability averaged across the 50 simulations is about 97% for a mean change in precipitation of 70%. However, reliability ranges between 80% and 100% across all 50 simulations for this mean precipitation change. This result is similar for many of the metrics and stressors tested.

Another result that emerges from Figure 23 is that climate variability may have more or less impact on system performance depending on the long-term climate or socioeconomic change. In

several instances (Figure 23(a,b,c,g)), the range of performance across the 50 simulations narrows substantially if the long-term change of a stressor exceeds some threshold. For example, in Figure 23(a), the range of water supply reliability is minimal if the mean precipitation change is 90% of baseline or greater. It is only when precipitation declines to 80% or less that climate variability begins to show a substantial impact on performance. However, this is different for Figure 23(d,e,f) which shows large variations in the upper bound of vulnerability for precipitation mean changes less than 100%, demand changes less than 120%, and temperature mean changes less than 2. In this scenarios, few demand shortfalls are occurring, enough so that as, for instance, precipitation mean is decreased from 80% to 70%, several shortfalls that were previously in the record no longer occur, and now one larger shortfall significantly increases the average shortfall, causing a quick rise in the upper bound from 80 to 70% precipitation mean change. On average of all the 50 stochastic climate trials, vulnerability decreases as precipitation mean increases, as expected.

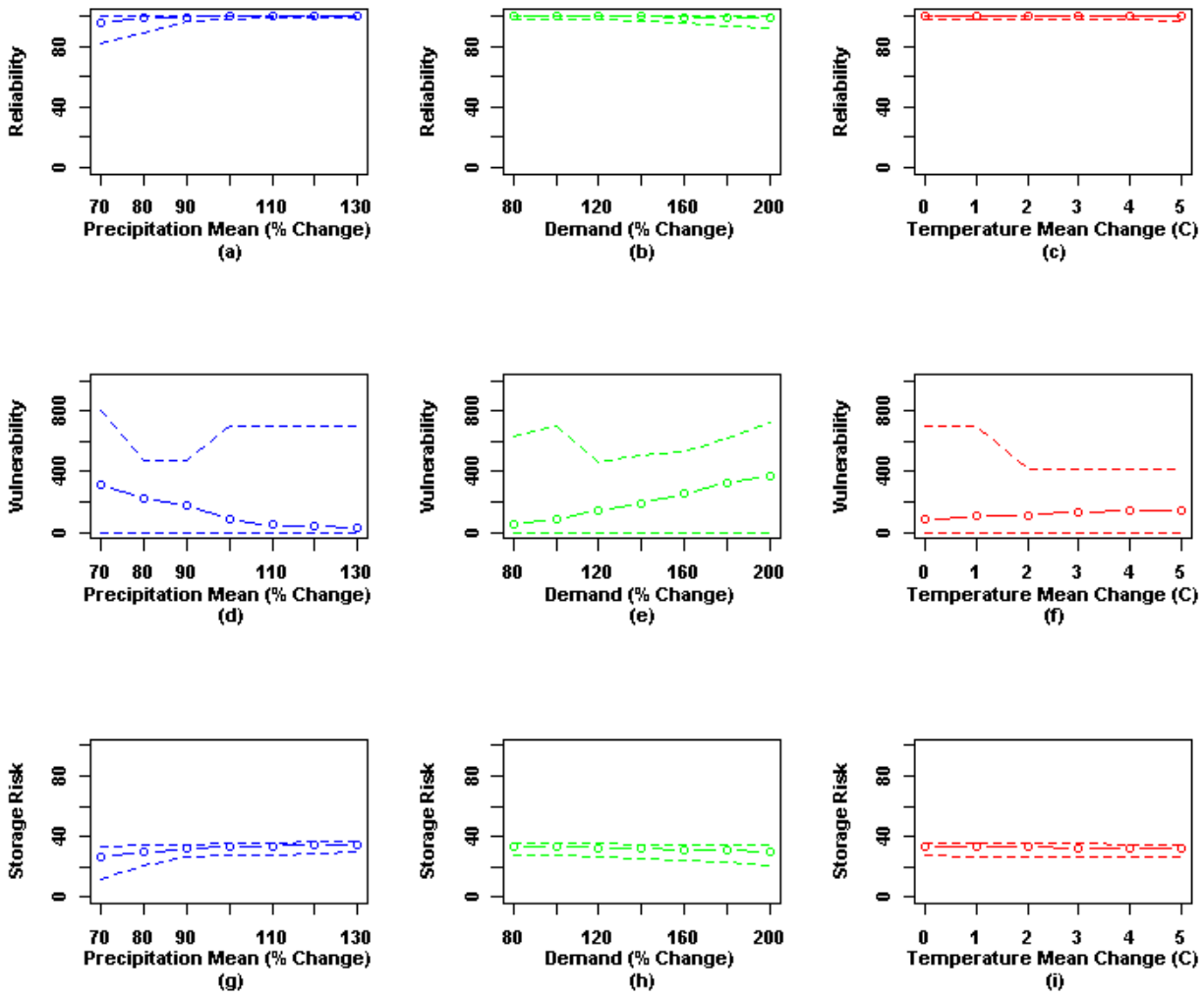

Figure 23 The response of each performance metric to a change in one stressor with the other two stresses held constant at their baseline levels. The solid line indicates the mean performance

metric under all 25 stochastic simulations, while the dashed lines represent the minimum and maximum metric from the 25 simulations.

In summary, the results of the stress test revealed that the water security of Fort Hood appears most vulnerable to declines in precipitation over the Belton Lake watershed region. Increases in water demand also contribute to the risk facing the water supply system, while the system appears only slightly sensitive to temperature increases. Internal climate variability also contributes significantly to the water supply risk of Fort Hood, particularly when long-term changes are unfavorable.

Likelihood of Future Climate Changes

After assessing the vulnerabilities of Fort Hood's water supply system to a range of future conditions, projections of future climate and water demands are used to determine how likely those futures are. Again, all information regarding future likelihoods is referred to as a "projection", while the time series of future conditions used in the stress test are referred to as "scenarios". To estimate the likelihood of future climate changes, climate projections were gathered from the Coupled Model Intercomparison Project (CMIP). Two generations of climate projections, CMIP3 and CMIP5, were gathered from this database (Reclamation, 2013). The CMIP database provides a large ensemble of future climate projections under a wide range of future carbon dioxide emissions scenarios and GCM structures. These data are available at very coarse resolutions, requiring that they be downscaled to the Belton Lake watershed. Here we use a single downscaling method for an initial assessment (the bias correction spatial disaggregation technique). Data from the downscaled climate projections were taken for a 30-year window around the year 2060, averaged over the entire Belton Lake watershed, and compared against data for 1950-2000 to determine the projected change factors for both precipitation and temperature. To estimate future changes in demand, the BRA (BGRWPG, 2011) and TWDB (2013) decadal municipal water use projections for the local communities are used.

Climate and demand projection data is shown in Figure 24. Both CMIP3 and CMIP5 climate projections show a slight co-variance between temperature mean and precipitation mean change. As temperature increases, precipitation mean tends to decrease. On average, CMIP3 projections estimate a decrease of 1.1% in precipitation and an increase in 2.4 degrees Celsius by 2060, whereas CMIP5 projections estimate and increase in 1.6% in precipitation and in increase in 2.5 degrees Celsius by 2060. The extremes of each climate projection data set do show significant differences. CMIP3 tends to have more high precipitation and low temperature changes, whereas CMIP5 tends to have more low precipitation and high temperature projections (which would significantly reduce system performance for Fort Hood). Each of the demand projections estimate significant increases in municipal water use demands by 2060. The estimate by the BRA shows a 48% increase whereas the TWDB estimate shows a 63% increase.

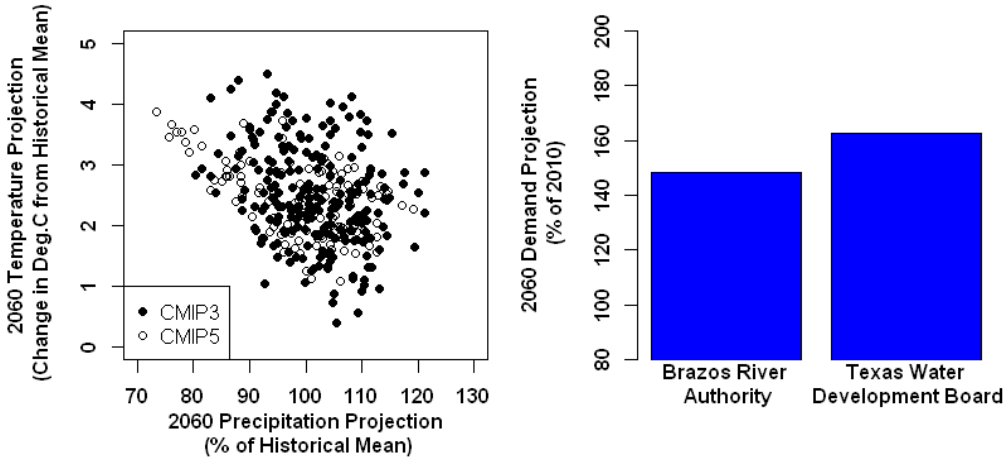

Figure 24 On the left, climate projections centered around the year 2060 from both CMIP3 and CMIP5 are shown. On the right, 2060 demand projections calculated by the BRA and TWDB are shown. The demand projections consider municipal water use changes for both Fort Hood and the surrounding communities with water rights to Belton Lake.

Assessment of Future Risks and System Robustness

The results of the vulnerability assessment can be coupled with the analysis of the likelihood of future change to determine how likely problematic futures are to occur and whether the water supply of Fort Hood is robust to these risks. Figure 25 shows the climate and demand projections superimposed on the contour plots of Figure 22.

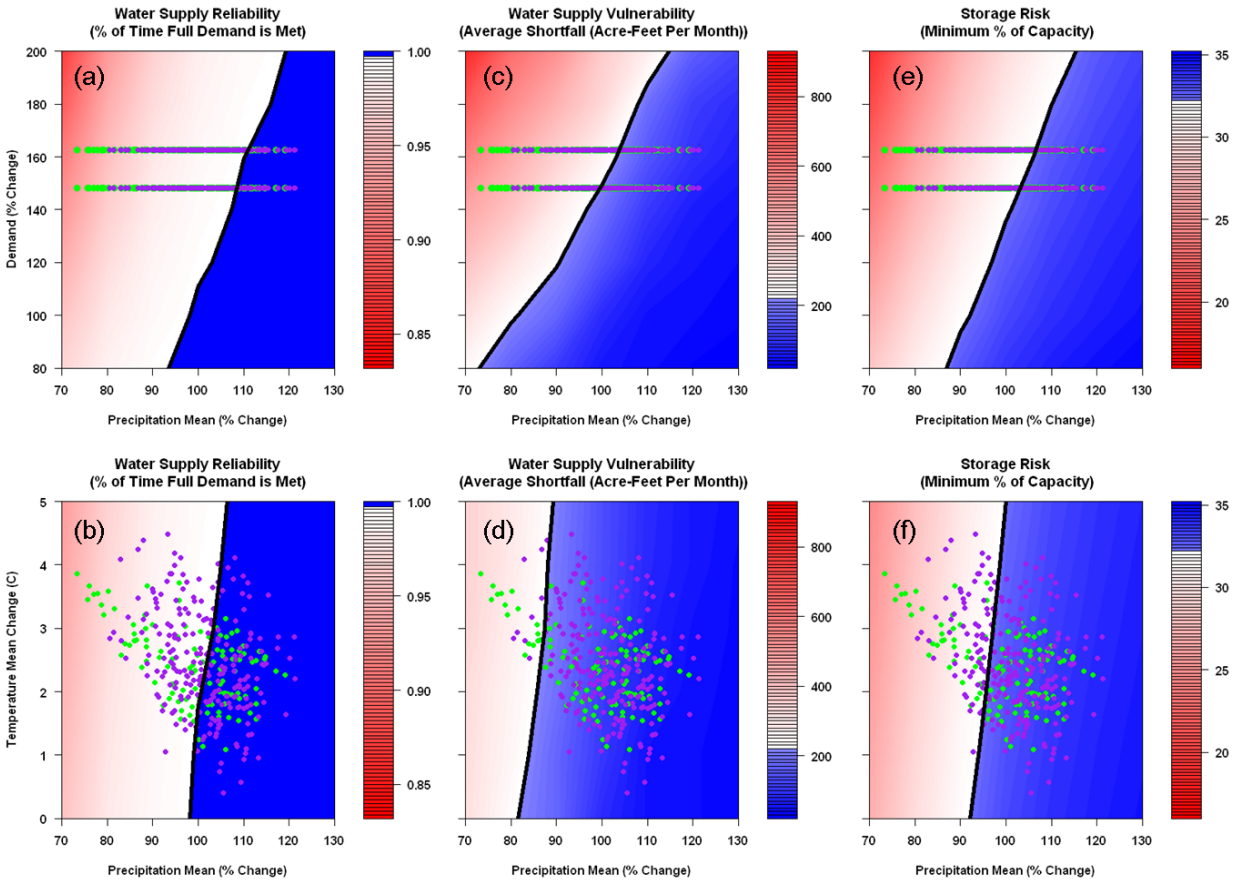

Figure 25 Filled contour plots of each performance metric coupled with both the CMIP3 (purple circles) and CMIP5 (green circles) climate projections and the BRA and TWRA demand projections for the year 2060. Because the climate and demand projections were developed independent of one another, each climate projection was coupled with every demand projection, leading to the horizontal orientation of the projections in (a), (c), and (e).

Unacceptable conditions (into the redder region) are compared against acceptable conditions (into the bluer region) and are separated by the performance threshold previously defined by the historical conditions baseline performance. In all cases projections both fall in acceptable and unacceptable conditions. The climate projections are spread throughout much of the impact space of the stress test, whereas the coupled demand and precipitation mean projections, while covering a wide range of precipitation, only coincide with two demand projections. For these levels of demand increase, a significant gain in precipitation must also occur to maintain the performance threshold set by the no change conditions. In Figure 25(a,b,c,e) the majority of projections are unacceptable, whereas only for Figure 25(d,f) the majority of projections are acceptable. Projections of future climate and water demand suggest that water supply at Fort Hood is at high risk of failure.

Two types of robustness measures are estimated for this system: unconditional and conditional. Each type of robustness is reported for each system model performance metric and is averaged over the 50 stochastic climate trials.

Unconditional robustness for a specific performance metric, Figure 26, is the percentage of the impact space developed in the stress test in which conditions are better than or equal to the performance metric threshold. Without taking into account any future projections, the unconditional robustness for each metric is between 40% and 45%. This is expected as the majority of runs performed in the vulnerability assessment cause less water to be in the lake (increase in demand, decrease in precipitation, and increase in temperature), causing unconditional robustness values to be less than 50%. These values indicate that water supply performance is very sensitive to many of the future scenarios that were tested.

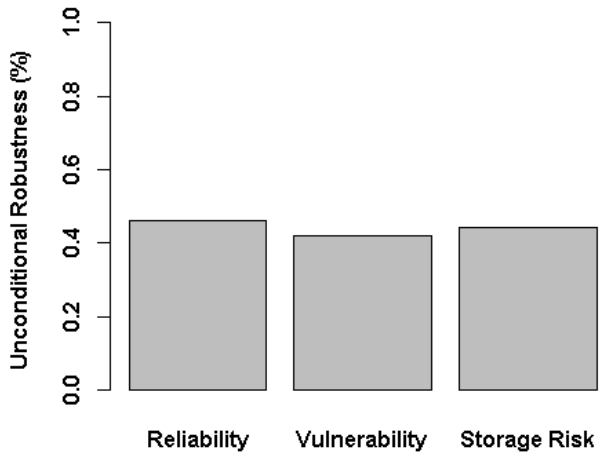

Figure 26 The unconditional robustness of each water supply performance metric, which equals the ratio of all acceptable climate and demand scenarios to the total number of scenarios tested.

Conditional robustness, Figure 27, is defined as the number of climate change and water demand projections (2 total – CMIP3 Climate / BRA+TWDB Demand, CMIP5 Climate / BRA+TWDB Demand) that fall into an acceptable space of water supply performance divided by the total number of projections considered. This conditional robustness value inherently weights all projections evenly. The results show that each of the performance measures are expected to perform worse than the historical baseline conditions. In particular, the CMIP3 climate projection combined with each demand projection results in approximately 32% for each metric. When using the CMIP5 climate projection instead, robustness values increase to approximately 38% for each metric, a significant increase in robustness when compared against the CMIP3 result. However, each of these results are significantly impacted by the two demand projections, versus the 112 CMIP3 and 234 CMIP5 projections. Because the demand increases are high, in the majority of scenarios the result is considered unacceptable, leading to a moderate to significant decrease when compared to the unconditional robustness metric.

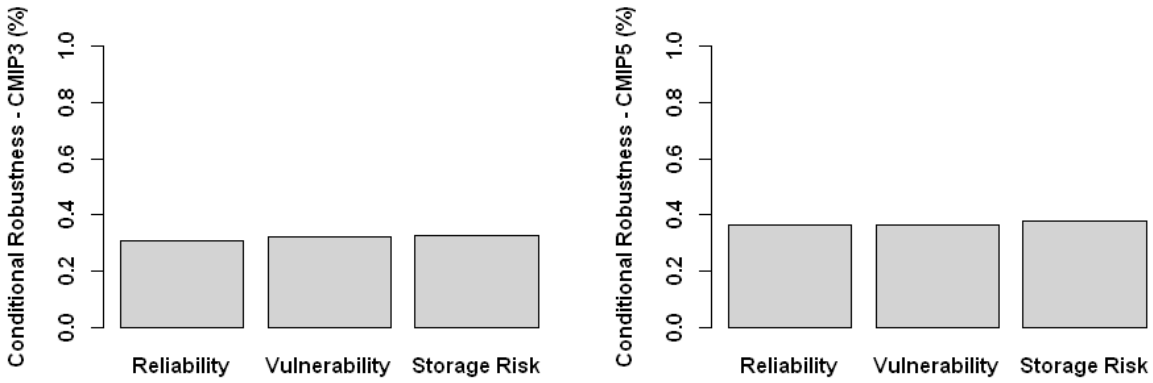

Figure 27 The conditional robustness of each water supply performance metric for the CMIP3 and CMIP5 projections. The conditional robustness equals the ratio of the number of climate and demand projections that are acceptable to the total number of projections examined.

Conclusions

This case study presented a risk assessment of the water supply system serving Fort Hood in Belton, TX. An initial vulnerability assessment was used to determine the future conditions that led to unacceptable water supply performance for the installation. This analysis showed that Fort Hood's water supply is highly sensitive to small decreases in average precipitation over the region, highly sensitive to increasing water demands, and relatively insensitive to increasing temperatures. Internal climate variability was also shown to strongly influence water supply performance, especially if underlying long-term trends were unfavorable for water supply security.

Climate and water demand information was then gathered to determine the likelihood of different future conditions. Climate projections showed a wide spread of possible outcomes, but many suggested that warmer and drier conditions were likely in the future. Demand projections all agreed that water demands would increase, but the magnitude of this increase ranged widely.

The results of the vulnerability assessment and the assessment of likelihoods of future change were combined to determine how robust Fort Hood's water supply system is to future change. Both unconditional and conditional robustness measures suggest that there is significant risk to the security of Fort Hood's water supply, although the conditional risks based on future climate and demand projections are significantly higher than the unconditional risks. Overall, the results of the analysis suggest that adaptation measures should be considered to make the water supply of Fort Hood more robust to future climate and socioeconomic conditions.

Case Study 3: U.S. Air Force Academy, CO

Background and Problem Framing

Any assessment of the climate-related water resource risks to the United States Air Force Academy (USAFA) needs to focus on the risks facing the serving utility, in this case the Colorado Springs Utility (CSU) (Figure 28(b)). The CSU water collection system serves an estimated 458,000 people, including the residents of Colorado Springs, the Ute Pass communities west of the city, and several military installations, including the USAFA. Currently, the firm yield of potable and non-potable water for the system is about 152,000 acre-feet per year, with potable deliveries at approximately 22 billion gallons per year. CSU estimates that they currently have enough water to meet the demand of their customers until approximately 2040, assuming average projections of population growth, per capita water demand changes, and the completion of planned infrastructure projects. These assumptions do not account for any changes in climate, however, and beyond 2040 additional water demands also become a substantial concern.

The CSU water collection system acquired their water from two primary sources, the Upper Colorado (Figure 28 (a)) and the Arkansas River Basins (Figure 28(b)). The Upper Colorado River Basin is one of the most developed and complicated water systems in the world. Waters from the Colorado serve people in seven states and Mexico and are allocated according to a complex set of compacts and water rights provisions. CSU holds one such water right, albeit a junior right, and acquires approximately 70% of its annual water supply through four trans-mountain diversions that divert water across the continental divide into storage reservoirs operated by CSU. In this way, the water supply security of the USAFA is directly linked to the broader water supply risks facing the entire Colorado River Basin. The remaining 30% of CSU water supply is derived from local runoff in the Arkansas River Basin that must also be shared with users downstream of Colorado Springs. In order to assess the climate-related risks to CSU (and thus USAFA) water supply, both the Upper Colorado and Arkansas systems need to be accounted for in the analysis. This presents a substantial challenge that required significant modeling efforts and persistent collaboration and communication with the CSU engineering team. The decision-scaling analysis presented below represents a multi-year collaboration with engineering support staff at CSU and composes a substantial portion of the ongoing CSU Integrated Water Resources Planning process.

In this USAFA case study, focus is given to a novel component of the analysis that relates to how we assess climate change uncertainty and integrate that evaluation with the vulnerability assessment to describe climate-related risks to water supply. Specifically, we explore the issue of climate model similarity – a phenomenon whereby climate models have similar code and parameterizations across global research centers, leading to correlated projections and reduced information content in model ensemble output - and demonstrate how this issue can affect decisions related to adaptation measures taken by water utilities serving training installations (and thus relevant to DoD decision makers).

In addition to the decision-scaling analysis applied to the case study of CSU, another major effort is given to additional hydrologic modeling efforts for Arkansas River, one of the two major water sources for the system that serves the USAFA. To do this, the Variable Infiltration

Capacity (VIC) hydrologic model (Liang et al., 1994) is designed to simulate the Arkansas River headwaters. We address how the model performance can be improved in terms of its ability to reproduce snow resources as well as streamflow by applying various calibration approaches.

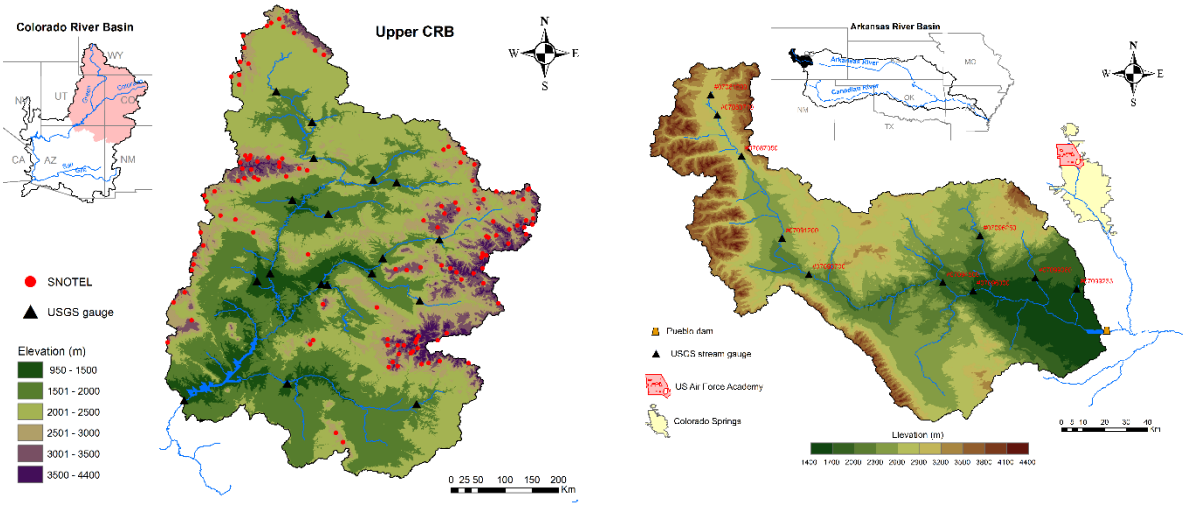

(a) (b)

Figure 28 (a) Map of the Upper Colorado River Basin. (b) Map of the Upper Arkansas River Basin and United States Air Force Academy located in Colorado Springs, CO.

Vulnerability Assessment

In the vulnerability assessment CSU system performance is systematically tested over a wide range of annual mean climate changes to determine under what conditions the system no longer performs adequately. This stress test is driven using a daily stochastic weather generator that creates new sequences of climate that simultaneously exhibit different long-term mean conditions and alternative expressions of natural climate variability. These weather sequences are passed through a series of hydro-system models of the relevant river basins and infrastructure network to estimate how these changes in climate will translate into altered water availability for the customers of CSU, including the Air Force Academy. The results of the stress test are summarized in a climate response surface, which provides a visual depiction of changes in critical metrics of system performance to changes in the climate parameters altered in the sensitivity analysis. The different components of the vulnerability assessment are detailed below.

Stochastic Climate Generator

This work utilizes a stochastic weather generator (Steinschneider and Brown, 2013) to produce the climate time series over which to conduct the vulnerability analysis. The weather generator couples a Markov Chain and K-nearest-neighbor (KNN) resampling scheme to generate appropriately correlated multi-site daily weather variables (Apipattanavis et al., 2007) with a Wavelet Autoregressive Modeling (WARM) framework to preserve low-frequency variability at

the annual time scale (Kwon et al., 2007). A quantile mapping technique is used to post-process simulations of precipitation and impose various distributional shifts under possible climate changes; temperature is changed using simple additive factors. The parameters of the model can be systematically changed to produce new sequences of weather variables that exhibit a wide range of characteristics, enabling detailed climate sensitivity analyses. The scenarios created by the weather generator are independent of any climate projections, allowing for a wide range of possible future climates to be generated. Furthermore, climate scenarios exhibiting the same mean climate changes can be stochastically generated many times to explore the effects of internal climate variability. The preservation of internal climate variability is particularly important for the CSU system because precipitation in the region exhibits substantial decadal fluctuations that can significantly influence system performance (Nowak et al., 2012; Wise et al., 2015). The stochastic model is designed to reproduce this low-frequency quasi-oscillatory behavior; many downscaled climate projections often fail in this regard (Johnson et al., 2011; Rocheta et al., 2014; Tallaksen and Stahl, 2014).

The WARM component of the weather generator was fit to annual precipitation data over the Upper Colorado River Basin. This data was provided by CSU and is derived from the DAYMET database (Thornton et al., 2014). The WARM model is used to simulate time series of annual precipitation averaged over the Upper Colorado Basin with appropriate inter-annual and decadal variability. A Markov Chain and KNN approach is then used to resample the historic daily data to synthesize new daily time series, with the resampling conditioned on the annual WARM simulation. The data is resampled for both the Upper Colorado and the Arkansas River Basins to ensure consistency between the synthesized climate data across both regions. In this way, the major modes of inter-annual and decadal variability are preserved in the simulations, as is the daily spatiotemporal structure of climate data across both the Upper Colorado and Arkansas River Basins.

CSU Hydro-Systems Models

The climate scenarios from the weather generator are used to drive hydrosystem models that simulate hydrologic response, water availability and demand, and infrastructure operations in the river basins that provide water to CSU. The output of the hydrosystem model simulations under each climate time series is used to create a functional link between water supply risk and a set of mean climate conditions. The CSU system requires two separate hydrosystem models because water is sourced from both the Upper Colorado River Basin on the western side of the continental divide, as well as from the headwaters of the Arkansas River on the eastern side of the divide. These models are described in more detail below.

- *Upper Colorado River Basin Hydrosystems Model*

The Water Evaluation and Planning System (WEAP) model (Yates et al. 2005) was used to simulate the hydrologic response, reservoir operations, withdrawals, and transmountain diversions of the Upper Colorado River Basin system. By necessity the WEAP model simplifies the extreme complexity of the Upper Colorado system, yet still requires nearly 40 minutes per 59-year (period-of-record) run on a standard desktop computer (HP Z210 Workstation with a 3.40 GHz processor and 18.0 GB of RAM). The WEAP model approximates how the climate scenarios developed above translate into changes in water availability for users throughout the

Colorado River system. Importantly, the WEAP model of the Upper Colorado simulates the availability of water for transfer across four trans-mountain diversion points that feed into the CSU system. Changes in these diversions substantially alter the water available for CSU and its customers (i.e., USAFA).

The WEAP model of the Upper Colorado was developed by David Yates at the University Corporation of Atmospheric Research and was made available for this project. Because of its complexity, WEAP model simulations were the rate-limiting step in the vulnerability analysis conducted for the CSU system. The computational expense of these simulations acted as a major motivation behind our choice of using a limited number of climate scenarios in the vulnerability assessment.

- *Upper Arkansas River Basin Hydrosystems Model*

The transmountain diversions estimated by the WEAP model are used to force a MODSIM-DSS model (Labadie et al. 2000) that represents the Eastern slope waterworks system operated by CSU. In addition to these diversions, the MODSIM model requires additional inflow data to a variety of nodes, but these inflows cannot be modeled as natural hydrologic response to meteorological forcings because there are legal constraints on the inflows not account for by MODSIM. Therefore, historical years of inflow data, which implicitly account for legal constraints, are resampled from the historic record in all future simulations. To ensure these flows are correctly correlated with the Western slope simulations from WEAP, the stochastic weather generator is used to produce synthetic weather simultaneously across both Western slope and Eastern slope regions. Natural streamflow response from the Eastern slope system under synthetic climate is estimated using the hydrologic model in WEAP calibrated to naturalized flows in the Arkansas River. A nearest-neighbor resampling scheme is then used to resample historic years based on a comparison between historical, naturalized Arkansas River streamflow and modeled hydrology of the Arkansas River under synthetic climate. Inflow to all MODSIM nodes besides those associated with Western slope diversions are then bootstrapped for use in future simulations based on the resampled years. One major drawback of this approach is the simplicity of the WEAP hydrologic model used to simulate natural flow in the Arkansas River. Part II of this case study addresses this limitation through the development of a more sophisticated hydrologic model of the basin.

Climate and Demand Alterations Considered

The weather generator described above is used to generate daily, 59-year (period-of-record length) climate sequences with different mean temperature and precipitation conditions that maintain the historic decadal variability in the observed data (McCabe et al., 2004; McCabe et al., 2007). To impose various climate changes in simulated weather time series, multiplicative (additive) factors are used to adjust all daily precipitation (temperature) values over the simulation period, thus altering their mean annual values. Annual changes are most important for the long-term planning purposes of the CSU system because the significant reservoir storage on both sides of the continental divide largely mitigates the impact of seasonal changes to runoff and snowmelt timing, consistent with classical reservoir operations theory (Hazen, 1914; Barnett et al., 2005; Connell-Buck et al., 2011). This does not preclude the importance of other hydrologic characteristics for long-term planning, such as the effects of climate extremes on

flood reduction capacity or water quality, but these issues are not addressed in this study. Annual changes to the precipitation mean are varied from -10% to +10% of the historic mean using increments of 5% (5 scenarios altogether), while temperature shifts are varied from approximately -1°C to +4°C using increments of 0.5°C (10 scenarios). These changes were chosen to ensure the identification of climate changes that cause system failure. Each of the 50=5×10 scenarios of climate change is simulated with the weather generator 7 times to partially account for the effects of internal climate variability while balancing the computational burden of the modeling chain, leading to a total of 350=5×10×7 weather sequences.

The 7 realizations of internal climate variability were selected in a collaborative process with the CSU engineering team as part of their Integrated Water Resources Planning process. The 7 series were chosen amongst 10,000 original weather generator simulations to span the range of natural climate fluctuations that could influence the system. This selection proceeded in two steps. First, 40 simulations were selected from the original 10,000 to symmetrically span the empirical distribution of a precipitation-based drought metric preferred by the utility. Second, the subset of 40 simulations was run through the hydrosystem models (described below), and 7 final simulations were chosen that spanned the empirical distribution of minimum total system reservoir storage across the 40 runs. Long-term climates changes were then imposed on these final 7 climate simulations and then used to force the hydrosystem models, producing a comprehensive vulnerability assessment that maps CSU system performance to long-term climate changes while also accounting for the effects of internal climate variability.

CSU considers two scenarios for water demands on their system. The first scenario is considered the Status Quo and reflected current water demands after accounting for the connection of several communities to the system's supply that is to be completed by 2016. The second demand scenario, referred to as "Build-Out Conditions", reflects a substantial increase in system demand. No date is associated with the water demands of the "Build-Out" scenario, but it is assumed that under current growth projections this level of demand will be reached around the year 2050. The stress test is repeated for both of these water demand scenarios to enable as assessment of the relative importance of climate and water demand changes on water resources vulnerability and risk.

Uncertainty Assessment of Future Climate Change

Background

Over the past decade the climate science community has proposed different techniques to develop probabilistic projections of climate change from ensemble climate model output. The most recent efforts (Groves et al., 2008; Manning et al., 2009; Hall et al., 2012; Christierson et al., 2012) for risk-based long-term planning have relied on climate pdfs from perturbed physics ensembles (PPEs) (Murphy et al., 2004), a Bayesian treatment of multi-model ensembles (MMEs) (Tebaldi et al., 2005; Lopez et al., 2006; Smith et al., 2009; Tebaldi and Sanso, 2009), or a combination thereof (Sexton et al., 2012). In a PPE, multiple climate runs are performed using a single model with unconstrained model parameters varied across the ensemble. PPEs, though systematic in addressing the parameter uncertainty of a single model, ignore structural uncertainties between models, or differences in the underlying assumptions of the governing

physics of certain physical processes. Bayesian methods for combining MMEs address these structural uncertainties, but they suffer from a variety of statistical challenges (Knutti et al., 2010), including the choice of metric(s) to judge model credibility and questionable assumptions of stationary model bias (Tebaldi and Knutti, 2007; Stephenson et al., 2012). Of interest here, probabilities of change based on MMEs often assume each individual climate model in an MME serves as an independent representation of the Earth system. This assumption ignores that many GCMs follow a common genealogy and supposes a greater effective number of data points than are actually available (Pennell and Reichler, 2011). Following Masson and Knutti (2011) and Knutti et al. (2013), we consider models to share a common genealogy, or be within the same family, if those models were developed at the same institution or if one is known to have borrowed a substantial amount of code from the other (e.g., the entire atmospheric model). It is common for model parameterizations and code to be shared not only between models developed at the same institution but also across modeling centers (Masson and Knutti, 2011). Models that share large blocks of code, especially in the atmosphere, often result in similar climate conditions, implying that they are not independent representations of the Earth's system (Knutti et al., 2013). Even models that fundamentally differ with respect to certain underlying processes have been shown to result in similar climate representations if they were developed at the same institution, possibly because modeling centers typically use the same observational datasets to evaluate and calibrate the present-day-climate conditions for all of their models (Abramowitz and Bishop, 2015).

To address this issue, recent work has explored methods to optimally choose a subset of models to capture the information content of an ensemble (Evans et al., 2013) or to weight models based on the correlations in their error structure over a hindcast period (Bishop and Abramowitz, 2013). This latter approach of independence-based weighting has recently shown promise in ensuring that observations and the ensemble of projections are more likely to be drawn from the same distribution (Abramowitz and Bishop, 2015) and consequently improve estimates of the ensemble mean and variance for climate variables of interest (Haughton et al., 2015). As noted in Haughton et al. (2015), improvements from independence-based weighting could provide substantial gains in projection accuracy and uncertainty quantification that may be relevant for informing adaptations to large climate changes.

Here we build on the work of Bishop and Abramowitz (2013), Abramowitz and Bishop (2015), and Haughton et al. (2015) to present an attempt to formally account for cross-model correlations in pdf development and risk assessment of local climate change. We use an ensemble of projections from the Coupled Model Intercomparison Project Phase 5 (CMIP5) to develop probabilistic climate information, with and without an accounting of inter-model correlations, for the river basins serving the CSU system and use the pdfs to estimate mid-century climate-related risks to the water supply security of CSU (and USAFA).

Methods

CMIP5 (Taylor et al., 2012) model output was bilinearly interpolated onto a 1º grid and then averaged over the CSU region. Rather than extending the independence-based weighting scheme of Bishop and Abramowitz (2013), probability distributions for mid-century temperature and precipitation change are developed based on adjustments to a previous lineage of Bayesian methods (Tebaldi et al., 2005; Lopez et al., 2006; Smith et al., 2009; Tebaldi and Sanso, 2009).

We let X_i^T and X_i^P be the temperature and precipitation, respectively, simulated by the i[th] climate model, annually and regionally averaged over a 30-year window representing current climate. Y_i^T and Y_i^P similarly represent average future temperature and precipitation. If we assume no correlation structure between models of the same family, then X_i^T, X_i^P, Y_i^T, and Y_i^P are all assumed to follow univariate Gaussian distributions:

$$X_i^T \sim N\left(\mu^T, {\lambda_i^T}^{-1}\right)$$
$$X_i^P \sim N\left(\mu^P + \tau(X_i^T - \mu^T), {\lambda_i^P}^{-1}\right)$$
$$Y_i^T \sim N\left(\nu^T + \beta^T(X_i^T - \mu^T), \theta^T {\lambda_i^T}^{-1}\right)$$
$$Y_i^P \sim N\left(\nu^P + \beta^P(X_i^P - \mu^P) + \tau(Y_i^T - \nu^T), \theta^P {\lambda_i^P}^{-1}\right)$$

Here, baseline means μ^T, μ^P and future means ν^T, ν^P are assumed to be the true mean values for the region. The parameters of interest $\Delta T = \nu^T - \mu^T$ and $\Delta P = \nu^P - \mu^P$ quantify the expected temperature and precipitation change. Precision (i.e., inverse variance) parameters λ_i^T, λ_i^P act as a measure of how well each model represents the temperature and precipitation response to natural and anthropogenic forcing. Baseline and future climate are assumed related through the linear coefficients β^T, β^P, and the parameters θ^T, θ^P allow the precision to vary from the current to the future period. The parameter τ allows for mean precipitation and temperature to be correlated across models. All parameters are estimated in a Bayesian framework, with prior distributions the same as found in previous studies (Smith et al., 2009).

The observed mean temperature and precipitation over the baseline period are also assumed normally distributed:

$$X_0^T \sim N\left(\mu^T, {\lambda_0^T}^{-1}\right)$$
$$X_0^P \sim N\left(\mu^P + \tau(X_0^T - \mu^T), {\lambda_0^P}^{-1}\right)$$

Here, the variance parameters ${\lambda_0^T}^{-1}, {\lambda_0^P}^{-1}$ are set equal to the variance of the observed data divided by the number of annual observations. Since these variances are relatively small with 30 years of baseline period data, the parameters $\mu^T$and μ^P are anchored near the observed means. If the differences $X_i^T - X_0^T$ and $X_i^p - X_0^P$ for the i[th] model are large, then the temperature bias $X_i^T - \mu^T$ and precipitation bias $X_i^p - \mu^P$ will also likely be large, requiring the precision parameters λ_i^T, λ_i^P for that model to decline. As λ_i^T and λ_i^P decrease, the i[th] model exerts less influence on the estimated climate changes ΔT and ΔP and is assumed to be less representative of the true regional climate system.

To account for intra-family model correlations, the above model is reformulated to consider all climate model data distributed according to a multivariate Gaussian model:

$$\boldsymbol{X^T} \sim N(\boldsymbol{\mu^T}, \boldsymbol{\Sigma^T})$$
$$\boldsymbol{X^P} \sim N(\boldsymbol{\mu^P} + \tau(\boldsymbol{X^T} - \boldsymbol{\mu^T}), \boldsymbol{\Sigma^P})$$
$$\boldsymbol{Y^T} \sim N(\boldsymbol{\nu^T} + \beta^T(\boldsymbol{X^T} - \boldsymbol{\mu^T}), \theta^T \boldsymbol{\Sigma^T})$$

$$\boldsymbol{Y^P} \sim N(\boldsymbol{\nu^P} + \beta^P(\boldsymbol{X^P} - \boldsymbol{\mu^P}) + \tau(\boldsymbol{Y^T} - \boldsymbol{\nu^T}), \theta^P \boldsymbol{\Sigma^P})$$

Mean temperature and precipitation data from all climate models are included in the vectors $\boldsymbol{X^T}, \boldsymbol{X^P}, \boldsymbol{Y^T}, \boldsymbol{Y^P}$. All elements of each mean vector $\boldsymbol{\mu^T}, \boldsymbol{\mu^P}, \boldsymbol{\nu^T}, \boldsymbol{\nu^P}$ are the same, i.e., $\boldsymbol{\mu^T}$ is a vector of repeated values μ^T. The variance-covariance matrices $\boldsymbol{\Sigma^T}, \boldsymbol{\Sigma^P}$ have the variance parameters $\lambda_i^{T^{-1}}, \lambda_i^{P^{-1}}$ along their diagonal. If all off-diagonal terms of the matrices $\boldsymbol{\Sigma^T}, \boldsymbol{\Sigma^P}$ are set to zero, the univariate and multivariate models are equivalent. However, the covariance matrices are augmented to account for intra-family model correlations. For models i and j that belong to the same model family, the ith,jth off-diagonal terms of $\boldsymbol{\Sigma^T}$ and $\boldsymbol{\Sigma^P}$ are set equal to $\rho^T \lambda_i^{T^{-1/2}} \lambda_j^{T^{-1/2}}$ and $\rho^P \lambda_i^{P^{-1/2}} \lambda_j^{P^{-1/2}}$, respectively. The model families are set to be the same as in a previous study on climate model genealogy (Knutti et al., 2013). The parameters ρ^T and ρ^P quantify the correlation between the climate information from the ith and jth models, are assumed to be constant across all model families, and are given uniform priors between -1 and 1. Off-diagonal covariance terms of $\boldsymbol{\Sigma^T}, \boldsymbol{\Sigma^P}$ corresponding to models not in the same family are set to zero.

Climate change pdfs from both methods are coupled with the previously described vulnerability assessment of the CSU water resources system to estimate climate-related risk to water supply. The probability that climate change will lead to inadequate future performance is estimated by sampling 10,000 samples of ΔT and ΔP using the pdfs from above and counting the fraction of samples that coincide with climate changes in the vulnerability assessment with indoor water demand shortfalls (Moody and Brown, 2013).

VIC Calibration

Hydrologic models have been an essential tool used to better understand how natural and anthropogenic impacts may affect water systems. A better understanding of the water system can be achieved by a well-calibrated hydrologic model leading to accurate prediction of water availability. There are many choices of hydrologic models each with their own set of calibration challenges, so there is a need to develop a strategy to improve calibration results.

The Variable Infiltration Capacity (VIC) is a gridded hydrologic model developed by Liang et al. (1994) which solves mass and energy balances to determine hydrological water fluxes (e.g., runoff, infiltration, evapotranspiration etc.) through each grid cell. Not only is the surface gridded, but each cell is further divided into various land covers and multiple soil layers. Outflows simulated by VIC for each grid cell are coupled with a separate routing model that produces streamflow at any locations of interest inside the basin (e.g., basin outlet). A snow module developed by Andreadis and Lettenmaier (2006) has been imbedded into VIC and outputs snow fluxes for each individual grid cell. Snow is an important part of the hydrologic cycle, and greatly impacts the surface energy and water balances of a system where snow forms a large part of the water resources. The importance of accurately modeling snow in a hydrologic model is widely acknowledged (Duethmann et al., 2014; Kim and Kaluarachchi, 2014), although here have not been many efforts to take the snow process into consideration for the model calibration purpose.

The headwaters of Arkansas River is such a snow-dominated basin. To define the area for VIC simulation, watershed delineation was performed based on the USGS gauge 07083710, which isolate a part of the Arkansas River headwaters as the VIC domain (as shown in Figure 29). This area of headwaters were analyzed since the gauges in this region represent more natural streamflow than further downstream where regulations will cause inaccurate flow values; calibration difficulties will arise when using regulated stream gauges.

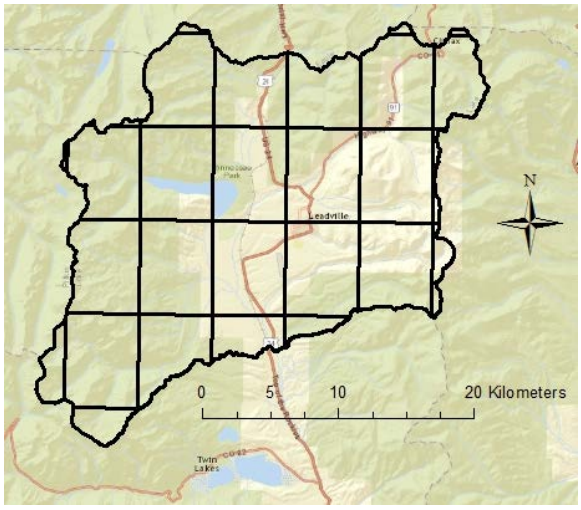

Figure 29 Arkansas River watershed headwaters with grid cells based on 1/16^{o} spatial resolution climate inputs.

To calibrate the VIC built on the Arkansas River headwaters, we employed the multi-objective optimization based on Genetic Algorithm (GA) (Wang, 1991) to help a compromise of two calibration targets that are important to take into account: streamflow at the basin outlet and snow covered area (SCA). This calibration effort is particularly important because well-calibrated models only against streamflow can lead to simulations with large errors in snow cover (Duethmann et al., 2014), basically leading to getting a seemingly good results with wrong representations of internal hydrological processes. Moreover, studies showed that models can be calibrated well to both streamflow and snow cover without large tradeoffs (Duethmann et al., 2014) and calibrating to snow cover and depth helps improve steamflow simulation (Tanmoyee et al., 2015).

Although VIC has been used successfully, many optimization schemes to calibrate VIC have not been used to its full potential, mainly due to the considerably high computational cost required to perform a large number of VIC runs. To manage the computation burden, we utilized the parallel computing power provided by the Massachusetts Green High-Performance Computing Center (MGHPCC), from which several thousands of processors are available. The calibration processes are described in more detail below.

Data

Gridded daily precipitation, temperature, and wind speed data were acquired to use as historic forces for the hydrologic model (available from 1915-2011) (Livneh et al., 2014). The State Soil Geographic Database (STATSGO) dataset data provided by the USGS was used for soil layer

information (available from 1995) (Schwarz and Alexander, 1995). Vegetation type was provided by the Advanced High Resolution Radiometer (AVHRR) satellite which contains global land cover information at 1 km resolution (available from 1981-1994) (Hansen et al., 2000). Fractional snow covered area (SCA) was obtained from the Terra sensor on the MODIS (MODERATE RESOLUTION IMAGING SPECTRORADIOMETER) satellite (MOD10A1) at 500m resolution; the data is provided by the national Snow and Ice Data Center (NSIDC) (daily data available from 2000 – 2014) (Hall et al., 2006).

Methods

The VIC model set-up is based on the version 4.1.2.g. A baseline run was first established by using the default parameter values, and then a sensitivity analysis was conducted to discern which parameters have large influences on the simulated hydrograph. To find an optimal parameter set of the VIC, the calibration was first executed for streamflow, and then a separate calibration task performed in which the SCA remote sensing data is used as calibration target. A multi-objective GA optimization was also run to calibrate to streamflow and SCA at the same time. More details on the GA are provided in following.

The VIC model was gridded at 1/16° resolution based on the climate inputs of Livneh et al. (2014), and in-grid variation in the soil and vegetation information was extracted for each cell. Consequently, for the Arkansas headwaters delineated for the USGS gauge 07083710, 29 grid cells are identified to overlap the VIC modeling domain (Figure 29).

To calibrate the VIC, we first determined a subset of the VIC parameters to be calibrated and then tested three different calibration approaches: two single objective calibrations (one objective is for streamflow and the other is for SCA) and a multi-objective calibration (both streamflow and SCA being targeted simultaneously). The USGS gage at the basin outlet provides the observed streamflow data available from 2004 – 2014. Consequently, the VIC runs for the period 2004-2011 for which both the streamflow observation and satellite SCA images are available. The model was allowed one year of ramp up (2004), the calibration period was defined over 3 years (2005-2007), and the following 4 years (2008-2011) was used for the purpose of validating VIC performance for periods other than the calibration period.

- *Selection of Calibration Parameters*

A sensitivity analysis was performed to determine which parameters would have large influences on the simulated hydrograph. After the baseline run was established, each parameter was varied individually by 10% increments throughout the parameter's feasible range. The results of the sensitivity analysis showed that varying b, Ds, Ws, snow roughness, and soil depth caused considerable changes in the hydrograph. Finally, 11 parameters were selected to be calibrated and their feasible ranges are shown in Table 4.

Table 4 VIC parameters selected for calibration and its feasible ranges

	Parameter	**Lower Bound**	**Upper Bound**
VIC	b (infiltration capacity)	0.005	0.4

	Ds (fraction non-linear baseflow)	0.001	1
	Ws (fraction max. soil moisture)	0.5	1
	Dsmax (max. velocity of baseflow, mm/day)	0	30
	Soil Layer 2 (soil depth, m)	0.2	1
	Soil Layer 3 (soil depth, m)	1	5
Routing	Velocity (m/s)	0.5	5
	Diffusivity (m^2/s)	200	4000
Snow	Snow roughness (surface roughness, mm or cm)	0.005	0.2
	Max Temp (when snow can fall, deg. C)	0	2
	Min Temp (when rain can fall, deg. C)	-2	0

- *MODIS Remote Sensing Processing*

Since MODIS imagery has a finer resolution (500m) than the VIC grid cell (1/16^o), the SCA values needed to be aggregated to the 1/16° resolution. The large volume of SCA information provided in a GIS-supported format was also compiled in a daily time series for all grid cells in the model domain. Additionally, any images containing more than 20% cloud cover for the Arkansas headwater watershed were excluded from the dataset to avoid calibration targets deemed large errors and uncertainty. This daily time series of MODIS provided SCA observations is compared to the simulated SCA from VIC.

- *GA Optimization*

There are many optimization approaches that have been proved useful for calibrating hydrologic models. One approach is to use a Genetic Algorithm (GA) (Wang, 1991); an iterative search method that works similarly to the way evolution works in nature. One advantage of using a GA over other methods is that it incorporates a mutation function within the algorithm which prevents the model from converging on a local solution and instead finds the global solution. Over time, GAs have been modified to be applicable to multi-objective applications (MOGA), as a result, there are various modified versions of GA algorithms that currently exist (Savic, 2002). Deb et al. (2002) introduced a version of GA, named NSGA-II (Non-dominated Sorting Genetic Algorithm II), by modifying MOGA approaches that had been criticized due to the computational complexity and lack of elitism, both of which made the algorithm slow. The NSGA-II fixed these issues and has been viewed as a superior method to other MOGAs in terms of its performance of searching optima. In this study, the single objective calibrations were carried out employing the GA (Wang, 1991) and the multi-objective calibration utilized the NSGA-II algorithm (Deb et al., 2002).

The GA set up starts with defining initial parameter sets. Each individual parameter set has 11 parameters; these are the number of parameters selected for calibration). A population of 100 (i.e., 100 different parameter sets) was chosen (roughly ten times the number of parameters to be calibrated), and 50 generations were run (100 parameter sets in a population is evolved through 50 evolutionary algorithm steps). This GA operation set, a population size of 100 and 50 generations, translates to 5,000 VIC runs. Running VIC in a parallel processing mode was

supported the MGHPCC super computing system by asking 100 processor so each processor takes a single run of VIC. Parallel processing allows VIC runs for the entire population within a generation to be processed at the same time, greatly reducing the computation time for model runs. Nash-Sutcliffe Efficiency (NSE) was selected as the objective function to evaluate simulated streamflow, while root mean square error (RMSE) was selected for SCA model performance.

Vulnerability Assessment Results

There are many metrics that can be used to assess the performance of the CSU system, but for screening purposed in the Integrated Water Resources Planning process, CSU initially wanted to focus on two measures: 1) storage reliability and 2) supply reliability. Storage reliability reflects the frequency that total system storage drops below a critical threshold set by the utility, while supply reliability represents the percentage of time that indoor water demands are met in a simulation. At the most basic level, system performance is considered adequate for a particular climate sequence if indoor water demands are met for the entire simulation (i.e., 100% supply reliability), since any drop in supply reliability suggests that the tap runs dry for some customers, which is considered unacceptable. We note that indoor water demand is a representative rather than encompassing measure of performance, but will be the metric of focus in this assessment.

We first present the results of the vulnerability assessment without any consideration of climate model output. Figure 30 shows the climate response surface of the CSU system to changes in mean precipitation and temperature under the Status Quo and Build-Out demand scenarios. The response surfaces, developed without the use of any projection-based data, shows the mean precipitation and temperature conditions under which the utility can provide adequate water services and those climate conditions where the reliability of their service falls below an acceptable level. Here, we define unacceptable performance as an inability to meet indoor municipal water demands. For the Status Quo system, the response surface suggests that the system can effectively manage moderately increasing temperatures and declining precipitation, but large changes beyond +2.2°C, coupled with declining precipitation, will cause the system to fail. For the Build Out demand scenario, the current system cannot adequately deliver water even under baseline climate conditions (no changes in temperature and precipitation), let alone reduced precipitation or increased temperatures. These results highlight that the CSU (and USAFA) system is at risk of water supply shortages simply due to the expected growth of water demands over the next several decades. These risks grow when the specter of climate change is considered, which is considered next.

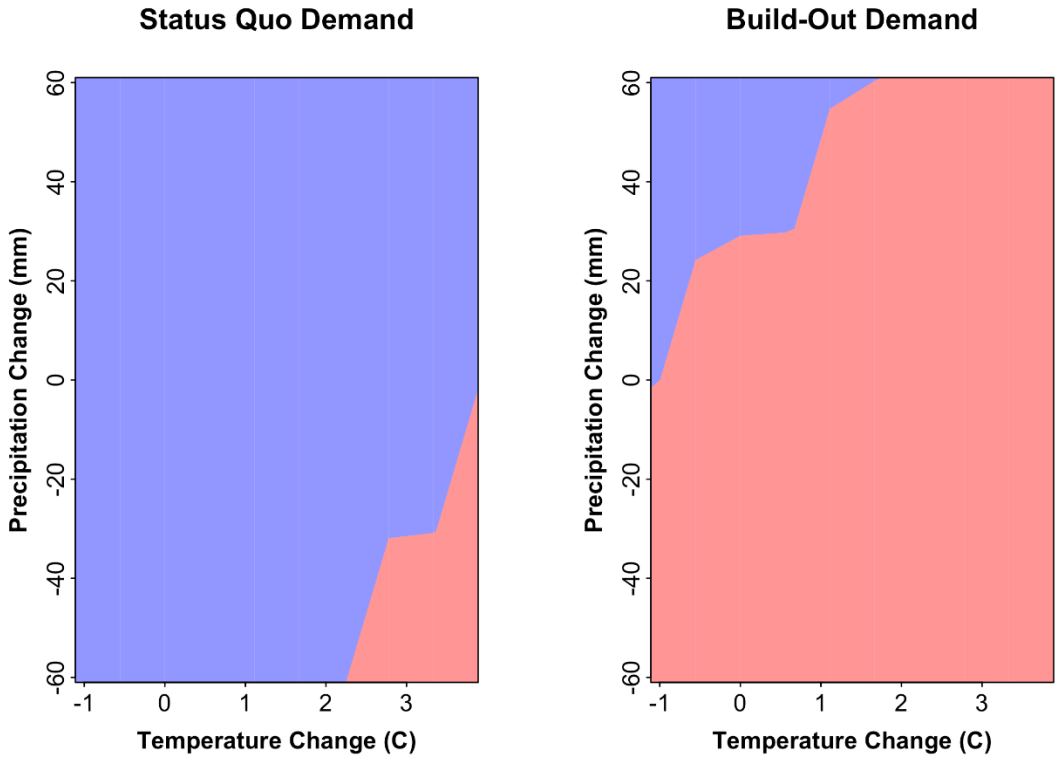

Figure 30 Climate response surfaces for the CSU system based on regions of climate change space that have 100% indoor water supply reliability. Acceptable (blue) and unacceptable (red) regions of performance are highlighted for both the Status Quo and Build Out demand scenarios.

Likelihood of Future Climate Changes

Regional mean annual temperature and accumulated precipitation for a baseline (1975-2004) and future (2040-2070) period averaged over the Upper Colorado and Arkansas River Basins are shown in Figure 31 (a) for the Representative Concentration Pathway (Meinshausen et al., 2011) (RCP) 8.5 scenario. Models that originate from the same institution or share large blocks of code are grouped into the families used in this analysis and denoted by the same color (Knutti et al., 2013). For example the models within the NCAR family all use key elements of the CCSM/CESM model developed at NCAR. Likewise, the MPI and CMCC models are combined because they are based on the ECHAM6 and ECHAM5 atmospheric models, respectively. Being in the same family does not guarantee that regional climate characteristics of related models will cluster, but global clustering analyses (Mason and Knutti, 2010; Knutti et al., 2013) suggest an increased likelihood of clustering even on small regional scales, a hypothesis which we test here.

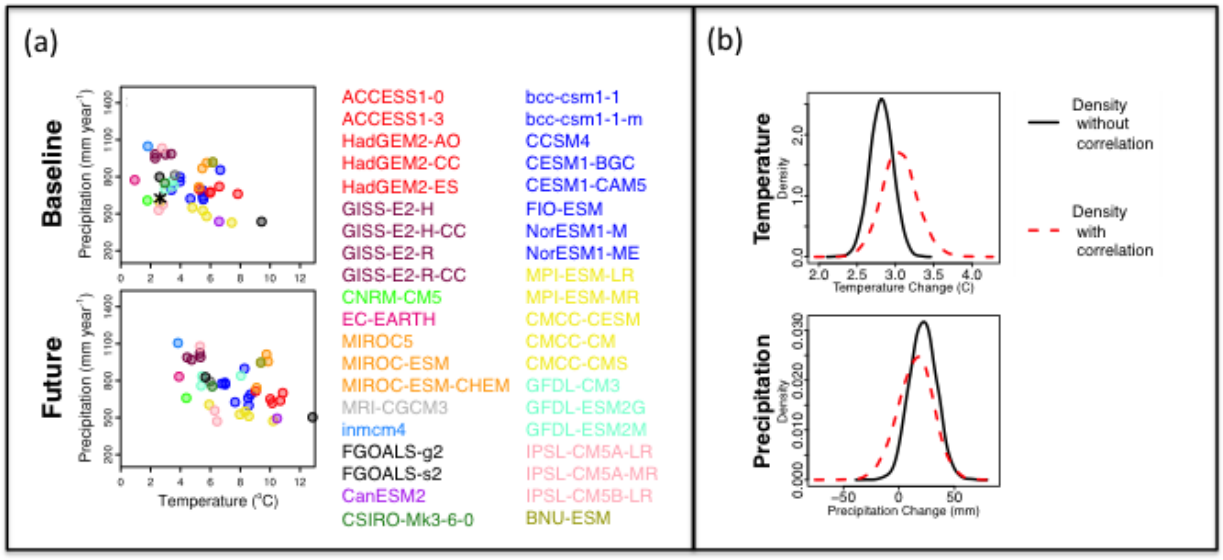

Figure 31 a) Scatterplot of mean temperature and precipitation over the Upper Colorado and Arkansas River Basin area from GCMs for a baseline (1975-2004) and future (2040-2070) period. The different models are colored according to their associated "families". b) Marginal probability density functions for midcentury temperature and precipitation change across the Upper Colorado and Arkansas regions developed with (red dashed) and without (black solid) an accounting of intra-family model correlations.

By visual inspection of Figure 31 (a), there is nontrivial clustering in both temperature and precipitation between models belonging to the same family. A formal hierarchical clustering of the baseline and future climatology (not show) confirms the tendency of models within the same family to cluster with respect to simulated regional precipitation and temperature averages. The degree to which clustering occurs within each family depends on the model family being considered (GISS and HadGEM cluster well, IPSL/CMCC less so). There is a tendency for models with very similar atmospheric structures to cluster, even if other components are different.

Clustering is very consistent within the GISS family of models. The GISS-E2-H/R models only vary in their ocean components and the CC version of each model indicates the addition of interactive terrestrial carbon and oceanic bio-geochemistry. While the four GISS models cluster in general, the interactive carbon versions of the models correspond almost exactly with their more standard counterparts. This finding suggests that within the GISS family, the choice of ocean model has a small influence on regional climate as defined in this study, while the inclusion of complex biological processes has almost no influence over regional results.

The HadGEM model family also clusters across most of the regions. Within this family, the HadGEM models and ACCESS1-0 all use similar versions of the HadGEM atmospheric model while ACCESS1-3 uses a different atmospheric component. Much like the GISS family, clustering within the HadGEM family suggests that similarities in the atmospheric model may be the dominant factor that results in clustered temperature and precipitation climatology over these timescales.

Within a few families, clustering occurs consistently between some members and not others. In many cases this is because the models that cluster have multiple, similar structural components while outlying model(s) are structurally different in at least one major component, usually the atmospheric model. For example, the two versions of IPSL-CM5A, differ only in their resolution (1.865º x 3.75º vs. 1.258º x 2.5º) and consistently cluster, while IPSL-CM5B has substantially different atmospheric physics parameterizations and gives a different solution. Within the GFDL family, GFDL-ESM2G/2M share a common atmospheric model (ATMO-CM2.1) and cluster well, while GFDL-CM3 is based on ATMO-AM3 and does not cluster with the other GFDL models. Likewise, in the MPI/CMCC family, the two MPI models differ only in their vertical resolution and always cluster, while the CMCC use a different version of ECHAM, the atmospheric model, and consequently do not cluster well with the MPI models.

While GCM clustering along family lines is well established, these results present the novel finding that models within a family, particularly those that share an atmospheric component, produce similar annual mean climate projections even on small regional scales. This result directly supports the idea that all the models within the CMIP5 ensemble do not provide independent information about regional climate changes, and therefore should not receive equal weighting in pdf development and impact risk studies. We now explore how the correlation between individual models within a family can influence the development of pdfs of local climate change and alter an impacts assessment of the CSU water supply system.

Probability models are fit to the climate model data with and without an accounting of the correlation between individual models within a family. Besides the inclusion of two additional correlation parameters for temperature and precipitation applied to all model families, the two pdfs are estimated identically. The estimate of intra-family model correlation for both annual mean temperature and precipitation are statistically different than zero at the 0.05 significance level. Figure 31 (b) shows pdfs of annual mean temperature and precipitation change with and without an accounting of within-family correlation. When inter-model correlations are included, an increase in variance is clear for both variables due to increased sampling uncertainty associated with a reduction in the effective number of data points. Beyond the increased variance of projected climate changes, high inter-model correlations also shifts the mean climate change estimate, since entire families of models are no longer regarded as independent data points, allowing, for example, centers with only a single model to assume more weight in the calculation.

Assessment of Future Risks and System Robustness

The pdfs of regional climate change can be used to determine the risk posed to the CSU water system. Figure 32 shows the climate response surface for the Colorado water utility under 2016 Demand conditions presented previously, but with the bivariate pdfs of annual temperature and precipitation change with and without intra-family correlations superimposed. We do not show the Build-Out demand conditions because system performance is unacceptable under that scenario even without climate change. The degree to which the pdfs extend into the region of unacceptable system performance in Figure 32 describes the risk that the water utility may face from climate change. Visually, it is clear that the tails of the pdf developed with an accounting of intra-family model correlations extend into the region of unacceptable system performance, while those of the pdf with an independence assumption do not. A climate robustness metric is

used to summarize the risk by numerically integrating the pdf mass in the region of unacceptable performance. For the pdf that does not account for model correlation, essentially 0% of its mass falls into the region of unacceptable performance. When correlations are accounted, the metric increases to 0.7%. While still small, this non-negligible probability (similar in magnitude to a 100-year event) is important because of the intolerable impact that such shortfalls would have on the local community. Any non-trivial probability that indoor water use will have to be forcibly curtailed would motivate the water utility to invest in measures to prevent such an outcome. Thus, there is an important increase in decision-relevant, climate-change related risk facing the water utility when we alter our interpretation of the information content present in the model ensemble.

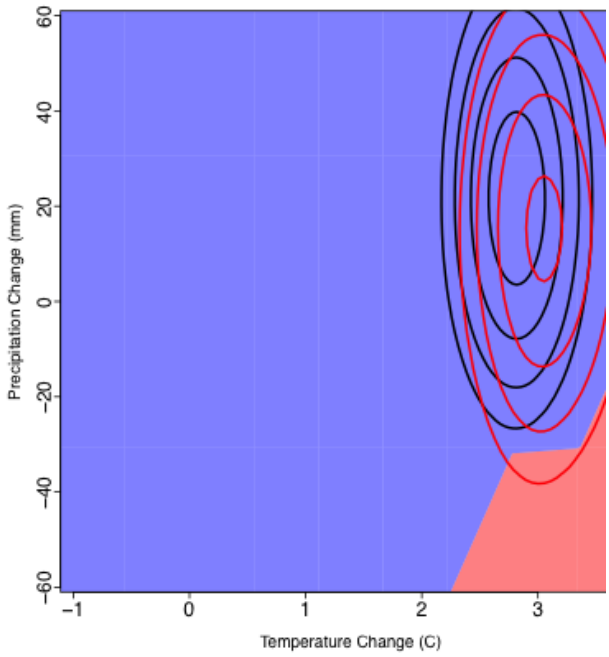

Figure 32 A climate response surface displaying the conditions of mean precipitation and temperature under which CSU can (blue) and cannot (red) provide reliable indoor drinking water. Bivariate pdfs of mean temperature and precipitation are superimposed on the response surface. The red pdf was developed with an accounting of intragroup model correlation, while the black pdf was not. Both pdfs are contoured at the same levels, with the final level equal to 1.5 × 10_3.

VIC Calibration Results

Single-Objective Calibration for Streamflow

The results of the single-objective calibration to streamflow showed that VIC can accurately represent streamflow for the Arkansas River headwaters. The calibration to streamflow was carried out ten times to explore the uncertainty level of calibration results and to choose among the best calibration. This is because each trial of GA optimization would end up with different calibration results owing to the stochastic processes in GA related to the initial population generation and evolutionary change of population. As a result, the 10 calibration results were

consistently close together, with NSEs for streamflow ranging from 0.90 to 0.92 for calibration and 0.85-0.87 for validation. RMSE values for SCA range from 0.32 to 0.34 for calibration and 0.34 to 0.36 for validation.

Figure 33(a) shows the best performing model in terms of streamflow prediction (NSE = 0.92 and 0.87 for calibration and validation periods respectively). SCA estimation was checked for this model to determine how well VIC predicts SCA when calibrating to streamflow alone; best performing VIC for streamflow resulted in RMSEs of 0.34 and 0.35 for calibration and validation, respectively (Figure 33(b)).

(a)

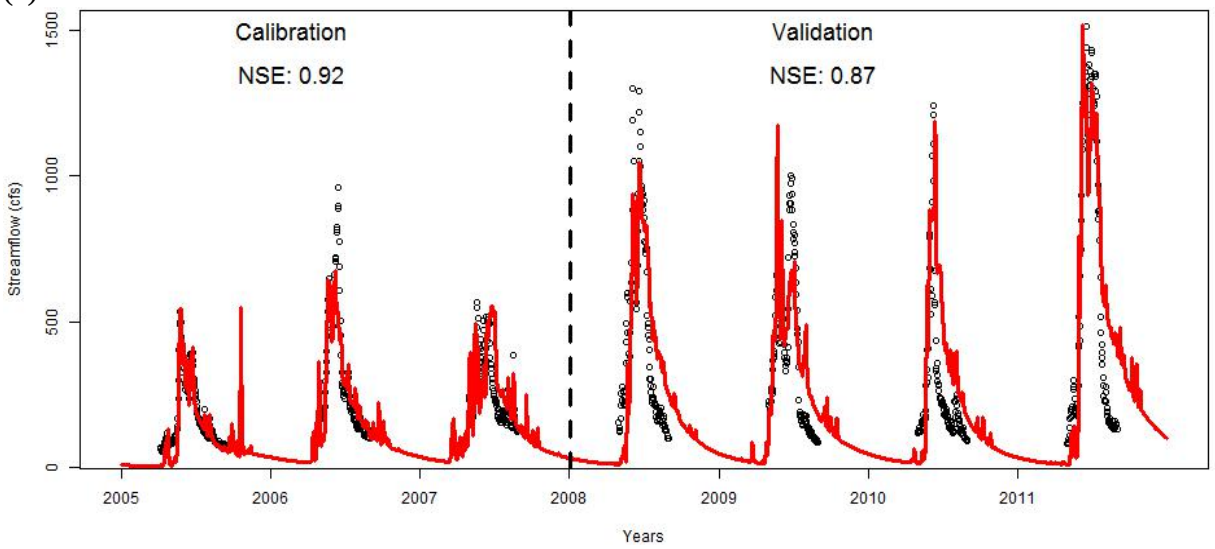

Observed: o Simulated: –

(b)

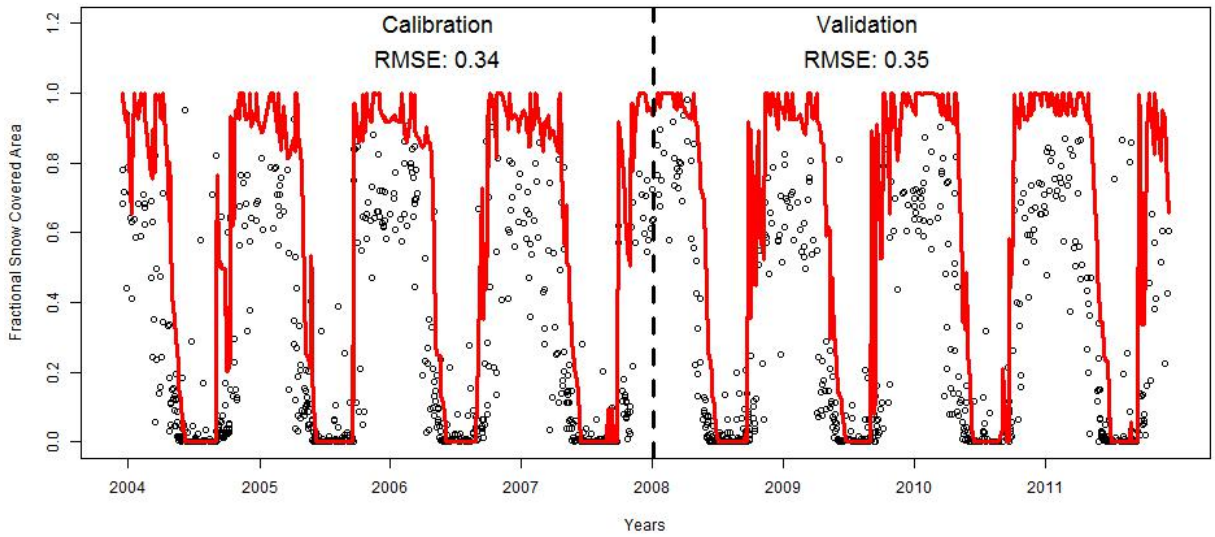

Figure 33 Calibration and validation results of the best streamflow model

Single-Objective Calibration for SCA

The results of the single-objective calibration to SCA showed improved prediction on SCA with marginal differences between 10 trials; RMSE values converged on 0.30 for the 10 trials for the calibration period and ranged from 0.33 to 0.34 for the validation period. These VIC performances for SCA predictions were not achieved by any of the streamflow calibrations. This implies that by having streamflow as an only calibration target the model cannot be fully functional for snow simulation process. The question then arises as to whether VIC can be functional in a satisfactory manner for both streamflow and SCA, depending on the level of degradation of NSE and RMSE (i.e., tradeoff between two objectives). This question will be addressed in the discussion for the results of the multi-objective calibration that follows this section.

The SCA calibration resulted in a wider range of streamflow NSEs compared to the streamflow calibrations, with NSE values ranging from 0.71 to 0.90 for the calibration period and 0.50 to 0.87 for the validation period. The lesson we can take from this result is that reliable streamflow predictions cannot be expected when using SCA as an only calibration target.

Figure 34(b) shows the best performing VIC in terms of SCA prediction (RMSE = 0.30 and 0.33 for calibration and validation periods respectively). This best performing model for SCA resulted in NSEs of 0.90 and 0.80 for calibration and validation, respectively. Interestingly, the calibration model best performing SCA prediction also performs best with respect to the streamflow prediction during the calibration period (Figure 34(a)); the NSE of 0.90 is the best among the NSE range of 0.71-0.90. This aligns with the argument made by Tanmoyee et al. (2015) that snow cover and depth used as calibration targets for hydrologic models help improve steamflow simulation. However, as described earlier RMSEs of SCA for all 10 calibration trials ended up with RMSE values of being very close to 0.30 but with large uncertainty in streamflow predictions, still emphasizing a need of caution when using SCA calibration results for the streamflow prediction purpose.

(a)

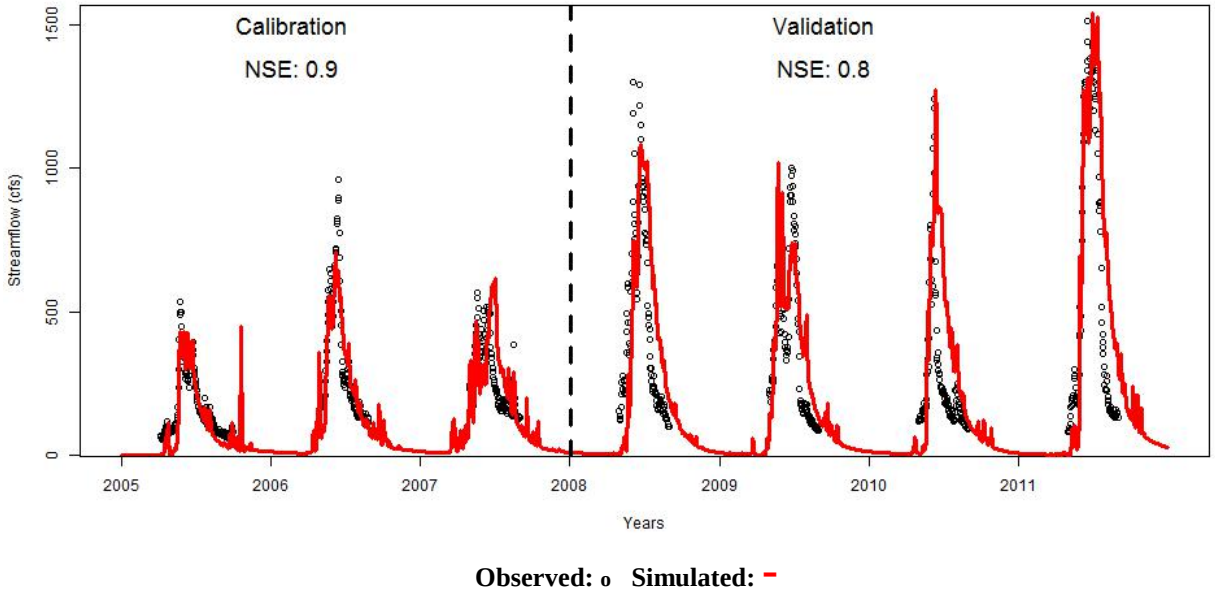

(b)

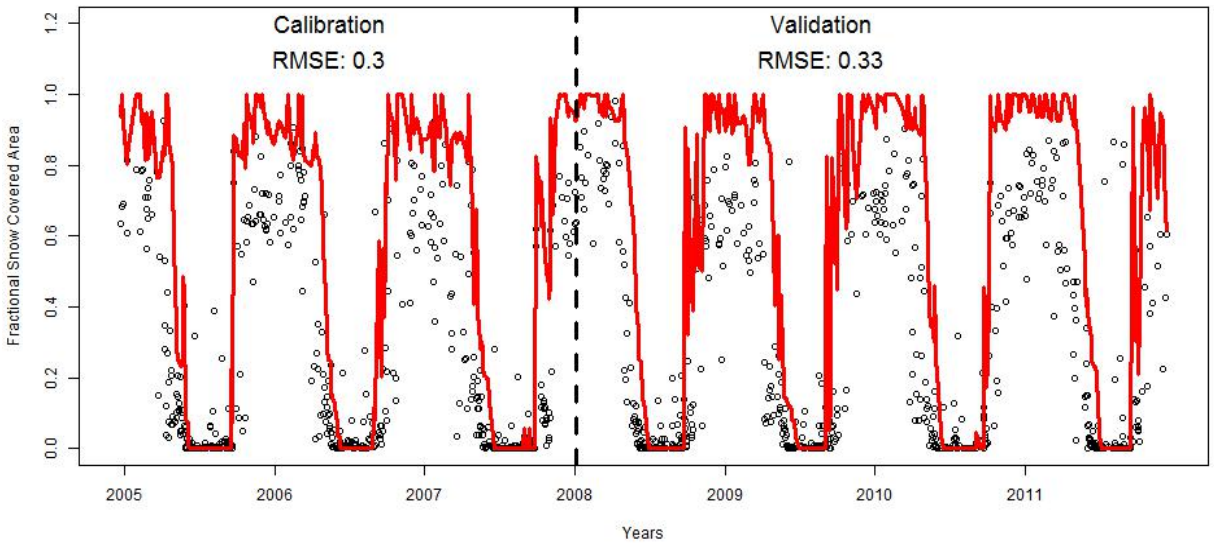

Figure 34 Calibration and validation results of the best SCA model

Multi-Objective Calibration

Ten trials of the multi-objective calibrations resulted in good representation for both streamflow and SCA. NSEs for streamflow range from 0.90 to 0.92 (for the calibration period) and 0.85 to 0.87 (for the validation period). The ranges of SCA RMSEs are 0.30-0.32 and 0.33-0.34 for calibration and validation period respectively. This multi-objective calibration results show a small tradeoff between streamflow and SCA; i.e., VIC can be calibrated to produce good predictions for both calibration targets without scarifying one target for another.

The best performing model identified by the multi-objective calibration task is represented in Figure 35. The model shows excellent performance for the streamflow prediction (NSE = 0.91 and 0.87 for calibration and validation period respectively), and also performs well for SCA with RMSE values (0.30 calibration period and 0.33 for validation) that are comparable to the best performing model calibrated to SCA alone.

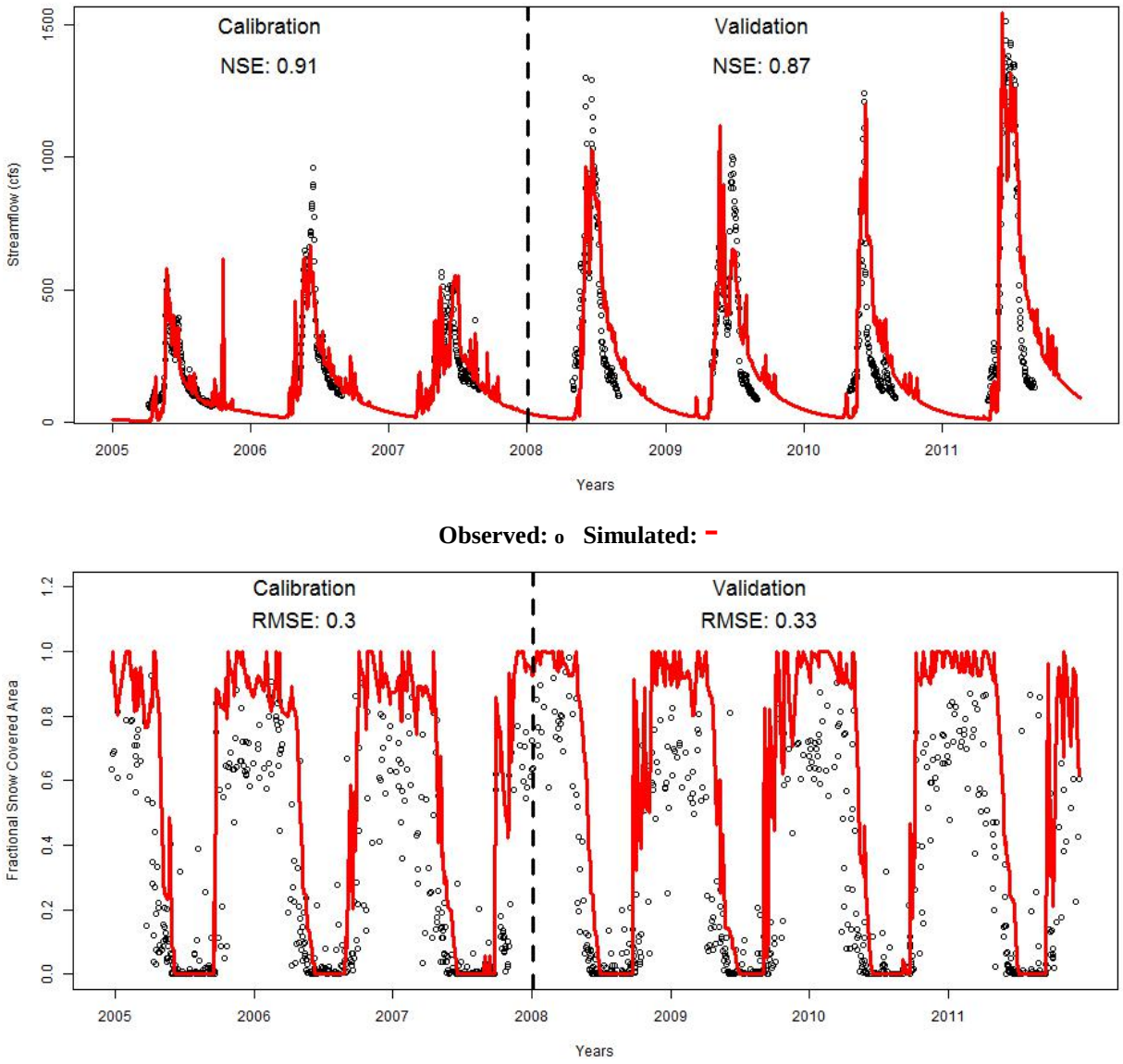

Figure 35 Calibration and validation results of the best multi-objective mode

Table 5 provides a summary of three calibration approaches: two single objective calibrations and multi-objective calibration using streamflow and SCA as calibration targets. Overall, the multi-objective optimization showed lower RMSE values for SCA than just calibrating to streamflow alone while still maintaining excellent performance in predicting streamflow (Table 5). More importantly, the NSEs for streamflow were more consistent (i.e., the uncertainty of streamflow predictions is greatly reduced) and higher (NSE > 0.90) compared to the single target calibration of SCA.

Table 5 Summary of calibration and validation ranges for calibration methods over 10 trials

	NSE		**RMSE**	
Calibration Target	**Calibration**	**Validation**	**Calibration**	**Validation**

Streamflow	0.90 - 0.92	0.85 - 0.87	0.32 - 0.34	0.34 - 0.36
SCA	0.71 - 0.90	0.50 - 0.87	0.30	0.33 - 0.34
Both	0.90 - 0.92	0.85 - 0.87	0.30 - 0.32	0.33 - 0.34

Conclusions

Given previous work at the global scale (Tebaldi and Knutti, 2007; Masson and Knutti, 2011; Knutti et al., 2013; Haughton et al., 2015), the lack of regional independence between models within the same family is not entirely unexpected. In the most extreme cases, climate models within a family are the same model configuration, simply run at different resolutions. In other cases they share common code and use the same assumptions to explain physical processes. Indeed, the genealogy of models may be evolving over time to favor and propagate model versions that perform better at the global scale, gradually reducing the independence among model variants. However, the extent of clustering in the confined geographic areas investigated in this study is somewhat surprising, and this work is the first attempt to quantify and account for model similarities at the regional scale in the development of climate change pdfs for use in impact studies. This work shows that accounting for inter-model correlations along family lines can give different climate change results for an impact assessment of the water supply related to a DoD training installation and alters the perception of climate-related risk. The effects of inter-model correlation on risk quantification will undoubtedly vary depending on the unique circumstances of each local system, and only a single demonstration for one system in a particular sector (the water sector) was shown here. However, the results presented in this study are generally applicable to all impact analyses (e.g., fire, training, energy risks) relevant to DoD decision makers.

While these results are important, there are a number of outstanding issues that require further research. First, it is important to remember that although the spread across the CMIP5 models is often used to express the uncertainty in future climate, even a completely independent model ensemble will not capture all of the structural uncertainty about the climate system. There are many physical processes that we do not understand and are not well represented in climate models. Therefore, the “probabilities” estimated in the case study cannot be interpreted in the traditional sense of probability distributions based on observed data, but rather as an interpretation of the uncertainty from the climate models. Other limitations of the analysis include a lack of “build-out” water demand conditions for the WEAP model of the Upper Colorado system, a lack of spatial variability in changes applied to climate scenarios, and the simplified hydrologic model of the Arkansas River used in the analysis. This last limitation is addressed in Part II of the USAFA case study analysis, which presents our novel approach to developing a sophisticated hydrologic modeling tool for the Arkansas that can support water supply climate risk assessments relevant to the USAFA and other DoD installations served by Arkansas River waters.

Good model performance with respect to streamflow at the basin outlet poses a problem about low performance in terms of models’ ability to reproduce snow cover area (Duethmann et al., 2014) as well as streamflow at interior points of the basin (Wi et al., 2015). Misleading internal

functioning of the models in spite of good streamflow simulations at the basin outlet implies that errors stemming from different internal processes or modeled spatial sub-domains are compensated as long as models seem to be satisfactory, so called “effect of error compensation.” (Seibert and McDonnell, 2002). Ideally, a calibration process should aim at dealing with this error compensation issue. In the hydrologic modeling effort for the Arkansas River headwaters using VIC, we addressed the issue by employing the remote-sensing provided spatial information of snow covered area as a calibration target in addition to the basin outlet streamflow. The multi-objective calibration based on the Genetic Algorithm successfully calibrated VIC for both streamflow and snow simultaneously, with small tradeoff between two calibration targets and significantly reducing the streamflow prediction uncertainty as compared the single target calibration for streamflow. This additional calibration effort devoted to improve the snow representation of VIC will have an important implication when the VIC is used as a future prediction tool (a main role people expect from models) of a watershed system under uncertain climate conditions. Our hypothesis is that the VIC (or any other hydrologic models) that is calibrated by this advanced calibration strategy would project different story about, for example, future water availability from the ones projected by models calibrated under the typical approach (say basin outlet calibration). Since in our decision scaling approach a hydrologic model plays a significant role in assessing the climate vulnerability of a water resources system under a variety of climate conditions, this hypothesis would have huge implication on the approach. Further exploration on this scientific question should be pursued for the future work.

By the year 2050, development in the Arkansas Basin is expected to grow considerably, causing projected water needs to be 28% higher than the present demands (approximately 102 billion gallons). A well-calibrated VIC hydrologic model designed for the Arkansas River is now available and will serve as an important tool to decision makers such as the Colorado Springs Utility, which receives 30% of their water supply from the Arkansas River.

Case Study 4: California Central Valley System

Background and Problem Framing

Managing water scarcity is one of the most pressing challenges society faces today in California. California's ongoing severe drought began in winter 2011-2012, and intensified in winter 2013-2014, a period that had very low winter precipitation, mountain snowpack, and spring runoff (Department of Water Resources, 2014b; U.S. Geological Survey, 2014; United States Drought Monitor, 2014). The continuing drought has drawn down reservoir storage in the state to dangerously low levels and threatens the state's agricultural production, drinking water supply, and fisheries (California Department of Fish and Wildlife, 2014; Department of Water Resources, 2014a; U.S. Department of Agriculture, 2014). The drought continues into water year 2015 and is now in its fifth year. The current drought has set a range of records, among them: 1) the years 2012-2014 constitute the driest three-year period in the state's observed record (measured as statewide total precipitation); 2) the most severe values of NOAA's National Climatic Data Center drought indicators; 3) the lowest calendar-year precipitation; 4) the lowest 12-month precipitation; 5) the warmest calendar-year temperatures; 6) the warmest winter temperature (year and temp, with reference temp); 7) the lowest April 1st snowpack; 8) the warmest 3-year period; and 9) the record-low water allocations for State Water Project and federal Central Valley Project contractors (California Department of Water Resources, 2015; Diffenbaugh et al., 2015). It has also taken a heavy toll on people and ecosystems, with wells running dry, farmers abandoning costs, wildfires raging, millions of trees dying, and fish species being pushed to the brink of extinction (Swain, 2015). These record-setting conditions speak to the need for continued improvement of our ability to respond to dry conditions.

The goal of this case study has been to better understand the vulnerability of California's water system, a huge and complex system called the California Central Valley System that encompasses multiple military bases (Beale AFB, McClellan AFB, Travis AFB, Naval Air Station Lemoore, etc.), to potential future droughts. In order to do so, we made use of an existing model of the water system, and bottom-up climate change vulnerability assessment techniques described in the Technical Approach section of this report. The vulnerability assessment involved repeated runs of the water resources system model in order to systematically trace out the response of the system to droughts of varying intensity and duration. The system response was further evaluated with the addition of temperature shifts in the range that might reasonably be expected to occur within the current planning horizon (to approximately year 2050).

The California Central Valley System

The catchment area of the Sacramento and San-Joaquin rivers (Figure 36) provide at least a portion of the water supply for about two-thirds of California's population, and provides a migratory pathway for four fish that are listed as endangered or threatened pursuant to the federal Endangered Species Act (Mount and Twiss, 2005). About half of California's average annual streamflow flows toward the Sacramento and San-Joaquin Delta, and most of California's farmland depends on water tributary to it (Lund et al., 2010). The Delta itself is a web of channels and reclaimed islands at the confluence of the Sacramento and San Joaquin rivers. It forms the eastern portion of the wider San Francisco Estuary, which includes the San Francisco, San Pablo, and Suisun bays, and it collects water from California's largest watershed, which

encompasses roughly 45 percent of the state's surface area (Lund et al., 2010). It is also a center for important components of California's civil infrastructure for such as electricity, gas transmission lines, underground storage of natural gas, transportation lines, and provides crucial habitat for many of California's fish species that live in or migrate through it. Not inconsequentially, the Delta is valued for its aesthetic appeal and support of recreational activities (Lund et al., 2010). The majority of usable water resources for the California Central Valley System can be approximated as the quantity of streamflow flowing into the Central Valley from the north-east downgradient regions that are comprised of twelve large sub-basins, referred to as the rim sub-basins (Figure 36).

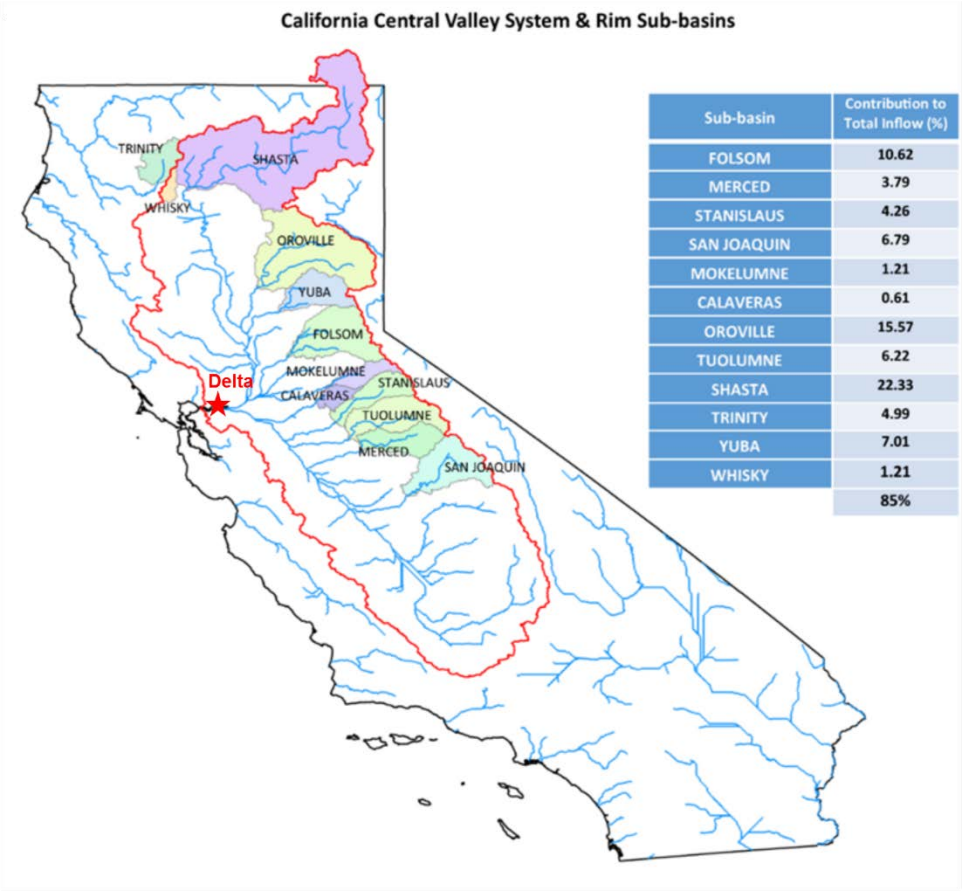

Figure 36 California Central Valley System and Rim Sub-basins

The California Department of Water Resources (DWR) and the United States Bureau of Reclamation (USBR), oversee the operation of the water systems that flow through the Sacramento-San Joaquin Delta, and use the Delta as a conveyance hub (see Figure 37). These systems include the infrastructure of the State Water Project (SWP), owned and operated by DWR, and the Central Valley Project (CVP), owned and operated by USBR. The CVP includes more than 13 million acre-feet of storage capacity. The SWP includes more than 30 storage facilities, reservoirs and lakes; about 700 miles of open canals and pipelines, providing water to approximately 25 million Californians and about 750,000 acres of irrigated farmland. The SWP is not the exclusive water supplier for those it serves, as many of its customers supplement the

water provided by SWP with local or other imported sources. Local water systems are outside of the jurisdiction of DWR.

Figure 37 State, Federal, and Local water infrastructure from the California Water Plan (2013) Volume 3, pg 7-6

Vulnerability Assessment

Previous exercises in hydro-economic optimization of climate change and extended drought have provided substantial insights for policy-making and public discussion in California (Connell-Buck et al., 2011; Harou et al., 2010; Null et al., 2014; Tanaka et al., 2011). Most of these studies show that California's water system, while not impervious, can be quite robust to substantial climate disturbances without widespread catastrophic losses, if well managed.

Connell-Buck et al. (2011) used CALVIN (CALifornia Value Integrated Network), a hydro-economic optimization model of California's statewide water supply system that minimizes costs subject to flow continuity at nodes and capacity constraints on links, to compare a warmer climate scenario and a warmer-drier scenario centered on 2085 with updated 2050 water demand estimates. The study thereby parsed out and analyzed the independent and combined effects on California water management adaptation of temperature and precipitation. However, because it based its exploration of future on a particular run of a particular GCM (the model GFDL CM2.1 and also a A2 emission scenarios specific), it is limited to that model's representation of a theoretical local climate future, and it relies on the model's potentially un-realistic representation of natural (inter and intra annual) climate variability. The study is not able to systematically explore the vulnerability of the system to meteorological droughts of varying intensity and duration.

Other attempts at evaluating the sensitivity of the California system to dry or drought conditions have been subject to similar limitations in the type and number of model runs. For example, Harou et al. (2010) tested the response of the CALVIN model to a single 72-yr synthetic hydrologic timeseries with half the mean historical inflow. The synthetic hydrologic timeseries was generated by random resampling from the 10 driest years of record (1922–1993). The random resampling does not facilitate risk assessment, which requires information on the relative likelihood occurrence of droughts of varying return periods. Null and Lund (2006) used an economic engineering optimization model to evaluate the water supply feasibility of removing O'Shaughnessy Dam, located in the Hetch Hetchy Valley of Yosemite National Park, by examining alternative water storage and delivery operations for San Francisco. The model was run under historical hydrology, and a single timeseries of a warmer drier hydrology with water demands increased to projected year 2100 demands. Similarly, Null et al. (2014) used the CALVIN model to evaluate the habitat and economic consequences of removing rim dams in California's Central Valley under historical conditions and a single warm and dry climate timeseries from the Geophysical Fluid Dynamics Laboratory (GFDL) CM2.1 model for the A2 emissions scenario. Rheinheimer et al. (2015) explored the effect of temperature increases on reservoir operating procedures to manage downstream temperatures with climate warming of 2, 4, and 6 ^{o}C. The study altered stream temperatures only and did not adjust water quantity or flow timing.

Two examples of studies that have explored a wider range of possible climate futures are Willis et al. (2011) and Groves and Bloom (2013). In order to understand the effect of climate change on flood operations in the Sacramento Basin, Willis et al. (2011) ran downscaled timeseries from 11 GCMs (each run twice, once for CMIP3 scenario A2 and once for B1) through the Army Corps' Hydrologic Engineering Center Reservoir Simulation (ResSim) model (after converting the climate information into reservoir inflow through application of the National Weather Service River Forecast System, NWS–RFS). Groves and Bloom (2013) used a Robust Decision Making (RDM) approach applied to the Water Evaluation and Planning (WEAP) Central Valley Model modeling environment (Joyce et al., 2010) to develop and compare robust water-management response packages that could ameliorate the vulnerabilities identified. The RDM approach explored the uncertainty associated with the system response to output from 6 GCMs (each run twice, once for scenario A2 and B1, as was done by Willis et al. (2011)). Although the ensemble of GCM projections (22, in the case of Willis et al. (2011) and 12 in the case of Groves

and Bloom (2013)) widens the range of future plausible hydrologic conditions relevant to the performance of California water system beyond that considered by previous more deterministic studies, they do not necessarily capture the range of uncertainty in future climate (Cayan et al., 2010), and they likely underestimate the range of future climate interannual variability, including the potential for multiyear droughts (Brown and Wilby, 2012). Furthermore, like other studies before them, they offer no systematic exploration of system response to the types of droughts of varying intensity and duration that might be experienced in the future.

This study addresses three limitations of the previous studies:

1) This study systematically explores system response to droughts of varying intensity and duration through the implementation of a novel modeling workflow. Climate timeseries are developed using a weather generator conditioned on historical climate statistics, with a range of temperature shifts applied to sample on conditions of potential future warming. Five thousand climate timeseries were generated by a stochastic daily weather generator, fifty of which were sampled in order to achieve a representative sample of: drought intensity levels of 1st, 25th, 50th, 75th, and 99th percentiles for 1-, 2-, 3-, 5-, and 10-yr droughts.
2) The water resources system model used (CalLite) includes urban, agricultural, and environmental aspects, connected to altered hydrology through probabilistic mechanisms in a novel workflow.
3) Because of its essential role in the quantification of available water on which water allocations to all water sectors is based, good performance is highly desired for the hydrologic model. This study introduces an advanced distributed, physically-based hydrologic model capable of supporting subsequent phases of the drought vulnerability assessment workflow.

A Modeling Workflow for Drought Vulnerability Assessment

Risk is a function of impact and likelihood (Dessai and Hulme, 2004), the most basic and uncontroversial version of which is presented mathematically as follows:

$$Risk = \sum_{i=1}^{all\ future\ states} Prob_i \times Impact_i$$

A straightforward technique for estimating average annual drought risk under the assumption of a stationary climate would be to multiply the total annual drought losses (e.g., in dollars) by 1/*n*, where n is the number of years of record, and sum over the period of record. If the interest were in the risk of losses from an *N*-year drought, then the approach would be limited to the sample of all *N*-year droughts in the historical record, in which measurements of drought impact are available. In order to explore risks to potential future droughts outside of the historical record, models are needed.

Water resources system models are the essential tools for exploring the impact of potential future hydro-climatological and socio-economic conditions on a water system (Brown et al., 2015). In modeling alternative droughts, a number of options are available. One could test the system

response to alternative meteorological, hydrological, agricultural, or socio-economic drought conditions, in order of increasing complexity and comprehensiveness. Given that the interest is to develop an understanding of impacts of drought on society, broadly defined (including urban, agricultural, and ecological sectors), it would be convenient to initiate the modeling workflow as far up the chain as possible. For example, with a model of the interactions between streamflow and agricultural production, the impacts might be calculated hydrological drought on societal well-being (using a water resources system model that connects available water to agricultural production to societal well-being). Unfortunately, it is very difficult to determine the future likelihood of a given hydrological drought, which is influenced by a number of non-independent factors, such as land cover, precipitation, temperature, antecedent moisture conditions, and groundwater table, all of which are subject to change.

In order to inform likelihood, it is necessary to begin with the most fundamental factors available – those describing conditions of meteorological drought, i.e., precipitation and temperature. This study uses a daily weather generator (Steinschneider and Brown, 2013) to develop timeseries of plausible alternative precipitation and temperature, which are then sampled systematically in order to explore a wide range of drought characteristics. An advanced hydrologic model translates descriptors of fundamental meteorological drought into measures of available water at the Earth's surface, which are in turn converted into measures of water system performance through the water resources system model. The second conversion is not straightforward, as it involves anthropogenic co-factors in the operation of water system infrastructure. This study demonstrates the inclusion of an important analytical step: the correlation of available water with historical outcomes of human behavior through quantile mapping procedures.

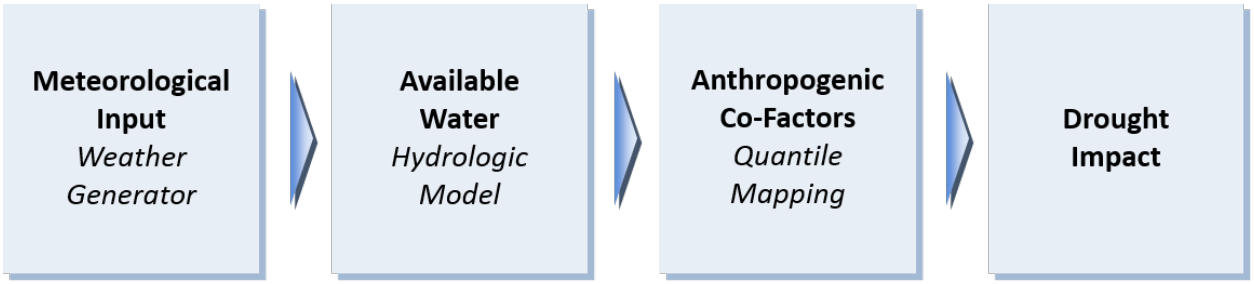

Figure 38 Modeling Workflow for Drought Vulnerability Assessment

The resulting workflow (Figure 38) allows the exploration of drought impact in response to a wide range of meteorological input. It does this by maintaining relative anthropogenic response to relative scarcity of available water through propagation of probabilistic relationships.

Stochastic Climate Generator

A weather generator has a number of advantages that distinguish it from sources of climate information that originate from global modeling efforts that serve primarily to assess the effects of greenhouse gas emissions on climate. A weather generator can be targeted specifically at the local climate characteristics, and altered systematically to explore changes to those climate characteristics that are informed by local observed changes in known climate drivers, such as atmospheric rivers and sea surface temperature correlations. It can also be adjusted to

exhaustively probe systems vulnerabilities. For questions of the sensitivity of the system to droughts of varying intensity and duration, the weather generator can be used to develop timeseries of climate metrics (e.g., precipitation and temperature) that contain exactly the type of drought characteristics of concern.

The weather generator used for this study (Steinschneider and Brown, 2013) resamples from the local historic record of temperature and precipitation (Maurer et al., 2002), while maintaining mean, standard deviation, and skew in the statistics. Because it resamples from the entire study area simultaneously, spatial correlations are maintained perfectly. The weather generator is capable of maintaining low-frequency variability in the climate signal, as described below, and long-term weather timeseries both with and without the low-frequency signal will be explored. There are approximately 1000 1/8th degree grid cells within the study area, each of which has contains daily climate data from 1950-2010.

The weather generator was conditioned on annual area-averaged gridded climate data (1950-2003) from (Maurer et al., 2002). Statistically significant (90% confidence) low frequency signals occur at between approximately 11 and 16 years (Figure 39). The identified 15-year periodicity in the precipitation signal is visible in the local paleo-record approximately 500 years into the past, but not before that (Dettinger and Cayan, 2014; Meko et al., 2014). According to Meko et al. (2014): "Cyclic variation, with an average wavelength of about 15 years, is evident in both observed and reconstructed flow series over the past 100 years, but is not a long-term feature of the hydroclimate of the basins studied. While some observed flow records have large inter-decadal swings, the near-15- year cycle in those records does not pass spectral analysis tests for statistical significance".

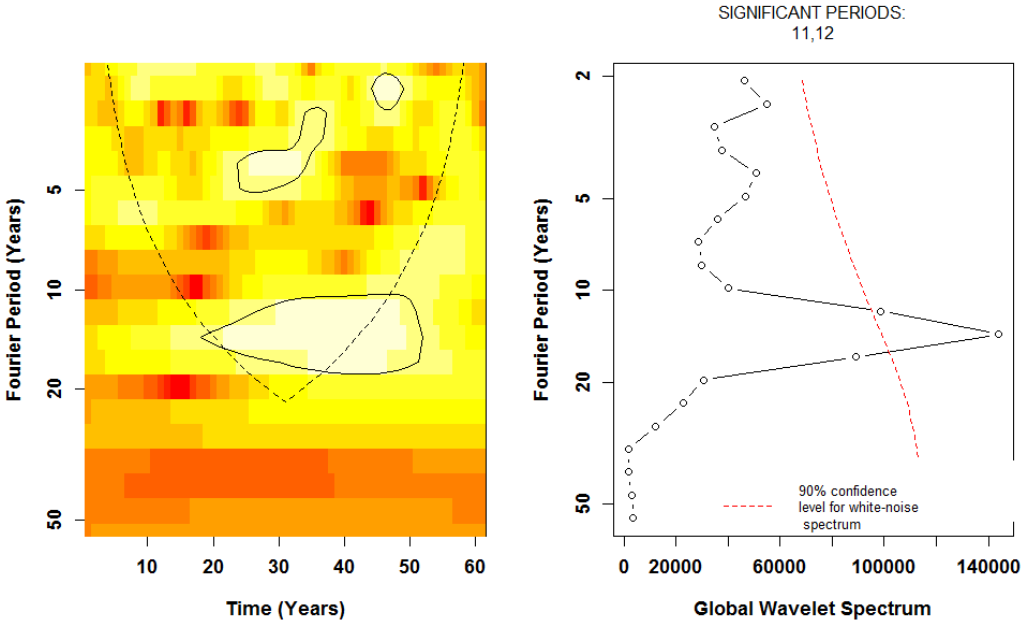

Figure 39 Power Spectrum

Figure 40 summarizes the procedure used to sample climate timeseries with the desired distribution of drought characteristics. The process follows after that used by Whateley et al. (2016). First, the weather generator was used to stochastically generate 5000 82-year timeseries that each approximately reproduced the mean, variance, skew, and power spectrum of the historical record. Then, the minimum *X*-year precipitation was identified in each timeseries (where *X* is 1 year, 2 years, 3 years, 5 years, or 10 years). Figure 40 shows the boxplots (n = 5000) of each sampled drought length, with the *X*-year historical drought of record identified by the horizontal red line. Finally, for each drought length, particular climate traces (2 of each) were chosen based on exceedance probability. The 82-year climate trace that is designated "1st-percentile 10-year drought", for example, contains a period of 10 years in which average annual precipitation is lower than the driest 10-year period in almost any other of the 5000 climate traces. A 1st-percentil drought has a 1 percent exceedance probability in terms of drought and a 99 percent non-exceedance probability in terms of precipitation.

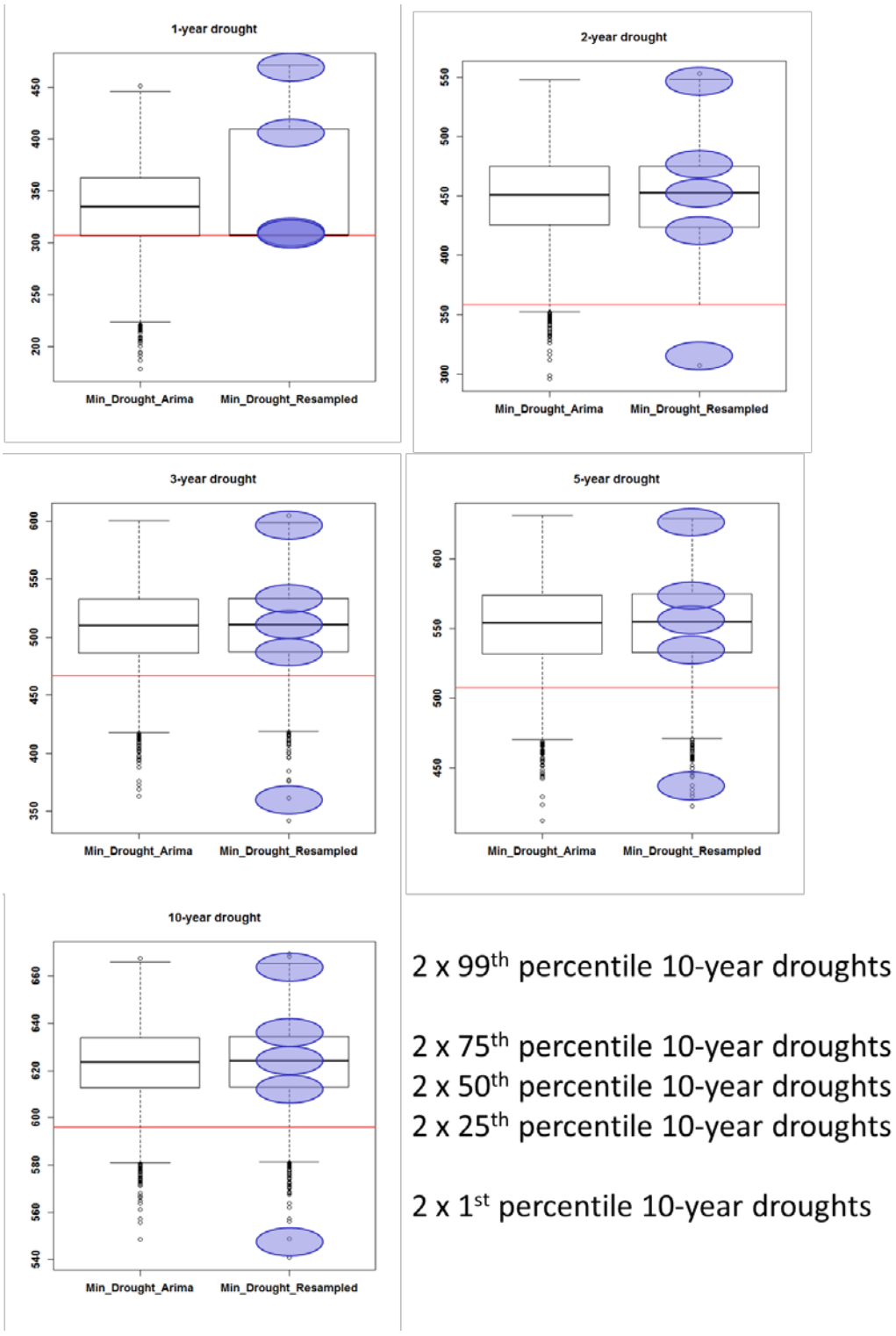

Figure 40 Procedure to sample climate timeseries with the desired distribution of drought statistics

Hydrologic Model

A distributed hydrologic model was developed specifically for this application based on the widely used lumped parameter Sacramento Soil Moisture Accounting model (SAC-SMA) model. To do so, the SAC-SMA model, a lumped conceptual hydrological model employed by the National Weather Service (NWS) of the National Oceanic and Atmospheric Administration (NOAA) to produce river and flash flood forecasts for the Nation (McEnery et al., 2005), is coupled with a river routing model to be suitable for modelling a distributed watershed system. We name it SAC-SMA _DS denoting the distributed version of SAC-SMA. The SAC-SMA_DS is composed of hydrological process modules that represent soil moisture accounting, evapotranspiration, snow processes, and flow routing. The model operates on a daily time step and requires daily precipitation and mean temperature as input variables.

The SAC-SMA_DS includes the Snow 17 module (Anderson, 1976) to deal with snow modelling process for the snow covered areas within the 12 rim sub-basins of the California Central Valley System (CVS). In this study the hydrologic modeling domains for 12 rim sub-basins are spatially disaggregated based on climate input grids of 1/8^{o} resolution and 200 m interval elevation bands. The runoff from each disaggregated area is weighted by its area fraction within the basin to obtain the total basin-wide runoff.

The overall model structure of the SAC-SMA_DS is described in Figure 41. More details on the model components are provided below by focusing on the descriptions for the modules additionally introduced to develop the distributed version of SAC-SMA.

- *Hamon Evapotranspiration Calculation*

The potential evapotranspiration (PET) is derived based on the Hamon method (Hamon, 1961), in which daily PET in millimeters (mm) is computed as a function of daily mean temperature and hours of daylight:

$$\mathrm{PET} = \mathrm{Coeff} \cdot 29.8 \cdot \mathrm{L_d} \cdot \frac{0.611 \cdot \exp\left(17.27 \cdot \frac{\mathrm{T}}{(\mathrm{T}+273.3)}\right)}{\mathrm{T}+273.3}$$

where, L_d is the daylight hours per day, T is the daily mean air temperature (^{o}C), and Coeff is a bias correction factor. The hours of daylight is calculated as a function of latitude and day of year based on the daylight length estimation model suggested by Forsythe et al. (1995).

- *In-grid Routing: Nash-Cascade Unit Hydrograph*

The within-grid routing process for direct runoff is represented by an instantaneous unit hydrograph (IUH) (Nash, 1957), in which a catchment is depicted as a series of N reservoirs each having a linear relationship between storage and outflow with the storage coefficient of K_q. Mathematically, the IUH is expressed by a gamma probability distribution:

$$\mathrm{u(t)} = \frac{\mathrm{K_q}}{\Gamma(\mathrm{N})}\left(\mathrm{K_q t}\right)^{\mathrm{N}-1}\exp\left(-\mathrm{K_q t}\right)$$

where, Γ is the gamma function. The within-grid groundwater routing process is simplified as a lumped linear reservoir with the storage recession coefficient of K_s.

- *River Channel Routing: Linearized Saint-Venant Eq.*

The transport of water in the channel system is described using the diffusive wave approximation of the Saint-Venant equation (Lohmann, et al., 1998):

$$\frac{\partial Q}{\partial t} + C\frac{\partial Q}{\partial x} - D\frac{\partial^2 Q}{\partial^2 x^2} = 0$$

where C and D are parameters denoting wave velocity and diffusivity, respectively.

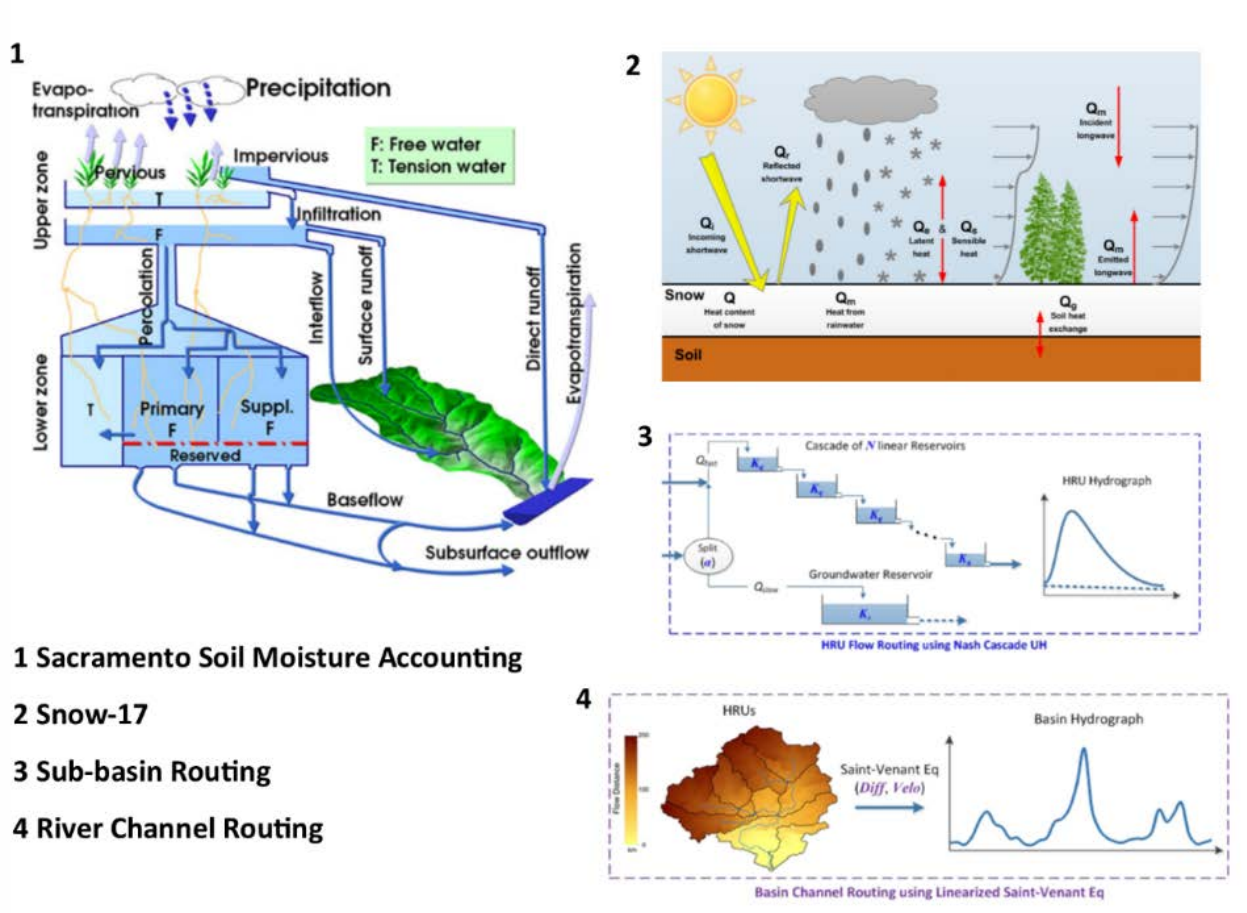

Figure 41 Schematic of distributed SAC-SMA hydrologic model

Water Resources System Model

CalLite is the water resources system model used in this study to assess the vulnerability of the Central Valley system to drought impacts. It is a screening level planning tool developed by DWR and United States Bureau of Reclamation (Reclamation) for analyzing Central Valley

water management alternatives. CalLite is the faster, streamlined version of CalSIM (Draper et al., 2004), designed to be accessible to policy and stakeholder demands for rapid and interactive policy evaluations. CalSIM, driven by the Water Resource Integrated Modeling System (WRIMS model engine or WRIMS) is "a generalized water resources modeling system for evaluating operational alternatives of large, complex river basins that integrates a simulation language for flexible operational criteria specification, a mixed integer linear programming solver for efficient water allocation decisions, and graphics capabilities for ease of use" (California Department of Water Resources and United States Bureau of Reclamation, 2011). As explained by Draper et al. (2014), "for each time period, the solver maximizes the objective function to determine a solution that delivers or stores water according to the specified priorities and satisfies system constraints. The sequence of solved MIP problems represents the simulation of the system over the period of analysis… CalSim also allows the user to specify objectives using a weighted goal-programming technique pioneered by Charnes and Cooper (1961)."

CalLite, a schematic of which is shown in Figure 42, represents reservoir operations, State Water Project (SWP) and Central Valley Project (CVP) operations and delivery allocation decisions, existing water sharing agreements, and Delta salinity responses to river flow and export changes on a monthly timestep. CalLite can also represent the effect on the water system of land use changes and sea level rise, features not planned for use in this study. CalLite 3.0, released in 2014, has 796 input parameters, and approximately 240 additional data tables that store all relational data, such as reservoir area-elevation-capacity data, wetness-index dependent flow standards, and monthly flood control requirements (California Department of Water Resources and United States Bureau of Reclamation, 2011; Draper et al., 2004). Output includes water supply indicators, environmental indicators, and water use metrics.

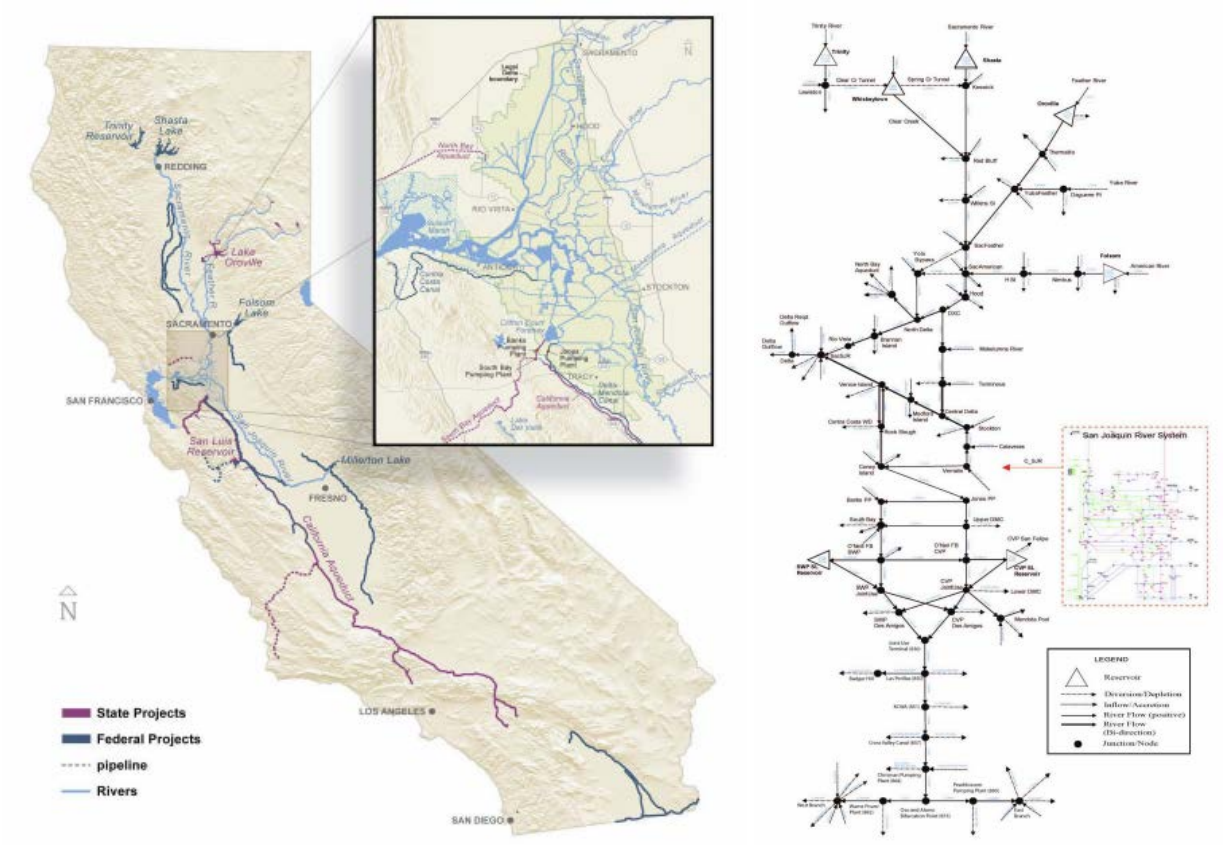

Figure 42 CalLite Schematic

- *Quantile Mapping Procedure for CalLite Inputs*

The water system model CalLite requires 796 parameters as inputs; those include inflow to the Central Valley System and water withdrawals (by demand and pumping) and diversions in the system. Of 796 CalLite inputs, 42 are concerned with inflows to the CVS; these 42 inflows consist of the 12 rim basin inflows and 30 local inflows.

To implement the drought vulnerability assessment of the CVS planned in this study, the CalLite inputs need to be generated corresponding to the synthetic climate conditions produced by the weather generator. In order to do so, we first applied the SAC-SMA_DS hydrologic model to simulate inflows of the 12 rim sub-basins, which historically take a majority of the total inflows to the CVS (approximately 85%). The simulated 12 inflows were then used to generate the 30 local inflows following the quantile mapping procedure described in detail below.

As a preliminary step to the quantile mapping, the historical local inflows, which take the portion of the system's total inflows other than 12 rim inflows (about 15%), were paired with one of the historical rim flows based on the statistical correlation. Specifically, each historical local inflow is tested for its Pearson's correlation coefficient with the 12 historical rim inflows and then

paired with the rim inflow that shows the highest correlation. For example, Figure 43 shows the correlation that two historical local inflows have (I18_FG and I18_SRJ) with the historical inflows of the 12 rim basins and the rim inflows of I_NHGAN and I_MLRTN are selected as the best pairs of I18_FG and I18_SRJ respectively. The pairs of local and rim inflows determined in this way are used in the quatile mapping procedure to generate new local inflows corresponding to new rim inflows. The quantile mapping procedure is detailed with a specific example in the following section. Table 6 shows pairs of local and rim inflows determined for all local inflows. Consequently, 6 of the rim inflows are selected based on which inflows are quantile-mapped.

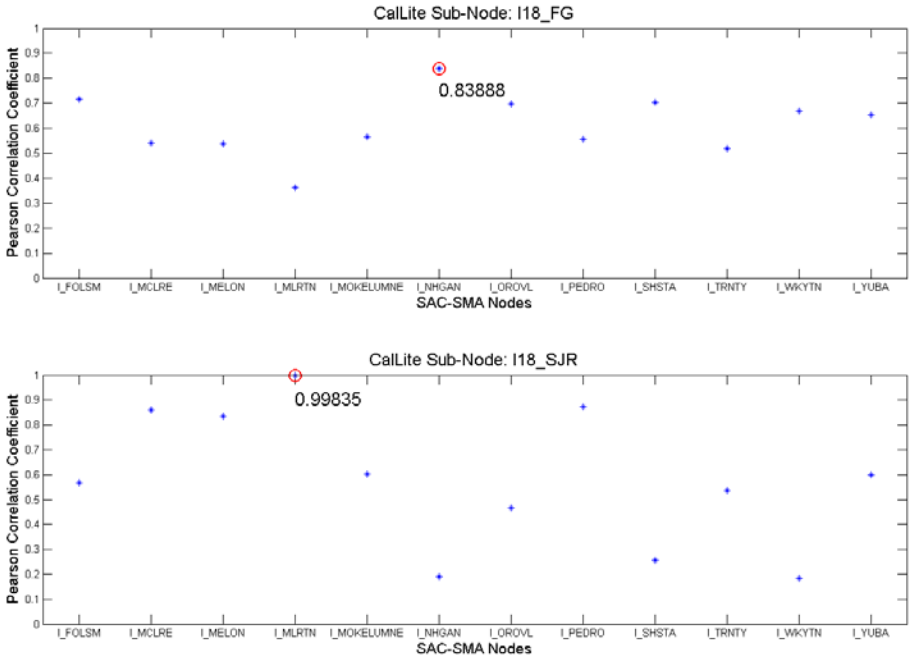

Figure 43 Pearson correlation coefficients of two historical local inflows (I18_FG and I18_SJR) with historical 12 rim inflows.

Table 6 Pairs of rim flows and local inflows determined by correlation. Blue bold text in parentheses represent the values of Pearson's correlation coefficient and red bold text represent contribution of local inflows to the total system inflows.

Rim Inflow Nodes	Local Inflow Nodes
I_NHGAN	I_STANGDWN(**0.99**, **0.01%**), I_NIMBUS(**0.94**, **0.03%**), I512(**0.93**, **0.20%**), I_ESTMN(**0.91**, **0.28%**), I_EASTBYP(**0.90**, **0.76%**) I_CALAV(**0.87**, **0.05%**), I_HNSLY(**0.87**, **0.33%**), I18_FG(**0.84**, **0.13%**), I_TERMINOUS(**0.83**, **0.22%**), I_BRANANIS(**0.79**, **0.32%**) I_STOCKTON(**0.77**, **0.06%**), I_MEDFORDIS(**0.76**, **0.18%**), I_HOOD(**0.72**, **0.05%**), I_SACSJR(**0.72**, **0.02%**), I_CONEYIS(**0.71**, **0.10%**) I422(**0.68**, **0.01%**), I_MARSHCR(**0.61**, **0.13%**), I_SJRMS(**0.57**, **0.09%**), I_SJRMSA(**0.57**, **0.09%**), I_TUOL(**0.42**, **0.79%**)

I_MELON	I_SJRMAZE (**0.58**, **1.45%**), I_SJRSTAN (**0.58**, **0.08%**), I_MERCED1B (**0.51**, **0.33%**)
I_MLRTN	I18_SJR (**0.99**, **6.66%**), I_KERN (**0.49**, **0.10%**), I_STANRIPN (**0.32**, **0.40%**)
I_FOLSM	I501 (**0.92**, **1.42%**), I_KELLYRIDGE (**0.38**, **0.50%**)
I_MOKELUMNE	I_MDOTA (**0.60**, **0.58%**)
I_TRNTY	I_LEWISTON (**0.99**, **0.03%**)

Here, we provide a detailed description on the quantile mapping procedure with an example for the local inflow of I18_SJR whose contribution to the total inflows (about 6.6%) is the largest among local inflows. For the I8_SJR, the rim inflow of I_NHGAN is selected as the best correlated inflow, with the correlation coefficient of 0.99. The quantile mapping procedure starts with fitting those two inflows to specific probability distributions. In this study, we employed two types of distributions: 1) empirical probability based on the Weibull plotting position, and 2) theoretical probability based on 2-parameter Gamma distribution. How the quantile mapping works for the I18_SJR with selected rim inflow I_NHGAN is illustrated in Figure 44. For those two inflows, both the empirical and theoretical distribution are fitted as shown in Figure 44; red line with asterisk dots represent the fit by the Weibull plotting position and blue line by the Gamma distribution. The red continuous empirical probability line is formed by doing a linear interpolation between values of asterisk dots. As shown in the figure, the new rim inflow lead us to the new local inflow value through those two quantile plots of local and rim inflows. The quantile mapping procedure is simply summarized in two steps: 1) find a quantile (i.e., non-exceedance probability) for the new rim inflow, 2) find the value of local inflow that corresponds to the quntile of the rim inflow. In our quantile mapping procedure, empirical distributions are used as long as new inflows are within historically observed range. In case the new inflows are beyond the historical range, Gamma distribution fit is used. This quantile mapping procedure is conducted on a monthly basis to take into account the seasonal variability of inflows (the example in Figure 44 is for June).

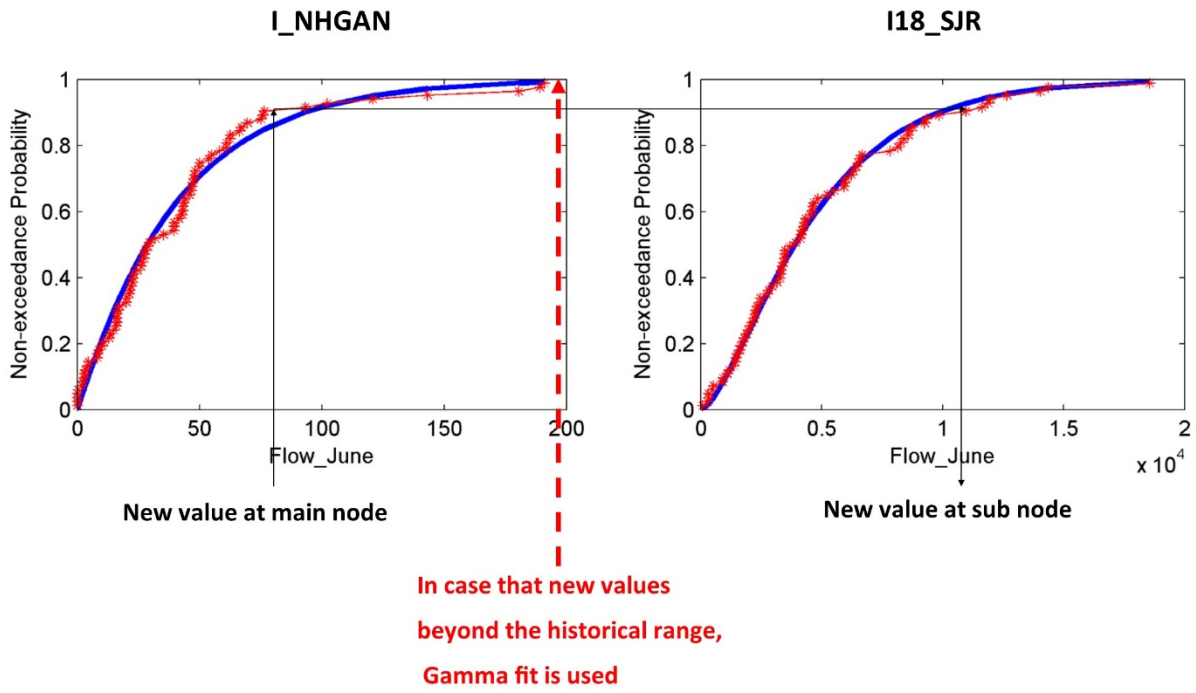

Figure 44 Quantile mapping procedure applied to example California sub-basin

This quantile mapping procedure is also applied to generate other CalLite inputs that relate to water withdrawals and diversions. Here, the CalLite inputs on which these withdrawals and diversions-related inputs are quantile-mapped based include 42 inflows and the time series of water year types, in which a system's condition is classified into one of five states every month: "wet" classification, two "normal" classifications (above and below normal), and two "dry" classifications (dry and critical).

Vulnerability Assessment Results

Hydrologic Model Results

The SAC-SMA_DS applied to reproduce historical inflows of the 12 rim sub-basins shows very good performance as shown in Table 7. The performance metrics of NSE evaluated on the monthly simulated streamflow show values of above 0.9 for all except for the sub-basin Mokelumne, for which NSE is 0.8. Considering the recommendation of Moriasi et al. (2007) that model simulation can be judged as satisfactory if NSE > 0.50, these simulation results are highly satisfactory and will greatly reduce the errors stemming from the hydrology.

Table 7 Hydrologic model performance for 12 rim sub-basins

Sub-basin	Nash Sutcliffe Efficiency
Folsom	0.96

Merced	0.95
Stanislaus	0.91
San Joaquin	0.92
Mokelumne	0.80
Calaveras	0.96
Oroville	0.95
Tuolumne	0.94
Shasta	0.97
Trinity	0.91
Yuba	0.91
Whiskeytown	0.95

System Model Results

- *System Model Calibration*

Three key outputs of CalLite 3.0 are the focus of this study, representing water supply (to municipal and agricultural water users) and ecological objectives. They are: 1) monthly SWP and CVP water deliveries, which indicate the ability of the system to meet demands given limitations of the available water, environmental regulations, and other competing water system goals; 2) end-of-April Shasta River reservoir storage, which represents the coldwater pool management of storage for water temperature control of the Sacramento River fisheries; and 3) X2 distance, the point identified by its distance from the Golden Gate Bridge to where salinity at the river's bottom is about 2 parts per thousand (ppt), which is the basis for standards to protect aquatic life. These three example outputs represent the types of water supply and ecological metrics of great interest to water system planners in California. Were any of the three to respond poorly to worsening drought conditions, adaptation measures would be in order. Figure 45 shows sample output of CalLite for two of these metrics, total annual water deliveries and X2 distance. The close correlation between the observed (black) and simulated (red) results demonstrates acceptable model performance.

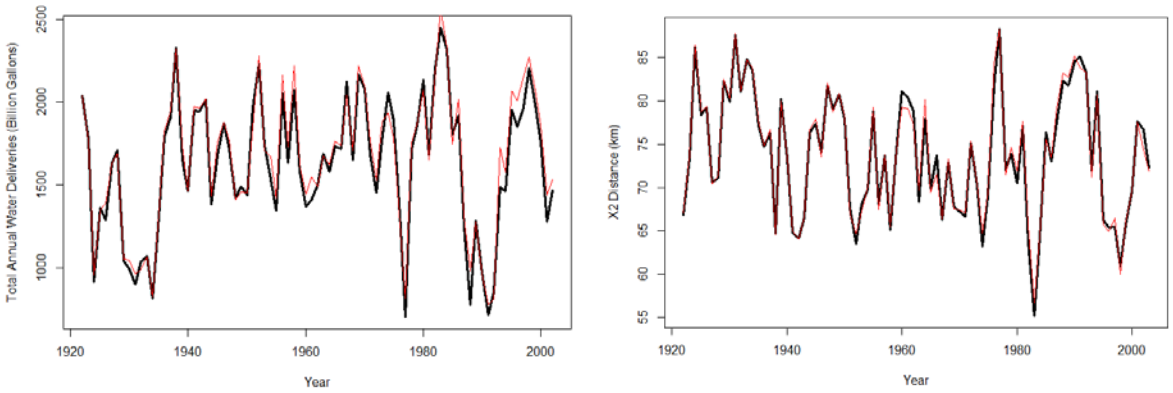

Figure 45 Water supply and environmental objectives: annual SWP and CVP water deliveries (left), which indicate the ability of the system to meet water demands and annual average X2

distance (right), which is the point identified by its distance from the Golden Gate Bridge to where salinity at the river's bottom is about 2 parts per thousand (ppt), which is the basis for standards to protect aquatic life. Historical data is shown in black and simulated values are shown in red.

- *Drought Sensitivity*

We broadly explored the hydrologic droughts spanning 2-20 years and ranging in severity from 0th percentile to 50th percentile (Figure 46). This analysis revealed that in nearly all simulations, delivery minima (2 year running average deliveries) occur during 2, 3 and 5 year droughts (not during 10 or 20 year droughts). Here, the key message is that the CVS is more sensitive to short duration severe droughts than longer duration droughts of the same severity.

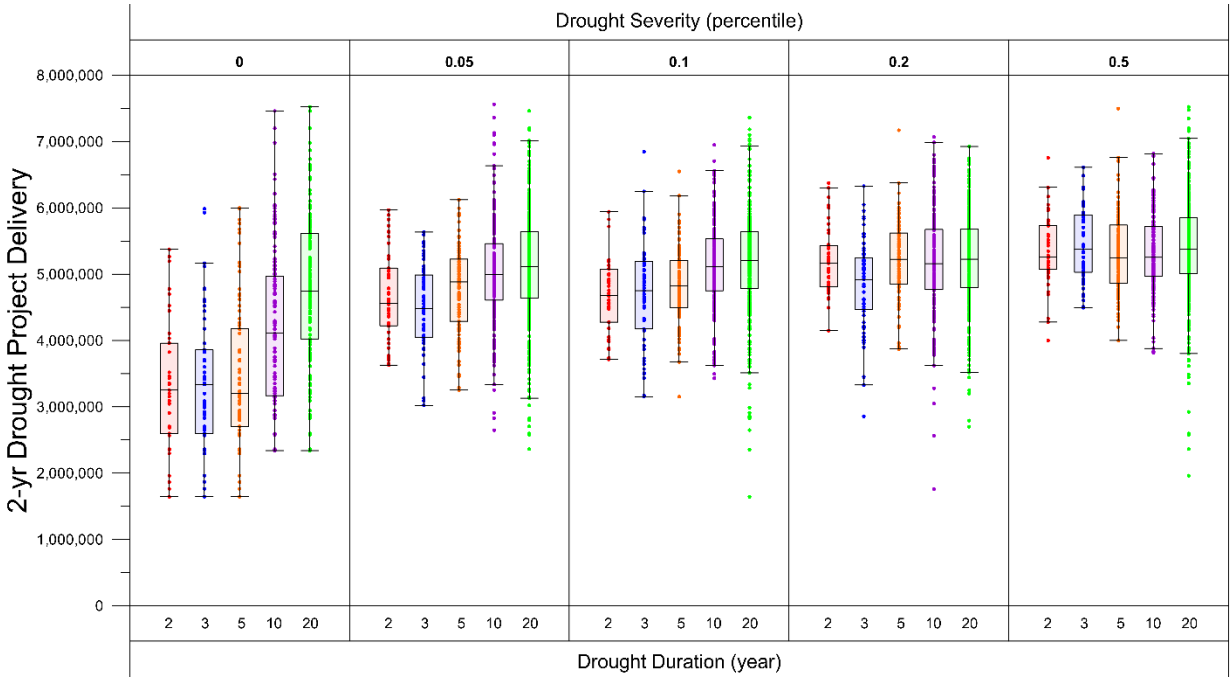

Figure 46 System sensitivity to drought

- *Internal variability vs. Climate Signal*

Figure 47 shows the system sensitivity with respect to the temperature changes (no change and increases of 0.5, 1.0, 2.0, and 3.0 ^{o}C). Each temperature change run was tested with 50 weather generator runs to explore the impact of internal variability of climates.

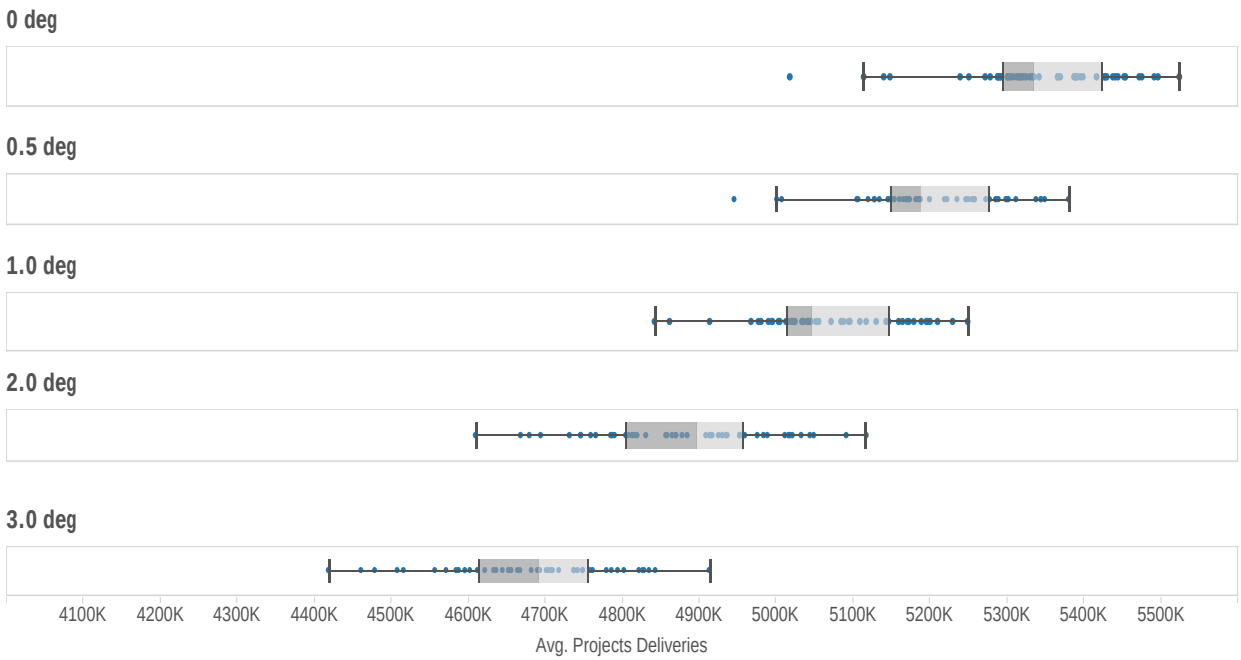

Figure 47 System sensitivity to temperature change and internal variability

For the evaluation of the system response to those temperature changes, instead of applying a constant temperature shift throughout a year we attempted to account for a seasonal variability informed by the set of global climate change simulations from the World Climate Research Programme's Coupled Model Intercomparison Project Phase 5 (CMIP5) multimodel ensemble (Talyor et al., 2012). Figure 48 shows the CMIP5 projection of monthly mean temperature changes between the historical period 1971-2000 and future period 2036-2065 for the CVS. Among the GCM ensembles of four emission scenarios (RCP 2.6, 4.5, 6.0, and 8.5), we used the ensemble mean temperature change pattern from the RCP 4.5 and incorporated the pattern into the temperature time series.

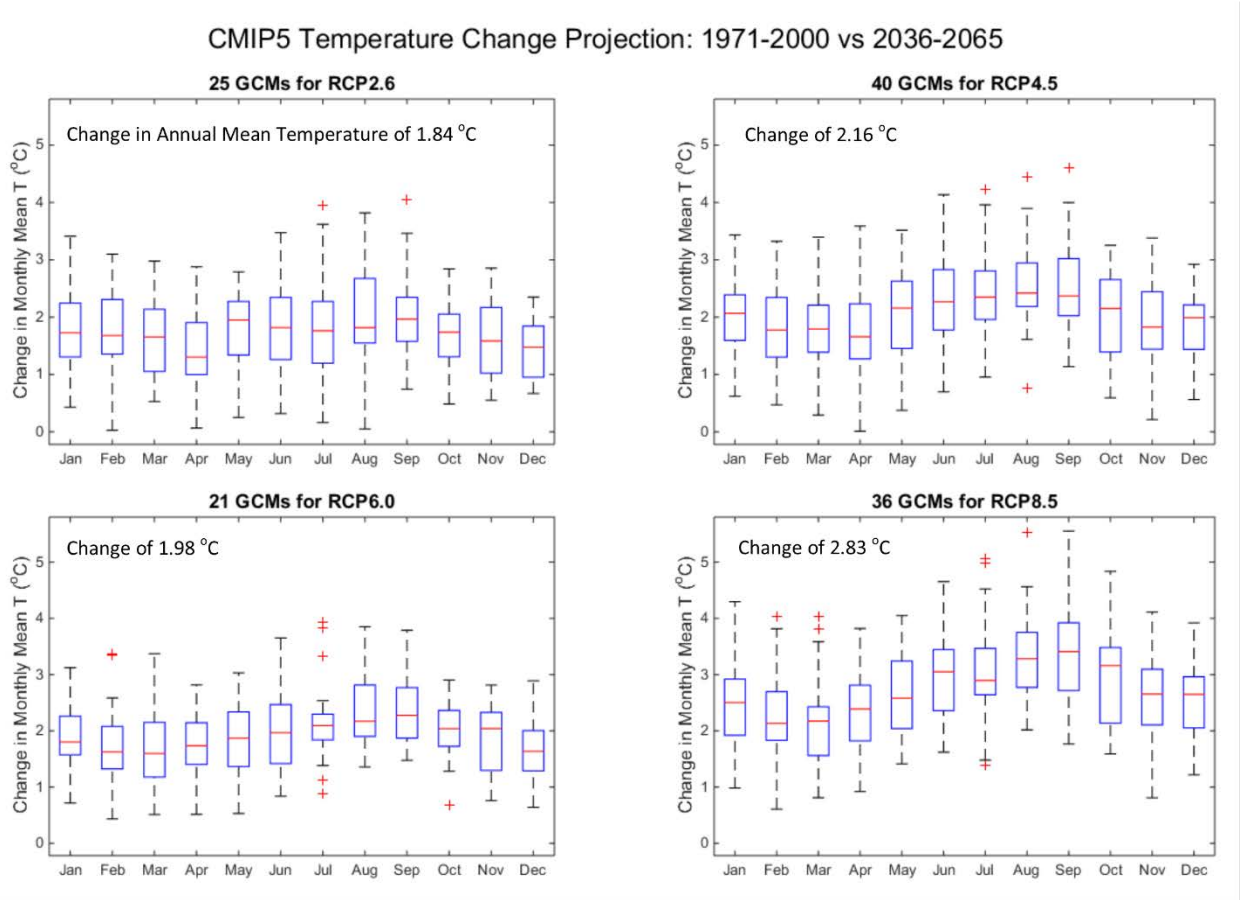

Figure 48 CMIP5 temperature change projection for the California Central Valley system.

Loss of deliveries caused by 0.5 °C increase in temperature still falls within the observed/historical climate distribution of performance. Internal variability can result in deviations in long-term delivery performance of ±4% from the mean. This internal variability is larger than the climate signal at lower levels of warming.

The effect of rising temperature only (no change in precipitation or sea level rise) has very significant effects on system deliveries. For each 0.5 °C increase in temperature the system losses approximately 110,000 acre-feet of delivery reliability. And internal variability appears to increase with rising temperature as well, with 3.0 °C warming, internal variability increases to nearly ±6%.

- *Individual Drought Tracing*

Hydrologic sequencing has large impacts on the severity of a drought. In Figure 49 four drought traces are shown that represent 5 year droughts of 5th percentile severity. All four have nearly identical average inflow over the course of the drought. However, each trace unfolds differently (Big dip, Erratic variation in inflow, Spike and Crash, and Steady Decline). The Big Dip results in the lowest annual minimum deliveries 2.5 MAF (50% below average), while the Erratic drought results in the highest annual minimum deliveries 4.2 MAF (just 14% below average).

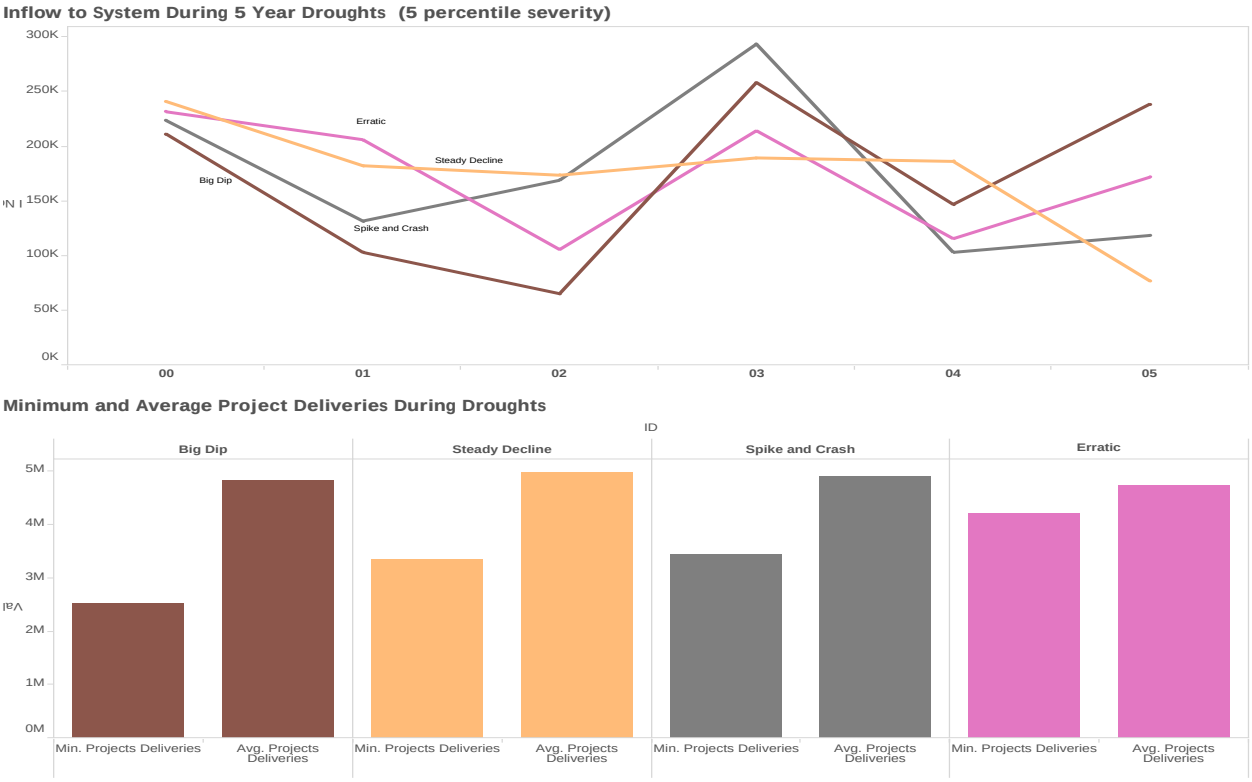

Figure 49 System sensitivity to drought shape

- *Sensitivity of SWP water delivery to climate changes*

Figure 50 presents the response of the annual average SWP water deliveries to changes in precipitation and temperature.

The performance metrics are contoured such that more favorable values are represented by blue while worse performance is represented by red. Seven precipitation changes (-30% to 30% compared to historical mean annual precipitation with a 10% interval) and nine temperature changes ranging from 0 to 4^{o}C with 0.5^{o}C increment are used to explore the response of annual average SWP deliveries to changing climate conditions. The climate trace used is the trace of observed historical climate (Oct 1922 - Sept 2003).

Both precipitation and temperature changes are influential factors for the CVS system. The historical average point is shown in the middle bottom of the plot. Temperature in excess of historical average temperature results in monotonically decreasing SWP deliveries. Precipitation greater than (less than) historical averages results in monotonically increasing (decreasing) SWP deliveries. The negative effect of temperature increase on SWP deliveries is due mostly to increases in loss by evaporation increases.

Finally, the projections of precipitation and temperature from the CMIP5 are superimposed onto the response surface, with colored dots: blue and red dots for RCP4.5 and RCP8.5 respectively. The GCMs show approximate change in CVS climate by mid-century (30-yr averages of the full ensemble of CMIP5 GCMs from 2035-2065 compared against 1971-2000). Judging by the likelihood of climate changes projected by CMIP5 GCMs (note that many of GCMs predict decreases in precipitation and almost all GCMs predict warmer conditions at least 1°C higher than the historical mean condition), the risk that the CVS system face a significantly reduced capacity of delivering water (i.e., water shortage) seems to be high, highlighting that well-planned adaptation that enhances the system's resilience to the droughts is advisable.

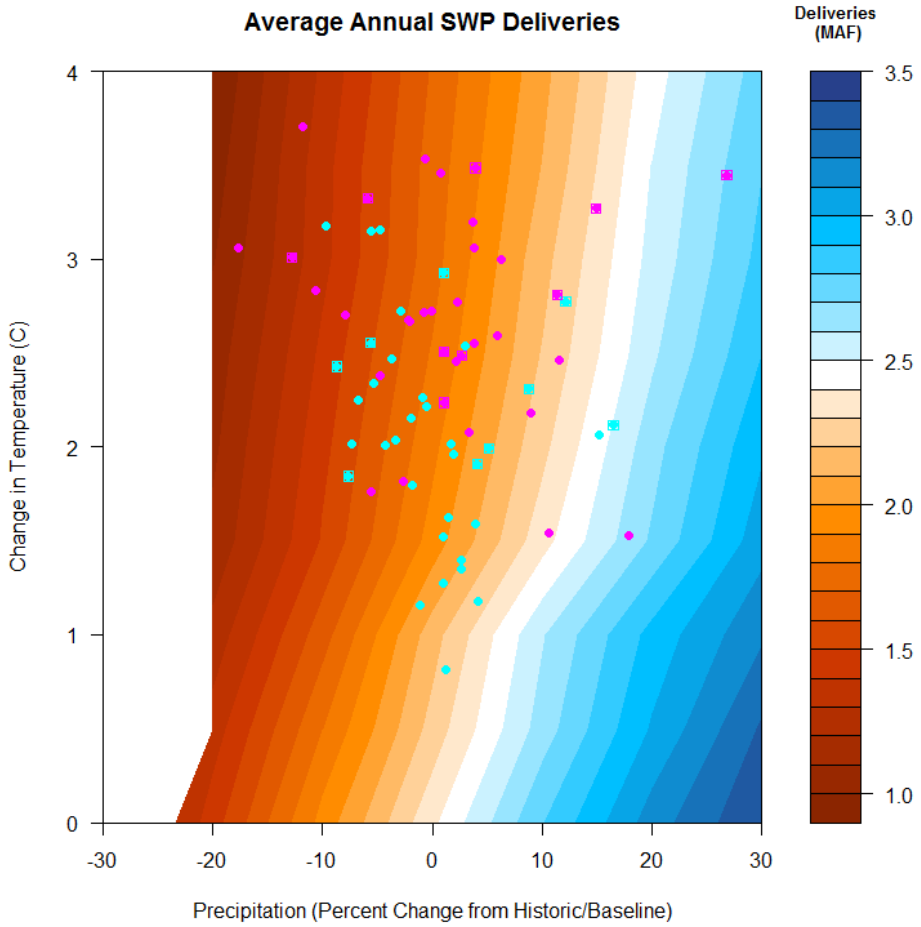

Figure 50 Response surface of the SWP water deliveries (in Million Acre Feet/year) averaged over 1951-2003. Dots represent CMIP5 projections of precipitation and temperature changes: blue for RCP4.5 and red for RCP8.5.

Conclusions

The past several years has revealed the current vulnerabilities to drought of California's water supply system and the economies and communities that depend on it. In this study, we conducted a drought vulnerability analysis of the water resources system in California's Central Valley by

using a stochastic weather generator to bootstrap on the historic climate record, a hydrologic model to generate new primary streamflows, and a quantile mapping to generate other system inputs. We test the system's response to a variety of other drought intensities and durations.

This study introduced a distributed version of the SAC-SMA model (named SAC-SMA_DS) capable of supporting subsequent phases of the drought vulnerability assessment workflow with a minimum propagation of uncertainty. The SAC-SMA_DS simulations for the historical inflows of the 12 rim sub-basins were highly satisfactory. The CalLite inputs generated by the quantile mapping procedure in which inflows to the system or water year types are main driver of other CalLite inputs properly drove the water system model, enabling us to further explore the vulnerability of the California water system to droughts of varying intensity and duration. Several valuable lessons we've learned from the vulnerability assessment are:

- The California Central Valley System is more sensitive to short duration severe droughts than longer duration droughts of the same severity. A broad exploration of hydrologic droughts spanning 2-20 years and ranging in severity from 0 percentile to 50th percentile revealed that in nearly all simulations, delivery minima (2 year running average deliveries) occur during 2, 3 and 5 year droughts (not during 10 or 20 year droughts.)

- Loss of deliveries caused by 0.5 ^{o}C increase in temperature still falls within the observed/historical climate distribution of performance. Internal variability can result in deviations in long-term delivery performance of +/-4% from the mean. This internal variability is larger than the climate signal at lower levels of warming.

- The effect of rising temperature only (no change in precipitation or sea level rise) has very significant effects on system deliveries. For each 0.5 ^{o}C increase in temperature the system losses approximately 110,000 acre-feet of delivery reliability. And internal variability appears to increase with rising temperature as well, with 3.0 ^{o}C warming, internal variability increases to nearly +/-6%.

- Hydrologic sequencing has large impacts on the severity of a drought. Four drought traces representing 5 year droughts of 5th percentile severity have nearly identical average inflow over the course of the drought. However, each trace unfolds differently (Big dip, Erratic variation in inflow, Spike and Crash, and Steady Decline). The Big Dip results in the lowest annual minimum deliveries 2.5 MAF (50% below average), while the Erratic drought results in the highest annual minimum deliveries 4.2 MAF (just 14% below average).

Chapter Conclusions

This chapter demonstrates the methodology for assessing climate change risks to water supplies for the four military installations considered. For the case of Edwards AFB, which is dependent on local groundwater resources (not effected by climate change) and the larger federal and state California water projects, the analysis focused on the larger system. In each case the analysis identified the specific climate change vulnerabilities of each system. Then, with the vulnerabilities known, climate model projections were used to estimate the relative probability of

the problematic climate conditions, which represents a measure of risk. The results for each installation are shown in the table below. Note that Colorado Springs represents water supply for the installations it serves. Edwards AFB is not listed as specific results for this installation were not estimated.

Installation	Risk of failure under historical condition	Risk of failure under climate change	Risk Increase
Fort Benning	5%	38%	33%
Fort Hood	5%	46%	41%
Colorado Springs	5%	5%	0%

The methods used in these assessments are complicated and time intensive, reflecting the complicated nature of these built and natural coupled systems. The estimation of vulnerabilities necessarily requires modeling of the entire system that supplies water to the installation because infrastructure plays such a critical role in determining the ability of a water supply to be reliable under climate change. Screening level analyses using regional climate change information might be used to flag whether a system requires further analysis. However, the efficacy of such a screening level assessment was not part of this analysis.

Results and Discussion: Fire Risk Installation-Level Assessment

Decision Framing

Fire management, both prescribed and for control and prevention of wildfires, is a significant land management activity on military installations. DoD fire management is an example of an installation management activity that is cross-cutting across domains of interest including operations, soldier and facilities safety, and natural resources management. Installation management activities for wildfire control and prescribed fire are directly related to climate factors that include wind speed and relative humidity. Failure to adequately reduce risk of wildfire can significantly compromise installation operations. Most installations have range regulations specifying under what weather conditions incendiaries (e.g. tracer rounds or smoke generating munitions) are prohibited to reduce wildfire risk, and ambient weather conditions must meet safety criteria for implementing prescribed burns. In 1996, major wildfires on Fort Hood caused by incendiaries used under hot, dry and windy conditions caused nearly complete cessation of installation training activities for a week and resulted in destruction of endangered species habitat beyond allowable limits. This resulted in the installation having to re-enter consultation with the U.S. Fish and Wildlife Service. In 2012, wildfires in proximity to the Air Force Academy resulted in closure and partial evacuation of cadets and staff from the academy.

Installations establish their own regulations for fire management and wildfire prevention. On Fort Hood III Corps & Fort Hood Regulation 350-40 prescribes what training activities may or may not be conducted under conditions of high fire risk. On Fort Hood the Directorate of Plans, Training, Mobilization, and Safety (DPTMS) Range Division has responsibility for implementing this regulation. As required by Army Regulation 200-1, Chapter 4 installations have developed Integrated Wildland Fire Management Plans (IWFMP). On Fort Hood, the Directorate of Emergency Services (DES), Fire and Emergency Services (FES) Fire Chief is designated as the Fort Hood Wildland Fire Program Manager (WFPM) and has responsibility for all of the duties assigned to the WFPM. However, implementation of fire management, suppression, and prevention activities is supported by many Fort Hood organizational elements including DPTMS, Directorate of Public Works Environmental Division. In addition the IWFMP must be consistent with objectives and activities under the Fort Hood Integrated Natural Resource Management Plan (INRMP) and the Integrated Cultural Resource Management Plan (INRMP). Fort Benning has similar range regulations governing wildland fire management and associated training regulations.

Installations generally use KBDI (described below) to establish wildfire risk ratings and determine suitable meteorological criteria for conducting prescribed burns. On Fort Benning, the Chief of Forestry calculates a daily KBDI. Fort Hood is a notable exception in that its fire risk determination is based on a site-specific fire model developed by Texas A&M University. The Range Safety Office makes the determination of daily fire risk ratings.

The decision by the Range Safety Office on allowable training activities as function of fire risk is made daily. Management objective for prescribed burn programs are established in INRMPs, which are 5-year plans. Annual work plans establish prescribed fire management goals annually contingent on current fiscal year appropriations. INRMP wildland fire management plans and prescriptions can be updated annually.

Non-meteorological factors that affect wildfire risk and implementation of prescribed burning programs include changes in intensity and types of munitions used in training exercises, access to ranges of personnel conduction prescribed burning activities, and habitat management activities to reduce fuel loads or construct permanent fire breaks.

Although most decisions regarding wildland fire management are made at the installation Directorate level, if future conditions significantly curtail ability to conduct necessary training activities or compromise ability to meet prescribed burning goals, decisions to modify training would be made at the level of the installation Commander or Installation Management Command (IMCOM) levels.

Analysis Methods

Keetch-Byram Drought Index Calculations

The Keetch-Byram Drought Index (KBDI), designated Q, is calculated on a daily interval (*dt* = 1 day) using the daily maximum temperature, *Tmax*, and daily precipitation P, as well as the annual mean precipitation *R*. The formulation for the daily change in KBDI, *dQ*, follows the revised and corrected English units equation of Alexander (1990) and Crane (1982) of the original Keetch and Byram (1968) index:

$$dQ = \frac{[800 - Q][0.968\exp(0.0486Tmax) - 8.30]dt\ x\ 10^{-3}}{1 + 10.88\exp(-0.0441R)}$$

The daily value Q is first decreased by the daily precipitation *P* (in hundreds of inches), and then increased by *dQ* in (1) above. The minimum Q value is kept at zero, the maximum at 800, which indicates 8 inches deficit in precipitation.

For the observed data analysis, as with the heat-related restrictions, the daily Tmax and P from the NOAA Global Summary of the Day (GSOD) stations with sufficient period of record for the installations are used to calculate the KBDI and the annual average number of days with KBDI in the range of the four color categories in Table 8.

Table 8 Live fire restriction table.

Fire Danger Condition	**Expected Fire Behavior**	**Training Restrictions**	**Fire Fighting Detail Requirements**	Derived KBDI*
GREEN	Fires are difficult to start and do not burn with vigor. Fires can easily be controlled using direct attack.	None.	None.	0-300
AMBER	Fires start easily and may burn quickly through grass	No aerial flares outside the live-fire training	None.	300-600

	and shrub fuels. Fires can be controlled using direct attack, but in some circumstances may require indirect attack methods.	areas. Pyrotechnics must be used on roadways, tank trails, or barren areas.		
RED	Fires start easily, move quickly, burn intensely, and may be difficult to control.	No pyrotechnics, incendiary munitions, tracers.	10-person fire fighting detail required. On-call helicopter required on 20-minute standby.	600-750
BLACK	Fires start very easily and are impossible to control.	No live-fire training. No pyrotechnics. Non-live-fire training must be authorized by the Senior Mission Commander.	None.	750-800

Projected Climate Impacts on Fire Risk – Mission Vulnerability

To assess the impact of a specific climate change projection on the fire risk at an installation, e.g. a change in mean monthly air temperature, dT_{air}, and a percentage change in average precipitation dP, we perturb the daily observed maximum temperatures T_{max} by dT_{air}, and scale the observed precipitation by a proportional change dP. We then compute projected number of days of each fire risk category under the projected climate change.

In estimating the projected heat impacts across the suite of CMIP 3 GCM projected results, we used the monthly mean temperature and precipitation changes from the bias corrected spatial disaggregated method of Maurer et al. (2002) for the climate changes at the 1/8 degree spatial resolution. These results are shown in the case studies below.

For the estimation of the fire risk across the wider range of climate changes, we computed the number of heat restriction categories across a range of +/- 5^{o}C, and change in precipitation of +/- 20%. The results across this range are shown in the case studies sections below.

Case Studies

The methods described above have been applied to our four selected installations for this project: Fort Benning, GA, Fort Hood, TX, Edwards Air Force Base, CA, and the Air Force Academy, CO.

Case Study 1: Fort Benning, GA

The annual number of days of each fire risk category for Fort Benning are shown in Figure 51 below for the observed daily data (left column) and for climate projections taken as the average of 36 model simulations from the CMIP3 A2 emission scenario for three 20-year periods. This figure includes only temperature changes, not precipitation changes.

For the observed record data (left column), Fort Benning experiences no days with the highest fire risk (KBDI > 750), and approximately 50 days with the category 4 fire risk (KBDI 600-750). The relatively frequent precipitation in the Southeast US maintains average KBDI values below 600 for most years, although the multiyear droughts that have occurred have pushed these values higher for these periods.

The projected temperature increases from the multi-model average increase the days with the higher two categories (red and black) to about 85 days per year by the 2080-2090 period, suggesting that significant increases in fire risks are possible, but will depend on the relative changes in precipitation, as well.

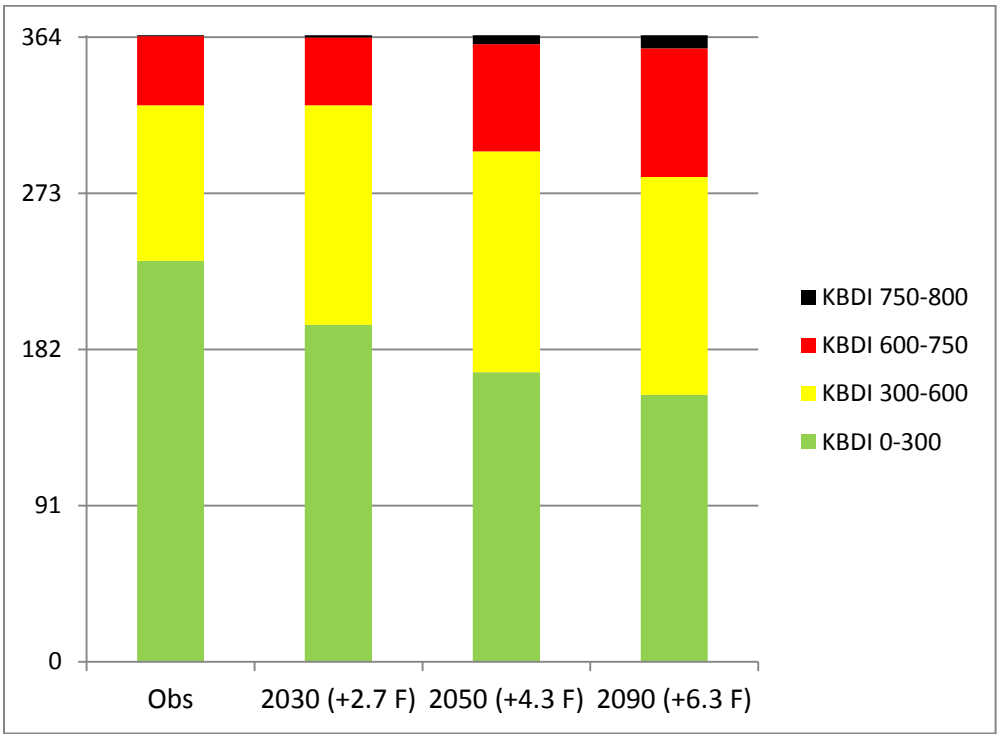

Figure 51 The annual number of days with live fire restrictions of each category for Fort Benning, based on daily computed KBDI, for the observed daily data (left column), and for projected temperature increases for 2030, 2050, and 2080.

The vulnerability of the installation to fire risks as a function of mean temperature and precipitation change in Figure 52 shows the expected increase in days for the two combined higher fire risk categories (KBDI from 600 to 800). The gradients of the fire risk days suggest there is an equivalent impact of 1 C temperature increase as an approximate 3% decrease in precipitation. The 36 GCM simulation results show a significant range in the change in mean precipitation among the models, from -17% to +15% for the 2080 timeframe, resulting in a potential range of high fire risk between 40 and 80 days.

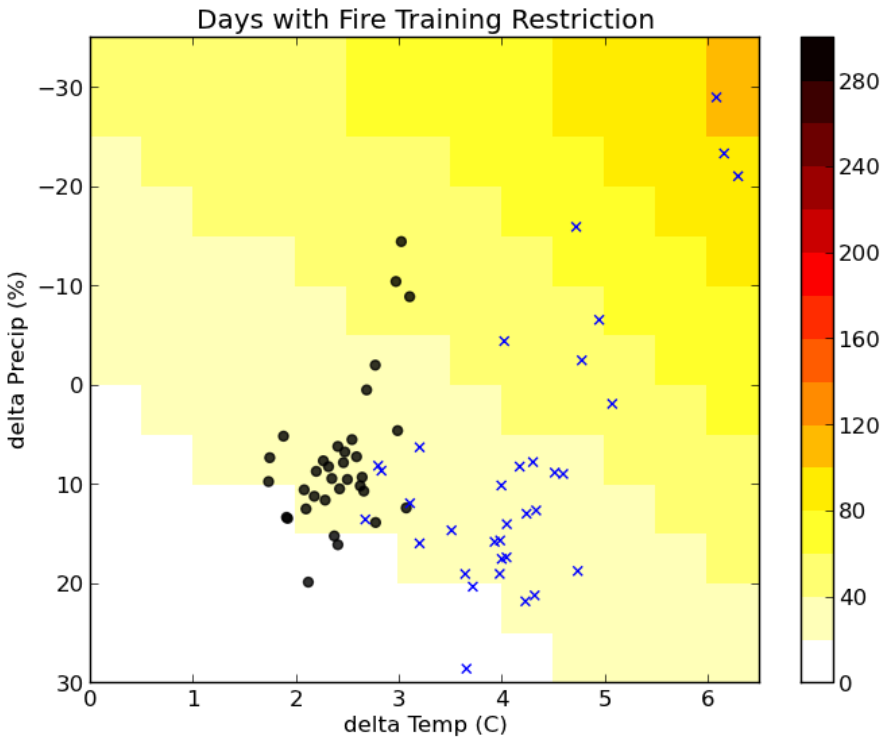

Figure 52 The dependence of number of days with the combined two fire risk categories (KBDI 600 to 800) on the mean temperature change (dT, ºC) and mean precipitiaton change (dP, %) for Fort Benning. The points represent the mean temperature and precipitation changes from 36 GCM simulations of the A2 scenario from the CMIP 3 archive, for years 2050 (black) and 2080 (blue).

Case Study 2: Fort Hood, TX

The annual number of days of each fire risk category for Fort Hood are shown in Figure 53 below for the observed daily data (left column) and for climate projections taken as the average of 36 model simulations from the CMIP3 A2 emission scenario for three 20-year periods. This figure includes only temperature changes, not precipitation changes.

For the observed record data (left column), Fort Hood experiences about 20 days with the highest fire risk (KBDI > 750), and approximately 90 days with the category 4 fire risk (KBDI 600-750). The relatively dry, high temperature conditions of the South central Texas climate maintains KBDI values that are frequently above 600 for most years.

The projected temperature increases from the multi-model average increase the days with the highest category (black) slightly to 30 days per year by the 2080-2090 period, but increases the next highest (red) category more to over 100 days.

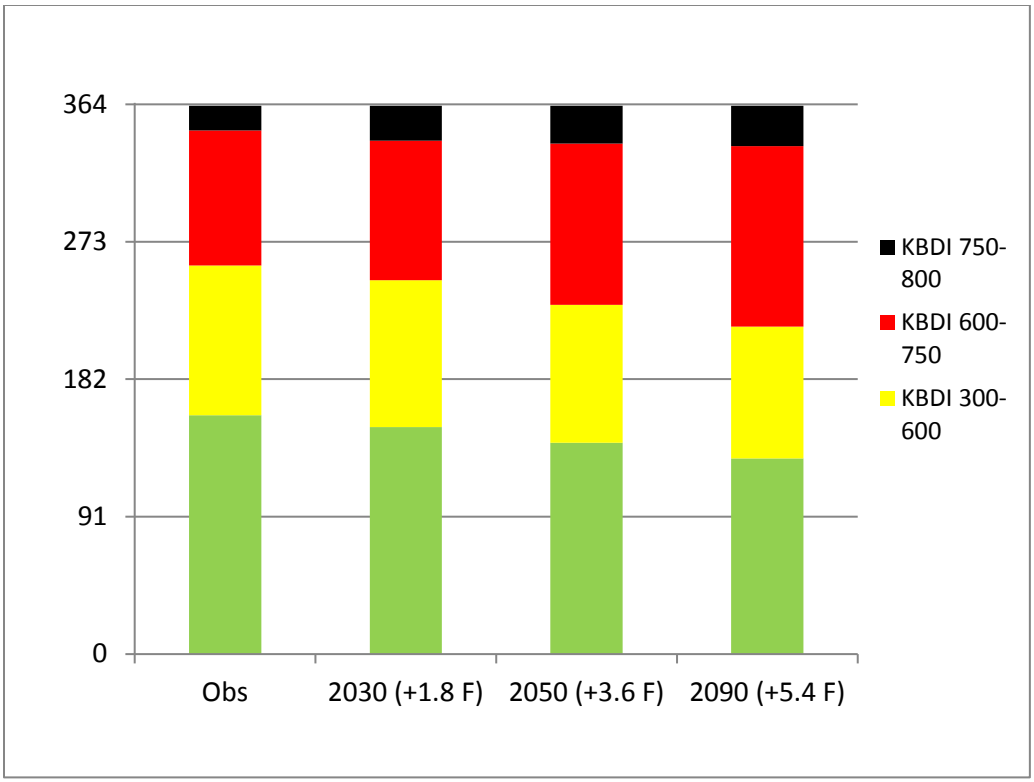

Figure 53 The annual number of days with live fire restrictions of each category for Fort Hood, based on daily computed KBDI, for the observed daily data (left column), and for projected temperature increases for 2030, 2050, and 2080.

Vulnerability Assessment

The vulnerability of the Fort Hood installation to fire risk is shown in Figure 54 below for the days with the highest fire risk category (KBDI > 750). There is substantially less dependence of high-risk days on the mean precipitation change, as the contours are more vertical across the +/- 20% precipitation range, but show a strong dependence on mean temperature change. The points of changes from the 36 GCM simulations for 2050 and 2080 timeframes have significant overlap in their ranges, with the fire risk days from 2050 from minimum of 15 days to maximum 30 days, and for 2080 from 20 to 32 days.

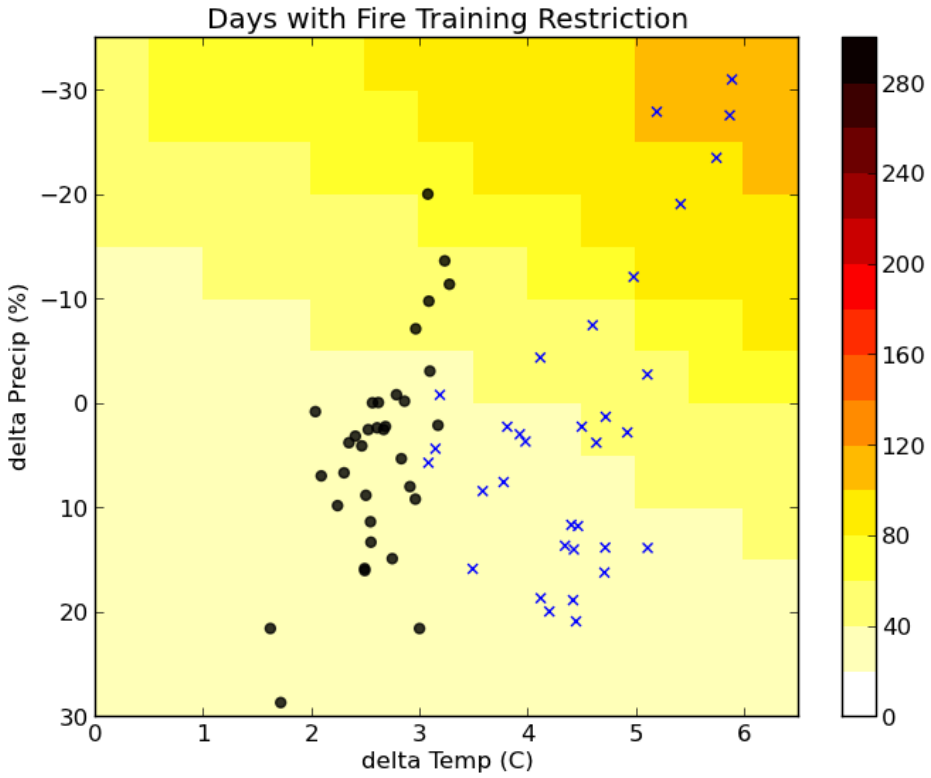

Figure 54 The dependence of number of days with the highest fire risk categories (KBDI 750 to 800) on the mean temperature change (dT, C) and mean precipitiaton change (dP, %) for Fort Hood. The points represent the mean temperature and precipitation changes from 36 GCM simulations of the A2 scenario from the CMIP 3 archive, for years 2050 (black) and 2080 (blue).

Case Study 3: U.S. Air Force Academy, CO

The annual number of days of each fire risk category for the US Air Force Academy are shown in Figure 55 below for the observed daily data (left column) and for climate projections taken as the average of 36 model simulations from the CMIP3 A2 emission scenario for three 20-year periods. This figure includes only temperature changes, not precipitation changes.

For the observed record data (left column), the Air Force Academy experiences about 25 days with the highest fire risk (KBDI > 600), but less days in the lower category of KBDI from 400 to 600. The relatively dry conditions of the Colorado location in the summer season keeps the KBDI values in the high range, while the frequency of snow and storms in the cold season in Colorado reduces the KBDI for the rest of the year. The future projections for this location expand the range of the lower fire risk days (yellow) and reduce the lowest risk days (green).

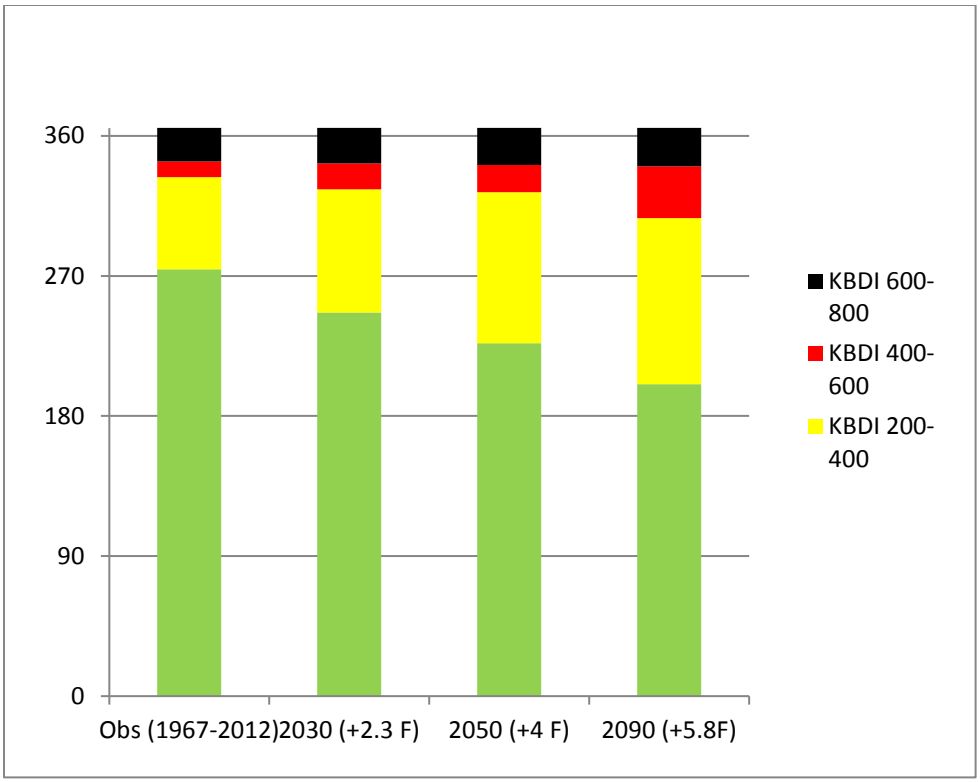

Figure 55 The annual number of days with live fire restrictions of each category for the Air Force Academy, based on daily computed KBDI, for the observed daily data (left column), and for projected temperature increases for 2030, 2050, and 2080.

Vulnerability Assessment

The vulnerability of the Air Force Academy to fire risk is shown in Figure 56 below for the days with the medium-to-high fire risk categories (KBDI > 400). There is dependence of these risk days to both the mean precipitation change and temperature change. The points of changes from the 36 GCM simulations for 2050 and 2080 timeframes have significant overlap in their ranges, with the fire risk days from 2050 from minimum of less than 5 days to maximum 25 days, and for 2080 from 5 to 35 days.

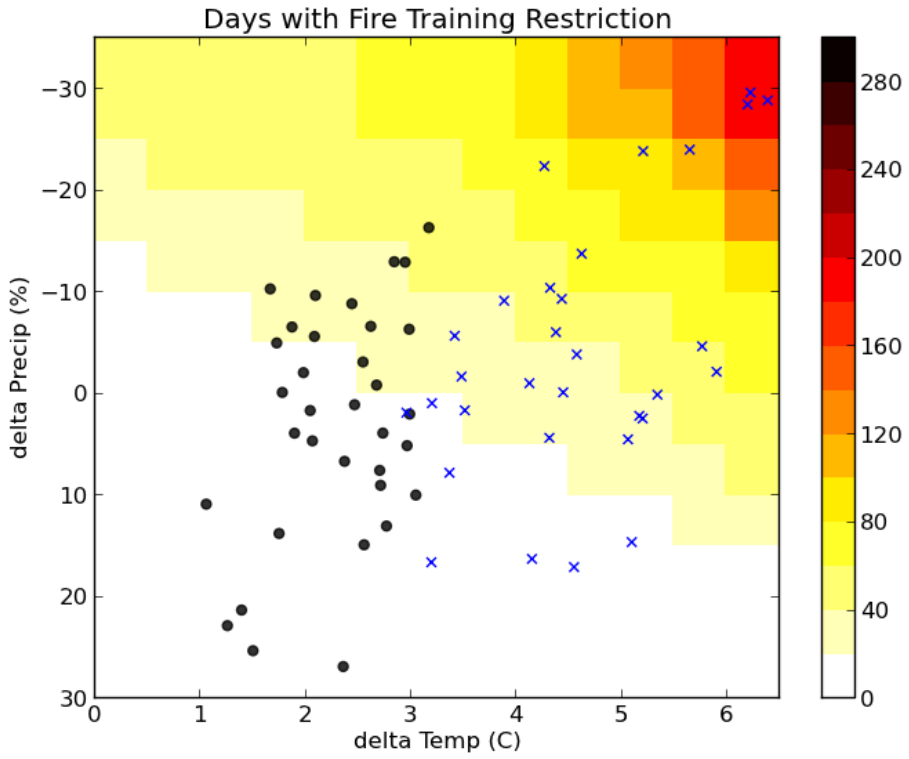

Figure 56 The dependence of number of days with the medium-to-high fire risk categories (KBDI 400 to 800) on the mean temperature change (dT, C) and mean precipitiaton change (dP, %) for the Air Force Academy. The points represent the mean temperature and precipitation changes from 36 GCM simulations of the A2 scenario from the CMIP 3 archive, for years 2050 (black) and 2080 (blue).

Case Study 4: Edwards Air Force Base, CA

The annual number of days of each fire risk category for Edwards AFB, in the dry southern California climate, are shown in Figure 57 below for the observed daily data (left column) and for climate projections taken as the average of 36 model simulations from the CMIP3 A2 emission scenario for three 20-year periods. This figure includes only temperature changes, not precipitation changes.

For the observed record data (left column), Edwards AFB experiences about 25 days with the highest fire risk (KBDI > 750), and about 200 days in the red category of KBDI from 600-750. The nearly year-round dry conditions at Edwards AFB keeps the KBDI values in the high range, with the lower KBDI values occurring in the winter storm season. The future projections for this location expand the range of the highest fire risk days, both red and black conditions.

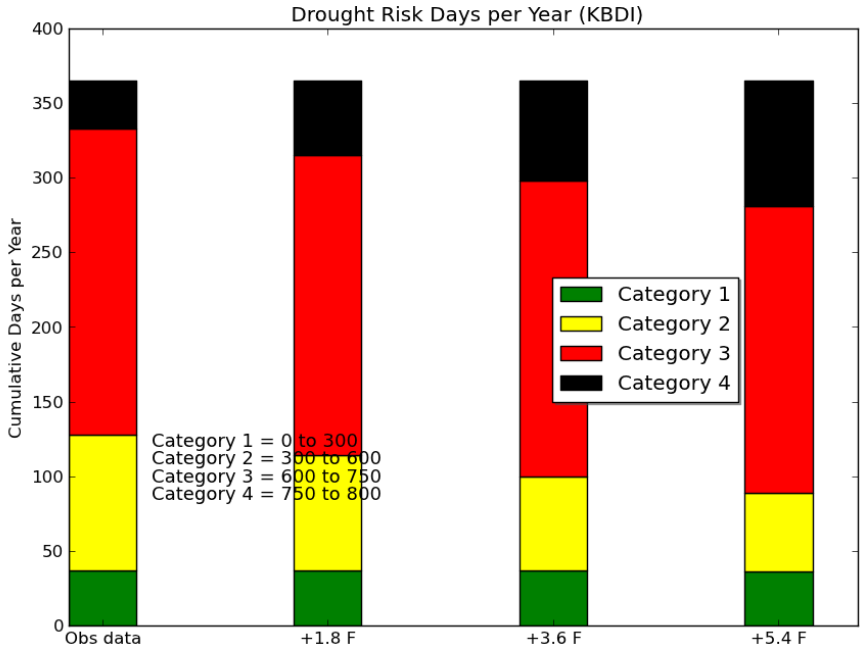

Figure 57 The annual number of days with live fire restrictions of each category for the Edwards AFB, based on daily computed KBDI, for the observed daily data (left column), and for projected temperature increases for 2030, 2050, and 2080.

Vulnerability Assessment

The vulnerability of Edwards AFB to fire risk is shown in Figure 58 below for the days with the highest fire risk categories (KBDI > 750). There is dependence of these risk days to both the mean precipitation change and temperature change. The points of changes from the 36 GCM simulations for 2050 and 2080 timeframes have less overlap in their ranges than with other sites. with the fire risk days from 2050 from minimum of 20 days to maximum 90 days, and for 2080 from 45 to 90 days.

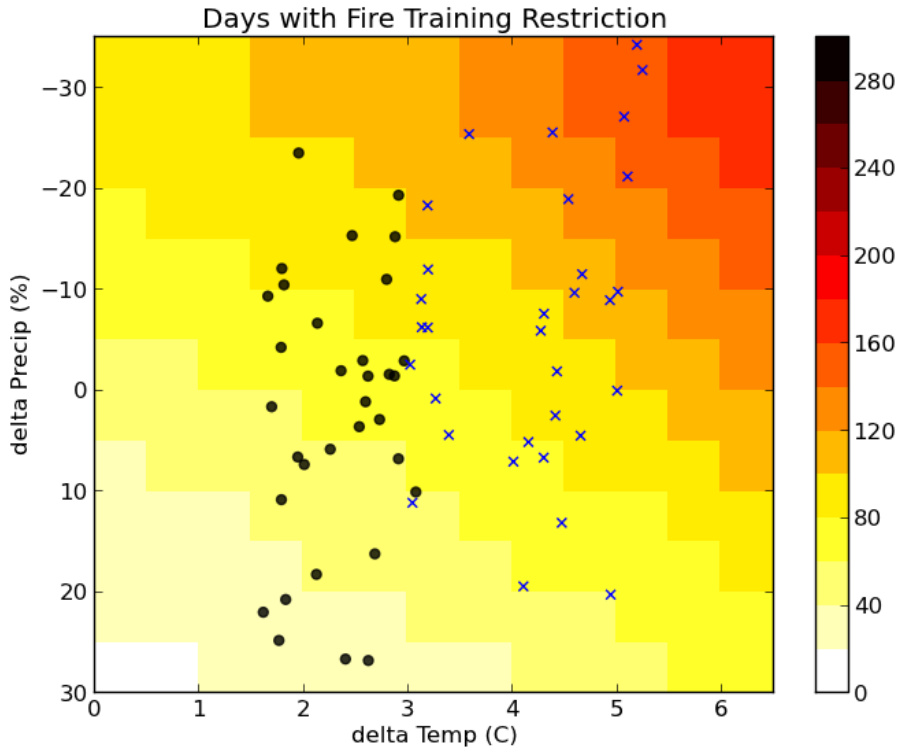

Figure 58 The dependence of number of days with the high fire risk categories (KBDI 750 to 800) on the mean temperature change (dT, C) and mean precipitiaton change (dP, %) for Edwards AFB. The points represent the mean temperature and precipitation changes from 36 GCM simulations of the A2 scenario from the CMIP 3 archive, for years 2050 (black) and 2080 (blue).

Results and Discussion: Training Installation-Level Assessment

Decision Framing

The risk of heat stress on soldier health, safety and operational readiness is a significant concern for DoD. This risk was highlighted and received wide-spread media coverage when a training exercise in June 2007 resulted in death of one soldier and emergency medical treatment for more than 2 dozen soldiers because of heat stress and dehydration. Under some conditions of heat and humidity, activity can be limited to as little as 10 minutes per hour. Increasing occurrences of these conditions could have significant negative effects on training.

For the Army, TB Med 507 provides the guidance for heat stress control and heat casualty management (See Figure 59 below). Processes and responsibility for determining heat stress risk varies at the installation level. To date, we have reviewed installation guidance and processes for determining heat stress risk and implementation of heat risk mitigation measures at Fort Benning, Georgia and Fort Hood, Texas. For example, at Fort Hood, III Corps & Fort Hood Regulation 350-16 "Prevention of Heat and Cold Injury" prescribes the policy and provides guidance to commanders in preventing environmental (heat or cold) casualties. In additions III Corps & Fort Hood Regulation 115-1 assigns responsibility to the Robert Gray Army Airfield Weather Station to provide weather data to Fort Hood agencies to calculate heat stress indices but does not provide the calculated indices. FH Reg 350-6 promulgates responsibility for assessing heat stress risk to installation Commanders. In essence this lays the responsibility on any unit commander leading soldiers working or training that may be subject to potential heat stress. Heat risk categories are determined using Wet Bulb Globe Temperatures (WBGT) as described below. At Fort Hood, personnel in the Range Safety Office calculate this measure hourly and transmit to units in the field via radio. On Fort Benning, each unit is supposed to conduct their own reading with their wet/dry bulb thermometer at the actual training site, and make decisions based on that reading. However, no consistent records are kept of just how many days/hours fall under some restriction over the year. The Fort Benning Army Medical Detachment (AMEDD) does record and post readings for the installation as a whole during the April to October "summer" season.

The time scale of the decision to implement activity restrictions in response to heat stress risk is potentially hourly and at least daily during periods of high temperatures. However, the impacts on training schedules resulting from reduction in allowable activity levels will be realized at monthly or yearly scales. Decisions to modify training schedules (e.g. conduct more night time training) and types of training (e.g. increase use of training simulators versus live field exercises) in response to increasing frequency of heat stress risk would have to be made at installation headquarter levels. The proximate decisions whether to restrict a units activities are obviously reversible contingent on environmental conditions. However, modification of training schedules or training type could require significant commitment of resources to modify training facilities and accommodate changes in support personnel scheduling.

Potential non-climate factors could mitigate impacts of future heat risk conditions resulting from climate change. Advances in soldier equipment and uniforms could reduce physical demands that exacerbate heat stress. Increasing reliance on simulator training could also reduce soldiers' exposure to extreme heat conditions.

Heat Category	WBGT Index, F°	Easy Work		Moderate Work		Hard Work	
		Work/Rest	*Water Intake (Qt/H)*	*Work/Rest*	*Water Intake (Qt/H)*	*Work/Rest*	*Water Intake (Qt/H)*
1	78° - 81.9°	NL	½	NL	¾	40/20 min	¾
2 (GREEN)	82° - 84.9°	NL	½	50/10 min	¾	30/30 min	1
3 (YELLOW)	85° - 87.9°	NL	¾	40/20 min	¾	30/30 min	1
4 (RED)	88° - 89.9°	NL	¾	30/30 min	¾	20/40 min	1
5 (BLACK)	> 90°	50/10 min	1	20/40 min	1	10/50 min	1

Figure 59 Heat-related activity restriction table based on Army TB Med 507 (2003).

Analysis Methods

Web bulb black globe Temperature Calculations

The sensitivity of training missions at individual installations is affected on the daily timescale by the restrictions to physical activities imposed by the Army's TB Med 501 guidelines. This guidance defines five categories of heat-related limitations from lowest (T_{wbgt} between 78° and 82°F) to highest (T_{wbgt} > 90°F). These restrictions are based on an on-site estimation of a wet bulb black globe temperature, T_{wbgt}. which is a blend of the ambient 2-m air temperature, wet-bulb temperature, and temperature measurement inside a sunlight black globe:

$$T_{wbgt} = 0.7\ T_{wb} + 0.2\ T_{globe} + 0.1\ T_{air}$$

Since records of measured Twbgt are not routinely kept, we compute T_{wbgt} based on the formulation by Dimiceli et al. (2011). In their formula T_{wbgt} is dependent on the measured surface air temperature, humidity, wind speed, and solar radiation. For our installation-level analysis, we use daily data records from the NOAA Global Summary of the Day (GSOD) for the observing station either on the installation, or closest to it, with a sufficiently long observation record. The variables in (1) for our analysis are defined as:

T_{air}: The daily maximum temperature (TMAX in NOAA data), as we are estimating the maximum heat impacts for the day.

T_{wb}: the wet-bulb temperature, can be measured in the field with a psychrometer or derived graphically using a skew-T chart based on the ambient temperature and humidity.

We used a computation tool from the National Weather Service to derive T_{wb} for a range of T_{air} and $T_{dewpoint}$ for summer at the installations, and derived a linear approximation for the maximum T_{wb} for each day based on the maximum T_{air} and mean (T_{mean}-$T_{dewpoint}$) depression.

$$T_{wb}\ (max) = T_{air}(max) - fwb*(T_{mean} - T_{dewpoint})$$

$fwb = .85 - .01*(T_{mean}-T_{dewpoint})$ for $(T_{mean}-T_{dewpoint}) < 50$ F
$fwb = .3$ for $(T_{mean}-T_{dewpoint}) > 50$ F

This allowed us to estimate the maximum T_{wb} for all stations where there was not hourly temperatures or dewpoint records. A more accurate computation for T_{wb} has been developed by Davies-Jones (2008), but that version has not been included into our present calculations.

T_{globe}: The black globe temperature computation is also described in Dimiceli et al. (2011), with an algorithm based on measurements inside a sunlit globe with surface albedo of 0.05 and emissivity 0.95. Their derived formulation is solved as

$$T_{globe} = (B + CT_{air} + 7680000) / (C + 256000)$$

$$B = S (f_{direct} / (4 \sigma \cos z) + 1.2 * f_{diffuse}/ \sigma) + \varepsilon T_{air}^4$$

Where S is the surface solar irradiance in Watts/m2, f_{direct} and $f_{diffuse}$ are the fractional direct and diffuse radiation, is the Stefan-Boltzmann constant, cos z is the cosine of the solar zenith angle z, and ε is the atmospheric emissivity (is assumed =1).

$$C = h u^{0.58} / 5.38 \text{ e-8}$$

Where h = 0.1, u is the wind speed in ***meters per hour*** (and is converted from knots from the NOAA data).For the NOAA GSOD daily data, there are no recorded values for solar radiation S, direct or diffuse radiation fractions. For the past years observations, we used

$f_{direct} = 0.7$
$f_{diffuse} = 0.3$
$S = S_{max} \cdot \cos Z$

where Z is the solar zenith angle at the site's latitude φ , at the maximum solar declination angle δ (23.6° N on the summer equinox) at local solar noon.

$$\cos Z = \sin \varphi \sin \delta + \cos \varphi \cos \delta$$

The maximum solar irradiance varies widely between locations and atmospheric conditions. For our installations in consideration, we have used:

Table 9 S_{max} for each location.

Location	Smax
Edwards AFB, CA	800 W m^{-2}
USAF Academy, CO	800 W m^{-2}
Ft Benning, GA	500 W m^{-2}
Ft Hood, TX	700 W m^{-2}

Using the daily maximum T_{wbgt} values over the period of record, the average number of days per year in each heat restriction category are calculated for the observed record.

Projected Climate Impacts on Heat Restrictions – Mission Vulnerability

To assess the impact of a specific climate change projection on the heat restrictions at an installation, e.g. a change in mean monthly air temperature, dT_{air}, and a change in relative humidity dRH, we perturb the daily observed temperatures and dewpoints and compute the project number of days of each heat restriction category under the projected climate change. Where there is a projected change in temperature, but not in humidity, we maintain the dewpoint depression from the perturbed maximum daily temperature. A specified increase in relative humidity translates to a proportional decrease in the dewpoint depression from the air temperature.

In estimating the projected heat impacts across the suite of CMIP 3 GCM projected results, we used the monthly mean temperature and precipitation changes from the bias corrected spatial disaggregated method of Maurer et al. (2002) for the climate changes at the 1/8 degree spatial resolution. These results are shown in the case studies below.

For the estimation of the mission vulnerability across the wider range of climate changes, we computed the number of heat restriction categories across a range of +/- 5 C, and change in relative humidity of +/- 20%. The results across this range are shown in the case studies sections below.

Case Studies

The methods described above have been applied to the four selected installations for this project: Fort Benning, GA, Fort Hood, TX, Edwards Air Force Base, CA, and the Air Force Academy, CO.

Case Study 1: Fort Benning, GA

The annual number of days of each heat restriction category for Ft Benning are shown in Figure 60 below for the observed daily data (left column) and for climate projections taken as the average of 36 model simulations from the CMIP3 A2 emission scenario for three 20-year periods. This figure includes only temperature changes, not relative humidity changes.

For the observed record data, Fort Benning experiences approximately 105 days with the highest heat restriction, with maximum T_{wbgt} > 90 F, so the installation training activities area already significantly affected by the climate of the Southeast U.S. The projected climate changes for 2030 onward result in greater increases in the highest heat category (black), and less changes in the lower categories. This is due in part by the consistently high temperatures and dewpoints in the Southeast, where any change in temperature increases the wet-bulb temperature accordingly.

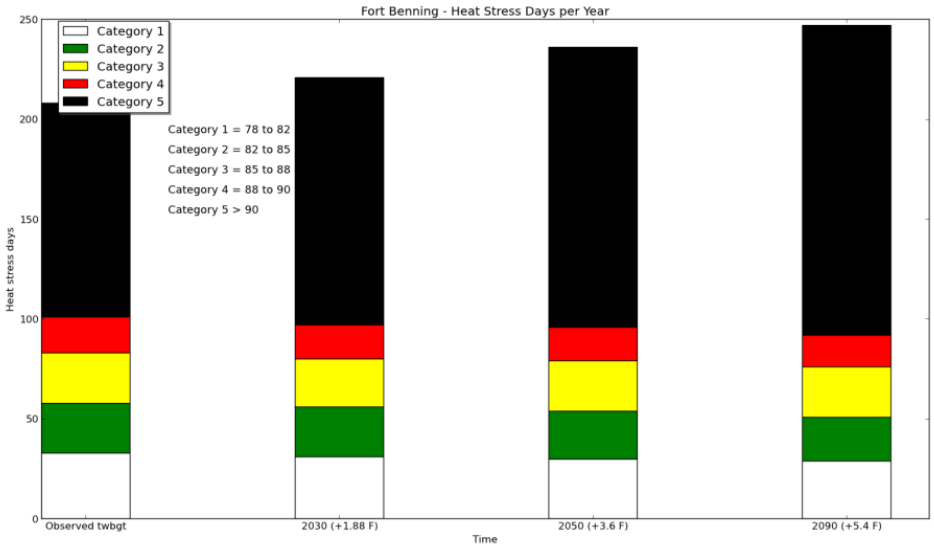

Figure 60 The annual number of days with heat related training restrictions of each category for Fort Benning, based on maximum daily Twbgt, for the observed daily data (left column), and for projected temperature increases for 2030, 2050, and 2080.

Vulnerability Assessment

The vulnerability of the training days to heat restrictions for Fort Benning under a range of projected temperature and humidity changes is analyzed in Figure 61. The days with highest category of heat restriction (T_{wbgt} > 90 F) show an expected increasing trend with temperature along any line of constant humidity, and also increasing with higher humidity. The *gradient* of increasing days also increases with temperature and humidity, as the contour lines are closer with increasing temperature and humidity. This is due to both the nonlinear function of T_{wbgt} and the frequent daily maximum temperatures and humidity at Fort Benning that approach the highest category.

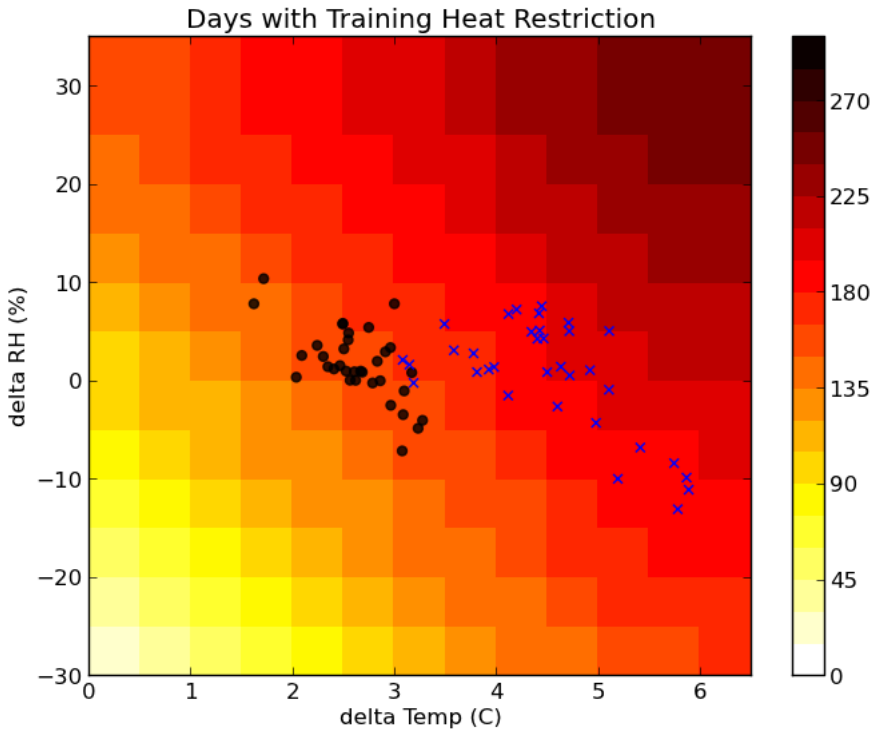

Figure 61 The dependence of number of days with category 5 heat restrictions (T_{wbgt} > 90 F) on the mean temperature change (dT, C) and relative humidity change (dRH, %) for Fort Benning. The points represent the mean temperature and humidity changes from 36 GCM simulations of the A2 scenario from the CMIP 3 archive, for years 2050 (black) and 2080 (blue).

Case Study 2: Fort Hood, TX

The annual number of days of each heat restriction category for Ft Hood, TX, are shown in Figure 62 below for the observed daily data (left column) and for climate projections taken as the average of 36 model simulations from the CMIP3 A2 emission scenario for three 20-year periods. Figure 62 includes only temperature changes, not relative humidity changes.

For the observed record data, Fort Hood experiences approximately 80 days with the highest heat restriction, with maximum T_{wbgt} > 90 F. The projected climate changes for 2030 onward result in greater increases in the highest heat category (black), and decreasing days in the lower categories, such that the majority of the days in the warm season become restricted with T_{wbgt} > 90 F).

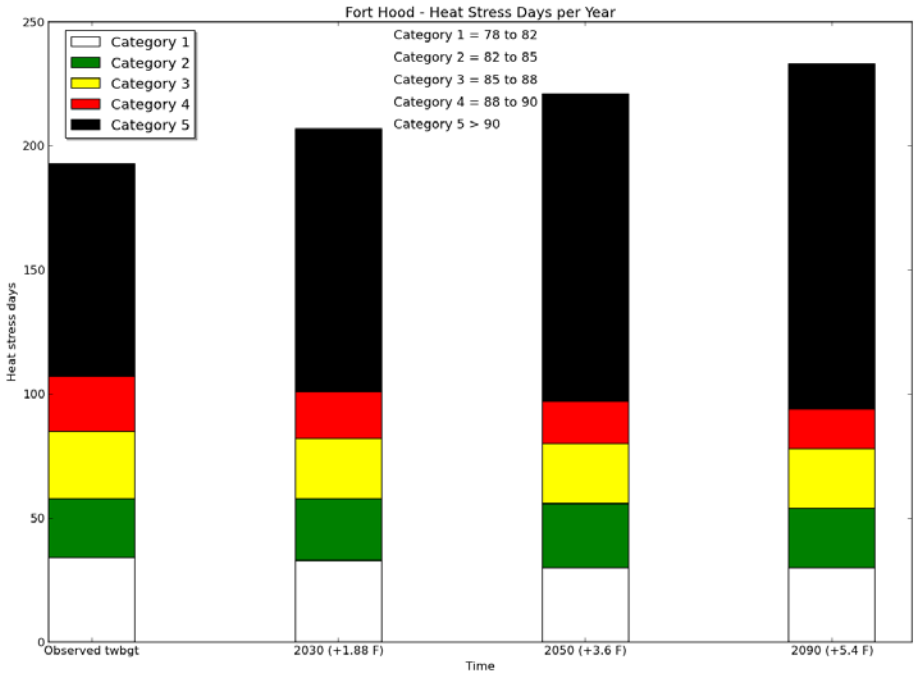

Figure 62 The annual number of days with heat related training restrictions of each category for Fort Hood, based on maximum daily Twbgt, for the observed daily data (left column), and for projected temperature increases for 2030, 2050, and 2080.

Vulnerability Assessment

The vulnerability of the training days to heat restrictions for Fort Hood under a range of projected temperature and humidity changes is analyzed in Figure 63. The days with highest category of heat restriction (T_{wbgt} > 90 F) show an expected increasing trend with temperature along any line of constant humidity, and also increasing with higher humidity. In a reverse sense from the Fort Benning site, the *gradient* of days is highest for the lesser temperature and humidity, and decreases with higher changes.

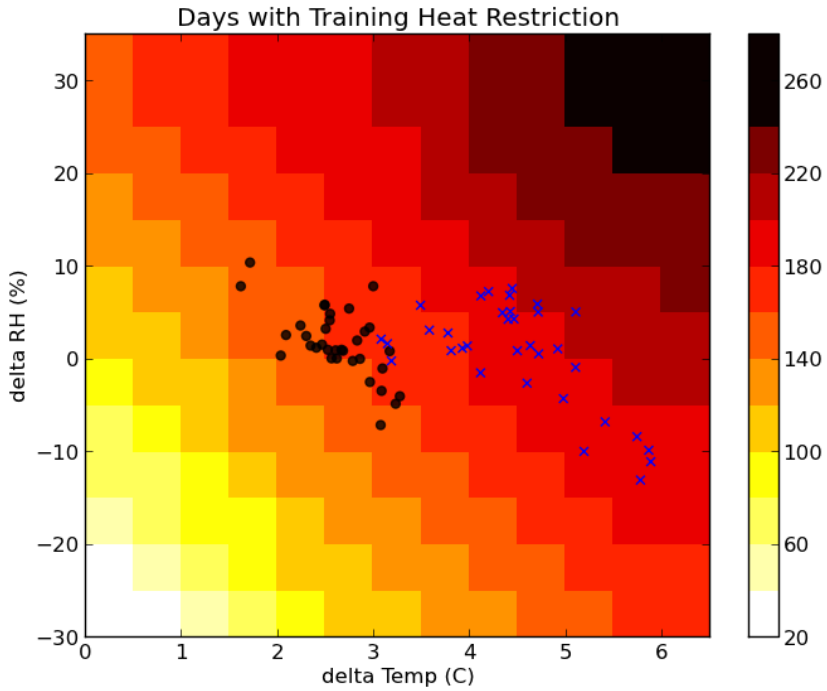

Figure 63 The dependence of number of days with category 5 heat restrictions (Twbgt > 90 F) on the mean temperature change (dT, C) and relative humidity change (dRH, %) for Fort Hood. The points represent the mean temperature and humidity changes from 36 GCM simulations of the A2 scenario from the CMIP 3 archive, for years 2050 (black) and 2080 (blue).

Case Study 3: U.S. Air Force Academy, CO

The annual number of days of each heat restriction category for the US Air Force Academy are shown in Figure 64 below for the observed daily data (left column) and for climate projections, taken as the average of 36 model simulations from the CMIP3 A2 emission scenario for three 20-year periods. This figure includes only temperature changes, not relative humidity changes.

For the observed record data, the USAFA experiences no days with maximum T_{wbgt} > 90 F, as it has lower mean relative humidity in the Colorado Springs area than the south central and southeast US, and fewer days with maximum temperatures above 90 F. The projected climate changes for 2030 onward result in increases in multiple categories, but mostly in the range of T_{wbgt} from 82 to 88 F.

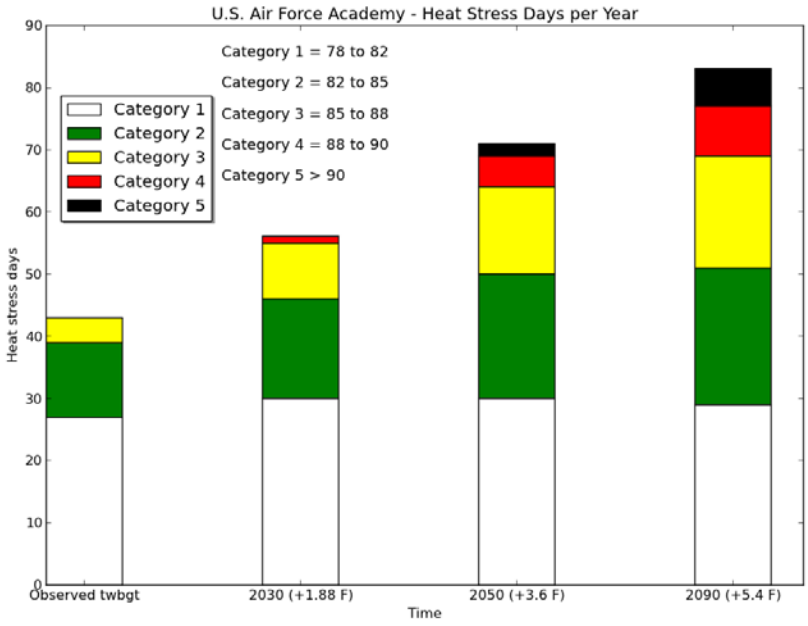

Figure 64 The annual number of days with heat related training restrictions of each category for US Air Force Academy based on maximum daily Twbgt, for the observed daily data (left column), and for projected temperature increases for 2030, 2050, and 2080.

Vulnerability Assessment

The vulnerability of the training days to heat restrictions for the Air Force Academy under a range of projected temperature and humidity changes is analyzed in Figure 65. There are fewer days overall with heat restrictions (T_{wbgt} > 88 F) with the drier Colorado climate, ranging from less than 5 days to about 40 days under the projected changes for 2050 and 2080. The range of projected relative humidity changes are within +/- 10%, so there is a stronger trend towards higher temperatures in future projections.

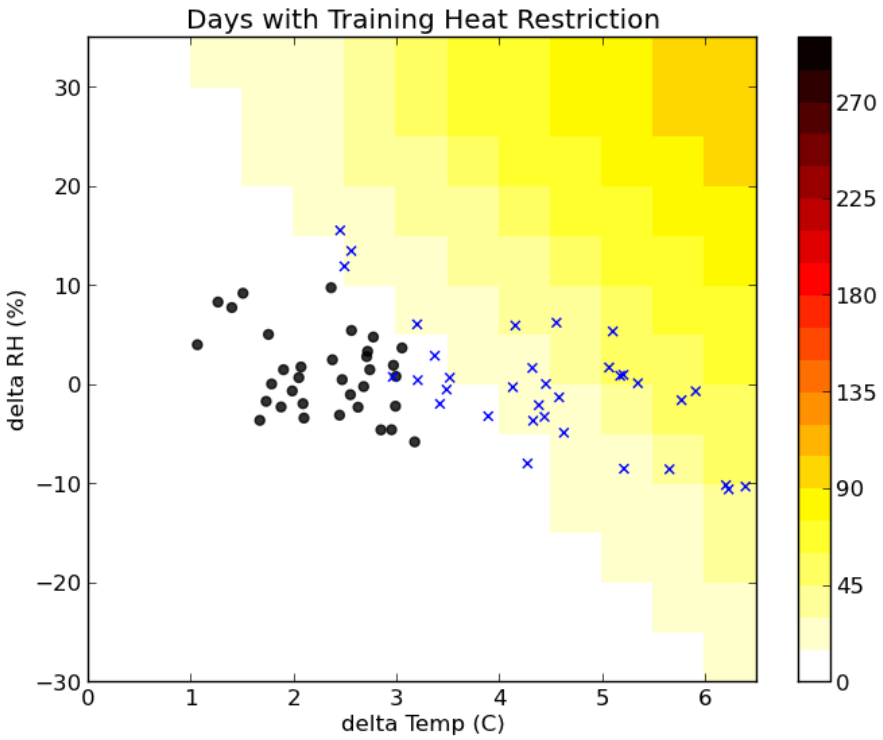

Figure 65 The dependence of number of days with categories 4 and 5 heat restrictions (Twbgt > 88 F) on the mean temperature change (dT, C) and relative humidity change (dRH, %) for the Air Force Academy. The points represent the mean temperature and humidity changes from 36 GCM simulations of the A2 scenario from the CMIP 3 archive, for years 2050 (black) and 2080 (blue x's).

Case Study 4 : Edwards Air Force Base, CA

The annual number of days of each heat restriction category for Edwards Air Force Base are shown in Figure 66 below for the observed daily data (left column) and for climate projections, taken as the average of 36 model simulations from the CMIP3 A2 emission scenario for three 20-year periods. This figure includes only temperature changes, not relative humidity changes.

For the observed record data, Edwards AFB experiences about 70 days with T_{wbgt} > 90 F, as it has frequent maximum summer temperatures above 90 F, but relatively low relative humidity. The increasing projected temperatures have the effect of increasing the days of highest heat category, and little change in the lower categories.

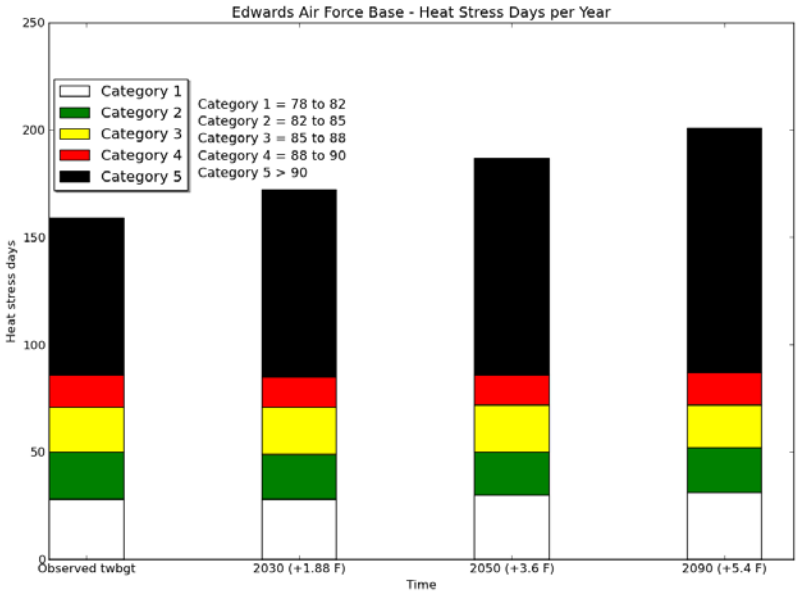

Figure 66 The annual number of days with heat related training restrictions of each category for Edwards Air Force Base based on maximum daily Twbgt, for the observed daily data (left column), and for projected temperature increases for 2030, 2050, and 2080.

Vulnerability Assessment

The vulnerability of the training days to heat restrictions for Edwards AFB under a range of projected temperature and humidity changes is analyzed in Figure 67. The days with highest category of heat restriction (T_{wbgt} > 90 F) show an expected increasing trend with temperature along any line of constant humidity, and also increasing with higher humidity. The range of high-risk days for the 2050 projected changes is 60 to 130 days, and for the 2080 timeframe the range is 90 to 150 days.

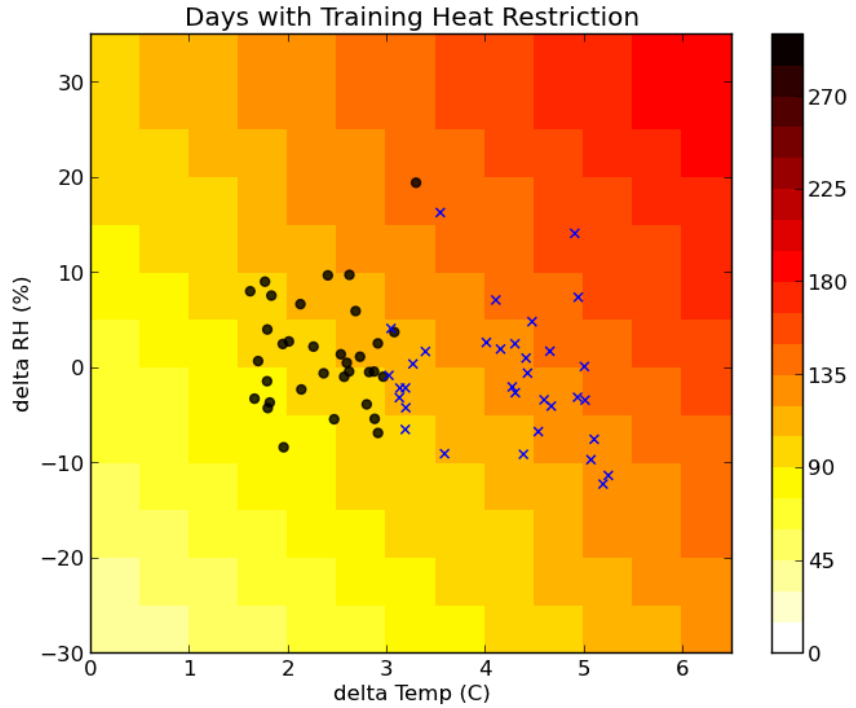

Figure 67 The dependence of number of days with category 5 heat restrictions (Twbgt > 90 F) on the mean temperature change (dT, C) and relative humidity change (dRH, %) for Edwards AFB. The points represent the mean temperature and humidity changes from 36 GCM simulations of the A2 scenario from the CMIP 3 archive, for years 2050 (black) and 2080 (blue x's).

Results and Discussion: Energy Resources Installation-Level Assessment

Decision Framing

This chapter develops science to support climate-related adaptation strategies for Department of Defense (DoD) to consider when determining the level of energy-related investment appropriate in construction of new facilities. As of FY 2011 the DoD spent nearly $4 billion on building energy for an inventory of 2.3 billion square feet. Decisions about energy efficiency in buildings are typically based on historical climate data. Thus, designers may under or over-specify performance requirements for components such as insulation, windows, roofs, and HVAC equipment if factors such as temperature, humidity, and cloudiness change from historical means. Because of the long life-span of DoD facilities, the impact of incorrectly specified facilities could be large in terms of energy consumption, cost, and security. This section describes an approach to estimating that impact in terms of sensitivity to climate-related changes. This section first discusses the decision processes and hierarchy for decision-making commonly used within the DoD when designing new facilities or retrofitting older ones. For this project the discussion scope is limited to decisions at the individual facility level, rather than with respect to installation-wide systems such as district energy systems. The current and potential use of climate information in making energy-related decisions is then discussed. Finally, this section reviews the regulations and directives that frame DoD decisions about energy measures applied to facilities.

DoD Decision Processes and Decision Hierarchy for Energy Adaptation

Decisions about facility energy measures are typically made at one of three levels: by the installation, by Architectural/Engineering organizations performing design work for the installation, or by higher headquarters. At the installation level, decisions occur on a day-to-day basis as part of Sustainment, Restoration, and Modernization (SRM) and during longer term Real Property Master Planning and Sustainability Planning. Maintenance activities in Operations and Maintenance (O&M) are reflected in decisions about replacement of consumables such as light bulbs, air filters, and fan coil units. Compared to the time scale of climate change, O&M decisions are made mostly in the short term and can readily be adapted to new conditions.

Installations may conduct fairly significant renovations (up to $750,000, more for some types of facilities) using locally administered SRM funds. Decisions regarding the building envelope (walls, foundation, and roof) may have long term implications for energy use. For instance, once a wall has had a particular thickness of insulation installed in walls, roof, or around a foundation, it is likely to be 20-30 years or more before an opportunity becomes available to reevaluate that decision. At the planning level, layout of facilities into compact, walkable communities, use of on-street parking, specification of maximum building Energy Use Intensity (EUI) in Installation Design Guides, and decisions about major capital investments for district heating, cooling, and power systems are all implicitly dependent on assumptions about regional climate.

Design work for new construction, renovations, and major repair is typically contracted to Architecture/Engineering (A/E) firms or may be done by an external organization such as the U.S. Army Corps of Engineers or the Naval Facilities command. These architects and engineers are constrained by statute and policy to produce technically sound products in a way that is cost effective. As professionals, they rely on their training, knowledge and experience. They are also

often immersed in a professional culture that is predominantly evaluated on executing projects on time and under budget. The combination of inter-organizational communication dynamics, policy restrictions, tradition, and time and budget schedule creates an environment that may be very resistant to the changes needed for adaptation to climate change. For instance, an installation might determine and document in its Installation Design Guide that barracks in their climate zone should have an annual Energy Use Intensity (including plug loads) no greater than 72 kBTU/ft^2, based on recommended targets from ASHRAE standard 189.1 (ASHRAE, 2010). An A/E firm, may determine that the level of insulation required to achieve this level of performance is not cost effective on a life cycle basis, because the estimated cost of a few more inches of insulation and supporting building structure may be determined to be more than the cost of the energy that would be saved over some period of time. The savings due to lower HVAC equipment cost may or may not be considered and could make the difference between feasibility and non-feasibility with respect to the cost effectiveness of higher insulation. There is considerable latitude in how these analyses are performed and assumptions made at the A/E level might rule out energy options that a different A/E would consider cost effective.

At the higher echelons, energy policy is set by the President, Congress, and agency Headquarters (H.Q.) in the form of statutes and policy directives. Specific examples will be discussed further on. Decision makers at this level include the services and the DoD as a whole, assigning relative priority to goals such as energy security, cost, fossil energy reduction, and greenhouse gases.

From an energy point of view, the current minimum standards for energy performance are set by ASHRAE 90.1 2010. There are some service differences. Further energy intensity restrictions are set by EPACT 2005 and EISA 2007, although the final rule for EISA 2007 has still not been issued. In the interim, goals come from policy in the form of Executive Orders (EO 13423, 2007 and EO 13514, 2009), Engineering Bulletins, and directives such as Army Directive 2014-02 (Net Zero Installations Policy). Further, the Environmenatl Proection agency (EPA) has determined that ‘source energy is the most equitable way to assess energy consumption, rather than ‘site’ energy. Site energy is a measure that represents electrical, thermal, and chemical energy, which is directly consumed at the point of use (e.g., for heating, cooling, lights, or plug loads), also referred to as “delivered” energy. Source energy represents all the energy used in delivering energy to a site; including the primary fuel (coal, natural gas, diesel fuel, uranium, etc.) consumed in the generation or conversion from one type of energy to another secondary type of energy (i.e., coal to electricity); transmission and distribution losses; as well as the point of use consumption.

The Department of Defense Unified Facility Criteria play a major role in specifying minimum standards. Formerly, DoD guidance was to refer to Chapter 13 of the International Building Code (IBC). UFC 1-200-01, General Building Requirements with changes, dated 01 Jul 2013 specified that DoD shall follow UFC 1-200-01, High Performance and Sustainable Building Requirements, dated 01 Mar 2013 (excerpted below). UFC 2-100-01, Installation Master Planning, contains general guidance on incorporating climate change into planning, as noted in the report text.

High Performance and Sustainable Building requirements. Section 2-4.1, Energy efficiency, specifies: “Design the building to achieve at least 30% energy consumption reduction from

ASHRAE 90.1 (2007) baseline or 12% energy consumption reduction from ASHRAE 90.1 (2010) baseline.

Design Federal low-rise residential buildings to achieve at least 30% energy consumption reduction from International Energy Conservation Code (IECC) baseline.
If a 30% reduction is not life-cycle cost-effective, the design of the proposed building must be modified so as to achieve an energy consumption level at or better than the maximum level of energy efficiency that is life-cycle cost-effective. (underlining added)

There are some differences in the UFC between the DoD services in that the minimum standard for the Army is ASHRAE 90.1 2010, while for the Navy and Air Force, it is ASHRAE 90.1 2007. However, the Department of Energy issues their final rule 2013-07-09, effective September 9, 2013, that makes ASHRAE 90.1, 2010 the minimum standard for new construction across the services. In summary, policy for all services is to do better than a minimum standard, subject to a life cycle cost analysis. This is relevant because the analysis is currently performed using historical data without weighing sensitivity to climate change.

Characteristics of DoD Decisions for Energy Demand Adaptation

The characteristics of the decisions made by the DoD for installation-level adaptation to energy demand risks vary greatly across the hierarchy described above. These characteristics include the frequency at which decisions are made, their reversibility, and whether actions can be phased in over time or must be carried through immediately. These characteristics are described below for each of the levels in the hierarchy.

Installation-level decision characteristics

Decisions made at the installation-level affect time scales ranging from short term to very long term, such as repair or replacement of equipment to Real Property Master Plans that determine policies such as types of development (e.g., sprawl versus compact), use of street trees, investment in district energy systems, construction of new buildings versus renovation of existing ones, and requirements for building energy performance in the Installation Design Guide. In the short term, repair and replacement policies can have a significant effect by specifying higher performance items such as lighting, furnaces, and chillers. The life of these items ranges from 5-10 years for equipment such as fluorescent lighting tubes to 12-20 years for equipment such as chillers [ASHRAE, 2013]. Compared to a climate change time scale, it is reasonable to make decisions about the above type of equipment in terms of life cycle cost analysis using current climate data. Decisions about Real Property Master Planning and certain configurations of building envelopes (insulation, windows, etc) have longer term implications. Many energy-related changes to the building envelope, such as insulation levels, windows, and mitigation of thermal bridges, can only be addressed economically either in the initial design or during a deep retrofit, which may only occur every 30-50 years, if at all. District energy strategies also have long term impacts and require long term planning. The goal of this energy section is to determine the sensitivity of these types of installation level decisions to climate change.

Architecture/Engineering decision characteristics

Architecture and Engineering firms make decisions primarily related to building energy features, especially with respect to the building envelope features such as insulation thickness, windows, and thermal bridges. Buildings are generally designed one at a time and the A/E firm may not be aware of higher level planning goals such as high performance building EUI requirements or strategic rationale to plan for connection to a district system. A/E firms are also often engaged to produce Real Property Master Plans and Installation Energy and Water Plans. These plans may extend over a long planning horizon relative to climate change effects. DoD policy is to consider climate change as part of the planning process. (See Framing Regulations and Drivers)

H.Q.-level decision characteristics

Decisions made at the highest level of the hierarchy, the H.Q. level and above, address statutes and policies. Without high level requirements and support, DoD decisions at lower echelons related to energy and adaptation will default to the lowest life cycle cost for historical conditions, which may not be the lowest life cycle cost for emerging conditions. Policy at the H.Q. level sets minimum requirements

Unique Aspects of DoD Energy Adaptation Decisions

DoD installations are similar in many ways to university campuses, in that there is a defined area of land and a set of buildings that are controlled by a centralized decision maker. This is in contrast to a small town or village in which energy decisions are made by private owners. There are a few differences, however, that make DoD installations unique or at least unusual. The dominant factor for installations is the need for mission assurance , defined as "*A process to protect or ensure the continued function and resilience of capabilities and assets—including personnel, equipment, facilities, networks, information and information systems, infrastructure, and supply chains—critical to the execution of DoD mission-essential functions in any operating environment or condition.*" [DoD, 2012] DoD decision making is strongly influenced by cost, but must also take into account the need to be able to continue installation missions in the face of possible interruption of external energy sources. The Defense Science Board published a finding in 2008 that "*Critical national security and Homeland defense missions are at an unacceptably high risk of extended outage from failure of the grid and other critical national infrastructure.*" [DoD, 2008]. Looking through the lens of energy security, DoD has subsequently initiated programs, including the Net Zero Energy initiatives, to reduce energy consumption and increase on-site energy generating capability, especially in the form of renewables. Energy security is defined in 10 USC 2924(3) to mean "having assured access to reliable supplies of energy and the ability to protect and deliver sufficient energy to meet mission essential requirements." This work addresses magnitude and characteristics of mission essential energy requirements that must be met with sufficient energy. During the decision making process, identification of critical missions and assignment of fiscal value to on-site generation for use in life cycle cost analysis can still be difficult.

The presence of tenant organizations on DoD installations presents another unique aspect. It is common for installations to host more than one governmental organization, including non-DoD organizations, providing land, facilities, and infrastructure services (including energy). In many cases, the garrison does not have control over resource use by the tenant or even a very good idea of the quantity of resources being consumed. In this case, the garrison has only indirect influence over energy adaptation measures undertaken by tenants, requiring long term planning

due to the difficulty in changing existing contracts and agreements. The situation is less clear when privatization is a factor, as in the case of programs such the Military Housing Privatization Initiative, Enhanced Use Leasing, or Power Purchase Agreements. Private parties are not necessarily required to build to Federal Standards on installation land, but can build to local and state standard in some cases. Thus, there may be tenants on the installation that will be able to build new facilities that do not meet minimum energy efficiency standards of federally constructed buildings on the installation. The installation must usually still provide utilities. These issues are not insurmountable, but require careful consideration during contract negotiations.

Current Use of Climate Information

Historical climate data is used extensively within DoD with respect to making decisions about energy performance of buildings. Whole building energy analysis programs such as EnergyPlus [Crawley, 2001] and eQuest/DOE 2.2[Hirsch, 2013] are often used to assess the performance of buildings and to demonstrate their compliance with codes and standards. These programs use the TMY3 (Typical Meteorological Year) data set published by the National Renewable Energy Laboratory [NREL, 2008]. This data set provides hourly values that include solar radiation, dry bulb temperature, dew point temperature, and wind speed. Source data for TMY3 data sets are drawn from the 1952-1975 SOLMET/ERSATZ database, the 1961-1990 National Solar Radiation Database (NSRDB), and the 1991-2005 NSRDB update. For each weather station in the database, a set of 12 typical meteorological months is concatenated. For each month, actual data from all months available is compared to select the most typical month for concatenation. Thus, each month contains data from an actual month, but not all of the months in a TMY3 file come from the same year. Stations in the TMY3 database draw from either 30 (24) years of data or 15(12) years of data, depending on data availability, with the numbers in parentheses showing the effective number of years of data in each case after removal of years associated with volcanic eruptions. Thus, current weather data used in whole building energy simulations is representative of the most typical months in either the last 30 years or the last 15 years, depending upon the station.

Non-Climate Factors

The need for Energy Security within DoD is driven by a number of factors other than climate, including mission assurance, geopolitics, national politics, national energy policy, energy costs, attempts to control greenhouse gases, and concerns over environmental impact of hydraulic fracturing ("fracking"). Energy decisions involve multiple criteria and a cost benefit analysis. The goal of this research is to investigate sensitivity of the "benefit" part of the decision analysis to climate change.

Framing Regulations or Directives

A number of laws and executive orders drive Army policies related to climate, such as EPACT 2005, EISA 2007, EO 13423, and EO13514. Master Planning policy documentation within the Army and Department of Defense has recently been rewritten, with the former Master Planning regulation, AR 210-20, Real Property Master Planning for Army Installations being rewritten and incorporated into AR 420-1, Army Facility Management. More detailed guidance on Master Planning is contained in Unified Facility Criteria UFC 2-100-01, Installation Master Planning as

revised May 15, 2012. Climate change adaptation is referred to indirectly in section 3-5.6.23, Environmental Conditions. The relevant section is quoted in its entirety below.

> ***3-5.6.2.3 Environmental Conditions.***
> *Where changing external conditions impact planning decisions, master planners will seek to understand, monitor and adapt to these changes. Such conditions include, but are not limited to, changes in land use and population density in the vicinity of installations; changes in climatic conditions such as temperature, rainfall patterns, storm frequency and intensity and water levels; and changes in infrastructure assets and configurations beyond and linking to the installation. These and other changes will impact existing facilities and infrastructure, and also will impact new facilities and infrastructure through their design life. Condition changes will be determined from reliable and authorized sources of existing data, but to anticipate conditions during the design life of existing or planned new facilities and infrastructure, "projections" may also be considered from reliable and authorized sources (e.g. such as Census Bureau for population projections, the U.S. Geological Survey for land use change projections, and the U.S. Global Change Research Office and National Climate Assessment for climate projections).*

The above text is a good start and ambiguous enough to be flexible in the face of emerging information over the coming decades, but begs the question of how to find or create authorized sources of existing data. For instance, the U.S. Army Corps of Engineers released Engineering Circular 1165-2-212 that specified "Sea-Level Change Considerations for Civil Works Program" on October 1, 2011, including equations showing the amount of sea level change that should be considered over the life of a project. In the context of energy decisions, decision makers need guidance on whether to use data from the current TMY3 data set or to use a set that has been adapted to reflect likely future conditions.

Analysis Methods

A methodology is proposed to identify which climate change adaptation steps, if any, should be considered in decision processes with respect to energy cost and security risks. This approach is designed to first identify energy-related stressors on installation energy use resulting from changes in temperature, with relative humidity held constant. Next, it identifies energy-related decisions that might be made differently in the face of such stressors and thresholds that might cause decisions to change. Finally, the methodology will produce input data appropriate for use in future climate change scenarios, including synthetic weather data and cost assumptions for use during planning.

Step 1.Framing the problem: Determine the appropriate context and scale of the analysis, identify key decision criteria and thresholds, and delimit adaptation options

The proposed methodology focuses on three principal inputs to energy security-related decisions: energy cost, measure costs, and weather. Energy costs reflect the price that is paid for electricity, natural gas, fuel oil, and other energy carriers. Federal agencies and contractors to federal agencies are required by 10 CFR 436 to use fuel prices, escalation rates, and discount rates published by the Energy Information Administration (EIA) and the National Institute of Standards and Technology (NIST) to calculate life cycle costs for energy and water related capital investment projects. Measure costs describe the cost to implement energy efficiency, distribution, or supply measures. Costs for established technologies used in new construction

and renovation can be obtained from published cost engineering data such as RS Means cost books [RSMeans 2013], although advance technology costs are more difficult to obtain. Finally, weather data for analysis purposes can be obtained from TMY3 weather files as described previously. In this decision context, possible climate scenarios can be explored by changing the weather files, while treating energy and measure costs as they are currently used. This is a building scale approach that addresses energy demands to be met by distribution and supply systems. Conceivably, climate could also affect region availability of energy from the commercial sector, but this is beyond the scope of this project.

When designing new buildings or retrofitting existing ones, a variety of adaptation options in the form of *energy efficiency measures* (EEM) are considered and a life cycle cost/benefit analysis is conducted. The decision criteria are *life cycle cost* and *energy use intensity (EUI)*, considering both site and source energy. Typical EEMs include (but are not limited to): high efficiency lighting, high efficiency electric equipment, higher levels of insulation, better windows, reduced air infiltration, higher efficiency Heating, Ventilation, and Air Conditioning (HVAC), and daylighting strategies. These EEMs can be considered individually or in combination. In fact, it is important that packages of these EEMs be analyzed together because of coupled effects between them. For instance, better insulation, air tightness, windows, and lighting might lead to the need for significantly smaller HVAC equipment. The savings from smaller equipment combined with lower energy use might make the difference in the entire package of EEMs being life cycle cost effective. Weather will directly affect the cost of energy use and the analysis seeks to identify how changes in temperature affect the cost effectiveness of EEM packages. If there is a significant effect, the argument could be made that climate-adjusted weather files should be used when doing building energy modeling.

Step 2. Stress test: Identify installation vulnerabilities to climate and other relevant stressors

The next step in the process is to conduct a vulnerability assessment, or stress test, on the current system. For this project, the system is represented using models and data from the Net Zero Planner tool [Case, 2014]. Net Zero Planner (NZP) is a web-based tool that support decisions about applying EEMs to buildings, making changes to thermal and electrical distribution systems, and choosing a mixture of supply systems, including cogeneration and large scale renewables such wind and solar energy systems. Only the building EEM capabilities are used here, the others are beyond this project's scope. NZP contains a library of EnergyPlus models for typical DoD facilities, eight of which have been selected because they are found on many installations and represent a broad spectrum of building types (Table 10). Five of these models were developed for a study on energy efficiency conducted by the U.S. Army Corps of Engineers in response to EISA 2007 [USACE 2011], with the others developed in response to a study conducted in response to EPACT 2005. The initial set of standard building types in Net Zero Planner was based on the most commonly built facility standards maintained by the U.S. Army Corps of Engineers, which is the construction agent for the Army and the Air Force. This set has also been applied to a Navy Installation (Portsmouth Naval Shipyard) and was calibrated against energy bills fairly easily. More importantly, the standard building types represent a broad spectrum of space and activity types likely to be found on installations (e.g., residential, dining, administration, small data centers, motor pools, etc.). For the purposes of scientific inquiry, the authors consider them adequately representative to address the question of whether historical

data or customized future climate projections should be used to select energy efficiency measures.

NZP also contains "packages" consisting of combinations of EEMs that are appropriate to consider for each type of model as well as a cost module that uses RSMeans data to estimate the first cost and maintenance costs of each EEM. It uses the closest existing TMY3 data file for each installation, with the capability to add modified files and use them to do EnergyPlus runs. NZP uses a server farm capable of running up to 40 EnergyPlus runs in parallel, with each run taking between 5-15 minutes depending on the complexity of the building model and EEMs considered. NZP contains a large number of EEM options. For the purpose of this analysis, however, a standard EEM package consisting of building insulation, low infiltration, better windows, and high efficiency LED lighting was selected for all building types. These EEMs represent investments and design decisions that should be prior to construction of a building, as they are costly to change afterwards. Some might consider lighting not to fall into this category, but high efficiency lighting design should include building design features and positioning of lighting fixtures to be most effective. Four EEM package combinations are automatically applied by the tool to each of the eight building types, resulting in a total of 32 EnergyPlus simulation runs to be made for each installation across the three climate change scenarios (+0C, +3C, +6C). For each installation, the scenarios to be include the Base Case, built to ASHRAE 90.1 – 2010, and the standard EEM package case

Table 10 NZP standard building types used in this analysis

Label	Name	Conditioned Area (sqft)	Floors
ARC	Army Reserve Center	19000	1
BDEHQ	Brigade Headquarters	13000	1
BNHQ	Battalion Headquarters	23000	1
CDC	Child Development Center	23000	1
COF	Company Operations Facility	14000	1
DFAC	Dining Facility	38000	1
TEMF	Tactical Equipment Maintenance Facility	10000	1
UEPH	Unaccompanied Enlisted Personnel Housing	55000	3

Weather data for each climate change scenario is generated by modifying the TMY3 weather file for an installation, using the existing file as a baseline, and then adding 3 degrees Celsius and 6 degrees Celsius to each hourly temperature of the 8,760 hours in a year. The range of temperatures was selected to insure that the problem was adequately bounded in consultation with climates scientists on the project team. Final results show that energy response to changing temperature is nearly linear, meaning that interpolation with the 0-6 degree Celsius range is reasonable. Lacking better information, relative humidity is held constant, resulting in a change in dew point.

The output of step 2 for each installation will show how electrical and natural gas usage change under the three climate scenarios for each building type and for each installation. For analysis purposes, we treat natural gas usage as an analog for heating requirements, including space heating, reheat, and domestic hot water. Results will be given both in Energy Use Intensity (EUI – kBtu/ft^2/year) and total energy usage and cost.

Step 3. Appraise the robustness of the installation's Energy Security

In the case of energy, the EEM packages represent the available adaptation strategies and are generated automatically. As long as design decisions depend upon an analysis of cost effectiveness of energy measures (as they currently do), then the choice of weather input is relevant because it affects projected energy performance of the building.

Case Studies

The analysis methods described above were applied to four installation case studies: Fort Benning, GA, Fort Hood, TX, Edwards AFB, and the U.S. Air Force Academy. In each case study, the entire methodology is presented, although most of the emphasis for this report is placed on framing the energy problem of each installation and conducting the stress test. In order to best compare results between installations, analysis was normalized to Energy Use Intensity in kBtu/ft^2/year and rolled up energy usage was calculated for a million square feet of conditioned area with a standardized mix of building types (Table 11). EUI and totals are calculated both in terms of site energy and source energy. Total results are easily customizable to a particular mix of buildings changing the total area and the percentage of total column in the underlying spreadsheet.

Table 11 A standardized mix of building types was used to enable comparisons between installations.

	Total Area (ft^2)	1,000,000
	Reference Area	**Percentage of total**
Army Reserve Center (ARC)	2,869	0.29%
Brigade HQ (BdeHQ)	73,296	7.33%
Battalion HQ (BnHQ)	284,305	28.43%
Child Development Center (CDC)	6,655	0.67%
Company Operations Facility (COF)	46,738	4.67%
Dining Facility (DFAC)	42,792	4.28%
Tactical Equipment Maintenance Facility (TEMF)	104,890	10.49%
Barracks (UEPH)	438,455	43.85%

A blended rate for electricity [EIA, 2015a] and natural gas [EIA, 2015b] was used for each installation, based on data from the U.S. Energy Information Administration (Table 12). In both cases, industrial rates were used (a conservative assumption). Electrical rates were as of October, 2015 and gas rates were annual averages as of 2014. Data for 2015 has not yet been released by the EIA.

Table 12 Energy rates used in analysis

	2015 EIA Electricity	**Used in analysis**	**2014 EIA Nat. Gas**
Blended rate	**$/kWh**	**$/kBtu**	**$/kcf**
Benning Elec	0.0573	0.016793	

Benning Gas		0.0059047	6.07
Hood Elec	0.0544	0.0159431	
Hood Gas		0.0045817	4.71
Edwards Elec	0.1396	0.0409127	
Edwards Gas		0.0074416	7.65
USAFA Elec	0.0725	0.0212477	
USAFA Gas		0.0066537	6.84

Case Study 1: Fort Benning, GA

Background and Problem Framing

An instance of each of the eight building types described in the analysis approach was placed at Fort Benning, GA using the Net Zero Planner (NZP). It is not necessary to draw the exact geometry of the building, as the NZP model library contains the reference geometry. The TMY3 weather file for Fort Benning, located in ASHRAE climate zone 3a, was modified by adding 3 degrees C and 6 degrees C, holding relative humidity constant as described in the approach. For each building type, the standard model uses fairly typical equipment and insulation values, compatibly with ASHRAE standard 90.1, 2010.

For a typical energy assessment, the parameters of each building type for its respective model would have been changed to better tune the models for the building inventory. For the purpose of this study, however, standard models were used across installations to allow for comparison across climate zones. At a screening level, the impact on the installation can be estimated by scaling to the total conditioned area of each facility type on each installation. Table 13 shows parameters used for an Army Reserve Center (ARC). Of course, not all of the parameters used in the Energy Plus model are shown. This table represents only those parameters that are changed to represent changes in the models. The Base Case column represent building to ASHRAE 90.1 – 2010, while the EEM column contains changes to the EnergyPlus input files that represent additional Energy Efficiency Measures that could be applied. The decision being framed is whether to build to the Base Case or the EEM case. In the interest of brevity, not all parameters are shown for all building types.

Table 13 Example of parameters changed in energy modeling for an Army Reserve Center model.

Name	Base Case Value	EEM Value	Unit	Description
Air Leakage Rate	1.4	1.0	cfm/ft^2	Air leakage rate when pressurized at 0.3 inch H2O (75 Pa)
Lighting Power Density - Assembly	1.3	0.625	W/ft^2	Electric lighting power density
Lighting Power Density - Classroom	1.3	0.625	W/ft^2	Electric lighting power density
Lighting Power Density - Corridor	0.5	0.25	W/ft^2	Electric lighting power density
Lighting Power Density - Fitness	0.9	0.44	W/ft^2	Electric lighting power density
Lighting Power Density - Kitchen	1.2	0.625	W/ft^2	Electric lighting power density
Lighting Power Density - Lockers	0.6	0.25	W/ft^2	Electric lighting power density

Lighting Power Density - Mechanical	1.5	0.625	W/ft^2	Electric lighting power density
Lighting Power Density - Net Ops	1.5	0.69	W/ft^2	Electric lighting power density
Lighting Power Density - Office	1.1	0.44	W/ft^2	Electric lighting power density
Lighting Power Density - Restroom	0.9	0.375	W/ft^2	Electric lighting power density
Lighting Power Density - Storage	0.9	0.44	W/ft^2	Electric lighting power density
Lighting Power Density - Weapon Sim	1.3	0.625	W/ft^2	Electric lighting power density
Roof Base Continuous Insulation	20	30	R	Roof base continuous insulation R-value
Slab Vertical Insulation	0	10	R	Slab vertical insulation R-value
Wall Base Cavity Insulation	0	19	R	Wall base cavity insulation R-value
Wall Base Continuous Insulation	5.7	15	R	Wall base continuous insulation R-value
Window SHGC	0.25	0.25	SHGC	Window solar heat gain coefficient
Window U-Value	0.75	0.41	U	Window U-value

The above steps set up energy rates, models for eight standard buildings types typically found on installations, and three weather files, making it possible to model the buildings under historical conditions, +3 degrees C, and +6 degrees C. In the next section, we run the models and compare the predicted performance and cost changes due to climate change.

Vulnerability Assessment

The Net Zero Planner model runs a baseline annual hourly analysis for each building type using EnergyPlus. It then analyzes the hourly output of the models, scaling it to the area of each building type, and produces summaries of total energy use (site and source) and cost. Table 14 shows Energy Use Intensities (EUI), total energy for the reference building mix, and energy costs for each of the modeled building types under the +0ºC scenario. In other words, the standard TMY3 weather file for Fort Benning was used. Table 15 shows results for the +3ºC scenario, while Table 16 shows results for +6ºC. The annual energy in Therms (100,000 Btu, 1000 kBtu) is calculated by multiplying the EUI of each building type by the area of that building type from Table 11. The annual energy cost for each building type is obtained by multiplying annual site energy by energy rates from Table 12.

Table 14. Energy Use Intensity, total energy use, and cost for zero temperature change at Fort Benning, GA

Temp +0	**Energy Use Intensity (kBtu/ft^2/yr)**						**Annual Energy (Therm)**		**Cost ($)**		
Energy Intensity (kBtu)/ft2/yr)	Elec site	Gas site	Tot Site	Elec src	Gas src	Tot src	site	src	Elec Cost	Gas Cost	Tot Cost
Army Reserve Center	31.8	22.6	54.3	106.2	23.6	129.8	1,559	3,723	$1,531	$382	$1,914
Brigade HQ	54.0	7.9	61.9	180.4	8.3	188.7	45,374	138,283	$66,481	$3,416	$69,897
Battalion HQ	42.9	9.7	52.5	143.2	10.1	153.3	149,377	435,900	$204,696	$16,228	$220,924
Child Development Center	33.2	26.6	59.8	110.8	27.9	138.7	3,980	9,231	$3,709	$1,046	$4,755
Company Operations Facility	23.0	18.4	41.4	76.9	19.3	96.2	19,363	44,962	$18,081	$5,076	$23,157
Dining Facility	114.4	125.0	239.4	382.0	130.9	512.9	102,445	219,477	$82,183	$31,593	$113,777
Tactical Equipment Maintenance Facility	26.7	23.6	50.3	89.2	24.7	113.9	52,760	119,467	$47,038	$14,614	$61,652
Barracks	62.2	46.0	108.1	207.7	48.1	255.8	474,177	1,121,616	$457,836	$119,003	$576,839
Totals							**849,035**	**2,092,661**	**$881,555**	**$191,359**	**$1,072,914**

Table 15. Energy Use Intensity, total energy use, and cost for +3°C temperature increase at Fort Benning, GA

Temp +3	Energy Use Intensity (kBtu/ft²/yr)						Annual Energy (Therm)		Cost ($)		
Energy Intensity (kBtu)/ft2/yr)	Elec site	Gas site	Tot Site	Elec src	Gas src	Tot src	site	src	Elec Cost	Gas Cost	Tot Cost
Army Reserve Center	34.7	17.2	51.8	115.8	18.0	133.7	1,487	3,837	$1,670	$291	$1,961
Brigade HQ	56.5	5.7	62.2	188.6	6.0	194.6	45,561	142,616	$69,511	$2,461	$71,972
Battalion HQ	45.3	6.9	52.2	151.4	7.2	158.6	148,430	450,962	$216,453	$11,535	$227,988
Child Development Center	36.0	21.3	57.3	120.2	22.3	142.5	3,812	9,481	$4,021	$837	$4,858
Company Operations Facility	26.3	12.8	39.0	87.7	13.4	101.0	18,230	47,223	$20,605	$3,519	$24,124
Dining Facility	129.5	98.6	228.1	432.7	103.2	535.9	97,608	229,309	$93,093	$24,901	$117,994
Tactical Equipment Maintenance Facility	27.5	14.1	41.6	91.9	14.7	106.6	43,616	111,811	$48,442	$8,721	$57,163
Barracks	68.0	38.2	106.1	227.0	40.0	267.0	465,390	1,170,585	$500,436	$98,837	$599,273
Totals							**824,135**	**2,165,824**	**$954,230**	**$151,103**	**$1,105,332**

Table 16. Energy Use Intensity, total energy use, and cost for +6°C temperature increase at Fort Benning, GA

Temp +6	Energy Use Intensity (kBtu/ft²/yr)						Annual Energy (Therm)		Cost ($)		
Energy Intensity (kBtu)/ft2/yr)	Elec site	Gas site	Tot Site	Elec src	Gas src	Tot src	site	src	Elec Cost	Gas Cost	Tot Cost
Army Reserve Center	38.2	13.0	51.3	127.7	13.6	141.4	1,471	4,056	$1,843	$221	$2,063
Brigade HQ	58.9	3.9	62.8	196.6	4.1	200.7	46,012	147,098	$72,447	$1,695	$74,142
Battalion HQ	47.8	4.6	52.4	159.6	4.9	164.5	149,054	467,634	$228,184	$7,778	$235,962
Child Development Center	39.4	17.2	56.7	131.7	18.0	149.7	3,770	9,964	$4,407	$677	$5,083
Company Operations Facility	30.8	8.4	39.2	102.8	8.8	111.6	18,303	52,149	$24,157	$2,313	$26,470
Dining Facility	150.0	79.3	229.3	501.0	83.1	584.1	98,139	249,939	$107,793	$20,046	$127,840
Tactical Equipment Maintenance Facility	28.8	7.7	36.5	96.1	8.1	104.2	38,257	109,273	$50,692	$4,766	$55,458
Barracks	75.2	32.3	107.5	251.1	33.8	284.9	471,157	1,249,233	$553,613	$83,544	$637,157
Totals							**826,164**	**2,289,345**	**$1,043,136**	**$121,039**	**$1,164,175**

Figure 68 illustrates the change in EUI at Fort Benning for the three climate scenarios, 0, +3, and +6°C. The trend, as might be expected, is that warmer average temperatures will increase required cooling energy and decreased required heating energy (Figure 69). The effect is nearly, but not quite linear with temperature increase. The buildings with higher internal loads (cooking equipment, domestic hot water), e.g. the dining facility (DFAC) and barracks (UEPH) are less linear, reflecting the need to remove heat from those loads. The tactical equipment maintenance facility (TEMF), shows a decrease in heating loads, but no increase in cooling load as these facilities are typically not air conditioned. Increased cooling and decreased heating nearly balance each other out with respect to site energy EUI (Figure 70).

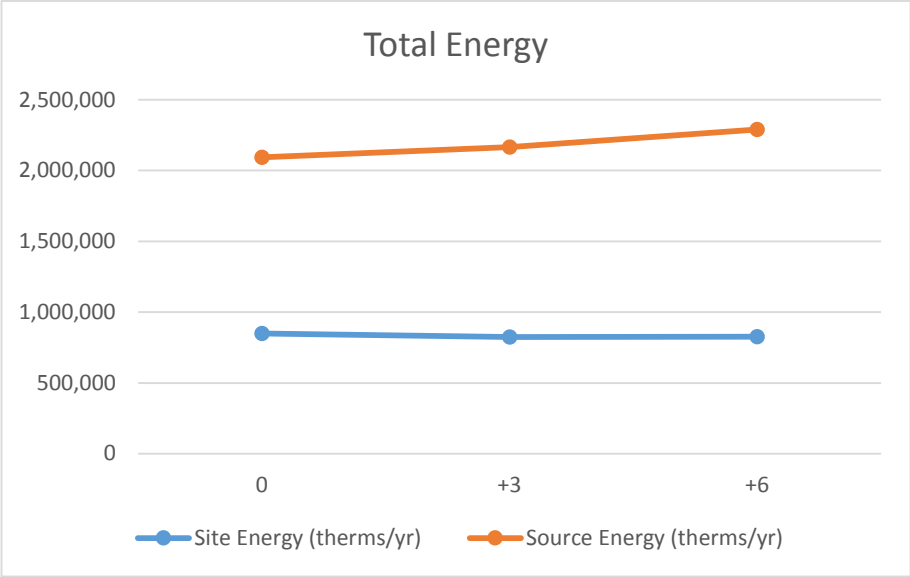

Figure 68. Annual energy use change per million square feet of conditioned building area for Fort Benning. Note that although total site energy usage is relatively constant, source energy use increases due to a shift from natural gas to electricity.

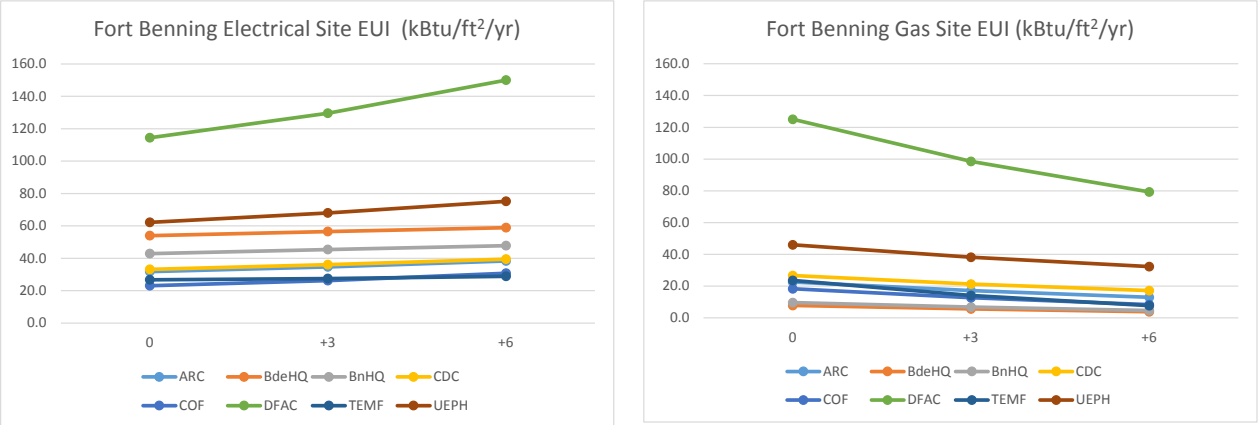

Figure 69. Electrical and gas EUI for all three climate change scenarios at Fort Benning, GA.

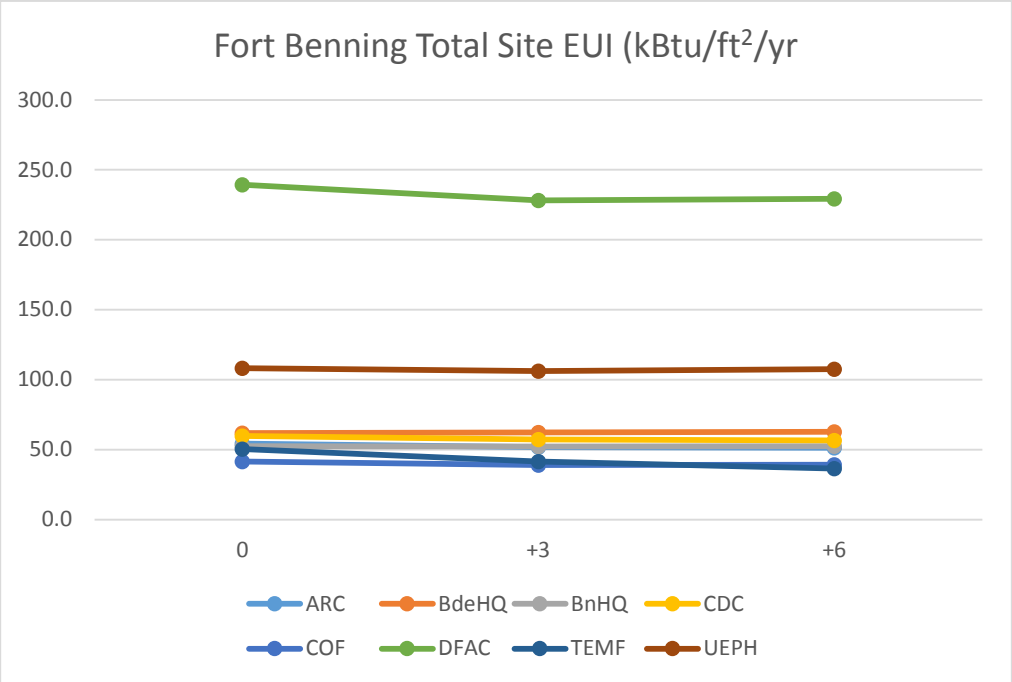

Figure 70. Total site EUI for all three climate change scenarios at Fort Benning, GA

A look at site and source energy together and scaled to the reference distribution of buildings, however, tells a different story. Although site energy stays relatively constant with increasing temperature, source energy grows significantly, reflecting the fuel switching from natural gas to electricity. Note that the site to source calculation was performed using a national average ratio, reflecting the mix of energy sources on the national grid. A regional electrical power grid with a higher than average mix of renewable sources would have a lower source to site ratio and the increase in source energy would be less. Figure 71 is instructive as well. The cost of the energy purchased increases even though the site energy consumption remains relatively flat, again because fuel switching from natural gas to higher priced electricity. The increase is not quite linear, about 1%/ºC for +3ºC and 1.4%/ºC for +6ºC.

The site versus source calculation is very sensitive to the mix of energy sources on the regional electric grid. The U.S. Environmental Protection Agency Portfolio Manager uses a national average site to source energy conversion factor of 3.14 for electricity and 3.05 for natural gas (https://portfoliomanager.energystar.gov/pdf/reference/Source%20Energy.pdf) to allow energy projects to be compared equitably on a national basis. Regional values can vary significantly to reflect different levels of hydropower, solar, wind, nuclear energy, etc. The important points to note are 1) that there can be a significant shift in the ratio between heating and cooling energy and 2) that the site energy results from the change may not reflect the actual change in source energy. The site to source conversion ratio should be taken into account and it is likely to change in the future based on the mix of energy sources.

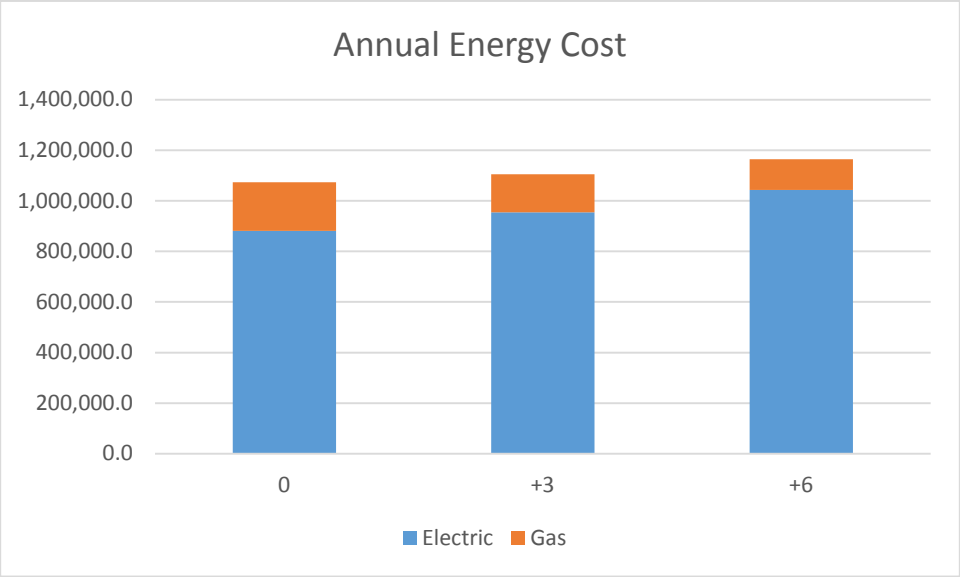

Figure 71. Annual energy cost at Fort Benning per million square feet of conditioned building area for three climate change scenarios. Note that natural gas used for heating decreases while electricity used for cooling increases.

Assessment of Future Risks and System Robustness

The assessment conducted so far indicates that current approaches to estimating heating and cooling loads for buildings at Fort Benning may be underestimating cooling needs and overestimating heating needs. Given the service life of Heating, Ventilation, and Air Conditioning (HVAC) equipment used to heat and cool buildings (measured in decades), future equipment replacement is likely to be an adequate strategy to adjust capacity as conditions change. However, design decisions made about EEMs such as wall thickness, insulation, air tightness and proper design to eliminate thermal bridges during new design or deep retrofit may underestimate the life cycle cost effectiveness of these strategies. These decisions can have implications lasting 30-50 years (time between major deep retrofits).

This section addresses whether climate change will a difference in decisions regarding employment of EEMs under the three climate change scenarios. This is done by simulating the buildings with envelope and lighting-related EEMS (additional insulation, better windows, more airtight, LED lighting) in each climate scenario and then assessing whether the cost effectiveness of the EEMS changes. Table 17 shows EUI, annual energy, energy and investment costs, and simple payback. The area of each building type is taken from Table 11 with the total showing values for a million square feet of conditioned area. Table 18 shows results for +3^{o}C and Table 19 shows results for +6^{o}C.

Table 17. Energy savings and simple payback per million square feet of conditioned area for envelope-related and lighting EEMs at Fort Benning under +0 ^{o}C climate change scenario.

Temp +0	Energy Use Intensity (kBtu/ft^2/yr)						Annual Energy (Therm)		Cost ($)			Invest $	Simple Payback
Energy Intensity (kBtu)/ft2/yr)	Elec site	Gas site	Tot Site	Elec src	Gas src	Tot src	site	src	Elec Cost	Gas Cost	Tot Cost		(yrs)
Army Reserve Center	22.8	17.4	40.2	76.2	18.2	94.4	1,153	2,708	$1,099	$294	$1,393	$11,476	22.1
Brigade HQ	44.3	4.8	49.2	148.1	5.1	153.1	36,045	112,242	$54,563	$2,098	$56,661	$329,831	24.9
Battalion HQ	35.9	6.0	41.9	119.8	6.3	126.1	119,137	358,519	$171,213	$10,146	$181,358	$1,279,371	32.3
Child Development Center	24.5	25.2	49.7	81.9	26.4	108.3	3,307	7,205	$2,741	$989	$3,730	$26,620	26.0
Company Operations Facility	15.1	14.4	29.5	50.4	15.1	65.5	13,785	30,607	$11,845	$3,975	$15,820	$186,951	25.5
Dining Facility	100.8	111.4	212.2	336.5	116.6	453.2	90,785	193,918	$72,406	$28,146	$100,552	$171,168	12.9
Tactical Equipment Maintenance Facility	20.5	20.3	40.8	68.4	21.3	89.7	42,806	94,082	$36,079	$12,590	$48,668	$419,562	32.3
Barracks	51.0	44.8	95.8	170.3	46.9	217.2	419,937	952,213	$375,363	$115,975	$491,338	$1,973,049	23.1
Totals							**726,955**	**1,751,495**	**$725,308**	**$174,213**	**$899,521**	**$4,398,028**	

Table 18. Energy savings and simple payback per million square feet of conditioned area for envelope-related and lighting EEMs at Fort Benning under +3 ^{o}C climate change scenario.

Temp +3	Energy Use Intensity (kBtu/ft^2/yr)						Annual Energy (Therm)		Cost ($)			Invest $	Simple Payback
Energy Intensity (kBtu)/ft2/yr)	Elec site	Gas site	Tot Site	Elec src	Gas src	Tot src	site	src	Elec Cost	Gas Cost	Tot Cost		(yrs)
Army Reserve Center	25.1	13.1	38.3	84.0	13.8	97.8	1,099	2,805	$1,212	$223	$1,434	$11,476	21.8
Brigade HQ	46.2	3.4	49.6	154.4	3.6	157.9	36,368	115,759	$56,891	$1,470	$58,361	$329,831	24.2
Battalion HQ	37.8	4.2	41.9	126.2	4.3	130.5	119,219	371,128	$180,384	$6,969	$187,353	$1,279,371	31.5
Child Development Center	26.7	20.2	46.9	89.0	21.2	110.2	3,119	7,333	$2,979	$794	$3,773	$26,620	24.5
Company Operations Facility	17.7	9.8	27.5	59.2	10.2	69.5	12,861	32,471	$13,919	$2,700	$16,619	$186,951	24.9
Dining Facility	114.5	88.3	202.7	382.4	92.4	474.8	86,754	203,160	$82,264	$22,300	$104,565	$171,168	12.7
Tactical Equipment Maintenance Facility	21.1	11.7	32.8	70.4	12.2	82.6	34,357	86,674	$37,133	$7,230	$44,363	$419,562	32.8
Barracks	56.4	37.7	94.1	188.4	39.4	227.9	412,502	999,052	$415,367	$97,519	$512,886	$1,973,049	22.8
Totals							**706,279**	**1,818,382**	**$790,147**	**$139,206**	**$929,354**	**$4,398,028**	

Table 19. Energy savings and simple payback per million square feet of conditioned area for envelope-related and lighting EEMs at Fort Benning under +6 ^{o}C climate change scenario.

Temp +6	Energy Use Intensity (kBtu/ft^2/yr)						Annual Energy (Therm)		Cost ($)			Invest $	Simple Payback
Energy Intensity (kBtu)/ft2/yr)	Elec site	Gas site	Tot Site	Elec src	Gas src	Tot src	site	src	Elec Cost	Gas Cost	Tot Cost		(yrs)
Army Reserve Center	28.0	10.1	38.0	93.4	10.6	104.0	1,092	2,983	$1,347	$171	$1,518	$11,476	21.1
Brigade HQ	48.0	2.3	50.3	160.4	2.4	162.8	36,868	119,293	$59,096	$990	$60,086	$329,831	23.5
Battalion HQ	39.6	2.7	42.3	132.3	2.8	135.2	120,371	384,339	$189,176	$4,558	$193,734	$1,279,371	30.3
Child Development Center	29.2	16.3	45.4	97.4	17.0	114.4	3,023	7,614	$3,258	$639	$3,898	$26,620	22.4
Company Operations Facility	21.1	6.4	27.5	70.6	6.7	77.2	12,860	36,103	$16,580	$1,764	$18,343	$186,951	23.0
Dining Facility	134.2	72.5	206.6	448.1	75.9	524.0	88,422	224,233	$96,419	$18,308	$114,727	$171,168	13.1
Tactical Equipment Maintenance Facility	22.1	6.3	28.4	73.9	6.6	80.5	29,777	84,406	$38,983	$3,875	$42,858	$419,562	33.3
Barracks	62.6	32.2	94.8	209.1	33.7	242.7	415,440	1,064,242	$460,856	$83,259	$544,115	$1,973,049	21.2
Totals							**707,852**	**1,923,213**	**$865,715**	**$113,564**	**$979,279**	**$4,398,028**	

Some interesting trends emerge from the above results. First, applying the package of EEMs significantly decreases both site and source energy usage and cost in all three climate change scenarios. The simple payback on investment ranges between 12.9 and 32.3 years in the +0^{o}C scenario. Further, the simple payback period decreases slightly for the +3^{o}C and +6^{o}C case for all building types except the TEMF (Figure 72). This is because the TEMFs are not air conditioned, so savings from tighter building and lower lighting loads do not accrue.

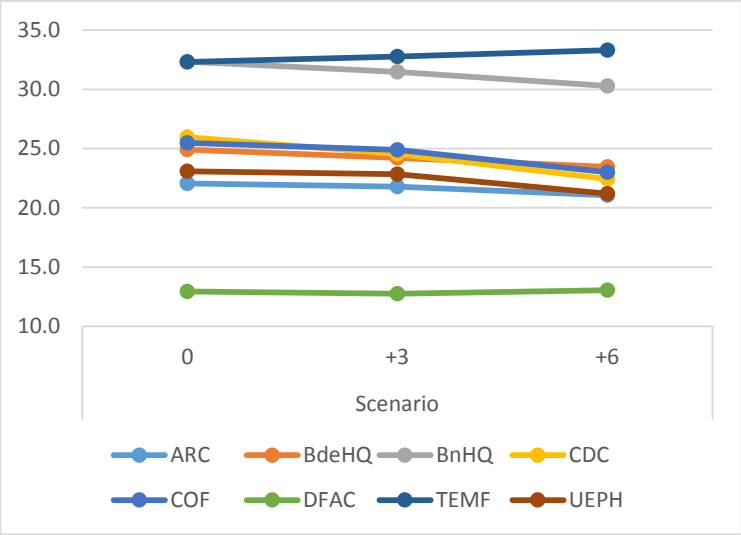

Figure 72. Simple payback in years versus climate change scenario for EEMs at Fort Benning.

Conclusions

For Fort Benning and the eight building types analyzed, rising temperatures will result in a decreased heating load and increased cooling load for most types of buildings. If the heating is provided by natural gas and cooling by electricity, this will result in significant fuel switching, even though overall EUI will remain fairly flat. With respect to the financial viability of applying envelope-related and lighting EEMs, results can be interpreted to show that if an EEM is cost effective, rising temperatures will only make it more so. Thus, a technical case can be made for conducting analysis using modified weather files.

Case Study 2: Fort Hood, TX

Background and Problem Framing

Like Fort Benning in the previous section, eight buildings were analyzed for Fort Hood, TX. Fort Hood is located in ASHRAE climate zone 2A, hotter than Fort Benning. The analysis procedure was identical and used the same EEM parameter values as show in Table 13.

Vulnerability Assessment

As before, results for +0ºC, +3ºC, and +6ºC are shown in Table 20, Table 21, and Table 22. Results are similar to Fort Benning. Examining EUI for cooling and heating shows higher cooling EUI and lower heating EUI, as one would expect in a hotter climate.

Table 20. Energy Use Intensity, total energy use, and cost for zero temperature change at Fort Hood, TX

Temp +0	Energy Use Intensity (kBtu/ft²/yr)						Annual Energy (Therm)		Cost ($)		
Energy Intensity (kBtu)/ft2/yr)	Elec site	Gas site	Tot Site	Elec src	Gas src	Tot src	site	src	Elec Cost	Gas Cost	Tot Cost
Army Reserve Center	34.7	16.3	51.0	115.8	17.1	132.8	1,462	3,810	$1,585	$214	$1,799
Brigade HQ	53.3	5.7	59.0	177.9	6.0	183.9	43,244	134,798	$62,243	$1,926	$64,169
Battalion HQ	45.0	6.7	51.7	150.4	7.0	157.3	146,901	447,264	$204,040	$8,669	$212,709
Child Development Center	35.6	20.7	56.3	118.8	21.7	140.5	3,744	9,347	$3,773	$631	$4,404
Company Operations Facility	26.0	12.0	38.0	86.8	12.6	99.4	17,751	46,435	$19,363	$2,569	$21,932
Dining Facility	125.1	97.8	222.9	417.8	102.4	520.3	95,401	222,637	$85,349	$19,182	$104,531
Tactical Equipment Maintenance Facility	27.1	15.5	42.6	90.6	16.2	106.8	44,722	112,043	$45,347	$7,458	$52,805
Barracks	67.1	36.5	103.6	224.1	38.3	262.3	454,405	1,150,279	$468,987	$73,418	$542,405
Totals							**807,630**	**2,126,613**	**$890,687**	**$114,067**	**$1,004,755**

Table 21. Energy Use Intensity, total energy use, and cost for +3°C temperature change at Fort Hood, TX

Temp +3	Energy Use Intensity (kBtu/ft²/yr)						Annual Energy (Therm)		Cost ($)		
Energy Intensity (kBtu)/ft2/yr)	Elec site	Gas site	Tot Site	Elec src	Gas src	Tot src	site	src	Elec Cost	Gas Cost	Tot Cost
Army Reserve Center	38.1	12.9	51.1	127.4	13.6	141.0	1,466	4,044	$1,745	$170	$1,915
Brigade HQ	54.8	4.0	58.9	183.2	4.2	187.4	43,160	137,362	$64,087	$1,357	$65,445
Battalion HQ	46.7	4.6	51.3	155.9	4.8	160.8	145,846	457,024	$211,594	$6,015	$217,608
Child Development Center	39.3	17.2	56.5	131.2	18.1	149.3	3,763	9,935	$4,169	$526	$4,695
Company Operations Facility	29.1	8.3	37.4	97.2	8.7	105.9	17,487	49,497	$21,685	$1,780	$23,465
Dining Facility	143.2	82.7	225.8	478.2	86.5	564.7	96,632	241,647	$97,670	$16,206	$113,876
Tactical Equipment Maintenance Facility	28.3	9.6	37.9	94.5	10.0	104.5	39,704	109,632	$47,323	$4,591	$51,914
Barracks	72.1	31.9	104.0	240.7	33.4	274.1	455,818	1,201,809	$503,787	$64,064	$567,851
Totals							**803,875**	**2,210,948**	**$952,059**	**$94,710**	**$1,046,769**

Table 22. Energy Use Intensity, total energy use, and cost for +6°C temperature change at Fort Hood, TX

Temp +6	Energy Use Intensity (kBtu/ft²/yr)						Annual Energy (Therm)		Cost ($)		
Energy Intensity (kBtu)/ft2/yr)	Elec site	Gas site	Tot Site	Elec src	Gas src	Tot src	site	src	Elec Cost	Gas Cost	Tot Cost
Army Reserve Center	42.3	10.7	53.1	141.4	11.2	152.6	1,522	4,379	$1,937	$141	$2,078
Brigade HQ	56.8	2.8	59.5	189.6	2.9	192.5	43,635	141,079	$66,326	$931	$67,258
Battalion HQ	48.7	3.1	51.8	162.6	3.3	165.8	147,279	471,483	$220,604	$4,082	$224,686
Child Development Center	43.7	14.9	58.6	146.1	15.6	161.7	3,900	10,759	$4,641	$453	$5,094
Company Operations Facility	34.2	6.1	40.3	114.3	6.4	120.7	18,856	56,429	$25,508	$1,309	$26,817
Dining Facility	166.8	70.2	237.0	557.2	73.5	630.7	101,431	269,880	$113,807	$13,767	$127,574
Tactical Equipment Maintenance Facility	30.0	5.8	35.7	100.1	6.0	106.2	37,480	111,350	$50,137	$2,764	$52,901
Barracks	77.9	28.6	106.5	260.2	30.0	290.2	467,060	1,272,371	$544,664	$57,468	$602,132
Totals							**821,163**	**2,337,731**	**$1,027,624**	**$80,915**	**$1,108,539**

Site electrical EUI rises more steeply with temperature than Fort Benning, while natural gas EUI falls less steeply (Figure 73). Overall site EUI rises moderately with temperature (Figure 74). Cost rises as well, moderated by Fort Hood's low electrical rates.

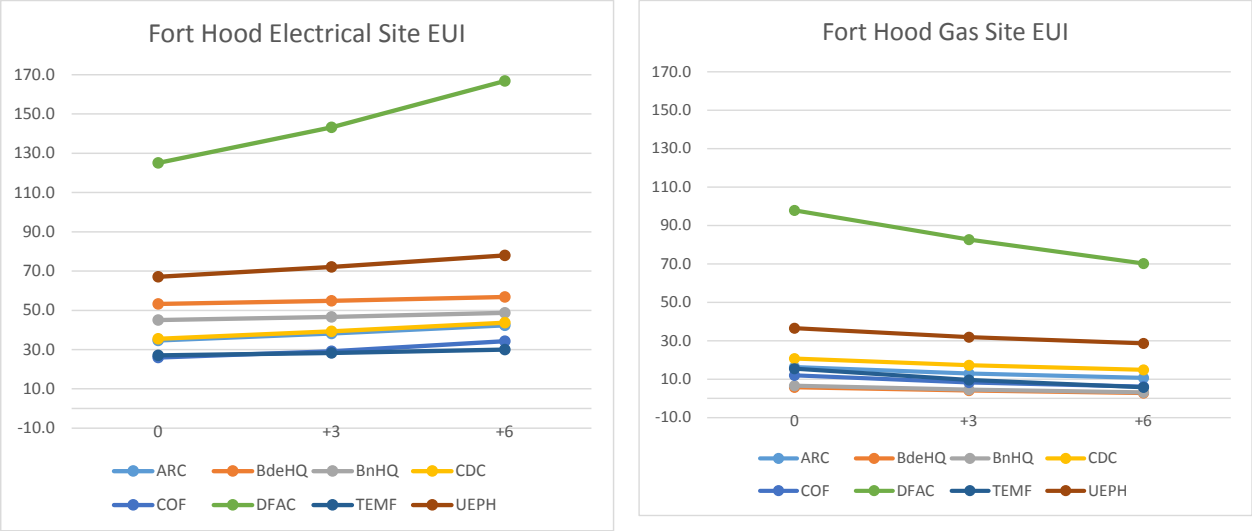

Figure 73. Electrical and gas EUI for all three climate change scenarios at Fort Hood, TX

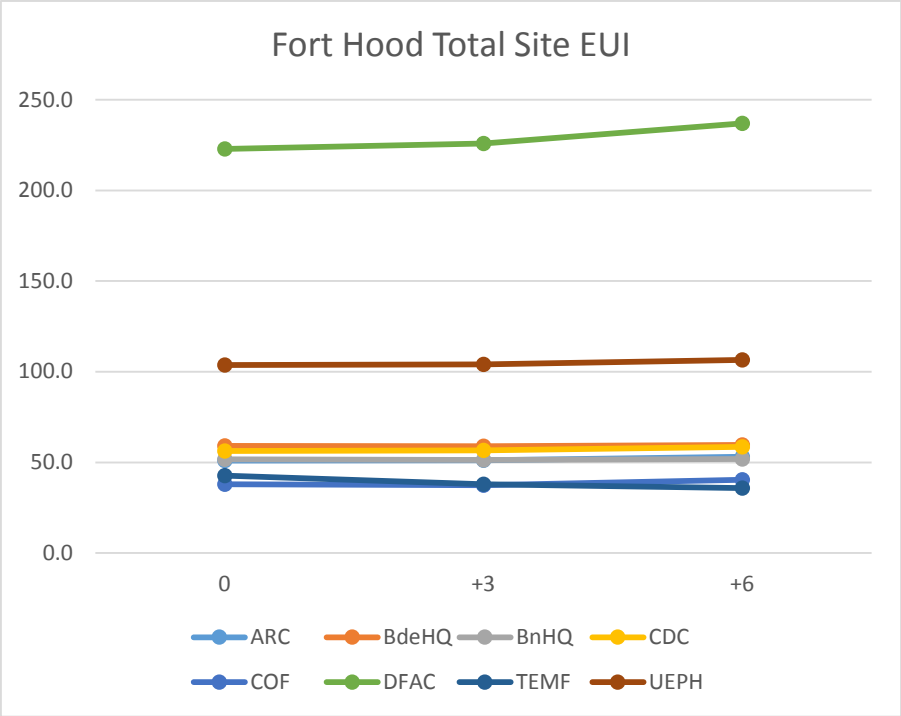

Figure 74. Total site EUI for all three climate change scenarios at Fort Hood, TX

Total site energy (Figure 75) rises only slightly, but total energy costs rise by about 10% for the +6°C scenario. (Figure 76) Like Benning, this is primarily because of fuel switching from natural gas for heating to electricity for cooling.

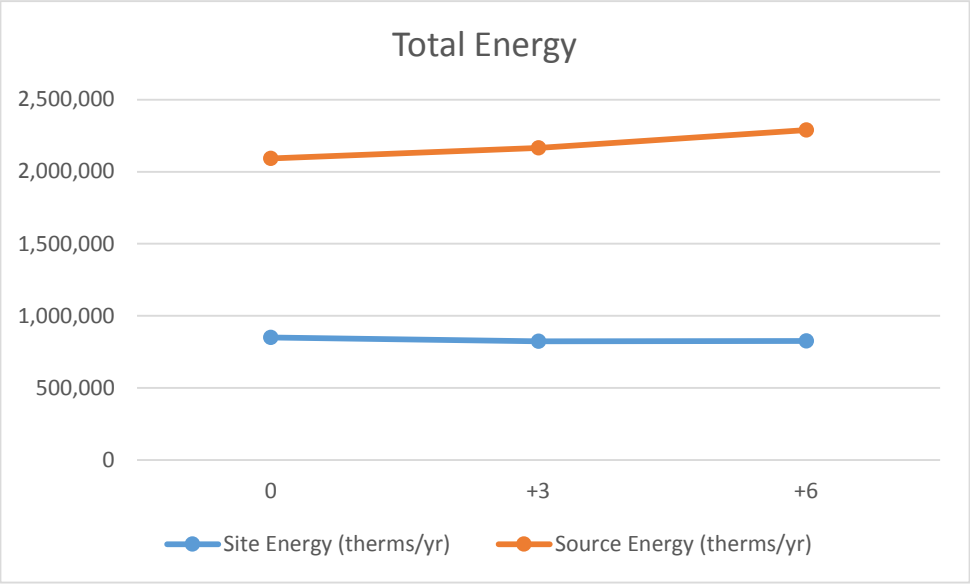

Figure 75. Annual energy use change per million square feet of conditioned building area for Fort Hood. Like Fort Benning, total site energy usage is relatively constant, but source energy use increases due to a shift from natural gas to electricity.

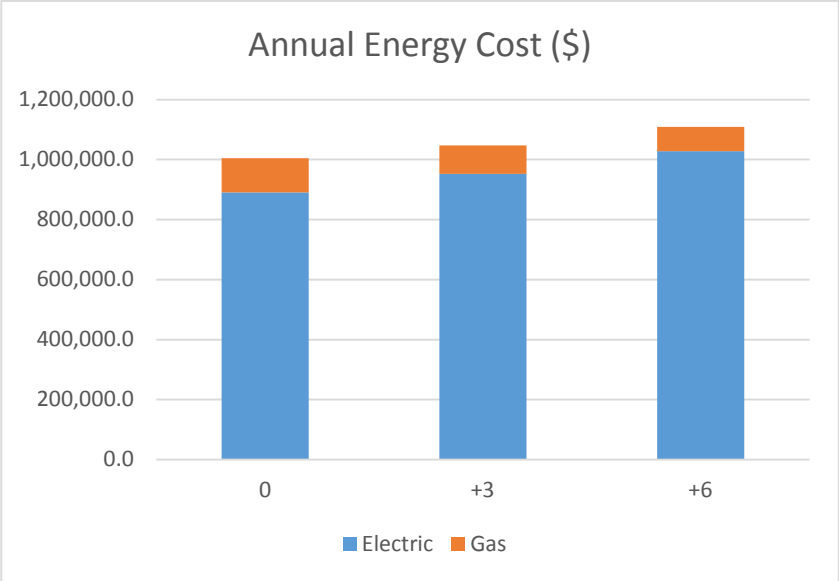

Figure 76. Annual energy cost at Fort Hood per million square feet of conditioned building area for three climate change scenarios. Also like Fort Benning, natural gas used for heating decreases while electricity used for cooling increases.

Assessment of Future Risks and System Robustness

The eight reference building models and EEM packages were simulated and produced tables Table 23, Table 24, and Table 25. Results were very similar, with a hotter climate and somewhat less expensive energy rates than Fort Benning.

Table 23. Energy savings and simple payback per million square feet of conditioned area for envelope-related and lighting EEMs at Fort Hood under +0°C climate change scenario.

Temp +0	Energy Use Intensity (kBtu/ft²/yr)						Annual Energy (Therm)		Cost ($)			Invest $	Simple Payback
Energy Intensity (kBtu)/ft2/yr)	Elec site	Gas site	Tot Site	Elec src	Gas src	Tot src	site	src	Elec Cost	Gas Cost	Tot Cost		
Army Reserve Center	24.9	12.5	37.4	83.2	13.1	96.3	1,074	2,763	$1,139	$164	$1,304	$11,476	23.2
Brigade HQ	45.9	3.3	49.2	153.5	3.4	156.9	36,062	114,975	$53,689	$1,093	$54,783	$329,831	35.1
Battalion HQ	37.6	4.0	41.6	125.6	4.2	129.8	118,272	369,058	$170,504	$5,189	$175,694	$1,279,371	34.6
Child Development Center	26.3	19.6	45.9	87.9	20.5	108.4	3,053	7,211	$2,791	$597	$3,388	$26,620	26.2
Company Operations Facility	17.0	8.9	26.0	56.9	9.3	66.3	12,138	30,973	$12,699	$1,912	$14,611	$186,951	25.5
Dining Facility	110.3	88.9	199.2	368.5	93.0	461.6	85,240	197,508	$75,274	$17,423	$92,696	$171,168	14.5
Tactical Equipment Maintenance Facility	20.9	13.2	34.1	69.8	13.8	83.7	35,803	87,771	$34,962	$6,357	$41,319	$419,562	36.5
Barracks	54.8	35.4	90.2	183.0	37.1	220.0	395,460	964,818	$382,948	$71,137	$454,085	$1,973,049	22.3
Totals							**687,104**	**1,775,077**	**$734,006**	**$103,873**	**$837,879**	**$4,398,028**	

Table 24. Energy savings and simple payback per million square feet of conditioned area for envelope-related and lighting EEMs at Fort Hood under +3°C climate change scenario.

Temp +3	Energy Use Intensity (kBtu/ft²/yr)						Annual Energy (Therm)		Cost ($)			Invest $	Simple Payback
Energy Intensity (kBtu)/ft2/yr)	Elec site	Gas site	Tot Site	Elec src	Gas src	Tot src	site	src	Elec Cost	Gas Cost	Tot Cost		
Army Reserve Center	27.6	10.0	37.6	92.3	10.5	102.8	1,080	2,949	$1,264	$131	$1,396	$11,476	22.1
Brigade HQ	47.1	2.3	49.4	157.5	2.4	159.8	36,213	117,147	$55,089	$761	$55,849	$329,831	34.4
Battalion HQ	38.9	2.7	41.6	129.8	2.9	132.7	118,280	377,142	$176,120	$3,579	$179,699	$1,279,371	33.7
Child Development Center	29.1	16.3	45.5	97.3	17.1	114.4	3,026	7,614	$3,091	$498	$3,589	$26,620	24.1
Company Operations Facility	19.3	6.2	25.4	64.4	6.5	70.8	11,887	33,100	$14,361	$1,319	$15,680	$186,951	24.0
Dining Facility	127.2	75.4	202.6	424.8	78.9	503.7	86,681	215,553	$86,771	$14,779	$101,550	$171,168	13.9
Tactical Equipment Maintenance Facility	21.8	8.4	30.2	73.0	8.8	81.7	31,678	85,700	$36,526	$4,017	$40,543	$419,562	36.9
Barracks	58.9	31.2	90.1	196.8	32.7	229.5	395,151	1,006,174	$411,927	$62,668	$474,594	$1,973,049	21.2
Totals							**683,996**	**1,845,379**	**$785,149**	**$87,752**	**$872,901**	**$4,398,028**	

Table 25. Energy savings and simple payback per million square feet of conditioned area for envelope-related and lighting EEMs at Fort Hood under +6°C climate change scenario.

Temp +6	Energy Use Intensity (kBtu/ft²/yr)						Annual Energy (Therm)		Cost ($)			Invest $	Simple Payback
Energy Intensity (kBtu)/ft2/yr)	Elec site	Gas site	Tot Site	Elec src	Gas src	Tot src	site	src	Elec Cost	Gas Cost	Tot Cost		
Army Reserve Center	30.9	8.4	39.3	103.1	8.8	111.9	1,127	3,211	$1,412	$111	$1,523	$11,476	20.7
Brigade HQ	48.6	1.6	50.1	162.2	1.6	163.9	36,743	120,109	$56,764	$522	$57,285	$329,831	33.1
Battalion HQ	40.4	1.9	42.2	134.8	1.9	136.7	120,016	388,730	$182,913	$2,422	$185,335	$1,279,371	32.5
Child Development Center	32.6	14.0	46.6	108.9	14.7	123.6	3,104	8,223	$3,458	$428	$3,886	$26,620	22.0
Company Operations Facility	23.2	4.5	27.6	77.5	4.7	82.1	12,923	38,389	$17,284	$954	$18,238	$186,951	21.8
Dining Facility	149.2	65.2	214.4	498.3	68.2	566.5	91,727	242,425	$101,782	$12,777	$114,558	$171,168	13.2
Tactical Equipment Maintenance Facility	23.1	4.9	28.0	77.2	5.1	82.4	29,377	86,379	$38,673	$2,346	$41,019	$419,562	35.3
Barracks	63.6	28.2	91.8	212.3	29.5	241.8	402,405	1,060,376	$444,333	$56,678	$501,011	$1,973,049	19.5
Totals							**697,421**	**1,947,843**	**$846,619**	**$76,237**	**$922,856**	**$4,398,028**	

Figure 77 shows that the simple payback period for the EEM packages studied decreases slightly with rising temperature, except for TEMFs and DFACs.

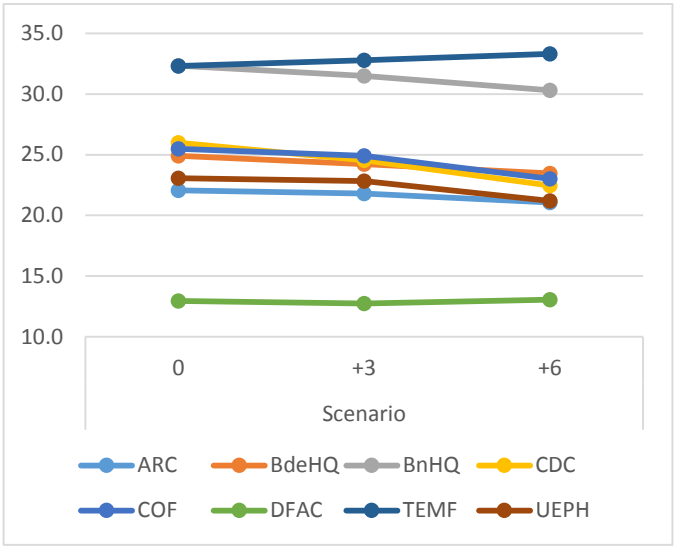

Figure 77. Simple payback in years versus climate change scenario for EEMs at Fort Hood. Except for TEMFs and DFACS, simple playback decreases with increasing temperature.

Conclusions

Simulation and analysis at Fort Hood yielded results very similar to results from Fort Benning. Simulation conducted with weather data that assumes stationarity will tend to be on the conservative side compared with weather data that has been adjusted for rising temperature. Based on the case studies examined so far, however, it is clear that rising temperatures may require higher electrical capacity and incur higher cost. There may be strategies to mitigate this trend to higher capacity requirements, such as moving to construction methods incorporating more thermal mass or generating electricity at point of use with solar photovoltaics, that are worthy of further study.

Case Study 3: U.S. Air Force Academy, CO

Background and Problem Framing

The U.S. Air Force Academy (USAFA) in Colorado Springs, Colorado, is located in ASHRAE climate zone 5B, which is considerably cooler and less humid than Fort Benning and Fort Hood. We would expect heating loads to exceed cooling loads and should not as high a degree of fuel switching as the previous two.

Because USAFA is in a significantly different climate zone, the parameter values applied from Table 13 to meet ASHRAE 90.1, 2010 in the base case are different, as are the EEM parameters applied in the simulation. Table 26 lists a subset of table 4 illustrating changes in insulation and window characteristics. That we used in simulation.

Table 26. Simulation parameters changed Table 13 for U.S. Air Force Academy energy base case and EEM simulation.

Name	Base Case Value	EEM Value	Unit	Description
Roof Base Continuous Insulation	20	50	R	Roof base continuous insulation R-value
Slab Vertical Insulation	0	20	R	Slab vertical insulation R-value
Wall Base Cavity Insulation	0	19	R	Wall base cavity insulation R-value
Wall Base Continuous Insulation	11.4	30	R	Wall base continuous insulation R-value
Window SHGC	0.55	0.35	SHGC	Window solar heat gain coefficient
Window U-Value	0.55	0.31	U	Window U-value

Vulnerability Assessment

Tables Table 27, Table 28, and Table 29 show results for the +0°C, +3°C, and +6°C climate scenarios. From Table 12, electrical power and gas are somewhat more expensive than for Fort Benning and Fort Hood.

Table 27. Energy Use Intensity, total energy use, and cost for +0°C temperature change at the U.S. Air Force Academy, Colorado Springs, CO

Temp +0	Energy Use Intensity (kBtu/ft²/yr)						Annual Energy (Therm)		Cost ($)		
Energy Intensity (kBtu)/ft2/yr)	Elec site	Gas site	Tot Site	Elec src	Gas src	Tot src	site	src	Elec Cost	Gas Cost	Tot Cost
Army Reserve Center	29.1	31.3	60.4	97.2	32.8	129.9	1,733	3,728	$1,773	$598	$2,371
Brigade HQ	44.1	11.4	55.5	147.4	11.9	159.3	40,688	116,760	$68,719	$5,553	$74,272
Battalion HQ	35.6	14.4	50.0	118.9	15.1	134.0	142,108	380,921	$215,103	$27,195	$242,298
Child Development Center	31.7	36.4	68.1	105.9	38.1	144.0	4,533	9,584	$4,482	$1,613	$6,095
Company Operations Facility	19.8	32.0	51.8	66.1	33.5	99.6	24,211	46,543	$19,639	$9,959	$29,598
Dining Facility	106.5	176.7	283.1	355.6	185.0	540.6	121,156	231,322	$96,807	$50,298	$147,105
Tactical Equipment Maintenance Facility	27.3	50.3	77.6	91.2	52.7	143.9	81,416	150,903	$60,843	$35,119	$95,962
Barracks	45.1	60.1	105.2	150.5	62.9	213.5	461,244	936,085	$419,914	$175,402	$595,316
Totals							**877,089**	**1,875,846**	**$887,281**	**$305,736**	**$1,193,018**

Table 28. Energy Use Intensity, total energy use, and cost for +3°C temperature change at the U.S. Air Force Academy, Colorado Springs, CO

Temp +3	Energy Use Intensity (kBtu/ft²/yr)						Annual Energy (Therm)		Cost ($)		
Energy Intensity (kBtu)/ft2/yr)	Elec site	Gas site	Tot Site	Elec src	Gas src	Tot src	site	src	Elec Cost	Gas Cost	Tot Cost
Army Reserve Center	29.9	24.3	54.2	99.8	25.4	125.2	1,554	3,593	$1,821	$464	$2,285
Brigade HQ	45.3	8.6	53.9	151.2	9.0	160.2	39,479	117,395	$70,480	$4,197	$74,677
Battalion HQ	36.7	10.8	47.5	122.6	11.3	133.9	134,996	380,581	$221,687	$20,401	$242,088
Child Development Center	32.3	29.6	61.9	107.8	31.0	138.8	4,118	9,237	$4,564	$1,310	$5,875
Company Operations Facility	20.9	23.9	44.8	69.7	25.1	94.7	20,937	44,282	$20,720	$7,442	$28,163
Dining Facility	110.3	140.3	250.6	368.3	146.9	515.3	107,245	220,487	$100,262	$39,961	$140,223
Tactical Equipment Maintenance Facility	27.0	34.5	61.6	90.3	36.1	126.5	64,568	132,637	$60,263	$24,090	$84,353
Barracks	47.6	50.0	97.6	158.9	52.4	211.3	428,055	926,514	$443,245	$146,012	$589,258
Totals							**800,952**	**1,834,725**	**$923,043**	**$243,878**	**$1,166,922**

Table 29. Energy Use Intensity, total energy use, and cost for +6°C temperature change at the U.S. Air Force Academy, Colorado Springs, CO

Temp +6	Energy Use Intensity (kBtu/ft²/yr)						Annual Energy (Therm)		Cost ($)		
Energy Intensity (kBtu)/ft2/yr)	Elec site	Gas site	Tot Site	Elec src	Gas src	Tot src	site	src	Elec Cost	Gas Cost	Tot Cost
Army Reserve Center	31.1	18.8	49.8	103.7	19.7	123.4	1,430	3,540	$1,893	$359	$2,251
Brigade HQ	46.4	6.3	52.7	155.0	6.6	161.6	38,644	118,431	$72,251	$3,087	$75,338
Battalion HQ	37.8	7.9	45.7	126.4	8.2	134.6	129,920	382,682	$228,559	$14,872	$243,430
Child Development Center	33.3	24.0	57.3	111.4	25.1	136.5	3,816	9,084	$4,715	$1,063	$5,778
Company Operations Facility	22.3	17.3	39.5	74.5	18.1	92.5	18,483	43,244	$22,139	$5,365	$27,505
Dining Facility	116.4	112.6	229.0	388.8	117.9	506.7	97,987	216,813	$105,841	$32,053	$137,894
Tactical Equipment Maintenance Facility	27.0	22.3	49.4	90.2	23.4	113.6	51,771	119,160	$60,191	$15,598	$75,788
Barracks	50.4	41.8	92.2	168.4	43.8	212.1	404,334	930,099	$469,581	$121,982	$591,564
Totals							**746,384**	**1,823,053**	**$965,169**	**$194,379**	**$1,159,548**

Graphs of electrical site EUI and natural gas site EUI (Figure 78) are much different for USAFA than for Fort Hood and Fort Benning. Natural gas heating loads are much higher compared to the previous case studies and there is very little increase in electrical cooling loads with temperature increase. The net effect is a decrease in EUI for all building type with increasing temperature in the range studied. Of course, if temperature were to increase enough, then

cooling loads would become more significant and EUI would start to increase again, but that inflection point was not investigated in this study, as +6°C was consider a high bound.

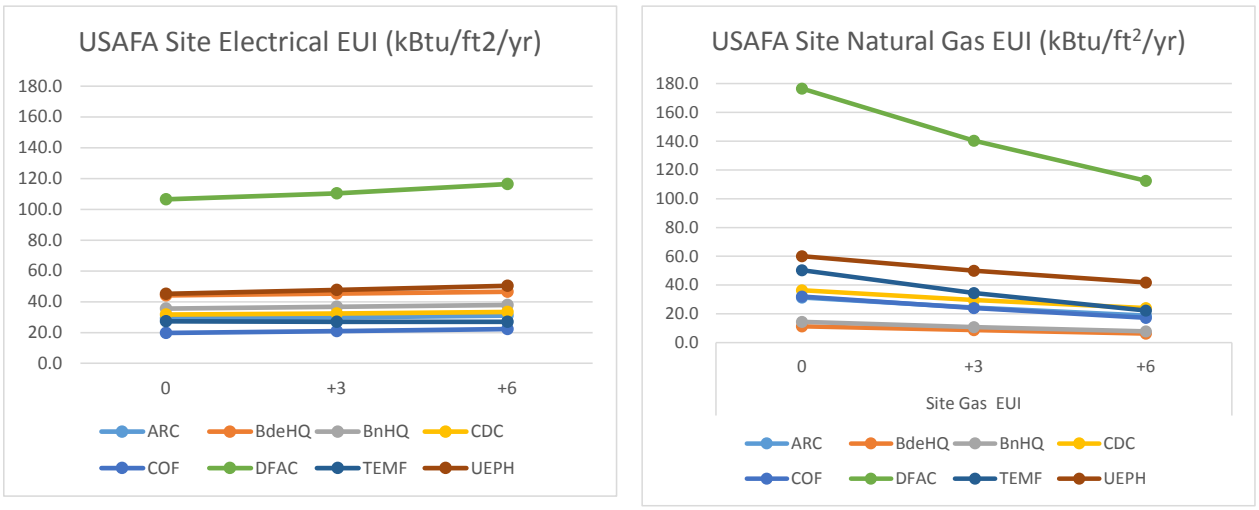

Figure 78. Electrical and gas EUI for all three climate change scenarios at the U.S. Air Force Academy.

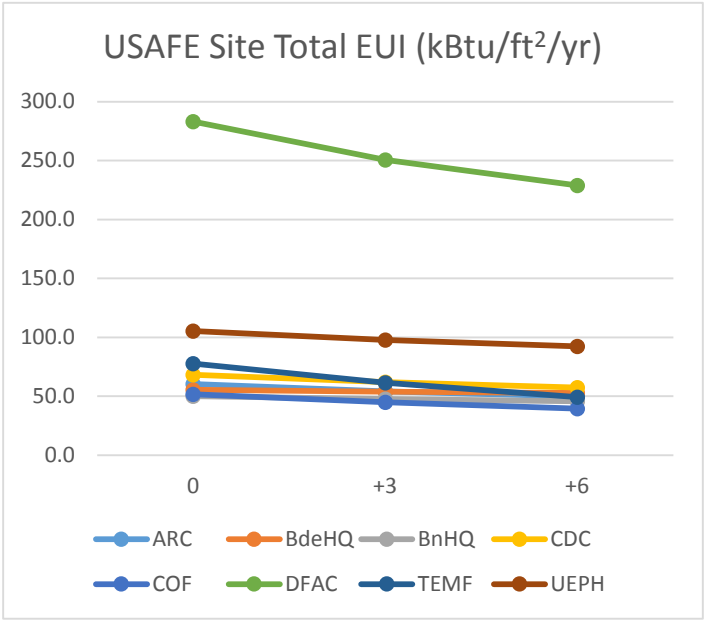

Figure 79. Total site EUI for all three climate change scenarios at the U.S. Air Force Academy.

Figure 80 shows total energy usage per mission square feet using the distribution of facility types from Table 11. It is noticeably different than the previous results in that both site energy and source energy decrease with increasing temperature. This difference can be attributed to the large decrease in required heating and a fairly small increase in required cooling. The total cost of energy also decreases (Figure 81).

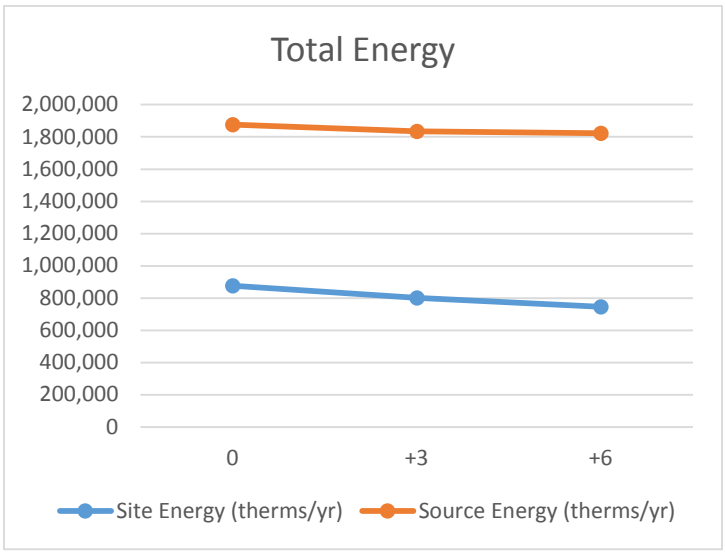

Figure 80. Annual energy use change per million square feet of conditioned building area for the U.S. Air Force Academy. Unlike Fort Hood and Fort Benning, both site and source energy decrease. Buildings in this climate zone are dominated by heating loads rather than cooling loads.

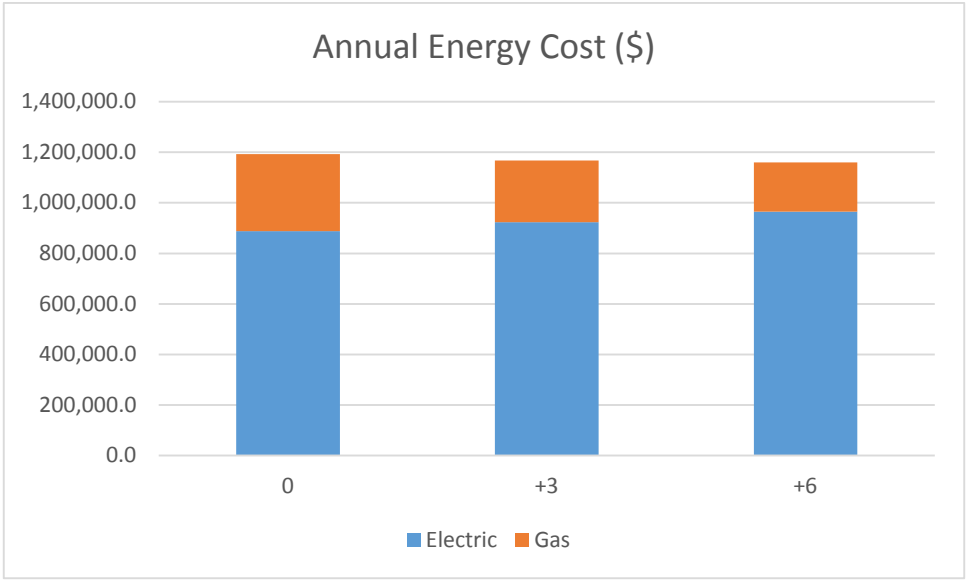

Figure 81. Annual energy cost at the U.S. Air Force Academy per million square feet of conditioned building area for three climate change scenarios. The slight increase in electricity for cooling is more than offset by the decreased heating requirements, resulting in lower overall energy costs.

Assessment of Future Risks and System Robustness

The USAFA case study is different in that increasing temperature actually saves the installation site and source energy as well as cost. Tables Table 30, Table 31, and Table 32 show results from simulation the application of the EEM package.

Table 30. Energy savings and simple payback per million square feet of conditioned area for envelope-related and lighting EEMs at the U.S. Air Force Academy, Colorado Springs, CO under +0°C climate change scenario.

Temp +0	Energy Use Intensity (kBtu/ft²/yr)						Annual Energy (Therm)		Cost ($)			Invest $	Simple Payback
Energy Intensity (kBtu)/ft2/yr)	Elec site	Gas site	Tot Site	Elec src	Gas src	Tot src	site	src	Elec Cost	Gas Cost	Tot Cost		
Army Reserve Center	20.6	23.8	44.4	68.9	24.9	93.8	1,274	2,691	$1,258	$454	$1,711	$11,476	17.4
Brigade HQ	38.7	6.8	45.5	129.4	7.1	136.5	33,362	100,034	$60,327	$3,307	$63,634	$329,831	31.0
Battalion HQ	30.1	8.8	38.9	100.6	9.2	109.8	110,605	312,137	$181,929	$16,622	$198,551	$1,279,371	29.2
Child Development Center	23.1	33.7	56.8	77.3	35.3	112.6	3,783	7,491	$3,271	$1,493	$4,764	$26,620	20.0
Company Operations Facility	12.1	23.4	35.5	40.4	24.5	64.9	16,591	30,330	$12,008	$7,279	$19,287	$186,951	18.1
Dining Facility	92.6	151.3	243.9	309.2	158.4	467.6	104,349	200,087	$84,170	$43,073	$127,243	$171,168	8.6
Tactical Equipment Maintenance Facility	20.7	41.9	62.6	69.2	43.9	113.0	65,685	118,575	$46,149	$29,253	$75,402	$419,562	20.4
Barracks	35.9	56.0	91.9	120.0	58.6	178.6	403,012	783,257	$334,795	$163,311	$498,106	$1,973,049	20.3
Totals							**738,661**	**1,554,603**	**$723,907**	**$264,792**	**$988,699**	**$4,398,028**	

Table 31. Energy savings and simple payback per million square feet of conditioned area for envelope-related and lighting EEMs at the U.S. Air Force Academy, Colorado Springs, CO under +3°C climate change scenario.

Temp +3	Energy Use Intensity (kBtu/ft²/yr)						Annual Energy (Therm)		Cost ($)			Invest $	Simple Payback
Energy Intensity (kBtu)/ft2/yr)	Elec site	Gas site	Tot Site	Elec src	Gas src	Tot src	site	src	Elec Cost	Gas Cost	Tot Cost		
Army Reserve Center	21.2	18.6	39.8	70.8	19.5	90.3	1,141	2,590	$1,292	$355	$1,647	$11,476	18.0
Brigade HQ	39.6	5.0	44.6	132.4	5.2	137.6	32,691	100,864	$61,748	$2,415	$64,163	$329,831	31.4
Battalion HQ	31.0	6.4	37.4	103.5	6.7	110.2	106,245	313,281	$187,219	$12,064	$199,284	$1,279,371	29.9
Child Development Center	23.6	27.6	51.2	78.9	28.9	107.8	3,409	7,174	$3,340	$1,223	$4,563	$26,620	20.3
Company Operations Facility	12.8	17.4	30.3	42.9	18.2	61.1	14,143	28,566	$12,748	$5,418	$18,167	$186,951	18.7
Dining Facility	95.8	121.1	217.0	320.1	126.8	446.9	92,846	191,242	$87,133	$34,491	$121,625	$171,168	9.2
Tactical Equipment Maintenance Facility	20.5	28.3	48.8	68.5	29.6	98.1	51,180	102,925	$45,720	$19,736	$65,456	$419,562	22.2
Barracks	38.0	47.3	85.3	127.1	49.5	176.6	374,194	774,289	$354,443	$137,984	$492,427	$1,973,049	20.4
Totals							**675,850**	**1,520,932**	**$753,645**	**$213,686**	**$967,331**	**$4,398,028**	

Table 32. Energy savings and simple payback per million square feet of conditioned area for envelope-related and lighting EEMs at the U.S. Air Force Academy, Colorado Springs, CO under +6°C climate change scenario.

Temp +6	Energy Use Intensity (kBtu/ft²/yr)						Annual Energy (Therm)		Cost ($)			Invest $	Simple Payback
Energy Intensity (kBtu)/ft2/yr)	Elec site	Gas site	Tot Site	Elec src	Gas src	Tot src	site	src	Elec Cost	Gas Cost	Tot Cost		
Army Reserve Center	22.1	14.5	36.6	73.8	15.2	89.0	1,050	2,553	$1,347	$277	$1,624	$11,476	18.3
Brigade HQ	40.5	3.5	44.0	135.3	3.6	138.9	32,236	101,842	$63,095	$1,691	$64,786	$329,831	31.3
Battalion HQ	31.9	4.5	36.4	106.4	4.7	111.1	103,395	315,960	$192,466	$8,526	$200,991	$1,279,371	30.1
Child Development Center	24.4	22.5	46.9	81.5	23.6	105.1	3,123	6,995	$3,452	$997	$4,449	$26,620	20.0
Company Operations Facility	13.8	12.5	26.3	46.1	13.1	59.2	12,292	27,660	$13,705	$3,887	$17,592	$186,951	18.9
Dining Facility	101.4	97.9	199.4	338.8	102.5	441.3	85,308	188,850	$92,230	$27,880	$120,109	$171,168	9.6
Tactical Equipment Maintenance Facility	20.5	18.1	38.6	68.5	18.9	87.4	40,486	91,701	$45,694	$12,629	$58,323	$419,562	24.0
Barracks	40.4	40.1	80.5	135.0	42.0	176.9	352,890	775,706	$376,425	$116,925	$493,350	$1,973,049	20.1
Totals							**630,781**	**1,511,265**	**$788,413**	**$172,811**	**$961,224**	**$4,398,028**	

Figure 82 shows the trends of the simple payback periods for the different building types. Unlike in the previous case studies, the periods increase, although not by very much. The TEMF is the only facility type with a large increase in simple payback period, indicating that using current TMY3 files might result in spending more than necessary from a purely economics view. However, the paybacks are all still within the 40 year period allowed by statute for new buildings.

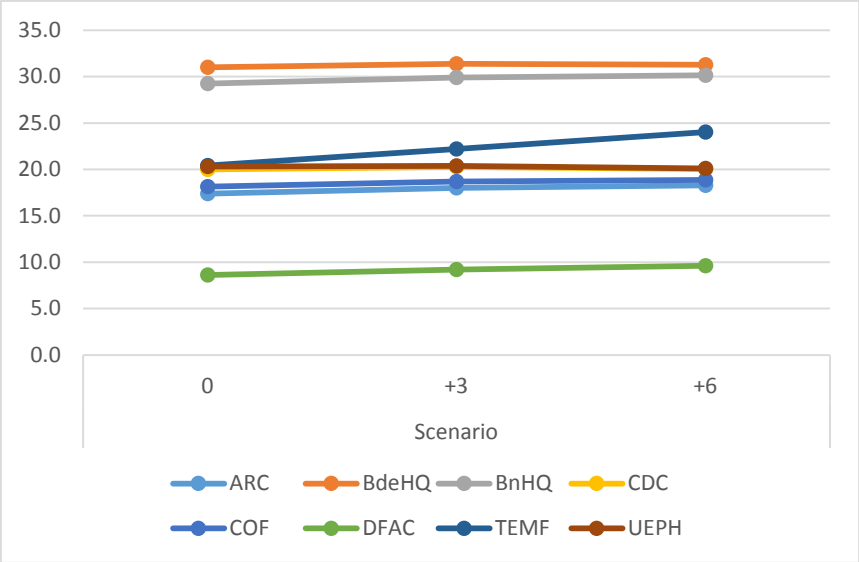

Figure 82. Simple payback in years versus climate change scenario for EEMs at the U.S. Air Force Academy. Unlike the other case studies, simple payback periods are flat to increasing as temperature increase.

Conclusions

This case study indicates that USAFA is not very vulnerable to temperature increase. In fact, temperature reduces site and source energy use intensity. Use of modified weather files in analysis to evaluate EEM packages might lead to less cost effective choices. I.E., more insulation, better windows, and better lighting might not be worth the investment. If other evaluation criteria are applied, however, such as Greenhouse Gas emissions, the EEM package evaluated is still more effective at reducing source energy consumption than the base case.

Case Study 4: Edwards Air Force Base, CA

Background and Problem Framing

Edwards Air Force Base is located in ASHRAE climate zone 3B, essentially as hot as Fort Benning, but much drier. Table 33 illustrates simulation parameters that were used.

Table 33. Simulation parameters changed from Table 13 for Edwards AFB, CA energy base case and EEM simulation.

Name	**Base Case Value**	**EEM Value**	**Unit**	**Description**
Roof Base Continuous Insulation	20	35	R	Roof base continuous insulation R-value
Slab Vertical Insulation	0	10	R	Slab vertical insulation R-value
Wall Base Cavity Insulation	0	19	R	Wall base cavity insulation R-value

Wall Base Continuous Insulation	7.6	20	R	Wall base continuous insulation R-value
Window SHGC	0.25	0.25	SHGC	Window solar heat gain coefficient
Window U-Value	0.65	0.41	U	Window U-value

Vulnerability Assessment

Tables Table 34, Table 35, and Table 36 show results for Edwards AFB. This installation is dominated by electrical cooling loads, although not to the degree that Fort Benning and Fort Hood. One difference is that the installation pays much higher rates for electrical power than is the case for the other three case studies.

Table 34. Energy Use Intensity, total energy use, and cost for +0°C temperature change at Edwards AFB, CA.

Temp +0	Energy Use Intensity (kBtu/ft²/yr)						Annual Energy (Therm)		Cost ($)		
Energy Intensity (kBtu)/ft2/yr)	Elec site	Gas site	Tot Site	Elec src	Gas src	Tot src	site	src	Elec Cost	Gas Cost	Tot Cost
Army Reserve Center	34.2	23.2	57.4	114.3	24.3	138.6	1,647	3,976	$4,016	$495	$4,512
Brigade HQ	49.1	9.2	58.3	164.0	9.6	173.6	42,707	127,253	$147,269	$4,994	$152,263
Battalion HQ	40.9	10.5	51.3	136.4	11.0	147.4	145,928	419,097	$475,163	$22,167	$497,330
Child Development Center	35.1	24.0	59.1	117.2	25.1	142.3	3,933	9,471	$9,552	$1,189	$10,741
Company Operations Facility	23.5	17.9	41.4	78.6	18.7	97.3	19,360	45,497	$45,012	$6,219	$51,232
Dining Facility	121.9	110.9	232.9	407.2	116.1	523.4	99,644	223,969	$213,469	$35,324	$248,792
Tactical Equipment Maintenance Facility	27.1	16.7	43.8	90.5	17.5	108.0	45,924	113,254	$116,283	$13,024	$129,307
Barracks	53.5	42.6	96.1	178.7	44.6	223.3	421,342	979,138	$959,909	$138,949	$1,098,859
Totals							**780,485**	**1,921,654**	**$1,970,673**	**$222,362**	**$2,193,035**

Table 35. Energy Use Intensity, total energy use, and cost for +3°C temperature change at Edwards AFB, CA.

Temp +3	Energy Use Intensity (kBtu/ft²/yr)						Annual Energy (Therm)		Cost ($)		
Energy Intensity (kBtu)/ft2/yr)	Elec	Gas	Tot Site	Elec src	Gas src	Tot src	site	src	Elec Cost	Gas Cost	Tot Cost
Army Reserve Center	35.9	16.4	52.4	120.0	17.2	137.2	1,503	3,937	$4,218	$351	$4,569
Brigade HQ	51.2	6.4	57.7	171.1	6.7	177.9	42,270	130,376	$153,658	$3,507	$157,165
Battalion HQ	43.0	7.1	50.2	143.7	7.5	151.2	142,611	429,735	$500,339	$15,119	$515,459
Child Development Center	36.8	18.6	55.3	122.8	19.5	142.2	3,684	9,466	$10,008	$921	$10,929
Company Operations Facility	25.4	11.4	36.8	84.9	12.0	96.9	17,221	45,274	$48,610	$3,973	$52,583
Dining Facility	130.6	84.9	215.5	436.1	88.9	525.0	92,215	224,659	$228,578	$27,047	$255,625
Tactical Equipment Maintenance Facility	27.4	8.7	36.1	91.4	9.1	100.5	37,840	105,425	$117,416	$6,802	$124,218
Barracks	57.8	34.5	92.2	192.9	36.1	229.0	404,415	1,004,112	$1,036,092	$112,495	$1,148,587
Totals							**741,758**	**1,952,983**	**$2,098,918**	**$170,216**	**$2,269,134**

Table 36. Energy Use Intensity, total energy use, and cost for +6°C temperature change at Edwards AFB, CA.

Temp +6	Energy Use Intensity (kBtu/ft²/yr)						Annual Energy (Therm)		Cost ($)		
Energy Intensity (kBtu)/ft2/yr)	Elec	Gas	Tot Site	Elec src	Gas src	Tot src	site	src	Elec Cost	Gas Cost	Tot Cost
Army Reserve Center	38.1	11.6	49.7	127.4	12.2	139.5	1,427	4,003	$4,477	$248	$4,725
Brigade HQ	53.4	4.4	57.7	178.3	4.6	182.9	42,318	134,029	$160,086	$2,373	$162,459
Battalion HQ	45.2	4.5	49.7	151.0	4.7	155.7	141,375	442,689	$525,762	$9,575	$535,337
Child Development Center	39.1	15.0	54.1	130.7	15.7	146.4	3,602	9,743	$10,654	$743	$11,397
Company Operations Facility	27.9	6.7	34.6	93.0	7.0	100.1	16,156	46,769	$53,266	$2,334	$55,600
Dining Facility	141.8	68.7	210.5	473.7	72.0	545.6	90,094	233,484	$248,288	$21,884	$270,171
Tactical Equipment Maintenance Facility	28.0	4.3	32.3	93.5	4.5	98.0	33,854	102,780	$120,142	$3,340	$123,482
Barracks	62.9	29.0	91.9	210.2	30.3	240.5	402,864	1,054,476	$1,128,850	$94,470	$1,223,320
Totals							**731,691**	**2,027,973**	**$2,251,524**	**$134,967**	**$2,386,491**

As can be seen in Figure 83, site electrical EUI increases fairly significantly with temperature, while heating load decreases even more sharply. Total site EUI (Figure 84) is reasonable flat, exhibiting fuel shifting.

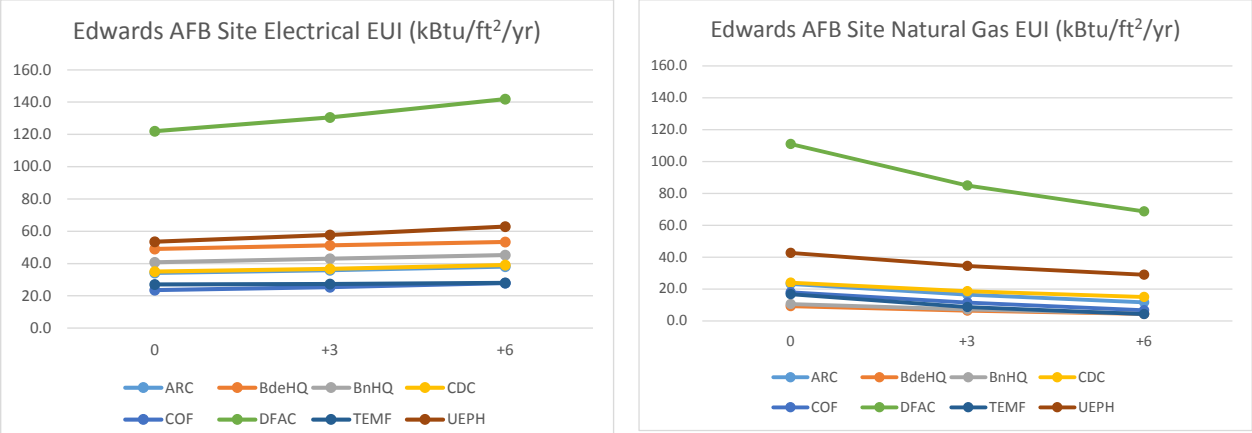

Figure 83. Electrical and gas EUI for all three climate change scenarios at Edwards AFB, CA

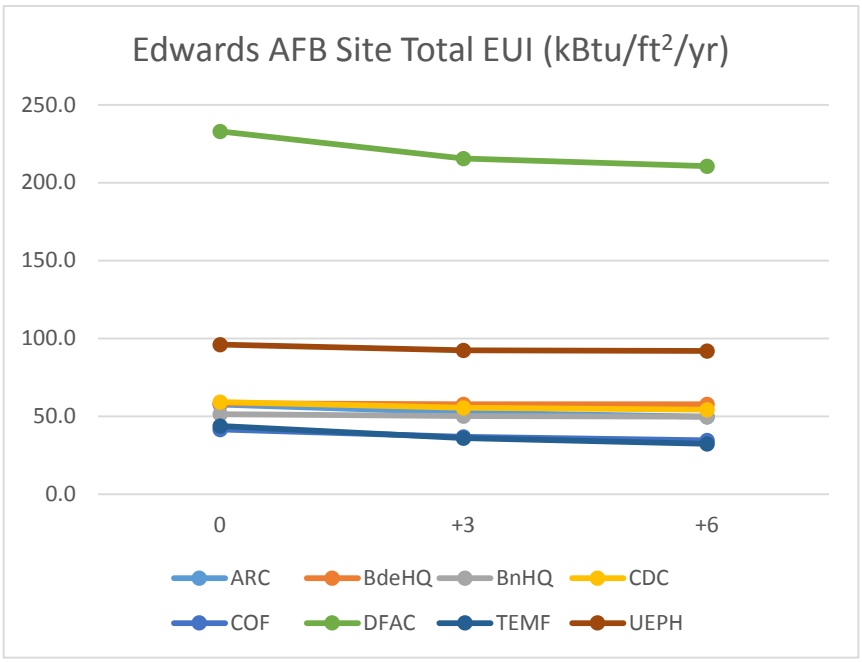

Figure 84. Total site EUI for all three climate change scenarios at Edwards AFB, CA

Total Energy for Edwards AFB, shown in Figure 85, is flat for site energy with increasing temperature, with source energy increasing due to switching from natural gas for heating to electricity. Costs increase significantly due to increased purchase of electricity, assuming electrical power is purchased from the grid.

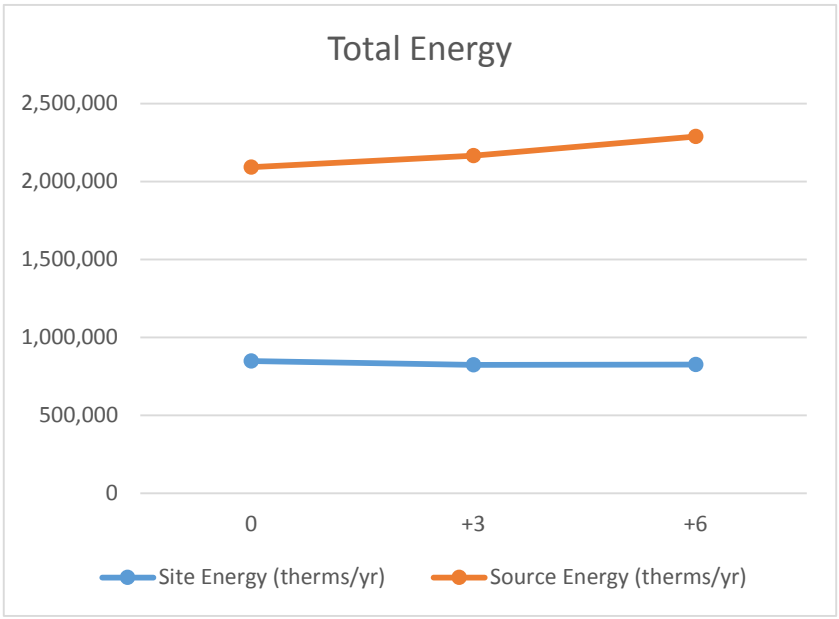

Figure 85. Annual energy use change per million square feet of conditioned building area for Edwards AFB, which shows a typical pattern for a cooling load dominated climate zone.

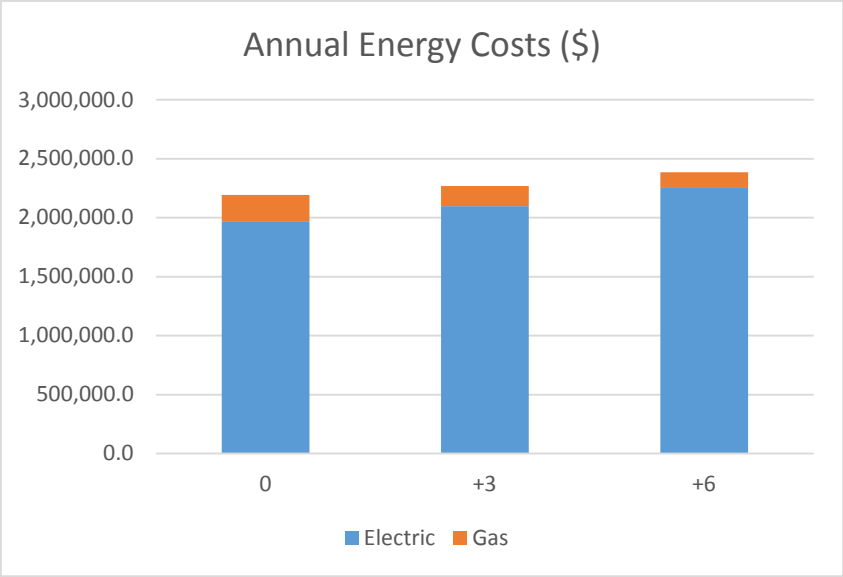

Figure 86. Annual energy cost at the Edwards AFB, CA per million square feet of conditioned building area for three climate change scenarios. Overall costs increase due to the strong increase in electrical cooling loads with increasing temperature.

Assessment of Future Risks and System Robustness

Tables Table 37, Table 38, and Table 39 show results of simulation of EEM packages for Edwards AFB. The simple payback periods are much lower than for the other case studies, reflecting the higher cost of electrical power.

Table 37. Energy savings and simple payback per million square feet of conditioned area for envelope-related and lighting EEMs at Edwards AFB, CA under +0°C climate change scenario.

Temp +0	Energy Use Intensity (kBtu/ft²/yr)						Annual Energy (Therm)		Cost ($)			Invest $	Simple Payback
Energy Intensity (kBtu)/ft2/yr)	Elec site	Gas site	Tot Site	Elec src	Gas src	Tot src	site	src	Elec Cost	Gas Cost	Tot Cost		
Army Reserve Center	24.4	16.3	40.8	81.5	17.1	98.6	1,169	2,830	$2,866	$349	$3,215	$11,476	8.8
Brigade HQ	42.5	5.0	47.5	142.1	5.2	147.3	34,850	107,994	$127,583	$2,728	$130,311	$329,831	15.0
Battalion HQ	34.1	5.9	40.0	114.0	6.2	120.2	113,820	341,756	$397,148	$12,463	$409,612	$1,279,371	14.6
Child Development Center	25.6	22.5	48.2	85.6	23.6	109.3	3,207	7,271	$6,982	$1,117	$8,098	$26,620	10.1
Company Operations Facility	15.0	13.1	28.1	50.1	13.7	63.8	13,132	29,822	$28,678	$4,556	$33,234	$186,951	10.4
Dining Facility	106.4	95.0	201.4	355.3	99.5	454.8	86,183	194,626	$186,261	$30,255	$216,516	$171,168	5.3
Tactical Equipment Maintenance Facility	20.7	13.2	33.9	69.2	13.8	83.0	35,586	87,082	$88,898	$10,312	$99,210	$419,562	13.9
Barracks	43.1	41.4	84.5	144.0	43.4	187.3	370,629	821,364	$773,140	$135,182	$908,322	$1,973,049	10.4
Totals							**658,576**	**1,592,744**	**$1,611,557**	**$196,961**	**$1,808,518**	**$4,398,028**	

Table 38. Energy savings and simple payback per million square feet of conditioned area for envelope-related and lighting EEMs at Edwards AFB, CA under +3°C climate change scenario.

Temp +3	Energy Use Intensity (kBtu/ft²/yr)						Annual Energy (Therm)		Cost ($)			Invest $	Simple Payback
Energy Intensity (kBtu)/ft2/yr)	Elec	Gas	Tot Site	Elec src	Gas src	Tot src	site	src	Elec Cost	Gas Cost	Tot Cost		
Army Reserve Center	25.7	11.7	37.4	86.0	12.2	98.2	1,073	2,816	$3,021	$249	$3,270	$11,476	8.8
Brigade HQ	44.2	3.5	47.7	147.7	3.6	151.4	34,965	110,935	$132,617	$1,898	$134,514	$329,831	14.6
Battalion HQ	35.8	3.8	39.7	119.6	4.0	123.7	112,766	351,572	$416,632	$8,135	$424,767	$1,279,371	14.1
Child Development Center	27.0	17.5	44.5	90.3	18.3	108.7	2,965	7,232	$7,364	$867	$8,231	$26,620	9.9
Company Operations Facility	16.3	8.4	24.7	54.5	8.7	63.2	11,525	29,545	$31,185	$2,904	$34,089	$186,951	10.1
Dining Facility	115.0	75.4	190.3	383.9	78.9	462.8	81,438	198,058	$201,250	$23,998	$225,247	$171,168	5.6
Tactical Equipment Maintenance Facility	21.0	6.9	27.9	70.1	7.2	77.3	29,233	81,106	$90,102	$5,365	$95,468	$419,562	14.6
Barracks	46.7	34.2	80.9	156.1	35.8	191.9	354,826	841,367	$838,353	$111,560	$949,913	$1,973,049	9.9
Totals							**628,790**	**1,622,630**	**$1,720,524**	**$154,975**	**$1,875,500**	**$4,398,028**	

Table 39. Energy savings and simple payback per million square feet of conditioned area for envelope-related and lighting EEMs at Edwards AFB, CA under +6°C climate change scenario.

Temp +6	Energy Use Intensity (kBtu/ft²/yr)						Annual Energy (Therm)		Cost ($)			Invest $	Simple Payback
Energy Intensity (kBtu)/ft2/yr)	Elec	Gas	Tot Site	Elec src	Gas src	Tot src	site	src	Elec Cost	Gas Cost	Tot Cost		
Army Reserve Center	27.4	8.5	35.9	91.4	8.9	100.3	1,029	2,878	$3,213	$181	$3,394	$11,476	8.6
Brigade HQ	45.9	2.2	48.1	153.3	2.3	155.6	35,241	114,019	$137,603	$1,197	$138,800	$329,831	13.9
Battalion HQ	37.5	2.4	39.9	125.3	2.5	127.8	113,382	363,327	$436,454	$4,988	$441,442	$1,279,371	13.6
Child Development Center	29.0	14.3	43.2	96.7	14.9	111.6	2,876	7,430	$7,885	$706	$8,591	$26,620	9.5
Company Operations Facility	18.0	4.9	22.9	60.3	5.1	65.3	10,703	30,543	$34,503	$1,689	$36,191	$186,951	9.6
Dining Facility	126.0	63.5	189.4	420.7	66.5	487.2	81,064	208,478	$220,538	$20,211	$240,750	$171,168	5.8
Tactical Equipment Maintenance Facility	21.5	3.5	25.1	71.9	3.7	75.6	26,304	79,329	$92,403	$2,767	$95,171	$419,562	14.8
Barracks	51.0	29.2	80.2	170.4	30.5	200.9	351,537	881,047	$915,295	$95,117	$1,010,412	$1,973,049	9.3
Totals							**622,137**	**1,687,050**	**$1,847,893**	**$126,857**	**$1,974,751**	**$4,398,028**	

Figure 87 shows that simple payback periods are relatively insensitive to temperature increase, with the TEMF and DFACS increasing and the others decreasing slightly.

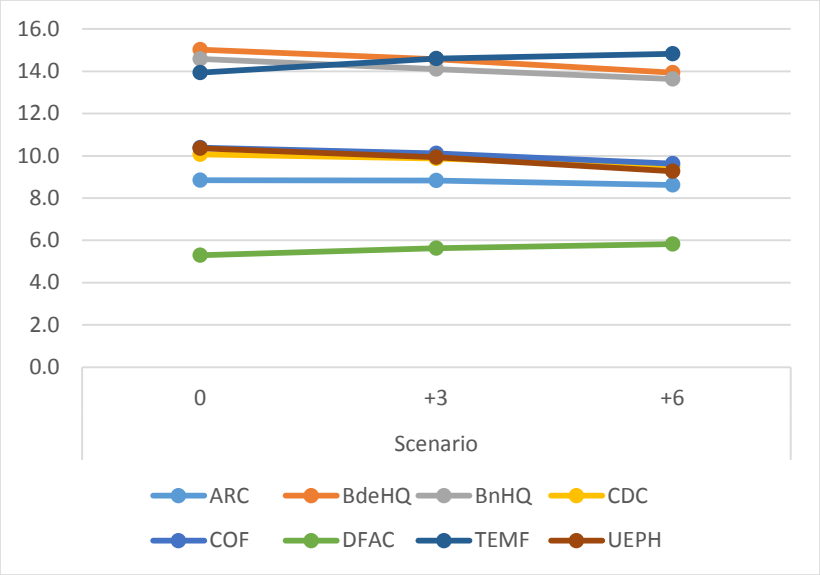

Figure 87. Simple payback in years versus climate change scenario for EEMs for Edwards AFB, CA. Like other hot climate zones, simple payback periods decrease, except for TEMFs and DFACs.

Conclusions

Given the insensitivity of simple payback periods, there is no real incentive to conduct the analysis with TMY3 weather files modified to reflect changing temperatures.

A study solely oriented towards climate-change related energy adaptation for each installation is probably not warranted. However, per the 31 March, 2016 Memorandum from OSD(EI&E), Installation Energy Plans, DoD installations are required to develop Energy Master Plans within three years of the Memo for installations that comprise 75% of each DoD Component. This includes a requirement to assess energy baselines and project future energy loads. If analysis for these plans is conducted using currently available tools (such as the NZP Tool used for this

analysis), it is very simple to conduct a sensitivity analysis using modified weather files at very low cost.

Results and Discussion: Climate Context at Installation Level

Regional Assessment Summary for Installations

Changes in Climate Based on the CMIP5

In order to create approximate comparability for the changes in climate simulated by the other climate models in the project (i.e., CMIP3 and NARCCAP suite) and the CMIP5 suite of simulations used in the recent IPCC 2013 Report, we focused on the results for the RCP 8.5 in the middle of the century (2046-2065). Among the new RCPs, RCP 8.5 follows a concentration and forcing path most similar to the A2 scenario in the CMIP3 and NARCCAP simulations.

We base these results presented in Table 40 on the maps presented in the Atlas of Regional Climate Change, Annex I of the WG1 IPCC Report, Supplementary Material for RCP 8.5. The maps portray the 25th, 50th, and 75th percentiles for seasonal changes (w.r.t. 1986-2005) in climate based on the total number of climate model simulations available (around 30) for three future time periods. We present the 25th to 75th percentile ranges for the mid-century. For precipitation the entire year is divided into two seasons. For temperature the four cardinal seasons are used.

Note that the values listed are approximate since they are determined from inspection of the maps available in the atlas supplementary material. This in a sense is a good thing, since greater precision likely is not warranted.

Table 40 Changes in temperature and precipitation for each installation

Locations	Winter		Summer	
	Temp °C	Precip (%)	Temp °C	Precip (%)
Fort Benning, GA	1.3 ~ 2.5	+5 ~ +15	2.0 ~ 3.0	-5 ~ +10
Fort Hood, TX	1.8 ~ 3.5	-5 ~ +5	1.8 ~ 2.5	-5 ~ +5
U.S. Air force Base, CO	1.8 ~ 3.5	-5 ~ +5	2.5 ~ 3.5	-5 ~ +5
Edwards Air Force Base, CA	1.8 ~ 3.5	-5 ~ +5	2.5 ~ 3.5	-15 ~ +5

For precipitation changes, the 25th-75th range covers 0 for all locations and both seasons (except for Ft. Benning in winter), thus indicating uncertainty about the direction of change. However, the changes are small and most are not significant. Hence many of the ranges should be interpreted as representing no significant change.
For temperature changes, values in both seasons generally range from 1.5 to 3.5^{o}C. The ranges tend to be narrower in summer. 75th percentile values are generally lower for Fort Benning than the other locations in both seasons.

Changes in Climate at Installation Level

Downscaled CMIP3 and CMIP5 projections were downloaded for Fort Hood, US Air Force Academy, Edwards Air Force Base, and Fort Benning. For each location of interest the mean temperature and precipitation was taken per projection. In other words, the precipitation and temperature at each grid cell for each time step was averaged for every projection. The time series analyzed where 2035 to 2065 and 2065 to 2095. This processes yielded a mean temperature and precipitation value for each projections for year 2050 and year 2080. Finally a

an overall average value for temperature and precipitation was taken for CMIP3 and CMIP5 per time series. The analysis for Fort Benning was done using a smaller set of projections because of a corrupt file. The data was graphed and is shown below.

Fort Benning, GA

Mean precipitation values for CMIP3 and CMIP5 suggest an increase of about 5% from historic values. The average CMIP3 projection is slightly above historic precipitation, while the average CMIP5 is modestly above historic precipitation. The range of values is large. One model expects precipitation to increase to almost 130% of historic precipitation while others expect precipiation to be less than 70% of historic by 2080.

All projections for both time series suggest increased temperature in the future. Mean values for CMIP3 and CMIP5 show an increase of around 1.75°C by 2050 and 2.75°C by 2080. The range is 0.5°C to 3.5°C for 2050 and 0°C to 5°C for 2080.

Fort Hood, TX

Both CMIP3 and CMIP5 projections for the Fort Hood area averaged around 100% of historic precipitation values. The CMIP3 mean value is slightly below historic, while the average CMIP5 is slightly above the historic mean. However, the range and scatter of the data is large. Minimum projected values drop below 80% and 70% of historic precipitaion for years 2050 and 2080, respectively. Max values hover around 120% and 130% by 2050 and 2080, respectively.

All projections for both time series suggest increased temperatures in the future. Mean values for CMIP3 and CMIP5 show an increase of 2°C by 2050 and 3°C by 2080. The CMIP5 values have larger ranges for both the 2050 and 2080 time series. The CMIP5 models vary from a small temperature change of less than 1° degree to a 6° increase.

U.S. Air Force Acadamy, CO

Mean precipitation values for CMIP3 and CMIP5 lie around 100% of historic values. The average CMIP3 projection is slightly below historic, while the average CMIP5 is slightly above historic mean. Again, here the range of values is large and increases from 2050 to 2080. By 2080 the range of projected precipitation values start at a low around 70% and a high above 130% historic values.

Almost all projections for both time series suggest increased temperature in the future. Mean values for CMIP3 and CMIP5 show an increase of around 1.75°C by 2050 and 2.75°C by 2080. Similar to the precipitation values, there is a large amount of scatter. The range is 0.5°C to 3°C for 2050 and 0°C to 5°C for 2080.

Edwards Air Force Base, CA

Mean precipitation values for CMIP3 and CMIP5 lie around 100% of historic values. The average CMIP3 projection is slightly below historic, while the average CMIP5 is slightly above the historic mean. The range of values is very large. One model expects precipitation to increase to almost 180% of historic precipitation while others expect precipiation to be 60% of historic mean by 2080.

Almost all projections for both time series suggest increased temperature in the future. Mean values for CMIP3 and CMIP5 show an increase of around 2°C by 2050 and 3°C by 2080. The range is 0.5°C to 3.5°C for 2050 and -0.25°C to 5.5°C for 2080.

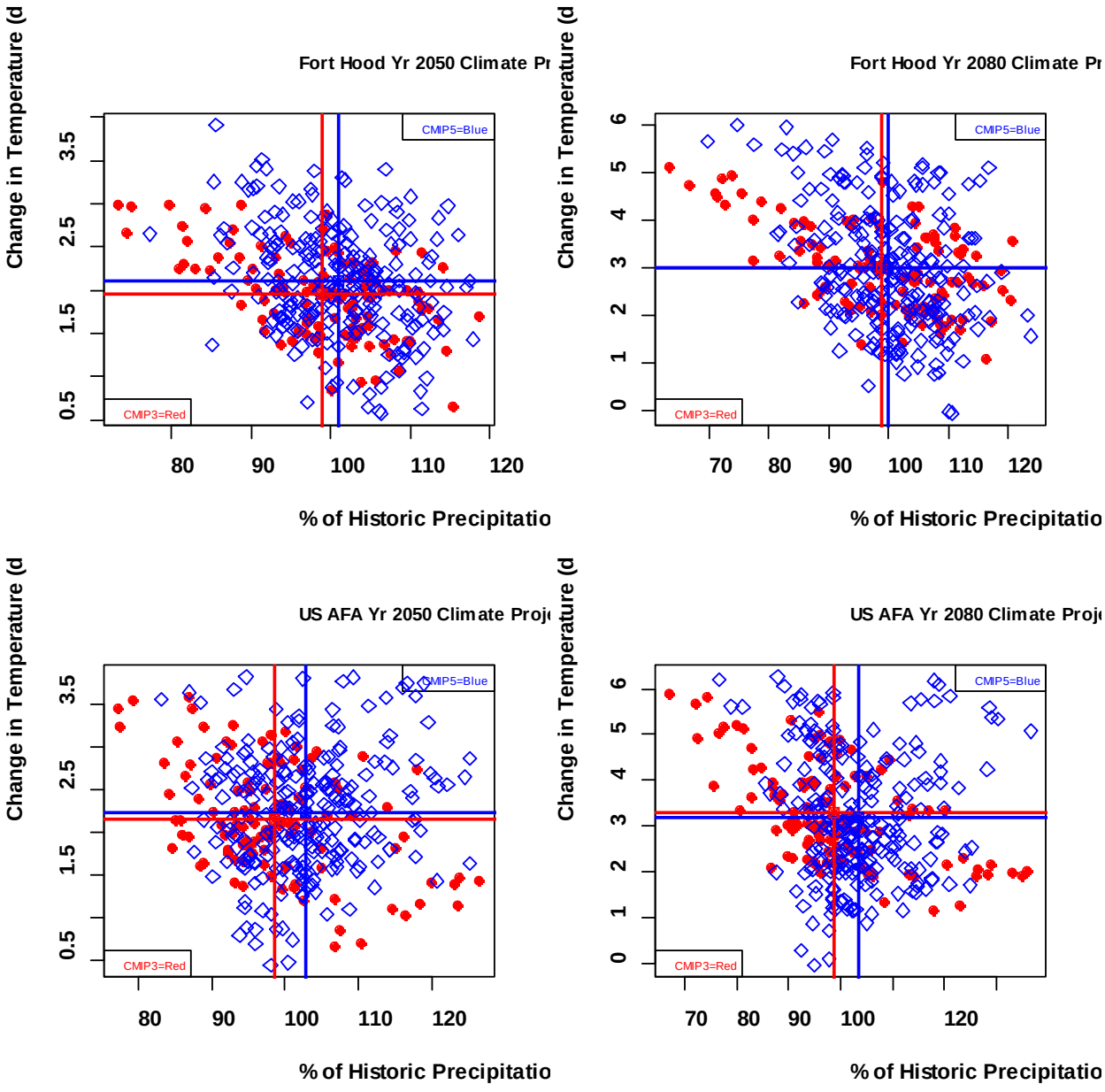

Figure 88 Climate change projections of changes in mean temperature and precipitation for Ft. Hood (top) and USAF Academy (bottom) for 2050 (right) and 2080 (left) based on CMIP3 and CMIP5 statistically downscaled projections.

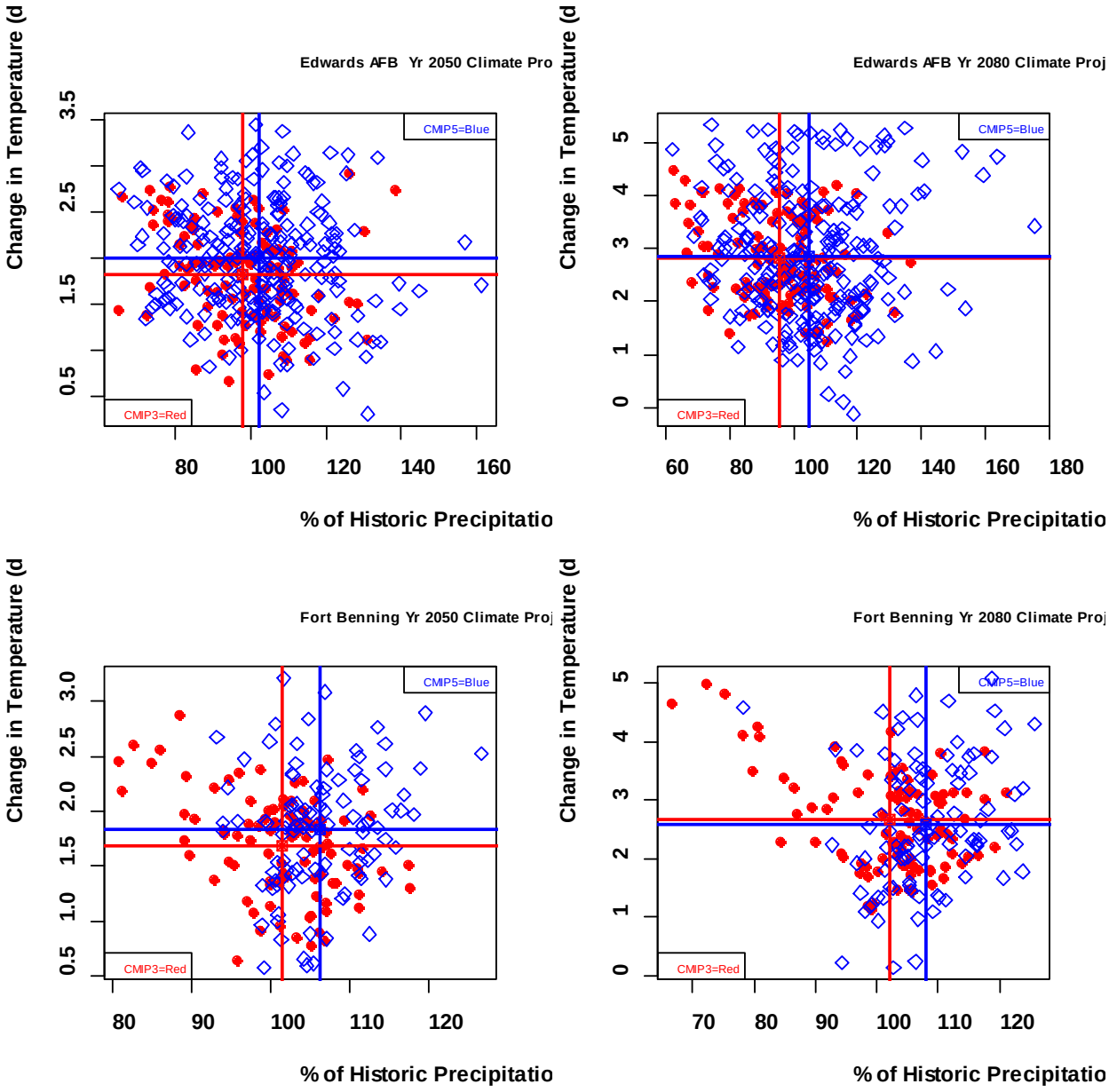

Figure 89 Climate change projections of changes in mean temperature and precipitation for Edwards AFB (top) and Ft. Benning (bottom) for 2050 (right) and 2080 (left) based on CMIP3 and CMIP5 statistically downscaled projections.

Initial results for relevant variables

Process Level Downscaling Credibility

Differential credibility of the NARCCAP simulations has been assessed using performance-based metrics that were developed within the European ENSEMBLES project for four regions encompassing all four military installations (see Table 41). Analysis regions are based on

ecoclimatic zones and are described in Bukovsky (2011). The metrics were developed to measure the performance of the RCMs in simulating sub-GCM scale climate features, where the RCMs should be capable of adding value of GCM performance. They are described in detail in Christensen et al. (2010). The metrics measure performance of the RCMs in simulating different aspects of temperature and precipitation. Performance in these two fields is indicative of performance in simulating many regional weather/climate processes. The results of the five metrics have been combined into one skill score for each region for each model simulation.

Table 41 Fire-risk categories based on the KBDI index and thresholds

Abbreviation	Name	Installation
DS	Deep South	Fort Benning
SP	Southern Plains	Fort Hood
SR	Southern Rockies	U.S. Air Force Academy
PSW	Pacific Southwest	Edwards Air Force Base

The five metrics measure the ability of the simulations to capture the spatial distribution of precipitation and temperature (f2), probability distributions of daily and monthly precipitation and minimum and maximum temperature (f3), extremes in precipitation and minimum and maximum temperature (f4), temperature trends (f5), and the annual cycle of precipitation and temperature (f6). Each metric is given equal weight when combined into the final skill score for each model. If a model performs poorly relative to the other models in any metric, this will be reflected in the final skill score. The metric measuring the ability to simulate temperature trends is not calculated for GCM-driven simulations, as they do not and are not expected to contain the same trends as observations because the natural internal variability of the driving GCMs does not cycle temporally with that of reality.

The results for each region and each metric for the NCEP-driven simulations are given in Figure 90. The greatest variability in performance between RCMs is seen in the mesoscale metric and trends metric, while the models perform with relatively equal skill in the pdf metric and the extremes metric. Some notable outliers include the HRM3, which performs best in capturing the spatial variability of precipitation and temperature in the PSW region in winter and SR region in summer. Also, the CRCM does not perform as well at simulating extremes as the other simulations in most regions and seasons. This known bias stems from the CRCM not simulating extreme precipitation events of a great enough magnitude, and may be due to the type of nudging used in the simulations. Finally, performance in simulating observed temperature trends is mixed, particularly in the DS and SP regions, and this is partly related to an ability to simulate the “warming hole” observed during the period of simulation. Trends and the ability of the models to simulate them in these simulations are further discussed in Bukovsky (2012).

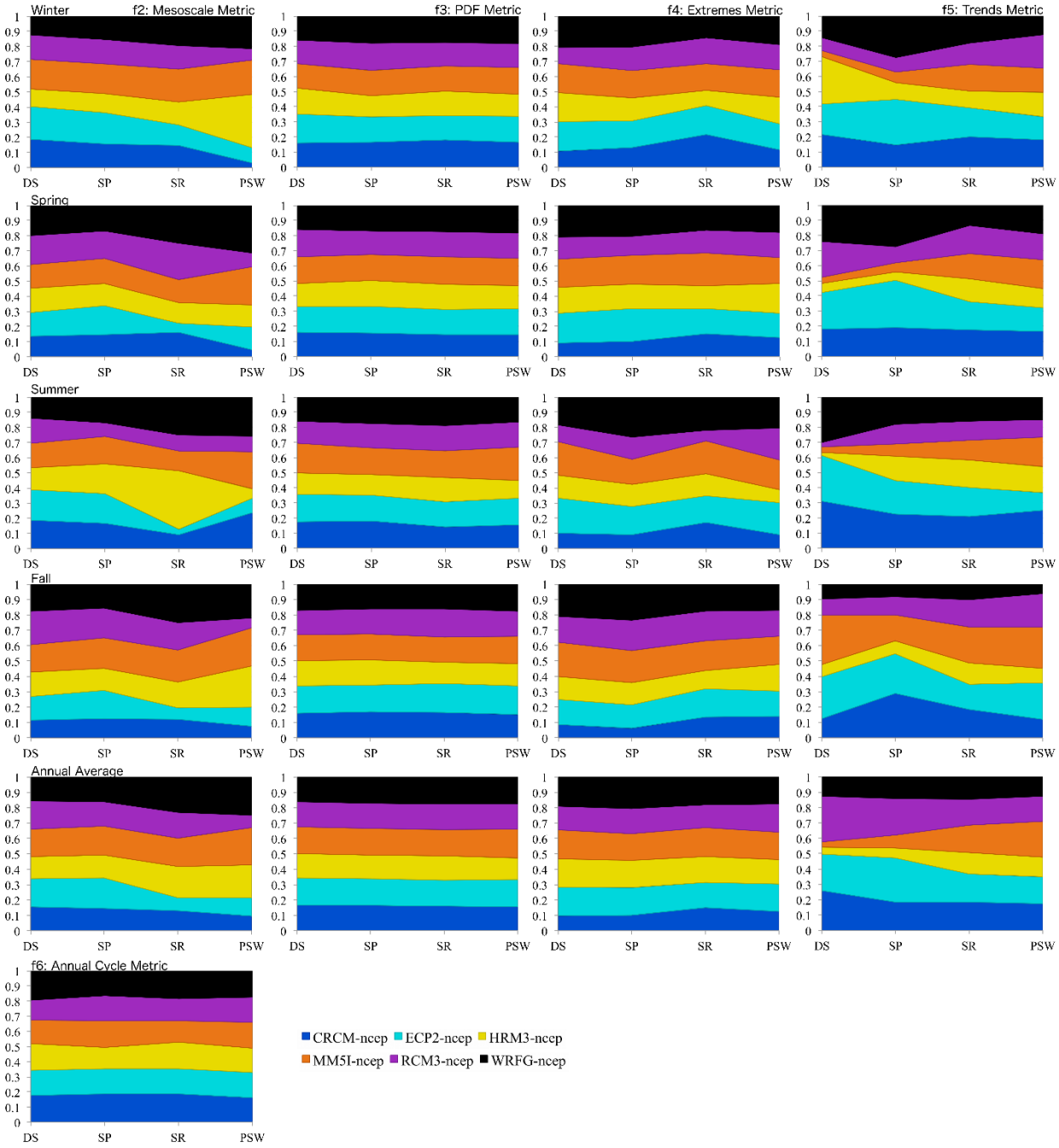

Figure 90 Individual metrics for each region (see Table 1 for regions) and NCEP-driven simulation. The thickness of a color above a given region indicates the value of the metric for the simulation assigned to that color. Since metrics are relative and must sum to one across all simulations, the thickness of the color over a region for any given simulation illustrates the performance of that simulation in that region relative to the other simulations (thicker is better).

Results for each region and metric for the GCM-driven simulations are shown in Figure 91. Results are similar to those in Figure 90, in that most of the relative variability in performance is in the mesoscale metric. Of note in the mesoscale metric are the MM5I-hadcm, which does not

perform well relative to the other simulations in any season or region due to problems simulating the spatial variability of temperature in these regions, and the WRFG simulations in the PSW in winter, which are generally perform better than the other simulations along with the MM5I-ccsm, due to better simulation of the precipitation spatial distribution. Similarly, we also see that the CRCM simulations perform at a lower skill level with extremes because of its precipitation bias.

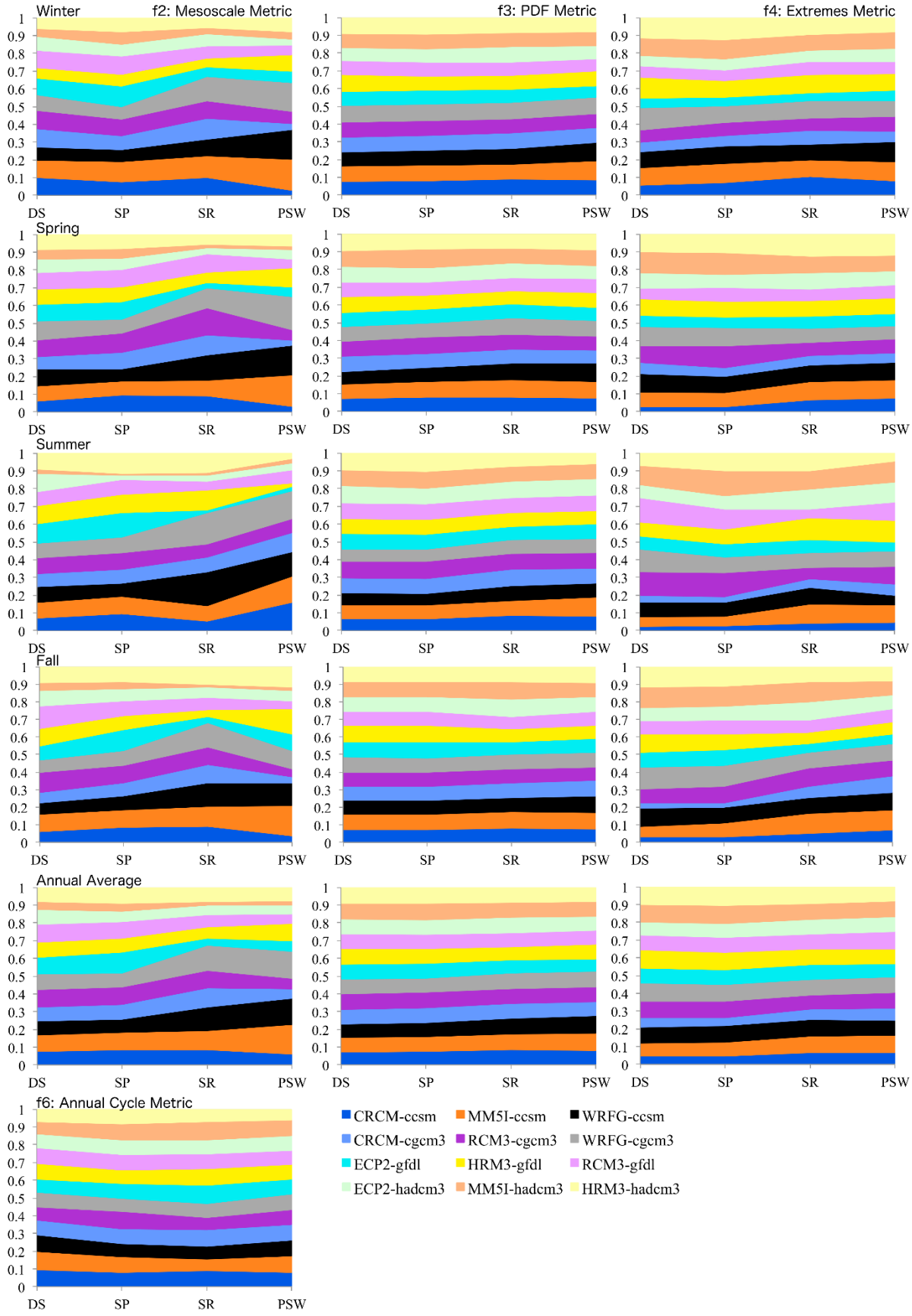
Winter
f2: Mesoscale Metric
f3: PDF Metric
f4: Extremes Metric
Spring
Summer
Fall
Annual Average
f6: Annual Cycle Metric
DS
SP
SR
PSW
CRCM-ccsm
MM5I-ccsm
WRFG-ccsm
CRCM-cgcm3
RCM3-cgcm3
WRFG-cgcm3
ECP2-gfdl
HRM3-gfdl
RCM3-gfdl
ECP2-hadcm3
MM5I-hadcm3
HRM3-hadcm3

Figure 91 Individual metrics for each region (see Table 1 for regions) and GCM-driven simulation. The thickness of a color above a given region indicates the value of the metric for the simulation assigned to that color. Since metrics are relative and must sum to one across all simulations, the thickness of the color over a region for any given simulation illustrates the performance of that simulation in that region relative to the other simulations (thicker is better).

Final skill score results from the NCEP-driven NARCCAP simulations are provided in Figure 92 for the annual mean, winter, and summer. The final skill scores use all of the above metrics. As is obvious from these results, no one model performs best in each region. However, there is some consistency in performance between models in the two eastern regions (DS and SP) and the two western regions (SR and PSW), likely due to the relative ability of the simulations to capture the patterns of precipitation and temperature and their forcing phenomena in each area. Most of the differentiation comes from the ability of the models to capture regional temperature trends and the spatial distribution of temperature and precipitation across the regions.

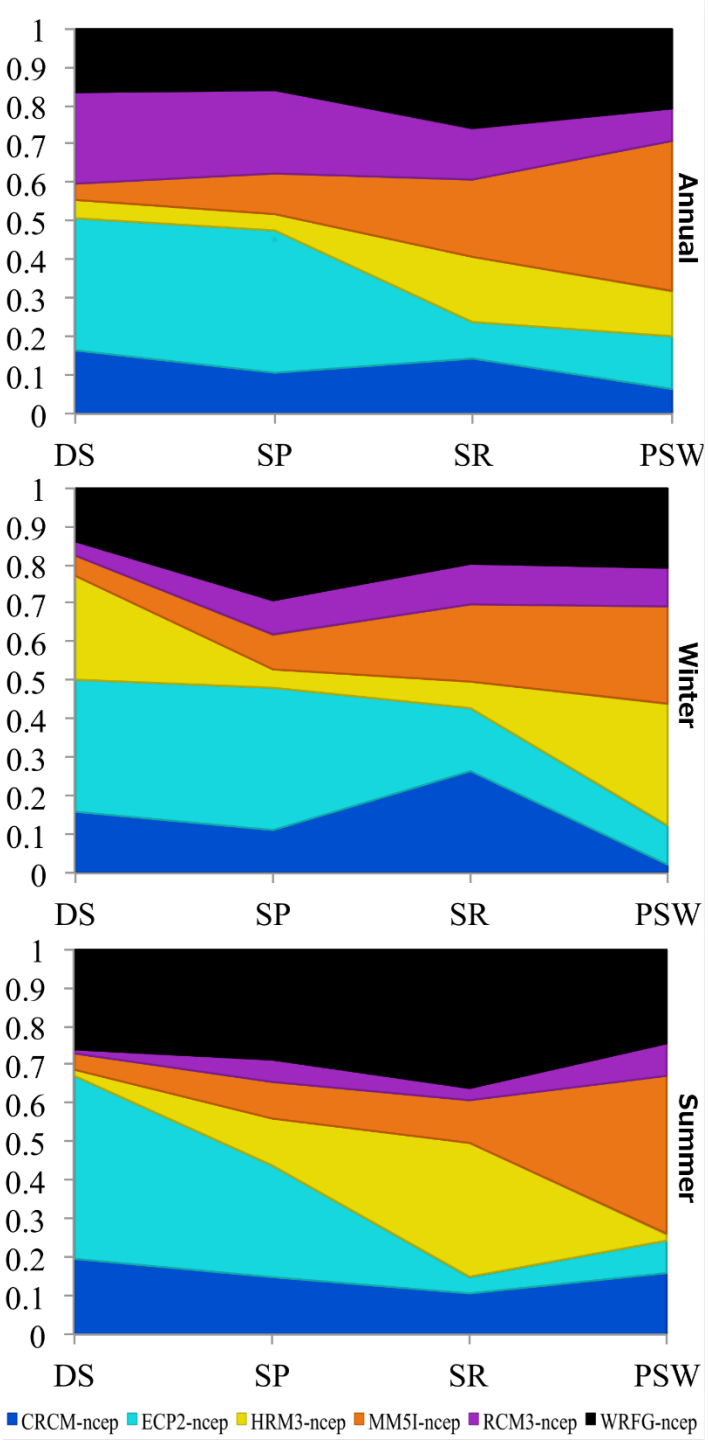

Figure 92 Skill scores for each region (see Table 1 for regions) and NCEP-driven simulation. The thickness of a color above a given region indicates the value of the score for the simulation assigned to that color. Since skill scores are relative and must sum to one across all simulations, the thickness of the color over a region for any given simulation illustrates the performance of that simulation in that region relative to the other simulations (thicker is better).

Final skill score results from the GCM-driven NARCCAP simulations are provided in Figure 93 for the annual mean, winter, and summer. In this case, most of the differentiation comes from the ability of the models to capture the spatial distribution of precipitation and temperature in each region and, to a lesser extent, extreme values of precipitation and temperature.

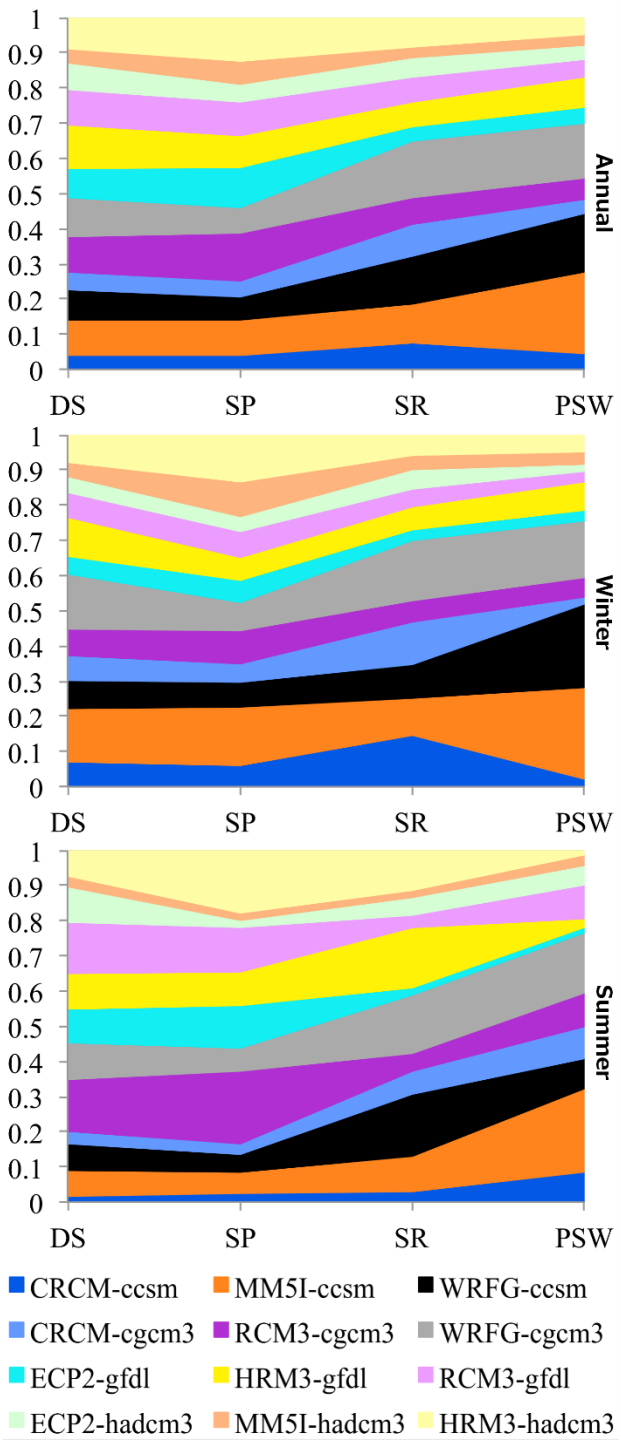

Figure 93 Skill scores for each region (see Table 1 for regions) and GCM-driven simulation. The thickness of a color above a given region indicates the value of the score for the simulation assigned to that color. Since skill scores are relative and must sum to one across all simulations, the thickness of the color over a region for any given simulation illustrates the performance of that simulation in that region relative to the other simulations (thicker is better).

While this exercise has provided useful information on the simulations, we have also found that the skill scores, when applied to the ensemble mean as weights for precipitation and temperature, change the mean by very little (not shown). Additionally, the using the skill scores as weights increase the ensemble mean bias by small amount during the baseline period in some regions/seasons. Therefore, we do not necessarily advocate for their use as weights, but as useful diagnostic tools.

These results will be included in a manuscript that will be submitted in the near future on metrics and weighting and their application to the NARCCAP ensemble (Bukovsky et al. 2016).

Comparison of Downscaling Performance

A number of methods have been implemented to translate coarse GCM climate projections down to the regional and local scale. These range from the simplest delta approach to complex dynamical downscaling methods. With so many diverse methods of downscaling now available, there is a need to perform robust comparisons and evaluations of the different techniques. In this section we explore how the choice of downscaling method may influence the climate change response of important impacts-related variables. Our goal is to identify the uncertainty in future climate change associated with different downscaling methods and investigate the effect of these differences when the resulting climate change information is applied to various impacts areas.

Downscaling Methods

Local climate changes are calculated using four downscaling techniques: the simple delta method, a bias correction method (KDDM), the statistical downscaling model (SDSM), and dynamical downscaling with NARCCAP. The configuration for downscaling comparisons is shown in Figure 94. Four CMIP3 GCMs are directly downscaled using three techniques: dynamical downscaling through NARCCAP, statistical downscaling through the SDSM, and the simple delta method. Then NARCCAP is further downscaled using SDSM, the delta method, and bias correction. Three different scales are considered for downscaling: 50km, 12km, and point or single station data.

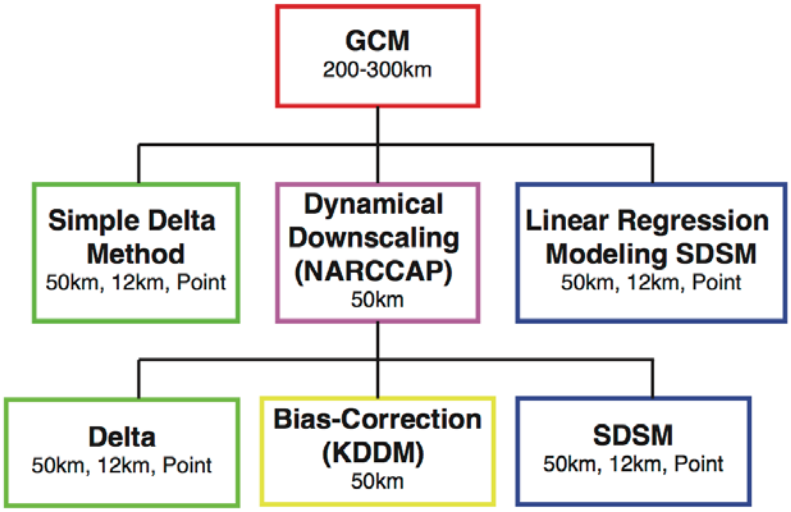

Figure 94 *Flowchart for the downscaling comparisons.*

In all cases the current climate is based on the 1971-2000 time period. Future changes are for mid-century, and extend from 2041-2070.

The simple delta approach is applied by calculating the monthly mean climatology shift in variables such as temperature or precipitation directly from the GCMs. Daily deltas are then calculated by linearly interpolating between months. Daily deltas added to the observed time record and the impacts relevant variables are re-calculated with these results. Hence the final spatial resolution is based on the locations of the station data, not the resolution of the GCMs.

For SDSM, a linear relationship is first found between surface observations of temperature and precipitation and large-scale atmospheric predictor variables from NCEP2. The linear relationship between large-scale predictor and surface predictands is then applied to the current and future GCM output to downscale GCM results. The scale of the downscaling depends on the scale of the observations used to calibrate the linear models.

In NARCCAP 6 regional models are forced with 4 GCMs from CMIP3 to produce dynamically downscaled results at 50km resolution. The NARCCAP results can be further downscaled using the approaches described above. The NARCCAP results have also been bias-corrected using the Kernel Density Distribution Mapping technique (KDDM, McGinnis et al., 2014).

The delta method, SDSM, and KDDM are all calibrated to observations. Since we are considering three different scales to downscale to, 3 different scales of observations are used. Station data is from the Global Summary of the Day archives (GSOD, obtained from the National Center for Environmental Information http://www.ncdc.noaa.gov). Gridded, interpolated observations are from the Maurer gridded meteorological data set (Maurer et al., 2002), which extends from 1949-2010, has a 1/8º resolution and daily output. To generate results at 50km using these methods, we re-gridded the Maurer meteorology using the "Patch" regridding method from the Earth System Modeling Framework (https://www.earthsystemcog.org/projects/esmf/).

Application of Downscaled Climate to Installation Sites

We apply these different climate changes to three impacts areas at the selected SERDP sites: energy demand, fire risk, and heat stress. Note that it was not possible to apply all the downscaling approaches in Figure 1 to all locations/impacts areas.

Energy Demand – US Air Force Academy

As temperatures rise, the demand for heating and cooling of buildings will change. It is expected that the demand to heat buildings will decrease while the demand to cooling buildings will increase.

Heating and cooling degree days (HDD and CDD) are used by engineers to estimate the heating and cooling energy demands for buildings. Both indices measure the difference between outdoor temperatures and temperature that people generally find comfortable indoors. In the United States, this "comfort" temperature is set to 65ºF.

A "degree day" is determined by comparing the daily average outdoor temperature to 65ºF. For example, if the average daily temperature on a particular day is 78ºF. then that day counts as 13 cooling degree days, as a buildings temperature would need to be cooled 13 degrees to reach the 65º "comfort" level. Conversely, if the average daily temperature is 34ºF, then it counts as 31 heating degree days. Both indices are cumulative and can be summed over months, seasons, or years.

In Colorado Springs, at the U.S. Air Force Academy (USAFA), the historical demand for heating buildings is high in winter, spring, and fall (Figure 95, red lines). During summer, there is some demand for cooling buildings (Figure 95, blue lines), but it is considerably lower than the demand for heat. There is some variability across the different scales of observations, however qualitatively they show very similar climatologies of HDD and CDD. Annually, average HDD sum to 7030 while CDD sum to 480.

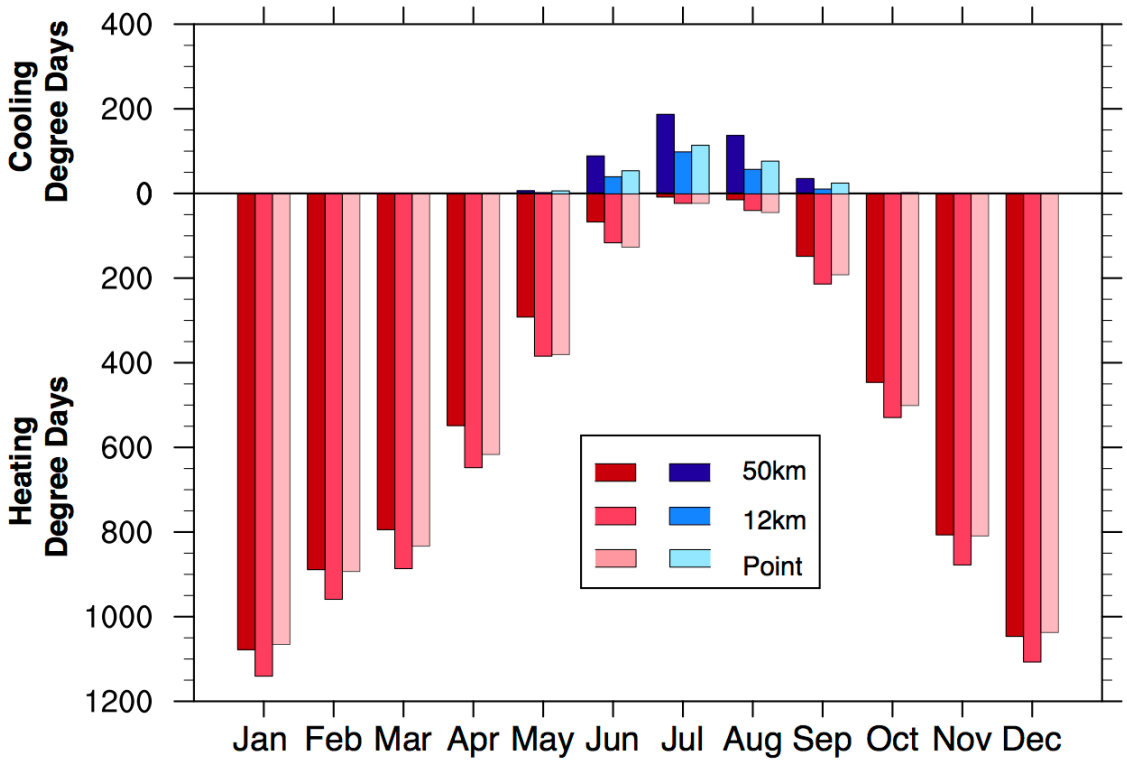

Figure 95 Observed average monthly climatology of heating degree days and cooling degree days for the USAFA based on 1971-2000 time period. Observations are from three different scales, 50km, 12km, and a point (station).

HDD and CDD as calculated by the GCMs used in this study during their current climate period (1971-2000), show some bias at the USAFA compared to observations (Figure 96a). While the overall pattern of the annual cycle of each index is similar in the GCMs, they all overestimate winter, spring, and fall HDD and they overestimate summer CDD. Turning to the future, the GCMs indicate a clear decrease in HDD during all months of the year and an increase in CDD in late spring, summer and early fall (Figure 96b). The increased demand for air conditioning may require a number of buildings to be retrofitted with cooling systems.

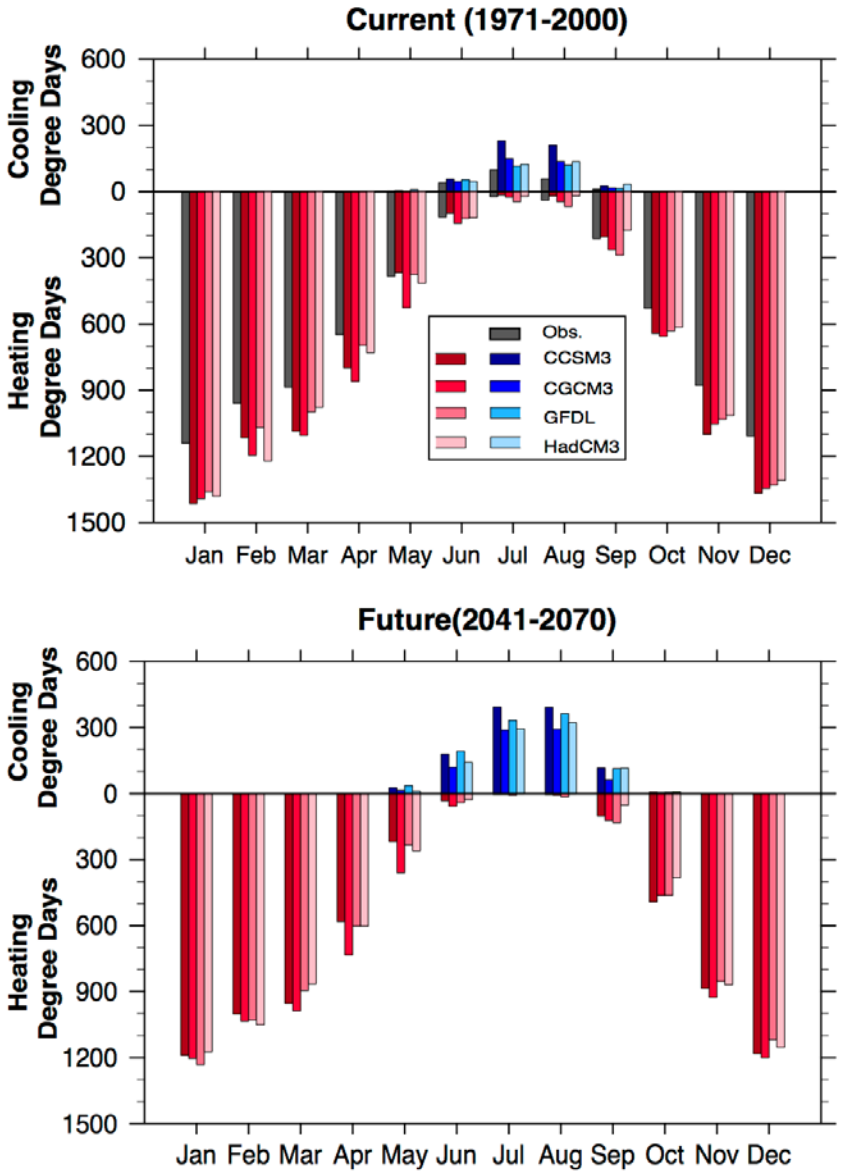

Figure 96 Average monthly climatology of heating degree days and cooling degree days for the USAFA from the 4 GCMs used in this study. Top (a): Current time period (1971-2000), Bottom (b): Future time period (2041-2070). Also shown are the 12km observations. GCM results are from the closest gridbox corresponding to the USAFA station.

The results from Figure 96 show the current and future values for HDD and CDD from the "raw" unchanged GCM output corresponding to the gridbox closest to the USAFA station. These results therefore correspond to a large area covering 150-300km on a side, depending on the GCM. In some cases it is desirable to get climate change information on a higher-resolution scale. Following the schematic of Figure 1, we have downscaled the GCM output in multiple ways, down to 50km, 12km, and a single point. The NARCCAP models are further downscaled using bias correction and the simple delta method.

Figure 97 shows the projected change in annual total CDD from the raw GCMs and the downscaling methods explored in this study. It is immediately clear from the figure that downscaling changes the uncertainty in future changes in CDD, however all methods, including the raw GCMs, show an increase in CDD by mid century. Taken alone, the raw GCMs show an increase in annual CDD ranging from 400-750, with two models showing an increase of about 575. Taken together, at the 50km scale, including all of the downscaling methods, the annual increase in CDD at the USAFA is projected to be between 0 and 900, with a median value of 430. One might expect that the downscaled results would be bounded by the GCM results, or at least centered about the GCM results, but this is not the case. For example, the delta method shifts the increase in CDD up to 500-900. SDSM contracts the increase in CDD spanning from 330-530. The NARCCAP models (which are fundamentally different than the other two methods), dramatically changes the mean and spread of the increase in CDD. The raw NARCCAP models show an expanded range in the increase in CDD from 100-620, with model results evenly spread-out through this range. Applying the delta method to the NARCCAP models, results in two regimes, some models exhibit very little change in CDD and others showing much larger increases in CDD. When the bias is accounted for in the NARCCAP models, the distribution of the change in CDD also contracts.

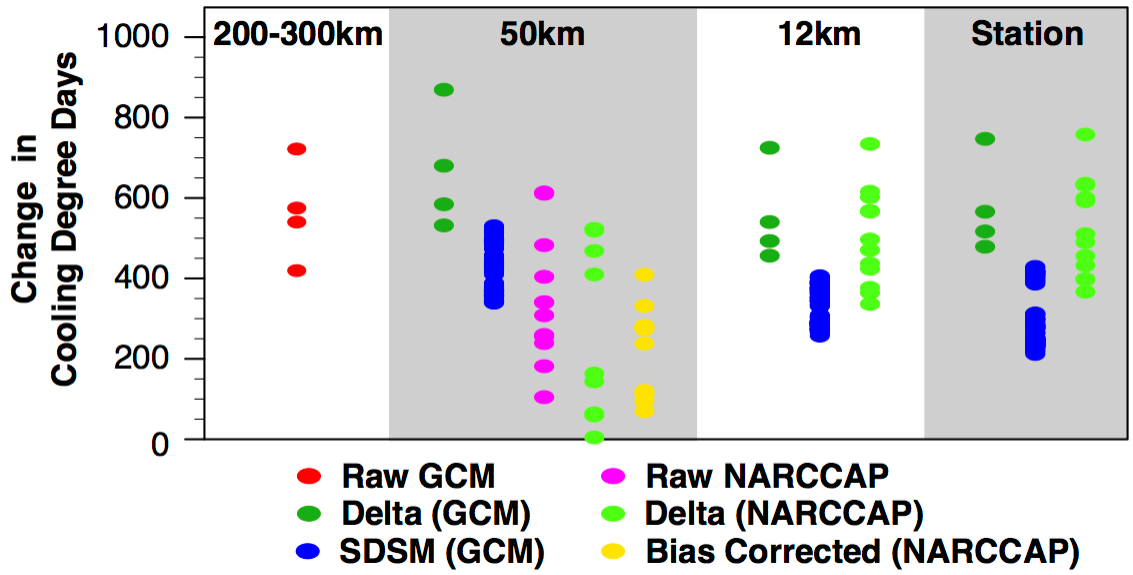

Figure 97 Change in annual total cooling degree days for USAFA based on GCM results and multiple downscaling methods attempting to get local-scale climate change results. Local scale in this case covers 50km, 12km, and point (station) results.

Fire Risk- Fort Hood

Persistent hot, dry conditions will increase the risk for wildfires. The Keetch-Byram Drought Index (KBDI) is used to examine future changes in the risk for wildfires at Fort Hood Texas. The KBDI index combines rainfall and maximum temperature to estimate how dry forested areas are and their risk for wild fires (Keetch and Byram, 1968). Table 42 outlines the fire risk thresholds based on the KBDI index and the description of the forest dryness. When the KBDI exceeds 600, wild fire risk is high. This index serves as a proxy for expert judgment and specific

knowledge of fuel moisture. It helps forest managers make decisions about prescribed burning, and where to locate important forest fire fighting resources.

Table 42 Fire-risk categories based on the KBDI index and thresholds.

Fire Risk	KBDI Threshold	Description
Low	0-200	Soil moisture and large class fuel moistures are high and do not contribute much to fire intensity
Moderate	200-400	Lower litter and duff layers are drying and beginning to contribute to fire intensity
High	400-600	Lower litter and duff layers contribute to fire intensity and will actively burn
Extreme	**600-800**	**Intense, deep burning possible**

Figure 98 shows the mean change in the KBDI as well as the change in the number of days per year where the KBDI is projected to exceed 600 from 4 downscaled products; the raw NARCCAP models, the delta method from NARCCAP applied to observations, bias-corrected NARCCAP using the KDDM method, and the 4 driving GCMs downscaled using SDSM. (Other comparisons at different scales (e.g., 12 km) are yet to be completed).

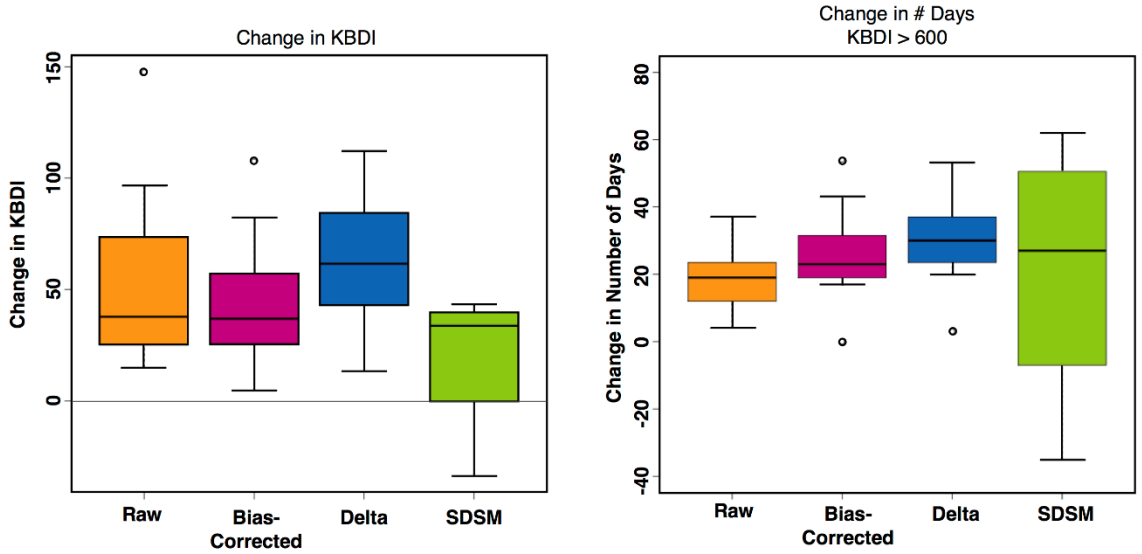

Figure 98 Change in annual mean KBDI values (left) and change in the number of days where KBDI > 600 (right) from 4 downscaling methods at the 50km scale for Fort Hood, Texas. The 4 downscaling methods shown are from the raw NARCCAP results, bias-corrected NARCCAP, and the delta method applied to Maurer from NARCCAP. Directly downscaled GCM results using SDSM are also shown.

The Raw, Bias-Corrected, and Delta method NARCCAP results all show increases in the mean KBDI ranging from ~10-150. Median values across these products range from increases in the KBDI from 35-65. The results from SDSM, on the other hand, show a different story. While

many of the results from SDSM show small increases in the mean KBDI, some downscaled results show the mean KBDI decreasing.

Mean changes in the KBDI value have important implications for changes in the number of days where KBDI>600 and the risk for wild fires is high. The raw, bias-corrected, and delta NARCCAP results show that the number of days where KBDI>600 is projected to increase. While the spread varies across each product, the median value is similar between the three – ranging from a 20-30 day increase in extreme wild fire risk days by mid-century. Again, the SDSM results tell a different story. While the median change is similar to the other methods, the spread is much larger in SDSM than the others, with some results suggesting that extreme wild fire risk days may actually decrease.

In the case of CDD, which only considers temperature, there was considerable spread across the different downscaling methods, but overall, the sign of the change was always positive. In the case of KBDI, which uses both temperature and precipitation in its calculations, the range of possible changes in values coming from SDSM, which are both positive and negative, might make future decisions more uncertain and thus perhaps more difficult. It is important to investigate why these changes occur, particularly when model simulations give such different and varied results.

Figure 99 shows the mean changes in maximum temperature and % change in precipitation from the individual models categorized by the downscaling method. By looking at this figure we see that the SDSM model results driven by the CCSM3 global model, exhibit large increases (up to 150%) in precipitation. Note also that the temperature changes are the smallest. In the SDSM model, this increase in precipitation is largely driven by increases in specific humidity. Analysis of the CCSM3 global model in Bukovsky et al. 2013 and 2015 demonstrate that the humidity field in CCSM3 may be suspect and not credible. Based on our expert judgment we might suggest that the SDSM CCSM3 results not be used for actual decision- making regarding future fire risk.

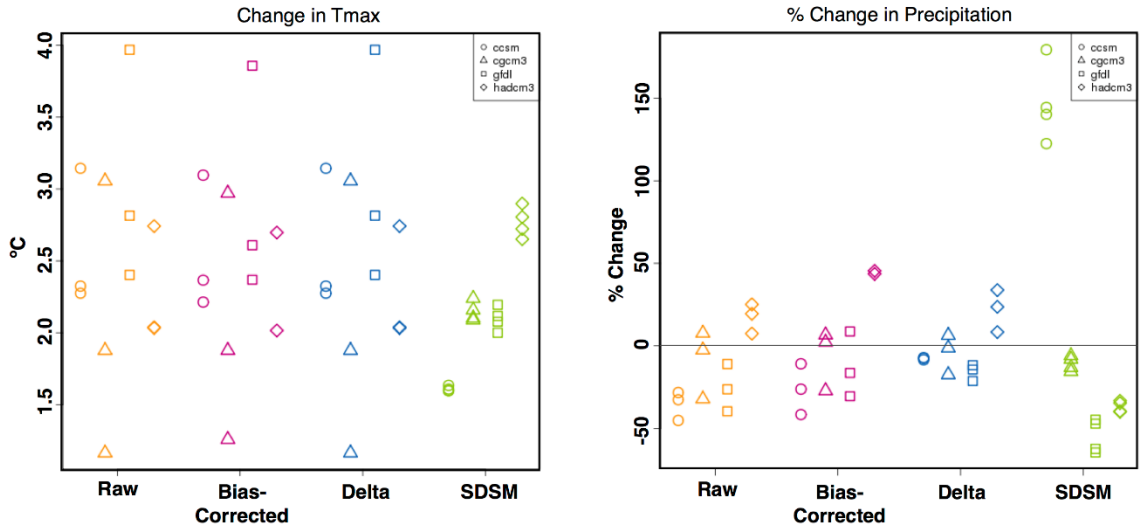

Figure 99 Change in annual maximum temperature (left) and % change in precipitation (right) from the individual models for each downscaling method at Fort Hood Texas. Under each downscaling method, the results are separated by the driving GCM (shape of marker).

Heat Stress and Training – Fort Benning

Increasing temperatures are expected to bring along with them, increases in the incidents of heat stress. Personnel exposed to extreme heat or working in hot environments may be at risk of heat stress. Exposure to extreme heat can result in occupational illnesses and injuries. Heat stress can result in heat stroke, heat exhaustion, heat cramps, or heat rashes.

The military uses the wet blub globe temperature (WBGT) as a way to identify environmental conditions under which individuals are likely to experience heat stress effects and for implementing protective controls to prevent heat related injuries. The WBGT is a weighted average of the wet bulb (Tw), dry bulb (Ta), and black globe (Tg) temperatures and is calculated as follows (Yaglou and Minard 1957):

$$WBGT = 0.7Tw+0.2Tg+0.1Ta$$

Unlike other measures of heat stress, the WBGT is designed to include not only the impacts of temperature and humidity, but also the influence of wind speed and the intensity of the sun. The multiplicity of variables involved limits some of the comparisons we can make because of limited data from the GCMs. Figure 100 shows the U.S. Army work-rest-water guidelines including the heat category determined by the WBGT. The military restricts outdoor activity based on the WBGT setting thresholds at different “flag” days. Where Red and Black flag days are the most severe and restrict outdoor activity significantly.

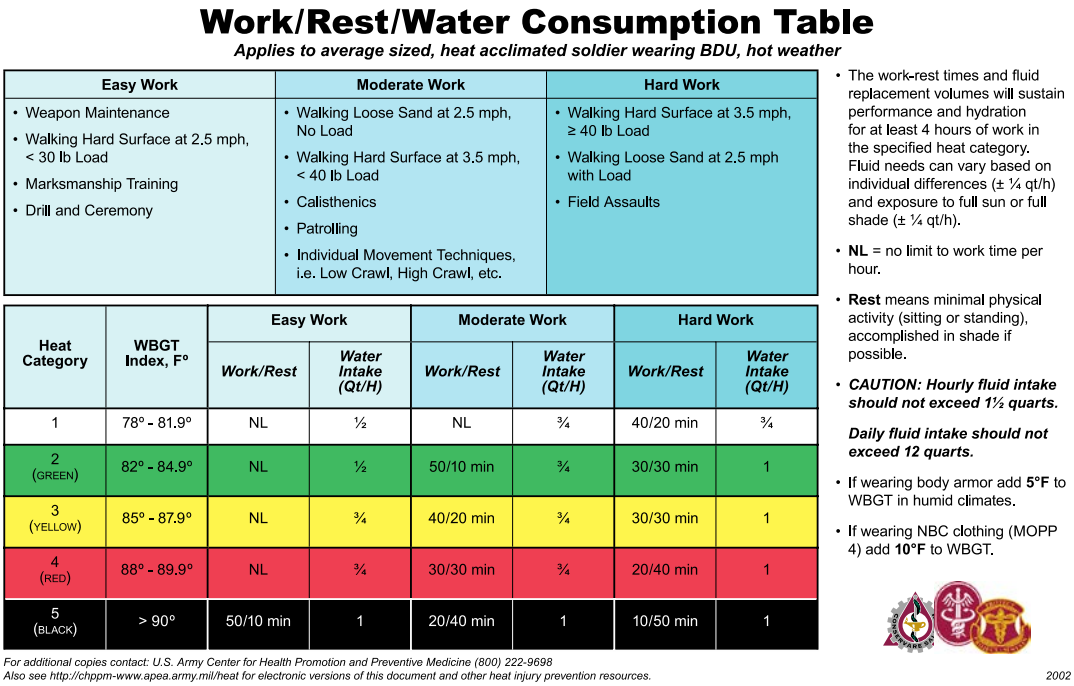

Work/Rest/Water Consumption Table

Applies to average sized, heat acclimated soldier wearing BDU, hot weather

Easy Work	Moderate Work	Hard Work
• Weapon Maintenance • Walking Hard Surface at 2.5 mph, < 30 lb Load • Marksmanship Training • Drill and Ceremony	• Walking Loose Sand at 2.5 mph, No Load • Walking Hard Surface at 3.5 mph, < 40 lb Load • Calisthenics • Patrolling • Individual Movement Techniques, i.e. Low Crawl, High Crawl, etc.	• Walking Hard Surface at 3.5 mph, ≥ 40 lb Load • Walking Loose Sand at 2.5 mph with Load • Field Assaults

Heat Category	WBGT Index, F°	Easy Work		Moderate Work		Hard Work	
		Work/Rest	*Water Intake (Qt/H)*	*Work/Rest*	*Water Intake (Qt/H)*	*Work/Rest*	*Water Intake (Qt/H)*
1	78° - 81.9°	NL	½	NL	¾	40/20 min	¾
2 (GREEN)	82° - 84.9°	NL	½	50/10 min	¾	30/30 min	1
3 (YELLOW)	85° - 87.9°	NL	¾	40/20 min	¾	30/30 min	1
4 (RED)	88° - 89.9°	NL	¾	30/30 min	¾	20/40 min	1
5 (BLACK)	> 90°	50/10 min	1	20/40 min	1	10/50 min	1

- The work-rest times and fluid replacement volumes will sustain performance and hydration for at least 4 hours of work in the specified heat category. Fluid needs can vary based on individual differences (± ¼ qt/h) and exposure to full sun or full shade (± ¼ qt/h).
- **NL** = no limit to work time per hour.
- **Rest** means minimal physical activity (sitting or standing), accomplished in shade if possible.
- ***CAUTION: Hourly fluid intake should not exceed 1½ quarts.***

  Daily fluid intake should not exceed 12 quarts.
- If wearing body armor add **5°F** to WBGT in humid climates.
- If wearing NBC clothing (MOPP 4) add **10°F** to WBGT.

For additional copies contact: U.S. Army Center for Health Promotion and Preventive Medicine (800) 222-9698
Also see http://chppm-www.apea.army.mil/heat for electronic versions of this document and other heat injury prevention resources.

2002

Figure 100 WBGT Flag Day work-rest-water guidelines for the Army.

Given that calculations of the WBGT requires inputs of temperature, humidity, winds and radiation, we use the high resolution North American Regional Reanalysis (NARR) to examine the observed frequency of WBGT Flag Day restrictions for Fort Benning, Georgia. Between 1979-2010 the area around Fort Benning experienced an average of 63 days with green flag restrictions, 45 days Yellow flag restrictions, 8 days with red flag restrictions and 8 days with black flag restrictions. These results are highlighted in Table 43.

Table 43 Frequency of flag- day restrictions based on NARR data for Fort Benning Georgia. Climatological results based on the 1979-2010 time period.

Flag Category	***WBGT Threshold***	***Number of Days***
White	*Below 80ºF*	***241***
Green	*80-84.9ºF*	***63***
Yellow	*85-87.9ºF*	***45***
Red	*88-89.9ºF*	***8***
Black	*Above 90ºF*	***8***

Based on the raw NARCCAP results the WBGT is projected to increase by 3-4.2 º F annually, and 3.6-5.3 ºF during the hot summer months (Figure 101). Increases in the WBGT will have important implications for the frequency of occurrence of flag day restrictions, to help prevent heat stroke in workers and trainees.

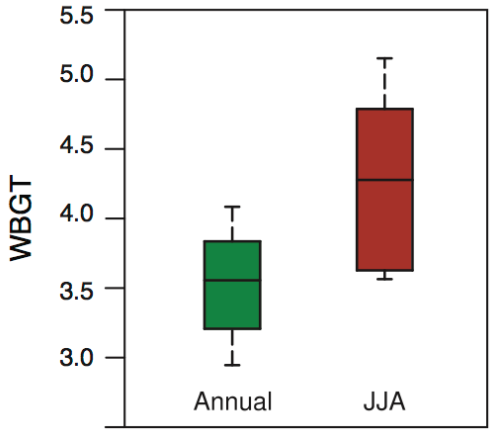

Figure 101 Mean change in WBGT by mid-century for Fort Benning, Georgia based on 11 NARCCAP models.

Figure 102a shows the projected changes in the frequency of heat related flag day restrictions based on the raw NARCCAP models. The uncertainty associated with these changes based on the raw NARCCAP models is quite large, especially for the most severe black flag day restrictions, with some models showing little to no change and others showing increases of 45 extremely hot days per year.

Investigation into the WBGT and Flag Day restrictions suggests that these threshold indices are sensitive to small changes in mean temperature. Model bias in the current climate time period may be playing a large role in the significant spread found in the change in flag-day frequency. To explore the role that model bias may play, we also apply changes in the WBGT to the NARR data from Fort Benning. This is essentially using the delta method, but on WBGT directly. In this case, the climatological shift in WBGT is applied to the WBGT time series calculated from NARR. Figure 102b shows the projected changes in the frequency of each flag-day category using the delta method approach. Here we see that the projected changes in each flag-day category are much narrower. With the largest increases found in the yellow flag-day category and smaller, much more manageable increases found in the black and red flag-day categories.

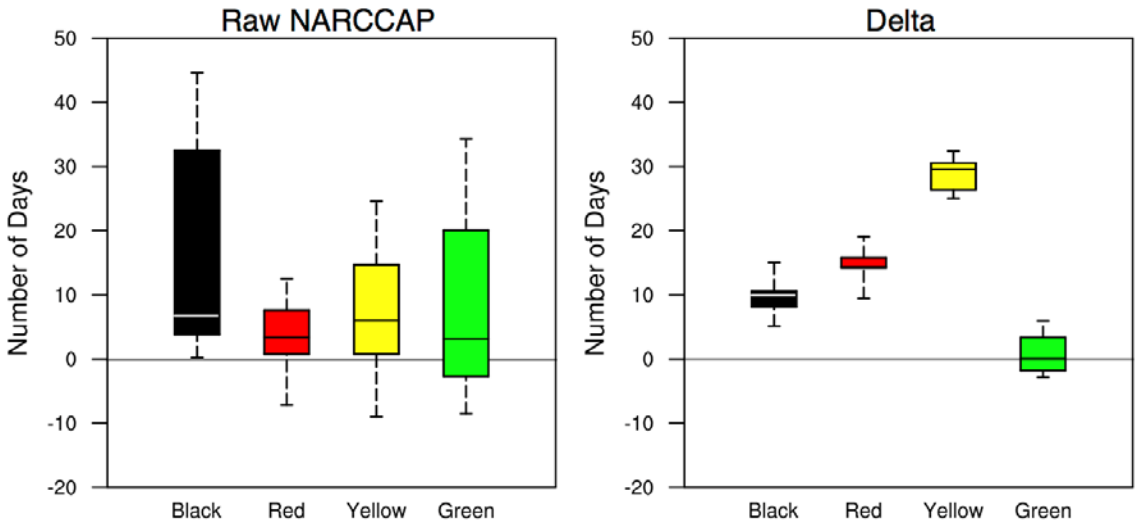

Figure 102 Change in the frequency of heat related flag-day restrictions from the raw NARCCAP models (a, left) and the delta approach applied to NARR (b, right).

Further investigation into model bias and the credibility of the delta method is being performed to help identify if one method may be more reliable, and better for planning purposes than the other.

Conditional Uncertainty Estimation

We explored a unique approach to development of a Bayesian joint probabilistic model (for temperature and precipitation) by forming the prior based on climate change results from the four GCMs that were used to drive the six RCMs. To our knowledge this is the first time such an approach to formation of a prior has been taken.
The basic joint Bayesian probabilistic model follows the work of Tebaldi and Sanso (2009).

Model

Likelihood

The temperature/precipitation changes (x) are assumed to follow a Gaussian distribution with mean μ and covariance Σ:

$$x_1,\ldots, x_n \sim N(\mu,\Sigma)$$

Prior

The prior for Σ is assumed to be an inverse-Wishart distribution that depends on GCM covariance and a parameter ν:

$$\Sigma \sim IW_n(\Lambda^{-1})$$

The prior for μ (conditional on Σ) is assumed to be Gaussian and depends on the GCM mean and a parameter κ:
$\mu|\Sigma \sim N(\mu_{GCM}, \Sigma/k)$

Note that parameters n and k control the influence of the prior.

Marginal posterior

The marginal posterior for μ is a multivariate t distribution. The mean is a weighted average between RCM ensemble mean and GCM prior mean:

$\kappa/(\kappa+n)\mu_{GCM} + n/(\kappa+n)\mu_{RCM}$

Covariance dominated by RCM covariance and prior covariance, also weighted. Can be driven to zero.

Posterior predictive distribution (PPD)

Posterior predictive distribution (PPD) for a "new" RCM is also a multivariate t distribution. The mean is a weighted average between RCM ensemble mean and GCM prior mean. The covariance is dominated by the RCM covariance and prior covariance, also weighted. It is limited by variance of the RCM ensemble. The weights are controlled by ν and κ.

We explored several different means of formulating the prior:

- The driving GCMs are used to compute the prior mean
- The prior GCMs can be used to compute the prior variance, but this is limited by the very small sample size. An alternative choice for the prior covariance is to use the full suite of GCMs from the CMIP3 data, from which the 4 driving GCMs came.

Joint Predictive Probability Distributions

We applied these models on the scale of the Bukovsky regions, for several regions. However, the main region we are concerned with regarding application to water resources is the southern Rockies. We present joint distributions for the different cases for forming the prior.

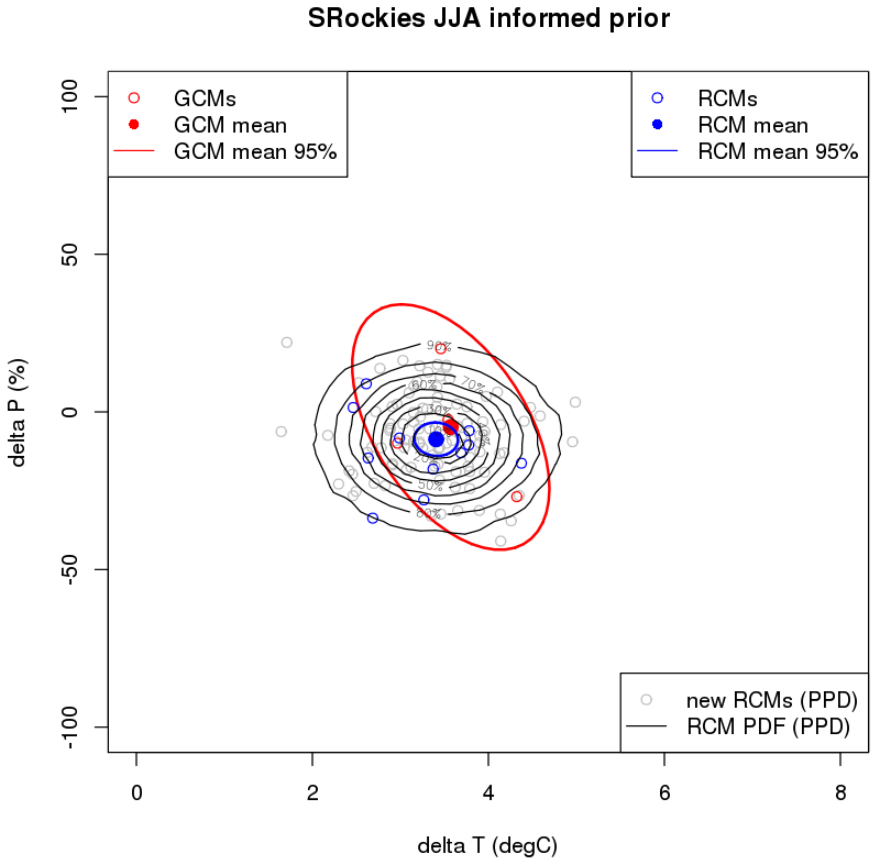

Figure 103 Joint predictive probability distribution (PPD) formed using the informed prior.

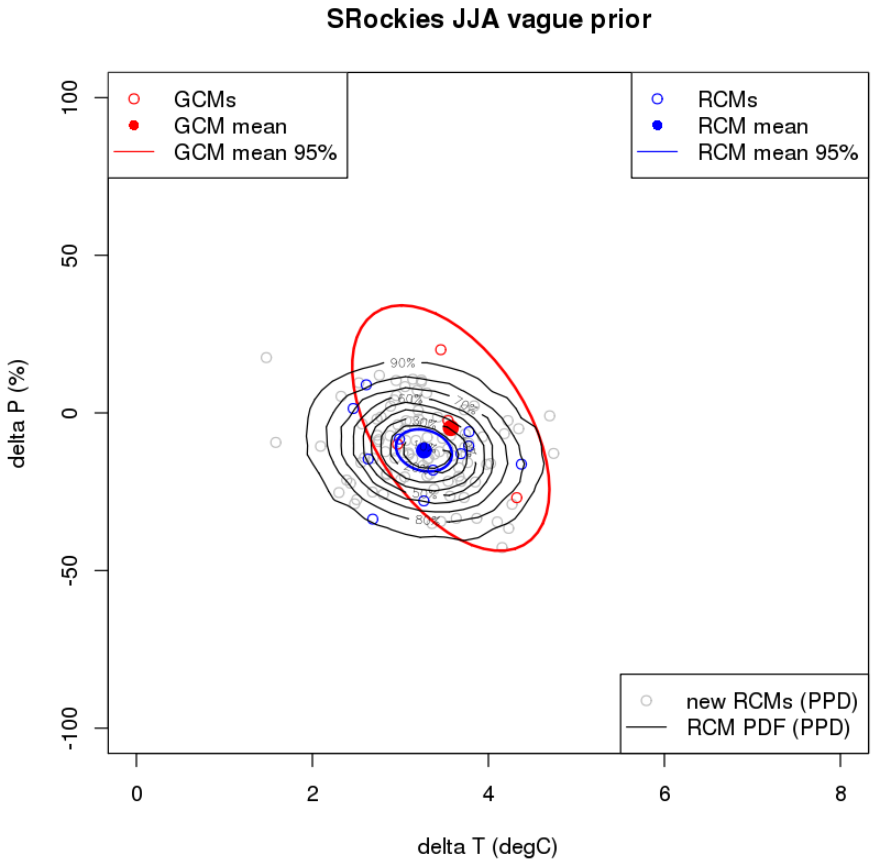

Figure 104 Joint PPD formed using an uninformed or vague prior.

Figure 103 and Figure 104 compare joint distributions for summer for the southern Rocky Mountain Region. Note that the joint distribution with the informed prior (Figure 103) is shifted to the right along the x-axis, indicating that the temperatures are a bit higher; and the distribution is shifted a bit higher along the y-axis.

In considering the use of the full CMIP3 suite of GCMs to form the covariance of the prior, we see in Figure 105 a somewhat different orientation of the distribution, and the ellipse is elongated. The use of the full CMIP3 suite for the covariance may be sensible, since the 4 GCMs used to drive the RCMs fall in the center of the distribution of the GCMs from the point of view of the Equilibrium Climate Sensitivity (ECS).

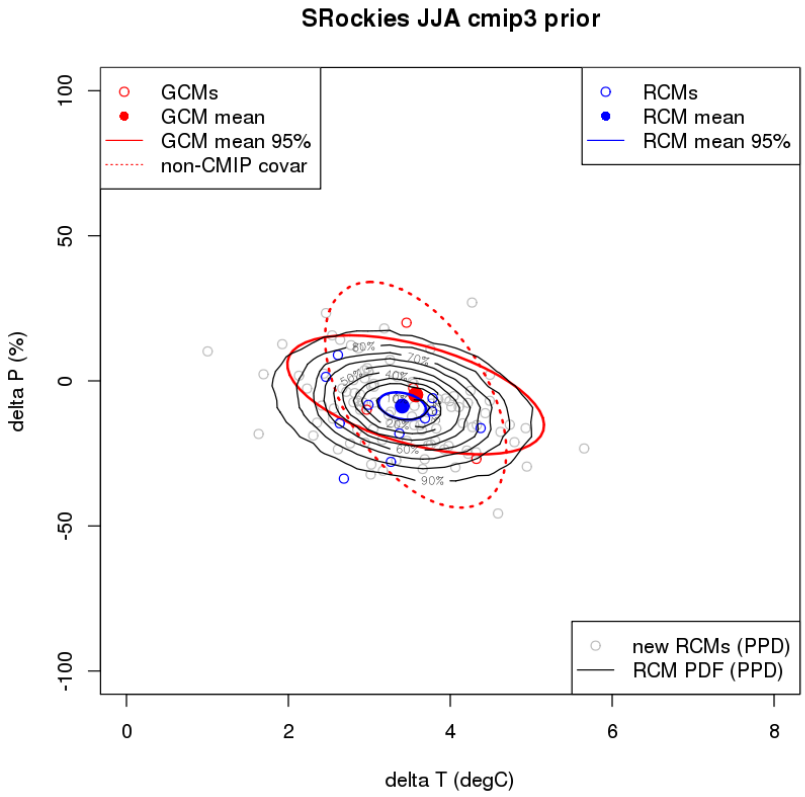

Figure 105 Joint Predictive Probability Distribution (PPD) using the full CMIP3 suite of climate change results to form the prior co-variance

Application to the Colorado Springs Utility (CSU) Water System

Two different water resource system models were used to formulate a water resource vulnerability assessment: The Water Evaluation and Planning System (WEAP) and a Decision Support System (MODSIM-DSS) model. These were used to model the hydrologic response, reservoir operations, withdrawals, and trans-mountain diversions of the water resources system located on both sides of the (continental) divide. For a particular climate sequence, the system is considered to perform adequately if indoor water demands are met for the entire simulation. The vulnerability assessment was constructed by systematically testing the CSU system performance over a wide range of annual mean climate changes to determine under what conditions the system no longer performs adequately. Alternative climate sequences with different mean temperature and precipitation conditions were developed using a daily stochastic weather generator. Changes to the precipitation mean ranged from -10% to +10% of the historic mean, while temperature shifts ranged from approximately -1°C to +4°C. For our case, ranges were extrapolated further for precipitation (to – 20%). Note that in the application to the CSU joint distributions were formulated for annual mean changes in precipitation and temperature, not seasonal ones. A similar vulnerability assessment was used in Steinschneider et al. (2015) to determine the effect of removing correlations among GCMs in the CMIP5 suite of models on the formation of PPDs when applied to a water resources future assessment.

There is an important difference in the percentage of the distribution(s) that fall in the unreliable zone based on which distribution is used. A smaller amount of the distribution falls into the unreliable category when the informed prior is used (Figure 106).

We plan to approach the water managers of CSU to determine if the differences in distributions is meaningful from a water management point of view.

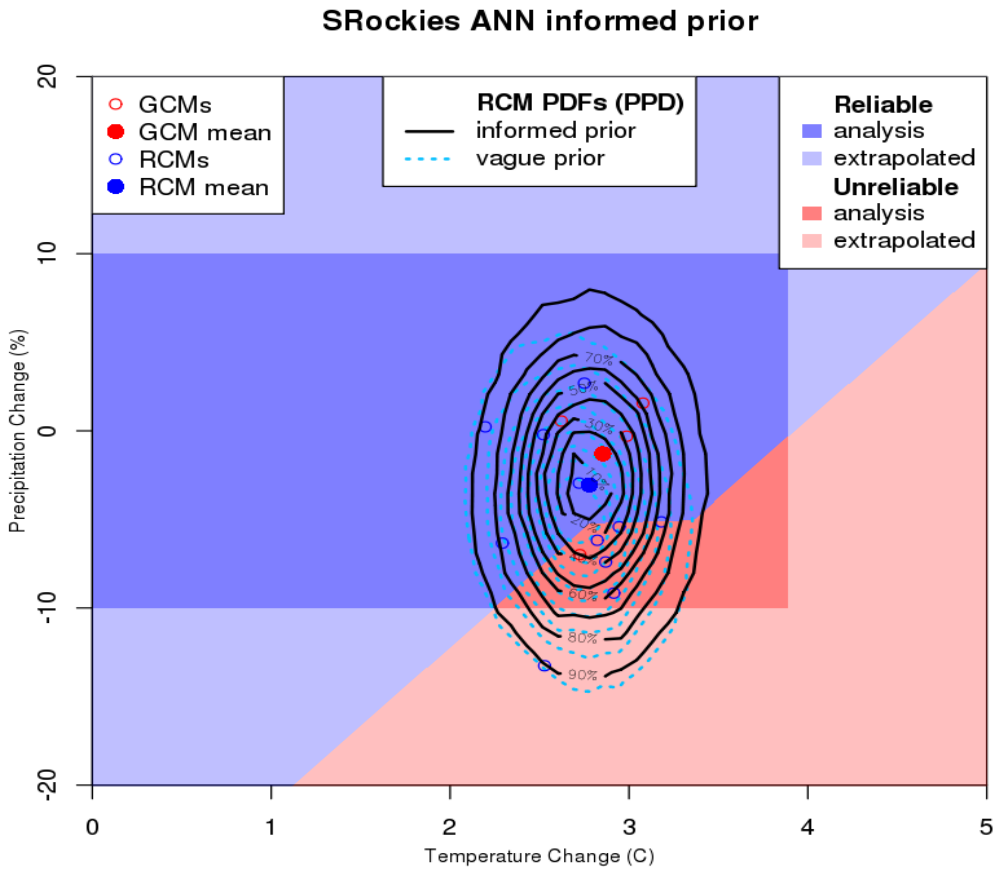

Figure 106 Differences in the reliability of the water resource system based on different joint PPDs. Using the informed prior, the percentage unreliable is 26%, whereas using the vague prior the percentage is 35%.

Literature Cited

AECOM, Maddaus Water Management, R2T Inc., 2009. Water Supply and Water Conservation Management Plan. Metropolitan North Georgia Water Planning District.

AghaKouchak, A., L. Cheng, O. Mazdiyasni, and A. Farahmand (2014), Global warming and changes in risk of concurrent climate extremes: Insights from the 2014 California drought, *Geophys. Res. Lett., 41*, 8847-8852.

Ajami, N. K., H. Gupta, T. Wagener, and S. Sorooshian (2004), Calibration of a semi-distributed hydrologic model for streamflow estimation along a river system, *Journal of Hydrology, 298*, 112-135.

Alexander, M.E., 1990: Computer Calculation of the Keetch-Byram Drought Index. *Canadian Forest Service Fire Management Notes*. Canadian Forest Service. Vol. 51 (4), pp 23-25.

Allen, R. G., Pereira, L. S., Raes, D., Smith, M., 1998. Crop evapotranspiration-guidelines for computing crop water requirements-FAO irrigation and drainage paper 56. FAO, Rome, 300, 6541.

Alley, W. M., 1984. On the treatment of evapotranspiration, soil moisture accounting, and aquifer recharge in monthly water balance models. Water Resources Research 20(8), 1137-1149.

Anderson, E. A. (1976). A point energy and mass balance model of a snow cover, NOAA Tech. Rep. NSW 19, 150 pp., Natl. Oceanic and Atmos. Admin., Silver Spring, MD.

Andreadis, K. M., & Lettenmaier, D. P. (2006). Assimilating remotely sensed snow observations into a macroscale hydrology model. *Advances in Water Resources*, *29*(6), 872–886. http://doi.org/10.1016/j.advwatres.2005.08.004

Apipattanavis, S., G. Podesta, B. Rajagopalan, and R. W. Katz (2007), A semiparametric multivariate and multisite weather generator, *Water Resour. Res.*, *43*, W11401, doi:10.1029/2006WR005714.

Arnell, N. W. & Delaney, E. K. Adapting to climate change: public water supply in England and Wales. Clim. Change 78, 227-255 (2006).

ASHRAE, 2010, *ANSI/ASHRAE/USGBC/IES Standard 189.1, Standard for the Design of High-Performance,Green Buildings Except Low-Rise Residential Buildings*. Atlanta: American Society of Heating, Air-Conditioning and Refrigeration Engineers, Inc.

ASHRAE, 2013, *Service Life and Maintenance Cost Database*, http://xp20.ashrae.org/publicdatabase/default.

Atlanta Regional Commission (ARC), 2009. Regional Snapshot.

Atlanta Regional Commission (ARC), 2011. Regional Snapshot.

Barnett, T.P., J.C. Adam, and D.P. Lettenmaier (2005), Potential impacts of a warming climate on water availability in snow-dominated regions, Nature, 438, 303-309, doi:10.1038/nature04141.

Beven, J. K. (2012), *Rainfall-Runoff Modelling: The Primer*, 2nd ed., Wiley-Blackwell, Chichester.

Bishop, C., and G. Abramowitz, Climate model dependence and the replicate Earth paradigm, Climate Dynamics, 41(3-4), 885-900, (2013).

Bolten, J. D., C. Lee, and P. Houser (2015), Satellite data for water resources management, Eos, 96, doi:10.1029/2015EO035971.

Boyle, D.P., H.V., Gupta, S., Sorooshian, V., Koren, Z., Zhang, and M., Smith, 2001. Toward improved streamflow forecast: value of semidistributed modeling, Water Resources Research, 37(11), 2749-2759.

Brazos G Regional Water Planning Group (BGRWPG). The 2011 Brazos G Regional Water Plan, Volume I – Executive Summary and Regional Water Plan, September 2010

Brekke, L. D. et al. Assessing reservoir operations risk under climate change. Water Resour. Res. 45 (2009).

Brown, C. and R. L. Wilby (2012), An alternate approach to assessing climate risks
, *EOS, Transactions, American Geophysical Union*, *92*, 401-412.

Brown, C. M., J. R. Lund, X. Cai, P. M. Reed, E. A. Zagona, A. Ostfeld, J. Hall, G. W. Characklis, W. Yu, and L. Brekke (2015), The future of water resources systems analysis: Toward a scientific framework for sustainable water management, *Water Resour. Res.*, *51*, 6110-6124.

Brown, C., Ghile, Y., Laverty, M. & Li, K. Decision scaling: Linking bottom-up vulnerability analysis with climate projections in the water sector. Water Resour. Res. 48 (2012).

Bukovsky, M.S., J. Thompson, and L. O. Mearns, 2015: The effect of weighting on the NARCCAP ensemble mean. Clim. Res., to be submitted 2016.

Bukovsky, M. S., 2011: Masks for the Bukovsky regionalization of North America. Regional Integrated Sciences Collective, Institute for Mathematics Applied to Geosciences, National Center for Atmospheric Research. doi:www.narccap.ucar.edu/contrib/bukovsky/.

Bukovsky, M. S., 2012: Temperature trends in the NARCCAP regional climate models. J. Climate, 25, 3985-3991.

Bukovsky, Melissa S., Carlos M. Carrillo, David J. Gochis, Dorit M. Hammerling, Rachel R. McCrary, Linda O. Mearns, 2015: Toward Assessing NARCCAP Regional Climate Model Credibility for the North American Monsoon: Future Climate Simulations. *J. Climate* **28**:17, 6707-6728.

Bukovsky, Melissa S., David J. Gochis, and Linda O. Mearns, 2013: Towards Assessing NARCCAP Regional Climate Model Credibility for the North American Monsoon: Current Climate Simulations. *J. Climate*, **26**, 8802–8826.

California Department of Fish and Wildlife (2014), CDFW moves to prevent fish loss, evacuates fish at American River and Nimbus Hatcheries, *California Department of Fish and Wildlife, 16 June*, Available at http://cdfgnews.wordpress.com/2014/06/16/cdfw-movesto-prevent-fish-loss-evacuates-fish-at-american-river-and-nimbus-hatcheries.

California Department of Water Resources (2013), California Water Plan 2013: Investing in Innovation and Infrastructure, *Bulletin 160-13, 3 - Resource Management Strategies*, 1-858.

California Department of Water Resources (2015), California's most significant droughts: comparing historical and recent conditions, *California Department of Water Resources*.

California Department of Water Resources and United States Bureau of Reclamation (2011), *CalLite: Central Valley Water Management Screening Model (Version 2.0) Reference Manual*, vol. October 2011, 161 pp., California Department of Water Resources, Sacramento, California.

Case, 2014, Case, M.P., Liesen, R., Zhivov, A., Stinson, J. "A Computational Framework for Low Energy Community Analysis and Optimization, *ASHRAE Transactions*, to appear.

Cayan, D. R., S. A. Kammerdiener, M. D. Dettinger, J. M. Caprio, and D. H. Peterson (2001), Changes in the onset of spring in the western United States, *Bull. Am. Meteorol. Soc.*, *82*, 399-415.

Cayan, D. R., T. Das, D. W. Pierce, T. P. Barnett, M. Tyree, and A. Gershunov (2010), Future Dryness in the Southwest US and the Hydrology of the Early 21st Century Drought, *Proceedings of the National Academy of Sciences of the United States of America, 107*, 21271-21276.

Charnes, A. and W. W. Cooper (1961), *Management Models and Industrial Applications of Linear Programming*, Wiley, New York.

Christensen, J. H., E. Kjellström, F. Giorgi, G. Lenderink, and M. Rummukainen, 2010: Weight assessment in regional climate models. Clim. Res., 44, 179–194.

Christierson, B. v., Vidal, J. & Wade, S. D. Using UKCP09 probabilistic climate information for UK water resource planning. Journal of Hydrology 424, 48-67 (2012).

Connell-Buck, C. R., J. Medellin-Azuara, J. R. Lund, and K. Madani (2011), Adapting California's water system to warm vs. dry climates, *Clim. Change, 109*, 133-149.

Connell-Buck, C. R., J. Medellín-Azuara, J. R. Lund, K. Madani (2011), Adapting California's Water System to Warm vs. Dry Climates. Climatic Change 109 (Suppl 1), S133–149.

Crane. W.J.B. 1982. Computing grassland and forest fire behaviour relative humidity and drought index by pocket calculator. Australian Forestry. 45(:1): 89-97.

Crawley, 2001, Crawley, D., L. Lawrie, F. Winkelmann, W. Buhl, Y. Huang, C. Pedersen, R. Strand, R. Liesen, D. Fisher, M. Witte, and J. Glazer. 2001. EnergyPlus: Creating a new-generation building energy simulation program. *Energy and Buildings* 33:319-331

Davies-Jones, R., 2008: An Efficient and Accurate Method for Computing the Wet-Bulb Temperature along Pseudoadiabats. *Mon. Wea. Rev.*, **136**, 2764–2785. doi: http://dx.doi.org/10.1175/2007MWR2224.1

Deb, K., Pratap, A., Agarwal, S., & Meyarivan, T. (2002). A fast and elitist multiobjective genetic algorithm: NSGA-II. *IEEE Transactions on Evolutionary Computation*, *6*(2), 182–197. http://doi.org/10.1109/4235.996017

Department of Water Resources (2014a), Water year 2014 ends as 3rd driest in precipitation, *California Department of Water Resources*, Available at http://www.water.ca.gov/waterconditions/.

Department of Water Resources (2014b), Year's final snow survey comes up dry, *California Department of Water Resources, 1 May*, Available at http://www.water.ca.gov/news/newsreleases/2014/050114.pdf.

Dept. of the Army, 2003: Heat Stress Control and Heat Casualty Management. *Army Technical Bulletin Medical 507*. Dept of the Army Headq., Washington DC, 65 pp.

Dessai, S. and M. Hulme (2004), Does climate adaptation policy need probabilities?, *Climate Policy, 4*, 107-128.

Dettinger, M. D. and D. R. Cayan (2014), Drought and the California Delta - A Matter of Extremes, *San Francisco Estuary and Watershed Science, 12*, 1-6.

Diffenbaugh, N. S., D. L. Swain, and D. Touma (2015), Anthropogenic warming has increased drought risk in California, *Proc. Natl. Acad. Sci. U. S. A., 112*, 3931-3936.

Dimiceli, V. E, S. F. Piltz, S. A. Amburn, 2011: Estimation of black globe temperature for calculation of the wet bulb temperature index. Proc. World Congress on Engineering and Comp. Sci. 2011. San Francisco, CA.

DoD, 2008, Report of *the Defense Science Board Task Force on DoD Energy Strategy*, February, 2008.

DoD, 2012, DoD *Policy and Responsibilities for Critical Infrastructure, Department of Defense Directive*, 3020.40 (change 2), September 21, 2012.

doi: http://dx.doi.org/10.1175/JCLI-D-12-00538.1

Draper, A. J., A. Munevar, S. K. Arora, E. Reyes, N. L. Parker, F. I. Chung, and L. E. Peterson (2004), CalSim: Generalized model for reservoir system analysis, *Journal of Water Resources Planning and Management-Asce, 130*, 480-489.

Duan, Q., Sorooshian, S., Gupta, V., 1992. Effective and efficient global optimization for conceptual rainfall-runoff models. Water Resources Research 28(4), 1015-1031.

Duethmann, D., Peters, J., Blume, T., Vorogushyn, S., & Guntner, A. (2014). The value of satellite-derived snow cover images for calibrating a hydrological model in snow-dominated catchments in Central Asia. *Water Resources Research*, 2002–2021. http://doi.org/10.1002/2013WR014382.Received

DUSD (I&E), 2012, Department of Defense Annual energy Report, Fiscal Year 2011.

EIA, 2015a, *Average Price of Electricity to Ultimate Customers by End-Use Sector*, http://www.eia.gov/electricity/monthly/epm_table_grapher.cfm?t=epmt_5_6_a, December 24, 2015.

EIA, 2015b, *Natural Gas Prices*, http://www.eia.gov/dnav/ng/ng_pri_sum_dcu_STX_a.htm, December 31, 2015.

Evans, J.P., F. Ji, G. Abramowitz, and M. Ekstrom, Optimally choosing small ensemble members to produce robust climate simulations, Environmental Research Letters, 8(4), doi: 10.1088/1748-9326/8/4/044050, (2013).

Forsythe, W. C., Rykiel Jr., E. J., Stahl, R. S., Wu, H., Schoolfield, R. M.: A model comparison for daylength as a function of latitude and day of year, Ecol. Model., 80, 87–95, 1995.

Franco, G., Cayan, D. R., Moser, S., Hanemann, M. & Jones, M. Second California Assessment: integrated climate change impacts assessment of natural and managed systems. Guest editorial. Clim. Change 109, 1-19 (2011).

Funk, C., A. Hoell, and D. Stone (2014), Examining the Contribution of the Observed Global Warming Trend to the California Droughts of 2012/13 and 2013/14, *Bull. Am. Meteorol. Soc., 95*, S11-S15.

Griffin, D. and K. J. Anchukaitis (2014), How unusual is the 2012-2014 California drought?, *Geophys. Res. Lett., 41*, 9017-9023.

Griffin, R.C. and Chang, C., 1990. Pretest analysis of water demand in thirty communities, Water Resources Research, 26(10), 2251-2255

Groves, D. G. and E. Bloom (2013), Robust Water-Management Strategies for the California: Water Plan Update 2013 Proof-of-Concept Analysis, *RAND Corporation, California Water Plan Update 2013*, 1-72.

Groves, D. G., Yates, D. & Tebaldi, C. Developing and applying uncertain global climate change projections for regional water management planning. Water Resour. Res. 44 (2008).

Hall, D. K., Riggs, G. A., & Salomonson., V. V. (2006). *MODIS/Terra Snow Cover Daily L3 Global 500m Grid V005, 2004-2010*. Boulder, Colorado: National Snow and Ice Data Center. Retrieved from http://nsidc.org/data/docs/daac/modis_v5/mod10a1_modis_terra_snow_daily_global_500m_grid.gd.html

Hall, J. et al. Towards risk-based water resources planning in England and Wales under a changing climate. Water and Environment Journal 26, 118-129 (2012).

Hamlet, A. F. & Lettenmaier, D. P. Effects of climate change on hydrology and water resources in the Columbia River Basin, Journal of the American Water Resources Association, 35: 1597–1623. doi: 10.1111/j.1752-1688.1999.tb04240.x (1999).

Hamon, W. R.: Estimating potential evapotranspiration, J. Hydr. Eng. Div.-ASCE, 87, 107–120, 1961.

Hansen, M., R DeFries, J.R.G. Townshend, and R. Sohlberg (2000), Global land cover classification at 1kim resolution using a decision tree classifier, International Journal of Remote Sensing, 21: 1331-1365.

Hargreaves, G. H., Samani, Z. A., 1982. Estimating potential evapotranspiration. Journal of the Irrigation and Drainage Division 108(3), 225-230.

Harou, J. J., J. Medellin-Azuara, T. Zhu, S. K. Tanaka, J. R. Lund, S. Stine, M. A. Olivares, and M. W. Jenkins (2010), Economic consequences of optimized water management for a prolonged, severe drought in California, *Water Resour. Res., 46*, W05522.

Haughton, N., G. Abramowitz, A. Pitman, and S.J. Phipps, Weighting climate model ensembles for mean and variance estimates, Climate Dynamics, DOI 10.1007/s00382-015-2531-3.

Hazen, A. (1914), Storage to be provided in impounding reservoirs for municipal water supply, Transactions of the American Association of Civil Engineers, 77, 1539-1669.

Hirsch, 2013, Hirsch, J., DOLE-2.2 Building Energy Use and Cost Analysis Program, James J. Hirsch and Associates, http://doe2.com/download/doe-22/DOE22Vol6-NewFeatures_47f.pdf

Horton, R.M., V. Gornitz, D.A. Bader, A.C. Ruane, R. Goldberg, and C. Rosenzweig, 2011: Climate hazard assessment for stakeholder adaptation planning in New York City. J. Appl. Meteorol. Climatol., 50, 2247-2266, doi:10.1175/2011JAMC2521.1

Jenicek, E.M., Carroll, R.A., Curvey, L.E., Hessel, M.S., Holmes, R.M., and Pearson, E., 2011. Water sustainability assessment for ten Army installations, Report TR-11-5, Engineering Research and Development Center (ERDC) / Construction Engineering Research Laboratory (CERL).

Johnson, F., Westra, S., Sharma, A., Pitman, A. J. (2011) An assessment of GCM skills in simulating persistence across multiple scales. Journal of Climate 24 (14), 3609-3623.

Joyce, B., D. Purkey, D. Yates, D. Groves, and A. Draper (2010), Integrated scenario analysis for the 2009 California water plan update, Vol. 4, *, California Dept. of Water Resources, Vol. 4*.

Keetch, J.J., and G.M. Byram, 1968. A Drought Index for Forest Fire Control. USDA Forest Service, Southeast Forest Experiment Station Research Paper SE-38. Asheville,

Keetch. J.J.; Byram. G.M. 1968. A drought index for forest fire control. *Res. Pap. SE-38.* Asheville NC: U.S. Department of Agriculture. Forest Service. Southeastern Forest Experiment Station. 32 p. [Revised November 1988.)

Kenny, J.F., Barber, N.L., Hutson, S.S., Linsey, K.S., Lovelace, J.K., and Maupin, M.A., 2009, Estimated use of water in the United States in 2005: U.S. Geological Survey Circular 1344, 52 p.

Khakbaz, B., B. Imam, K. Hsu, and S. Sorooshian (2012), From lumped to distributed via semi-distributed: Calibration strategies for semi-distributed hydrologic models, *Journal of Hydrology*, *418*, 61-77.

Kim, D., & Kaluarachchi, J. (2014). Predicting streamflows in snowmelt-driven watersheds using the flow duration curve method. *Hydrology and Earth System Sciences*, *18*(5), 1679–1693. http://doi.org/10.5194/hess-18-1679-2014

Knutti, R., Furrer, R., Tebaldi, C., Cermak, J. & Meehl, G. A. Challenges in combining projections from multiple climate models. J. Clim. 23, 2739-2758 (2010).

Knutti, R., Masson, D. & Gettelman, A. Climate model genealogy: Generation CMIP5 and how we got there. Geophys. Res. Lett. 40, 1194-1199 (2013).

Koren, V., S. Reed, M. Smith, Z. Zhang, and D. J. Seo (2004), Hydrology Laboratory Research Modeling System (HL-RMS) of the US National Weather Service, *Journal of Hydrology, 291*, 297-318.

Kwon, H.-H., Lall, U., and Khalil, A.F., 2007. Stochastic simulation model for nonstationary time series using an autoregressive wavelet decomposition: Applications to rainfall and temperature, Water Resour. Res., 43, W05407, doi:10.1029/2006WR005258.

Kwon, H.-H., U. Lall, and A. F. Khalil (2007), Stochastic simulation model for nonstationary time series using an autoregressive wavelet decomposition: Applications to rainfall and temperature, *Water Resour. Res., 43*, W05407, doi:10.1029/2006WR005258.

Labadie, J., Baldo, M. & Larson, R. MODSIM: decision support system for river basin management: Documentation and user manual. Dept. of Civil Eng., Colo. State Univ., Ft. Collins, CO (2000).

Liang, X., Lettenmaier, D. P., Wood, E. F., & Burges, S. J. (1994). A Simple hydrologically Based Model of Land Surface Water and Energy Fluxes for GSMse. *Geophysical Research Letters*, *99*.

Liu, Yongqiang, S. L. Goodrick, and J. A. Stanturf, 2013: Future US Wildfire potential trends projected using a dynamically downscaled climate change scenario. *Forest Ecology and Management* 294: 120-135.

Livneh, B., Rosenberg, E. a., Lin, C., Nijssen, B., Mishra, V., Andreadis, K. M., … Lettenmaier, D. P. (2014). A Long-Term Hydrologically Based Dataset of Land Surface Fluxes abd States for the Conterminous United States: Upade and Extensions. *Journal of Climate*, *27*(1), 477–486. http://doi.org/10.1175/JCLI-D-13-00697.1

Lohmann, D., Raschke, R., Nijssen, B., and Lettenmaier, D. P.: Regional scale hydrology: I. Formulation of the VIC-2L model coupled to a routing model, Hydrolog. Sci. J., 43, 131–141, 1998.

Lopez, A. et al. Two approaches to quantifying uncertainty in global temperature changes. J. Clim. 19, 4785-4796 (2006).

Lund, J., E. Hanak, W. Fleenor, W. Bennett, R. Howitt, J. Mount, and P. Moyle (2010), *Comparing Futures for the Sacramento-San Joaquin Delta*, Freshwater Ecology Series, vol. 3, 232 pp., Univ California Press, Berkeley; 2120 Berkeley Way, Berkeley, CA 94720 USA.

Manning, L., Hall, J., Fowler, H., Kilsby, C. & Tebaldi, C. Using probabilistic climate change information from a multimodel ensemble for water resources assessment. Water Resour. Res. 45 (2009).

Mao, Y., B. Nijssen, and D. P. Lettenmaier (2015), Is climate change implicated in the 2013-2014 California drought? A hydrologic perspective, *Geophys. Res. Lett., 42*, 2805-2813.

Martinez, G. F., & Gupta, H. V., 2010. Toward improved identification of hydrological models: A diagnostic evaluation of the "abcd" monthly water balance model for the conterminous united states. Water Resources Research 46(8), W08507, doi:10.1029/2009WR008294.

Masson, D. & Knutti, R. Climate model genealogy. Geophys. Res. Lett. 38 (2011).

Maurer, E. P., A. W. Wood, J. C. Adam, D. P. Lettenmaier, and B. Nijssen (2002), A long-term hydrologically based dataset of land surface fluxes and states for the conterminous United States, *J. Clim., 15*, 3237-3251.

Maurer, E.P., A.W. Wood, J.C. Adam, D.P. Lettenmaier, and B. Nijssen, 2002, A Long-Term Hydrologically-Based Data Set of Land Surface Fluxes and States for the Conterminous United States, *J. Climate 15(22)*, 3237-3251.

Maurer, E.P., A.W. Wood, J.C. Adam, D.P. Lettenmaier, and B. Nijssen, A Long-Term Hydrologically-Based Data Set of Land Surface Fluxes and States for the Conterminous United States, J. Climate 15(22), 3237-3251 (2002).

Maurer, E.P., A.W. Wood, J.C. Adam, D.P. Lettenmaier, and B. Nijssen, 2002: A Long-Term Hydrologically-Based Data Set of Land Surface Fluxes and States for the Conterminous United States, *J. Climate* 15: 3237-3251.

Maurer, E.P., L. Brekke, T. Pruitt, and P.B. Duffy. 2007. Fine-resolution climate projections enhance regional climate change impact studies, *Eos Trans. AGU*, 88(47), 504.

McCabe, G. J., Betancourt, J. L. and Hidalgo, H. G. (2007), Associations of Decadal to Multidecadal Sea-Surface Temperature Variability with Upper Colorado River Flow. JAWRA Journal of the American Water Resources Association, 43: 183–192. doi: 10.1111/j.1752-1688.2007.00015.

McCabe, G.J., M. Palecki, and J. Betacourt (2004), Pacific and Atlantic Ocean influences on multidecadal drought frequency in the United States, Proceedings of the National Academy of Sciences of the United States of America, 101 (12), 4136-4141.

McEnery, J., Ingram, J., Duan, Q., Adams, T., and Anderson, L., 2005. NOAA'S Advanced Hydrologic Prediction Service – Building pathways for Better Science in Water Forecasting. Bulletin of the American Meteorological Society, March, 375-385.

McGinnis, S., D. Nychka, and L.O. Mearns, 2014: A new distribution mapping technique for climate model bias correction. 4th International Workshop on Climate Informatics.

Meinshausen, M. et al. The RCP Greenhouse Gas Concentrations and their extensions from 1765 to 2300. Climatic Change, 109, 213-241 (2011).

Meko, D. M., C. A. Woodhouse, and R. Touchan (2014), Klamath/San Joaquin/Sacramento Hydroclimatic Reconstructions from Tree Rings, *Draft Final Report to California Department of Water Resources, Agreement 4600008850*.

Mesinger, F., and Coauthors, 2006: North American Regional Reanalysis. *Bull. Amer. Meteor. Soc.,* 87: 343-360.

Moody, P., and C. Brown, Robustness indicators for evaluation under climate change: Application to the upper Great Lakes, Water Resour. Res., 49, 3576–3588, doi:10.1002/wrcr.20228, (2013).

Moradkhani, H., K. Hsu, H. Gupta, and S. Sorooshian, 2005b. Uncertainty assessment of hydrologic model states and parameters: Sequential data assimilation using particle filter, Water Resour. Res., 41, W05012, doi:10.1029/2004WR003604.

Moradkhani, H., S. Sorooshian, H. Gupta, and P. Houser., 2005a. Dual state-parameter estimation of hydrological models using ensemble Kalman filter, Adv. Water Resour., 28(2), 135–147.

Mosiasi, D. N., Arnold, J. G., Van Liew, M. W., Bingner, R. L., Harmel, R. D., and Veith, T. L. (2007), Model Evaluation guidelines for systematic quantification of accuracy in watershed simulations, Transactions of the American Society of Agricultural and Biological Engineers, 50, 885-900.

Mote, P. W., A. F. Hamlet, M. P. Clark, and D. P. Lettenmaier (2005), Declining mountain snowpack in western north America, *Bull. Am. Meteorol. Soc., 86*, 39-49.

Mount, J. and R. Twiss (2005), Subsidence, sea level rise, and seismicity in the Sacramento-SanJoaquin Delta, *San Francisco Estuary and Watershed Science, 3*.

Murphy, J. M., D.M.H Sexton, D.N Barnett, G.S Jones, M.J Webb, M Collins, Matthew and Stainforth, and A. David (2004): 'Quantification of Modelling Uncertainties in a Large Ensemble of Climate Change Simulations', Nature, Volume 430: 12. August 2004.

Murphy, J. M., D.M.H Sexton, D.N Barnett, G.S Jones, M.J Webb, M Collins, and D.A. Stainforth. Quantification of Modelling Uncertainties in a Large Ensemble of Climate Change Simulations. Nature 430, 768-772 (2004).

Nash, J. E.: The form of the instantaneous unit hydrograph, International Association of Science and Hydrology, 3, 114–121, 1957.

NC, 32 pp.

Nowak, K., M. Hoerling, B. Rajagopalan, and E. Zagona (2012), Colorado River Basin Hydroclimatic Variability. J. Climate, 25, 4389–4403. doi: http://dx.doi.org/10.1175/JCLI-D-11-00406.1

NREL, 2008, Users Manual for TMY3 Data Sets, NREL/TP-581-43156, May 2008.

Null, S. E. and J. R. Lund (2006), Re-Assembling Hetch Hetchy: Water Supply Implications of Removing O'Shaughnessy Dam, *Journal of the American Water Resources Association*, *42*, 395-408.

Null, S. E., J. Medellin-Azuara, A. Escriva-Bou, M. Lent, and J. R. Lund (2014), Optimizing the dammed: Water supply losses and fish habitat gains from dam removal in California, *J. Environ. Manage.*, *136*, 121-131.

Palmer, R.N., Rowden, W., Trungale, J., and Hamlet, A., 1995. Documentation for the modified schematic models. Report to the basinwide working group of the ACT/ACF Study. Department of Civil Engineering, University of Washington, Seattle.

Parajka, J., & Blöschl, G. (2008). The value of MODIS snow cover data in validating and calibrating conceptual hydrologic models. *Journal of Hydrology*, *358*(3-4), 240–258. http://doi.org/10.1016/j.jhydrol.2008.06.006

Pennell, C. & Reichler, T. On the effective number of climate models. J. Clim. 24, 2358-2367 (2011).

Ray, P.A.; Brown, C.M.. 2015. Confronting Climate Uncertainty in Water Resources Planning and Project Design: The Decision Tree Framework. Washington, DC: World Bank.

Reclamation, 2013. Downscaled CMIP3 and CMIP5 Climate and Hydrology Projections: Release of Downscaled CMIP5 Climate Projections, Comparison with preceding Information, and Summary of User Needs, prepared by the U.S. Department of the Interior, Bureau of Reclamation, Technical Services Center, Denver, Colorado. 47pp.

Reed, S., V. Koren, M. Smith, Z. Zhang, F. Moreda, D. J. Seo, and DMIP Participants (2004), Overall distributed model intercomparison project results, *Journal of Hydrology*, *298*, 27-60.

Rheinheimer, D. E., S. E. Null, and J. R. Lund (2015), Optimizing Selective Withdrawal from Reservoirs to Manage Downstream Temperatures with Climate Warming, *J. Water Resour. Plann. Manage.*, *141*, 04014063.

Rocheta, E., Sugiyanto, M., Johnson, F., Evans, J. and Sharma, A. (2014), How well do general circulation models represent low-frequency rainfall variability? Water Resources Research, 50, 2108-2123.

RS Means, 2013, Building Construction Cost Data 2013. http://rsmeans.reedconstructiondata.com/

Savic, D. (2002). Single-objective vs Multiobjective Optimisation for Integrated Decision Support. *Proceedings of the First Biennial Meeting of the International Environmental Modelling and Software Society*, 7–12.

Schwarz, G. E., & Alexander, R. B. (1995). Soils data for the Conterminous United States Derived from the NRCS State Soil Geographic (STATSGO) Data Base. Retrieved May 1, 2015, from http://water.usgs.gov/GIS/metadata/usgswrd/XML/ussoils.xml

Sexton, D. M., Murphy, J. M., Collins, M. & Webb, M. J. Multivariate probabilistic projections using imperfect climate models part I: outline of methodology. Clim. Dyn. 38, 2513-2542 (2012).

Sexton, D.M.H., J.M. Murphy, M. Collins, and M.J. Webb (2012), Multivariate probability projections using imperfect climate models part I: outline of methodology, *Climate Dynamics, 38 (11-12)*, 2513-2542.

Smith, M. B., D. J. Seo, V. I. Koren, S. M. Reed, Z. Zhang, Q. Duan, F. Moreda, and S. Cong (2004), The distributed model intercomparison project (DMIP): motivation and experiment design, *Journal of Hydrology, 298*, 4-26.

Smith, M. B., V. Koren, S. Reed, Z. Zhang, Y. Zhang, F. Moreda, Z. Cui, N. Mizukami, E. A. Anderson, and B. A. Cosgrove (2012), The distributed model intercomparison project - Phase 2: Motivation and design of the Oklahoma experiments, *Journal of Hydrology, 418*, 3-16.

Smith, M. et al. (2013), The distributed model intercomparison project - Phase 2: Experiment design and summary results of the western basin experiments, *Journal of Hydrology, 507*, 300-329.

Smith, R. L., Tebaldi, C., Nychka, D. & Mearns, L. O. Bayesian modeling of uncertainty in ensembles of climate models. Journal of the American Statistical Association 104, 97-116 (2009).

Srikanthan, R. and McMahon, T. A., 2001. Stochastic generation of annual, monthly and daily climate data: A review. Hydrol. Earth Syst. Sci., 5, 653-670, doi:10.5194/hess-5-653-2001.

Stainforth, D. A., et al. (2005), Uncertainty in predictions of the climate response to rising levels of greenhouse gases, Nature, 433, 403–406.

State of Georgia, 2010. Georgia 2030 Population Projections. Office of Planning and Budget.

Stedinger, Jery R. and Veronica W. Griffis, 2011. Getting From Here to Where? Flood Frequency Analysis and Climate. *Journal of the American Water Resources Association* (JAWRA) 47(3):506-513. DOI: 10.1111/j.1752-1688.2011.00545.x

Steinschneider S., Wi S. and Brown C. (2014), The integrated effects of climate and hydrologic uncertainty on future flood risk assessments, Hydrol. Process., doi: 10.1002/hyp.10409

Steinschneider, S. & Brown, C. A semiparametric multivariate, multisite weather generator with low‐frequency variability for use in climate risk assessments. Water Resour. Res. 49, 7205-7220 (2013).

Steinschneider, S. and C. Brown (2013), A semiparametric multivariate, multisite weather generator with low-frequency variability for use in climate risk assessments, *Water Resour. Res., 49*, 7205-7220.

Steinschneider, S., R. McCrary, L. O. Mearns, and C. Brown, 2015: The Effects of Climate Model Similarity on probabilisitc climate simulations and implications for Local, Risk-Based Adaptation Planning. *Geophysical Research Letters* DOI: 10.1002/2015GL064529.

Steinschneider, S., McCrary, R., Wi, S., Mulligan, K., Mearns, L., and Brown, C. (2015), Expanded Decision-Scaling Framework to Select Robust Long-Term Water-System Plans under Hydroclimatic Uncertainties, J. Water Resour. Plann. Manage. ,10.1061/(ASCE)WR.1943-5452.0000536 , 04015023.

Stephenson, D. B., Collins, M., Rougier, J. C. & Chandler, R. E. Statistical problems in the probabilistic prediction of climate change. Environmetrics 23, 364-372 (2012).

Swain, D. L. (2015), A tale of two California droughts: Lessons amidst record warmth and dryness in a region of complex physical and human geography, *Geophysical Research Letters, 42*, 9999-10003.

Swain, D. L., M. Tsiang, M. Haugen, D. Singh, A. Charland, B. Rajaratnam, and N. S. Diffenbaugh (2014), The Extraordinary California Drought of 2013/2014: Character, Context, and the Role of Climate Change, *Bull. Am. Meteorol. Soc., 95*, S3-S7.

Tallaksen, L. M., and K. Stahl (2014), Spatial and temporal patterns of large-scale droughts in Europe: Model dispersion and performance, Geophys. Res. Lett., 41, 429– 434, doi:10.1002/2013GL058573.

Tanaka, S. K., C. Buck, K. Madani, J. Medellin-Azuara, J. Lund, and E. Hanak (2011), Economic Costs and Adaptations for Alternative Regulations of California's Sacramento-San Joaquin Delta, *San Francisco Estuary and Watershed Science, 9*, 28.

Tanmoyee, B., V, R. P., & Abdul, H. (2015). Climate Change Impact on Snowmelt Runoff Modelling for Alaknanda River Basin. *Journal of Environment and Earth Science*, *5*(9), 139–150.

Taylor, K. E., R. J. Stouffer, and G. A. Meehl, A Summary of the CMIP5 Experiment Design, Bull. Amer. Meteor. Soc, 93, 485–498 (2012).

Tebaldi, C. & Knutti, R. The use of the multi-model ensemble in probabilistic climate projections. Philos. Trans. A. Math. Phys. Eng. Sci. 365, 2053-2075 (2007).

Tebaldi, C. & Sansó, B. Joint projections of temperature and precipitation change from multiple climate models: a hierarchical Bayesian approach. Journal of the Royal Statistical Society: Series A (Statistics in Society) 172, 83-106 (2009).

Tebaldi, C. and B. Sansó, 2009: Joint Projections of Temperature and Precipitation Change from Multiple Climate Models: A Hierarchical Bayesian Approach. J. Royal Statistical Society 172: 83-106.

Tebaldi, C., Smith, R. L., Nychka, D. & Mearns, L. O. Quantifying uncertainty in projections of regional climate change: A Bayesian approach to the analysis of multimodel ensembles. J. Clim. 18, 1524-1540 (2005).

Tebaldi, Claudia, Richard L. Smith, Doug Nychka, Linda O. Mearns, 2005: Quantifying Uncertainty in Projections of Regional Climate Change: A Bayesian Approach to the Analysis of Multimodel Ensembles. *J. Climate*, **18**, 1524–1540. doi: http://dx.doi.org/10.1175/JCLI3363.1

Texas Water Development Board, 2013. Projection nethodology – Draft population and municipal water demands, http://www.twdb.state.tx.us/waterplanning/data/projections/index.asp

Thornton, P.E., M.M. Thornton, B.W. Mayer, N. Wilhelmi, Y. Wei, R. Devarakonda, and R.B. Cook (2014), Daymet: Daily Surface Weather Data on a 1-km Grid for North America, Version 2. ORNL DAAC, Oak Ridge, Tennessee, USA. Accessed July 07, 2013. http://dx.doi.org/10.3334/ORNLDAAC/1219

U.S. Department of Agriculture (2014), California drought 2014: Farm and food impacts, *United States Department of Agriculture*, Available at http://www.ers.usda.gov/topics/in-the-news/california-drought-2014-farm-and-food-impacts.aspx.

U.S. Geological Survey (2014), California Water Science Center, Available at http://ca.water.usgs.gov/data/drought/surfacewater.html.

United States Army Corps of Engineers, 1997. ACT/ACF comprehensive water resources study surface water availability, volume 1: Unimpaired Flows. Mobile District, Hydrologic Engineering Center.

United States Drought Monitor (2014), California drought intensifies and U.S. drought spreads, *United States Drought Monitor, 6 Feb*, Available at http://droughtmonitor.unl.edu/USDMNews/NewsArchive.aspx.

USACE 2011, *MILCON Energy Efficiency and Sustainability Study of Five Types of Army Buildings,* U.S. Army Corps of Engineers, Washington DC, 2011.

Vandewiele, G., Xu, C. Y., 1992. Methodology and comparative study of monthly water balance models in Belgium, China and Burma. Journal of Hydrology 134(1), 315-347.

Vigerstol, K. L., & Aukema, J. E. (2011). A comparison of tools for modeling freshwater ecosystem services. *Journal of Environmental Management*, *92*(10), 2403–2409. http://doi.org/10.1016/j.jenvman.2011.06.040

Vogel, R. M., Sankarasubramanian, A., 2003. Validation of a watershed model without calibration. Water Resour. Res 39, *1292, doi:*10.1029/2002WR001940,10.

Wagener T., Boyle D.P., Lees M.J., Wheater H.S., Gupta H.V., Sorooshian S., 2001, A framework for development and application of hydrological models. Hydrol Earth Syst Sci;5(1): 13–26.

Wang, H. and S. Schubert (2014), Causes of the Extreme Dry Conditions Over California during Early 2013, *Bull. Am. Meteorol. Soc., 95*, S7-S11.

Wang, Q. J.: The Genetic Algorithm and Its Application to Calibrating Conceptual Rainfall-Runoff Models, Water Resour. Res., 27, 2467–2471, 1991.

Whateley, S., S. Steinschneider, and C. Brown (2016), Selecting stochastic climate realizations to efficiently explore a wide range of climate risk to water resouces systems, *Journal of Water Resources Planning and Management, submitted*.

Wi, S., Y. C. E. Yang, S. Steinschneider, A. F. Khalil, and C. M. Brown (2015), Calibration approaches for distributed hydrologic models using high performance computing: Implication for streamflow projections under climate change, *Hydrology and Earth System Sciences*, *19*, 857-876.

Wilby, R. L. and S. Dessai (2010), Robust adaptation to climate change, *Weather, 65*, 180-185.

Willis, A. D., J. R. Lund, E. S. Townsley, and B. Faber (2011), Climate Change and Flood Operations in the Sacramento Basin, California, *San Francisco Estuary and Watershed Science, 9*, 18.

Wise, E.K., M. L. Wrzesien, M. P. Dannenberg, and D. L. McGinnis, (2015), Cool-Season Precipitation Patterns Associated with Teleconnection Interactions in the United States. J. Appl. Meteor. Climatol., 54, 494–505. doi: http://dx.doi.org/10.1175/JAMC-D-14-0040.1

Xie, Z., Yuan, F., Duan, Q., Zheng, J., Liang, M., & Chen, F. (2007). Regional Parameter Estimation of the VIC Land Surface Model: Methodology and Application to River Basins in China. *Hydrometeor*, (8), 477–468.

Yates, D., Sieber, J., Purkey, D. & Huber-Lee, A. WEAP21—A demand-, priority-, and preference-driven water planning model: part 1: model characteristics. Water Int. 30, 487-500 (2005).

Zhang, J. Y., Wang, G. Q., Pagano, T. C., Jin, J. L., Liu, C. S., He, R. M., & Liu, Y. L. (2012). Using Hydrologic Simulation to Explore the Impacts of Climate Change on Runoff in the Huaihe River Basin of China. *Journal of Hydrologic Engineering*, (September 2015), 389. http://doi.org/10.1061/(ASCE)HE.1943-5584.0000581

Zhang, X., Srinivasan, R., & Liew, M. Van. (2008). Multi-site calibration of the SWAT model for hydrologic modeling. *Transactions of the ASABE*, *51*(2007), 2039–2049.

Zhao, F., Chiew, F. H. S., Zhang, L., Vaze, J., Perraud, J.-M., & Li, M. (2012). Application of a Macroscale Hydrologic Model to Estimate Streamflow across Southeast Australia. *Hydrometeor*, *13*, 1233–1250.